



UNIVERSITAT DE  
BARCELONA

# Relevant Molecular and Functional G-Protein Coupled Receptor Interactions in Neuroinflammation and Addiction

Interaccions moleculars i funcionals de receptors acoblats  
a proteïna G rellevants en neuroinflamació i addició

Edgar Angelats Canals

**ADVERTIMENT.** La consulta d'aquesta tesi queda condicionada a l'acceptació de les següents condicions d'ús: La difusió d'aquesta tesi per mitjà del servei TDX ([www.tdx.cat](http://www.tdx.cat)) i a través del Dipòsit Digital de la UB ([diposit.ub.edu](http://diposit.ub.edu)) ha estat autoritzada pels titulars dels drets de propietat intel·lectual únicament per a usos privats emmarcats en activitats d'investigació i docència. No s'autoritza la seva reproducció amb finalitats de lucre ni la seva difusió i posada a disposició des d'un lloc aliè al servei TDX ni al Dipòsit Digital de la UB. No s'autoritza la presentació del seu contingut en una finestra o marc aliè a TDX o al Dipòsit Digital de la UB (framing). Aquesta reserva de drets afecta tant al resum de presentació de la tesi com als seus continguts. En la utilització o cita de parts de la tesi és obligat indicar el nom de la persona autora.

**ADVERTENCIA.** La consulta de esta tesis queda condicionada a la aceptación de las siguientes condiciones de uso: La difusión de esta tesis por medio del servicio TDR ([www.tdx.cat](http://www.tdx.cat)) y a través del Repositorio Digital de la UB ([diposit.ub.edu](http://diposit.ub.edu)) ha sido autorizada por los titulares de los derechos de propiedad intelectual únicamente para usos privados enmarcados en actividades de investigación y docencia. No se autoriza su reproducción con finalidades de lucro ni su difusión y puesta a disposición desde un sitio ajeno al servicio TDR o al Repositorio Digital de la UB. No se autoriza la presentación de su contenido en una ventana o marco ajeno a TDR o al Repositorio Digital de la UB (framing). Esta reserva de derechos afecta tanto al resumen de presentación de la tesis como a sus contenidos. En la utilización o cita de partes de la tesis es obligado indicar el nombre de la persona autora.

**WARNING.** On having consulted this thesis you're accepting the following use conditions: Spreading this thesis by the TDX ([www.tdx.cat](http://www.tdx.cat)) service and by the UB Digital Repository ([diposit.ub.edu](http://diposit.ub.edu)) has been authorized by the titular of the intellectual property rights only for private uses placed in investigation and teaching activities. Reproduction with lucrative aims is not authorized nor its spreading and availability from a site foreign to the TDX service or to the UB Digital Repository. Introducing its content in a window or frame foreign to the TDX service or to the UB Digital Repository is not authorized (framing). Those rights affect to the presentation summary of the thesis as well as to its contents. In the using or citation of parts of the thesis it's obliged to indicate the name of the author.



UNIVERSITAT DE  
BARCELONA

UNIVERSITAT DE BARCELONA  
FACULTAT DE BIOLOGIA  
DEPARTAMENT DE BIOQUÍMICA I BIOMEDICINA MOLECULAR

**RELEVANT MOLECULAR AND FUNCTIONAL G-PROTEIN COUPLED  
RECEPTOR INTERACTIONS IN NEUROINFLAMMATION AND  
ADDICTION**

**INTERACCIONS MOLECULARS I FUNCIONALS DE RECEPTORS  
ACOBLATS A PROTEÏNA G RELLEVANTS EN NEUROINFLAMACIÓ I  
ADDICCIÓ**

Memòria presentada pel graduat en Biomedicina  
**Edgar Angelats Canals**  
per optar al grau de Doctor per la Universitat de Barcelona

Aquesta tesi s'ha adscrit al Departament de Bioquímica i Biomedicina Molecular de la  
Universitat de Barcelona, dins del programa de doctorat de Biomedicina

El treball experimental i la redacció de la present memòria han estat realitzats per Edgar  
Angelats Canals, sota la direcció del Dr. Rafael Franco Fernández i la Dra. Gemma  
Navarro Brugal.

Dr. Rafael Franco Fernández

Dra. Gemma Navarro Brugal

Edgar Angelats Canals

Barcelona, Juny de 2018



Una tesi doctoral podria definir-se, en certa manera, com un camí que decidim recórrer. Sens dubte hi ha moments en que el camí fa pujada i es fa feixuc, tan cert com que en d'altres moments, fa baixada i bé tot rodat. En qualsevol cas, tot i semblar un viatge d'un sol protagonista o d'un sol autor, no pot entendre's sense tota aquella gent que en algun punt del procés, t'han acompanyat, ajudat o fet gaudir d'aquest camí que sembla arribar al seu final.

Així doncs, amb la intenció de no deixar-me a ningú, m'agradaria donar-vos les gràcies a tots aquells que, d'una manera o un altra, m'heu ajudat a que avui sigui jo qui arribi al final del trajecte.

En primer lloc, voldria agrair als directors de tesi, la confiança dipositada en mi des d'un primer moment. Sense aquesta confiança, aquest projecte no hagués estat possible. Al Rafa, agrair-li el fet de tenir la porta del despatx sempre oberta, volent solucionar qualsevol entrebanc i problema que sorgeixi amb la major brevetat possible. A la Gemma, sense cap mena de dubte, agrair-li la passió que m'ha contagiada per aquesta professió, reconeixent-li també els esforços i l'interès perquè tingues una beca i pogués realitzar la tesi al grup.

Tanmateix, no voldria oblidar-me de la resta de membres sèniors del grup. L'Enric, la Pepi, l'Antoni i el Vicent. Durant aquest camí, he pogut viure i aprendre de moltíssimes situacions que no serien possibles sense el grup de Neurobiologia Molecular, al qual estaré sempre agraït per tot aquests anys.

Tampoc voldria deixar-me alguns que fa temps que van acabar la seva etapa al laboratori, com el Victor i l'Isaac. Tinc el plaer d'haver gaudit 48 hores al 'camarote', i això sense haver donat sang als últims vampirs de NBM. Al Marc, qui va suggerir-me la idea de fer pràctiques d'estiu al grup on ell treballava i que tot plegat ha acabat amb una tesi al grup... Mencionar també el 'poli' del grup, el Dani, i totes les seves tècniques en l'art de la seducció.

Passant a tots aquells més contemporanis, i amb aquells amb qui he compartit el meu dia a dia al laboratori durant aquest temps, desitjar sort a la Estefa en la nova etapa que l'espera en un mesos, i a la Vero amb l'última passa que li queda per convertir-se en doctora. A la Jas, recordar-li que haurà de trobar a algú altre amb qui inventar-se cançons. Es fa difícil entendre que diu ('mi gozo en seis pozos') o que li passa pel cap a la Jas molts cops, però és un membre indispensable perquè funcioni el lab. Gràcies per tota l'ajuda que m'has ofert durant aquests anys. Després mencionar al David, l'Agui. Company de lab i de pis. Gràcies per obrir-me les portes del 'bunquer' (les de les finestres ja les obro jo, ni que sigui per ventilar...) i per tots els moments viscuts durant aquests anys (sense guants per tenir més 'grip' en parets verticals, peixeres per Copenhage o les festes a casa...). Què dir de la Mireia Medrano... Un exemple com a científica i de qui he après més del que ella pugui imaginar. Apart (menys certes discrepàncies futbolístiques) amb qui coincideixo en molts aspectes. Què, quan fem un pàdel? (XD)... La Mar, la paciència i bondat personificades alhora que una gran companya de coffee breaks (també una gran Queen Cobra)... M'ha encantat poder compartir aquests últims mesos colze a colze, mentre escrivíem la tesi! A la Irene, agrair-li les moltes coses bones que han passat amb ella al

lab. No sé si és coincidència o gràcies a ella, però justament va ser després de que arribes ella que tots vam passar de ser companys de laboratori per ser amics. A l'Iñigo, els vídeos, bromes, i moments autènticament inversemblants al laboratori. Molta sort Doctor Etayo! A l'altra Mireia, la 2.0, molta sort en el camí que tot just comences. A vegades es fa dur, però segur que amb la teva alegria te'n surts amb facilitat. També desitjar sort al Rafa Junior, 'Cordobés', el més 'nou' dels meus contemporanis al lab, i el més vell de les noves generacions. Finalment dins d'aquest grup, no puc deixar-me a la Patri, lletuga (saps que és el millor dels molts 'apodos' que t'han posat...). La nostra amistat, va patir serioses turbulències tot just quan s'enlairava, però d'ençà només ha fet que millorar, convertint-te en una part indispensable del laboratori per mi en aquests últims mesos!

No vull deixar-me d'expressar els meus millors desitjos per a tots aquells que comenceu i que ara sou al lab. Caty, Laura, Iu, Alejandro, Jaume i companyia, molta sort. Igualment, m'agradaria mencionar aquelles dues noies a les quals espero haver pogut ajudar a créixer científicament. La primera TFG a càrrec va ser la Cristina, una autèntica princesa sortida de una pel·lícula de Disney. I la Marta, ara a l'estranger i obrint-se camí. Que seguiu valorant la meva opinió (ja sigui per feina o altres coses) m'omple d'orgull i alegria.

Let me acknowledge to Horst Vogel, Thamani and Catarina all what they did during my fruitful stay in the EPFL. Those months were such an experience, maybe the best months of the entire thesis. All what I learnt in the lab or in the SyncSignal Meeting, is knowledge that I will carry wherever I go and definitely will help me in a near future.

En aquest apartat, agrair novament al Marc, fer-me sentir com a casa a Suïssa. També a l'Anna i la petita Judit, per obrir-me les portes del Mont Pelerin i per convertir els mesos a Lausanne en una experiència inoblidable.

En aquest camí que és la tesi, no tot és ciència. Els moments per desconectar són més que necessaris, i en aquest sentit, agrair als 'peixets', amics de tota la vida, a ajudar-me a aïllar-me dels problemes del dia a dia científic. Al Marc i la Cris, per fer-nos partícips (en certa manera) a tots de la seva relació. A l'Hèctor, per portar l'Anna al grup. I l'Anna, per ser ella, per ser com és. També al Mario, Panter, Corrales o el Muñoz (el més car de veure'l però...) per tots els moments, els anys junts i ser-hi sempre. A la Marina, sempre disposada a cuinar-nos petites meravelles. A l'Albert agrair-li no haver-me venut cap hipoteca i a la Laura que no fugís corrents quan ens va conèixer a la Sede. I també al Pinguino, ben tornat!

Vull agrair també a la Mar, Laura, Nago i la Dra. Sílvia Garcia Monclús, no únicament per no repetir errors d'altres que no se'n recorden dels seus amics de la uni, sinó perquè sempre és motiu d'alegria recordar moments on les coses eren més senzilles, més fàcils i on les complicacions menys complexes. Uns grans anys.

Dins els agraïments a aquells que no són del món científic però que són indispensables i més que necessaris per mi, hi entra la meva família. Als qui els hi dec molt. Sens dubte som un reflex de les experiències i històries viscudes, i en aquest sentit,

sense tot el que he viscut i m'ha ensenyat la meva família, no hagués pogut recórrer aquest camí.

Així doncs, agrair als tiets i cosins, per les reunions, dinars i sopars interminables i que sempre arranquen més d'un somriure. També a la iaia Fefa, a qui aviat podré dir-li que sí, que els estudis ja els he acabat. A l'Èric i la Espe, que són un exemple i demostren una valentia immensa a l'hora de perseguir els seus somnis. I òbviament als meus pares. A la meva mare, qui segurament més s'ha preocupat en els moments durs i a qui més il·lusió li fa aquest moment. Al meu pare, per el suport constant i incondicional, i per tot el que m'ha ensenyat, potser sense que ell ho sàpiga i més del que mai li voldré reconèixer.

I ja per acabar, no puc deixar-me qui ha estat, I en certa manera segueix sent, algú molt important per a mi. A la iaia Carmen, a qui trobo molt a faltar cada dia. A la lliçó de vida que era passar una estona amb tu. Per la teva complicitat, la teva alegria i la felicitat amb que inundaves l'estança on fossis, independentment de la quina fos la situació. Perquè res m'enorgulleix més que et sentissis orgullosa de nosaltres i de tota la família. Allà on siguis, un petó molt fort.

A tots els que sortiu en aquestes línies, I aquells dels quals potser m'he oblidat; de tot cor, moltes gràcies.

Edgar Angelats Canals



*A la meua àvia Carmen,  
per la seva alegria, vitalitat i somriure etern.*





## INDEX

I. INTRODUCTION .....	15
I.1 G-Protein coupled receptors .....	17
I.1.1 General characteristics.....	17
I.1.2 GPCR structure.....	17
I.1.3 GPCR classification.....	19
I.1.4 GPCR ligands and constitutive activation.....	21
I.1.5 GPCR activation and signalling pathways.....	22
I.1.6 Regulation of GPCR activity.....	25
I.2 GPCR oligomerization.....	27
I.2.1 GPCR interaction.....	27
I.2.2 Architecture of GPCR heteromers.....	29
I.2.3 Techniques used to identify GPCR oligomers.....	32
I.2.4 Functional consequences of GPCR oligomerisation.....	37
I.3 The endocannabinoid system.....	40
I.3.1 Components of the endocannabinoid system.....	40
I.3.2 Cannabinoid receptors.....	43
I.3.2.1 Cannabinoid receptor 1.....	43
I.3.2.2 Cannabinoid receptor 2.....	44
I.3.3 Cannabinoid receptor heteromers.....	46
I.3.4 Cannabinoids role in neuroinflammation process.....	48
I.4 Calcium sensor proteins.....	51
I.4.1 Relevance of calcium in neuron physiology.....	51
I.4.2 Calmodulin.....	52
I.4.3 Neuronal calcium-binding proteins.....	53
I.4.4 Neuronal Calcium Sensor.....	54
I.4.5 Calcium sensor proteins as regulators of GPCR activity.....	56
I.5 Cocaine addiction .....	58
I.5.1 The reward system .....	58

I.5.2 Drug addiction development .....	59
I.5.3 Cocaine mechanism of action .....	60
I.5.4 Sigma receptors and their relationship with cocaine .....	63
I.5.5 Ghrelin, ghrelin receptors and the control of food intake .....	67
I.5.6 Ghrelin in the reward pathway and its involvement in addiction processes.....	70
II. AIMS.....	73
III. MATERIALS AND METHODS.....	79
IV. RESULTS.....	99
IV.1 Chapter 1: Modulation of the expression and signalling of CB <sub>1</sub> , CB <sub>2</sub> and CB <sub>1</sub> -CB <sub>2</sub> receptor heteromers in activated microglia.....	101
IV.2 Chapter 2: Identification of a neuronal calcium- cAMP signalling cross-talk at cannabinoid CB <sub>1</sub> R mediated by interactions with EF-hand calcium sensors.....	121
IV.3 Chapter 3: Determination of the functional role for the truncated Ghrelin receptor GHS-R1b.....	131
IV.4 Chapter 4: Investigation of the relationship between cocaine and the loss of appetite.....	151
V. CONCLUSIONS.....	169
VI. BIBLIOGRAPHY.....	175

## LIST OF ABBREVIATIONS

- 2-AG – 2-Arachidonoylglycerol
- 5-HT<sub>n</sub>R – Serotonin Receptor n
- Å – Angstrom
- AC – Adenylyl Cyclase
- ACEA – Arachidonyl-2'-chloroethylamide
- AD – Alzheimer's disease
- AEA - Anandamide
- AIM – Abnormal Involuntary Movement
- ALS – Amyotrophic Lateral Sclerosis
- A<sub>1</sub>R – Adenosine Receptor 1
- A<sub>2A</sub>R – Adenosine Receptor 2a
- ATP – Adenosine-5'-triphosphate
- BiFC – Bimolecular Fluorescence Complementation
- BiLC – Bimolecular Luminescence Complementation
- BiP/GRP-78 – Immunoglobulin Binding Protein/ 78 kDa Glucose-Regulated Protein
- BRET – Bioluminescence Resonance Energy Transfer
- Ca<sup>2+</sup> - Calcium Ion
- CaM – Calmodulin
- cAMP – cyclic Adenosine monophosphate
- CNS – Central Nervous System
- CRF-R – Corticotropin-releasing Factor Receptor
- DAG – Diacylglycerol
- DAG-lipase – Diacylglycerol lipase
- DAT – Dopamine Transporter
- DMEM – Dulbecco's Modified Eagle's Medium
- DMR – Dynamic Mass Redistribution
- DMSO – Dimethyl sulfoxide
- DNA – Deoxyribonucleic Acid
- D<sub>n</sub>R – Dopamine Receptor
- ECL – Extracellular Loop
- ER – Endoplasmic Reticulum
- ERK – Extracellular Regulated Kinase

FAAH – Fatty Acid Amide Hydrolase  
FBS – Foetal Bovine Serum  
FRET – Förster Resonance Energy Transfer  
GABA<sub>xn</sub> – *gamma* aminobutyric acid receptor n  
GDP – Guanosine-5'-diphosphate  
GEF – Guanine nucleotide exchange factor  
GFP – Green Fluorescent Protein  
GHS-1xR – Ghrelin Receptor 1x  
G<sub>n</sub> – G-protein subunit  
GPCR – G-Protein Coupled Receptor  
GRK – GPCR kinase  
GTP – Guanosine-5'-triphosphate  
HBSS – Hank's Balanced Salt Solution  
HD – Huntington Disease  
HEK-293T – Human Embryonic Kidney 293T  
HFIP – 1,1,1,3,3,3-hexafluoro-2-propanol  
HTRF – Homogeneous Time-Resolved Fluorescence  
ICL – Intracellular Loop  
INF- $\gamma$  - Interferon gamma  
IP<sub>3</sub> – Inositol-1,4,5 triphosphate  
JNK – c-Jun N-terminal kinases  
kDa – KiloDalton  
LPI – Lysophosphatidylinositol  
LPS – Lipopolysaccharide  
LTD – Long Term Depression  
M-MLV – Moloney Murine Leukemia Virus  
MAGL – Monoacylglycerol lipase  
MAPK – Mitogen Activated Protein Kinases  
MEK – Mitogen Activated Kinase Kinase  
Mg<sup>2+</sup> - Magnesium ion  
mM – milliMolar  
mRNA – messenger Ribonucleic Acid  
MS – Multiple Sclerosis  
N-arachidonoyl-PE – N-arachidonoyl-phosphatidylethanolamine

NAcc – Nucleus Accumbens  
NAGly – N-Arachidonoylglycine  
NAPE-PLD – N-acyl-phosphatidyletanolamine phospholipase D  
nCaBP – Neuronal Calcium-Binding Protein  
NCS – Neuronal Calcium Sensor  
NED - N-1-naphthylethylenediamine dihydrochloride  
NIDA – National Institute on Drug Abuse  
nm – Nanometer  
nM – nanoMolar  
Ox-R – Orexin Receptor  
PD – Parkinson's disease  
PEI – PolyEthylenImine  
PFA – Paraformaldehyde  
PKA – Protein Kinase A  
PKC – Protein kinase C  
PLA – Phospholipase A  
PLA – Proximity Ligation Assay  
PLC – Phospholipase C  
R – Receptor  
RAMPs – Receptor Activity-modifying Protein  
RET – Resonance Energy Transfer  
RGS – Regulator of G-protein signalling protein  
Rluc – *Renilla* luciferase  
RPMI 1640 – Roswell Park Memorial Institute 1640 medium  
RTK – Receptor Tyrosine Kinase  
SRET – Sequential Resonance Energy Transfer  
TH – Tyrosine Hydroxylase  
TIRF – Total Internal Reflection Fluorescence  
TM - Transmembrane  
TRPV-1 – Vanilloid receptor 1  
VGCC – Voltage Gated Calcium Channels  
VTA – Ventral Tegmental Area  
YFP – Yellow Fluorescent Protein  
 $\Delta^9$ -THC -  $\Delta^9$ -tetrahydrocannabinidiol

$\mu\text{M}$  – microMolar

$\sigma_n\text{R}$  – Sigma Receptor

# **I. INTRODUCTION**







## **I. INTRODUCTION**

### **I.1 G PROTEIN COUPLED RECEPTORS**

#### **I.1.1 General Characteristics**

G-Protein Coupled Receptors (GPCR) or seven transmembrane domain (7-TM) receptors constitute the biggest and most versatile protein superfamily of membrane receptors involved in signal transduction. Almost a 2% of human genome codes for GPCR (*Fredriksson et al., 2003; Jacoby et al., 2006*), resulting in more than a thousand proteins, 90% of which are expressed in Central Nervous System (CNS) (*George et al., 2002*).

A diverse and wide range of endogenous and exogenous ligands can activate GPCRs, *inter alia* amines, glucopeptides, lipids, nucleotides, ions and even light photons. As shown in Figure 1, through activation of different effector proteins such as Adenylyl Cyclase (AC), phospholipase C (PLC) or ion channels, GPCR trigger multiple functions within the CNS and periphery, controlling cell survival, metabolism, cell differentiation, inflammatory and immune responses or neuronal transmission (*Getber, 2000; Marinissen and Gutkind, 2001*). Alterations in GPCR function or even polymorphisms in these receptors are linked to several diseases or disorders (*Rana et al., 2001*), making GPCR good candidates for drug discovery. Nowadays, it is estimated that the 40% of the commercialised drugs (*Lu and Wu, 2016; Schlyer and Horuk, 2006*) and almost the 25% of the 200 most sold drugs are targeting and modulating GPCR activity (*Flower, 1999; Howard et al., 2001; Marinissen and Gutkind, 2001*).

#### **I.1.2 GPCR Structure**

The first characteristic to define GPCR is that they have seven connected transmembrane domains that span the plasma membrane. These domains are formed by 25-35 amino acids with a relative high degree of hydrophobicity. While the N-terminal domain of the protein is facing the extracellular space, the C-terminal is going to be found in the cytosol. The other main characteristic of these receptors is their ability to couple heterotrimeric G-proteins, through which the receptor mainly transduces its signal.

In 2000, Palczewski et al. published the first GPCR crystal structure, defining the structure of bovine rhodopsin (*Palczewski et al., 2000*). With a resolution of 2.3 Å, the demonstration of the arrangement in seven  $\alpha$ -helix domains forming the TM receptor core, with the six alternative connecting intracellular (ICL) and extracellular (ECL) loops, was



## INTRODUCTION

obtained. The integration and the conformation of the GPCR structure is done in the endoplasmic reticulum (ER), where the  $\alpha$ - helices are stabilized inside the lipid bilayer due to the molecule high hydrophobicity. Polar residues face the receptor core, then minimizing the hydrophobic interactions with the membrane, and the tertiary structure is achieved by specific interaction between helices that lead to the ring-shape stable conformation of the receptors. Finally, after the post-translational modifications and numerous steps of quality control, the receptors are delivered to the plasma membrane, where exert their function.

Several GPCR structures are now available (Rosenbaum *et al.*, 2009; Weis and Kobilka,

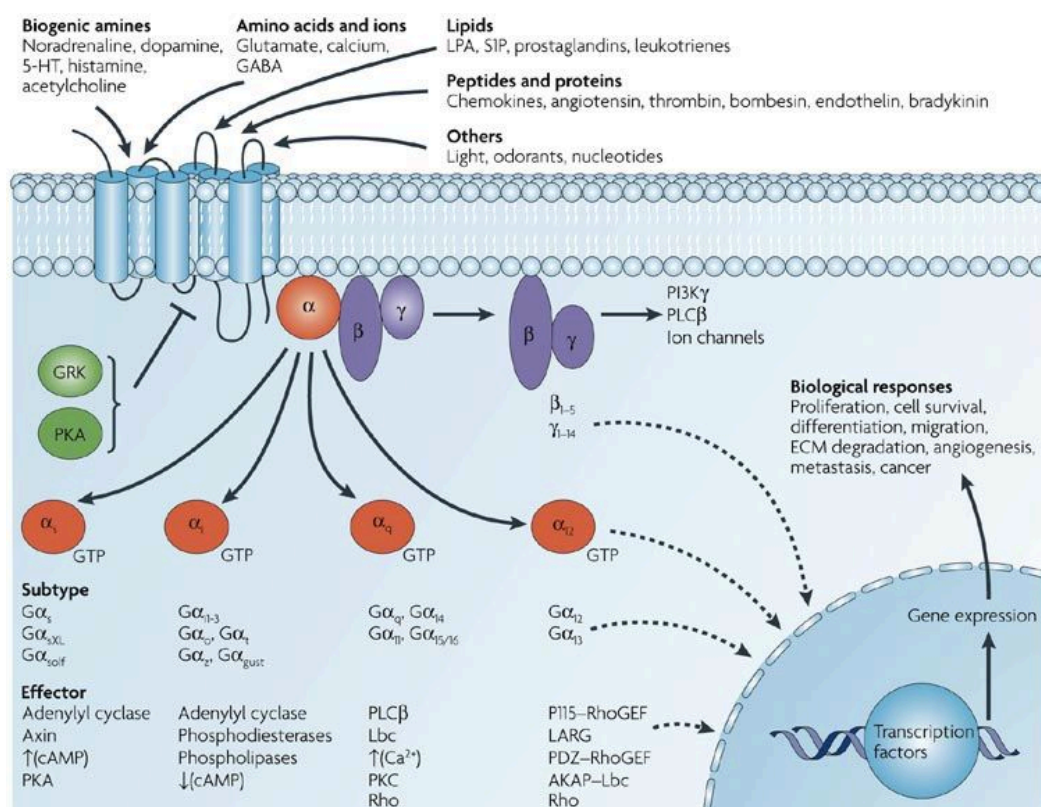


**Figure II. GPCR endogenous ligands and signalling mechanisms.** A wide variety of ligands use GPCR to stimulate cytoplasmic and nuclear targets through heterotrimeric G-protein –dependent and independent pathways. Such signalling pathways regulate key biological functions such as cell proliferation, cell survival and angiogenesis (Dorsam and Gutkind, 2007).

2008). The  $\beta_2$ -adrenergic receptor (Cherezov *et al.*, 2007) (Figure 2) or the A<sub>2A</sub> adenosine receptor (Jaakola *et al.*, 2008) were among those whose structure was elucidated first. To date, more than a hundred crystal GPCR structures have been published (Shonberg *et al.*, 2015; Yin *et al.*, 2016). The obtain of the opsin receptor crystal structure coupled to a G-protein provide clues for interpret the conformational changes during signal transduction (Park *et al.*, 2008; Scheerer *et al.*, 2008). Structural advances have not only had an impact on GPCR architecture knowledge, but have let the concept of biased agonism evolve from a theoretical frame towards a realistic approach in pharmacology and drug discovery (Kenakin and Christopoulos,

2013; Whalen *et al.*, 2011). Biased agonism could be described as the ability of ligands to stabilise different conformations of a GPCR, enabling the activation of some signalling pathways in detriment of others (Costa-Neto *et al.*, 2016; Klein Herenbrink *et al.*, 2016). Therefore, this new paradigm opens the possibility of generating new drugs favouring the signal transduction through one pathway and, at the same time, reducing the action of those pathways that provoke undesired side effects (Klein Herenbrink *et al.*, 2016). To achieve this goal, it is necessary to understand how different ligands modify and stabilise the receptor structure.

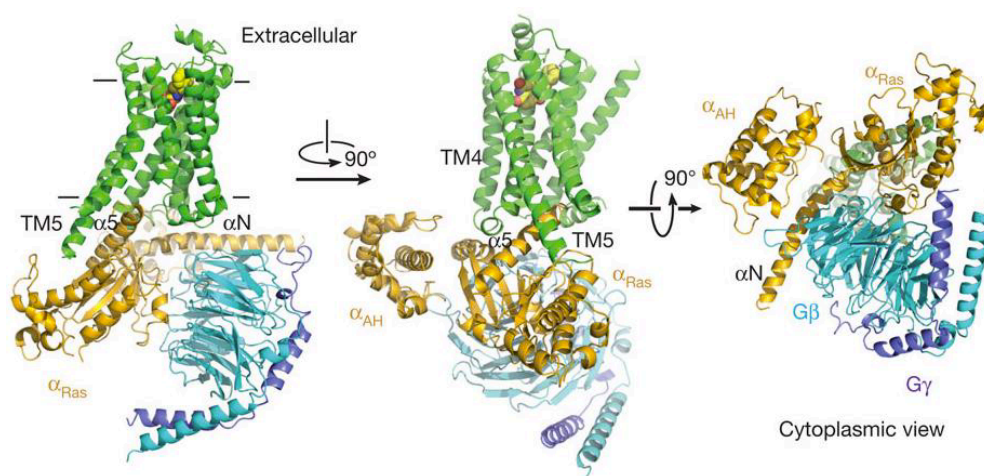


**Figure I2.** Crystal structure of the  $\beta_2$ -adrenergic receptor coupled to a Gs protein (Rasmussen *et al.*, 2011).

### I.1.3 GPCR Classification

GPCR share structural common features, including the seven TM domains, the alternative ICL and ECL loops and, in most of them, two cysteine residues located in the ECL1 and ECL2 that form a disulphide bond with implications in packaging and stabilising the multiple conformations of the seven TM (Baldwin, 1994; Probst *et al.*, 1992). Nonetheless, other structural characteristics of these receptors like N and C-terminus length or even the overall sequence homology are very diverse (Kolakowski, 1994). Due to this divergence, several GPCR classifications have been proposed. One of the oldest is the proposed by Kolakowski (Kolakowski, 1994), that gathers GPCR in six different groups according their sequence and structure (A to F). The families A, B and C are the biggest ones, while the families D, E and F are formed by few receptors (Kolakowski, 1994).

Family A, or rhodopsin-like family includes almost the 90% of all GPCR. The wide variety of receptors included in this family, that range from hormone to neurotransmitter receptors, make them share few homology traits. These are a palmitoylated cysteine in the C-



## INTRODUCTION

terminus that anchors the receptor at the membrane, a disulphide bond between ECL1 and ECL2, and the conserved amino acid residue of arginine in the Asp-Arg-Tyr (DRY) motif located on the cytoplasmic side of the third transmembrane domain (Probst *et al.*, 1992), and believed to be involved in the receptor activation. The ligand is mainly bound to the cavity formed by the TM domains, although in some cases the interaction occurs at the N-terminus domain or at the extracellular loops (George *et al.*, 2002; Jacoby *et al.*, 2006).

The family B includes approximately 50 receptors, most of them receptors for hormones or neuropeptides. This family lacks of the DRY motif presented in family A, but contains a large N-terminus domain (100 amino acids) with multiple cysteine residues that form, presumably, a net of disulphide bonds (de Graaf *et al.*, 2017; Ulrich *et al.*, 1998).

Family C is characterised by a large C-terminus and N-terminus domains (500 to 600 amino acids). According to crystallography studies with solubilised metabotropic receptor bound to glutamate, it was deduced that, in these receptors, ligand binding takes place in the N-terminal domain (Pin *et al.*, 2003). Besides the two conserved cysteine residues that form a disulphide bond between ECL1 and ECL2, there is no other common trait with families A and B. In addition, the 3<sup>rd</sup> intracellular loop of these GPCR is short and highly conserved.

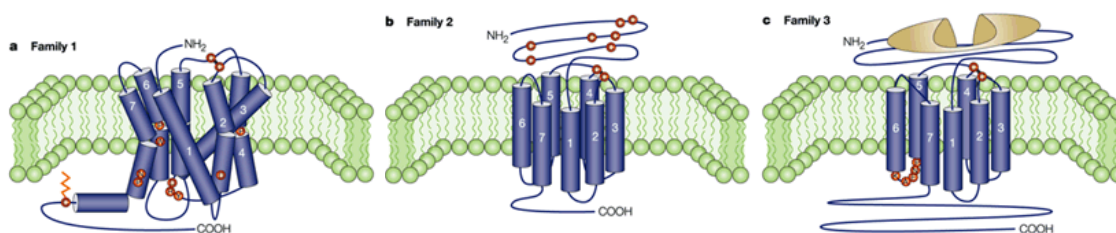


**Figure I3. Schematic representation of the principal GPCR families.** A) Family A, rhodopsin-like. B) Family B. C) Family C. The highly conserved residues are indicated with red circles (George *et al.*, 2002).

As mentioned above, families D and E are formed by few receptors, that include pheromone and yeast receptors, while the family F is composed of four cAMP receptors from *Dictyostelium discoideum* (Kolakowski, 1994).

The Kolakowski system is widely accepted. However, after a phylogenetic analysis of mammalian GPCR genome, Fredriksson and collaborators proposed a more accurate GPCR classification. This classification, named GRAFS, divides GPCR in five different groups, gathered by common evolutionary origin, and resulting in the glutamate, rhodopsin, adhesion, *frizzled*/taste and secretin families (Fredriksson *et al.*, 2003). The families Rhodopsin, Secretin and Glutamate of GRAFS classification are compatible with the Kolakowski system (families A, B and C respectively), although the other two families are not related to any family of Kolakowski system. The authors of this new classification defend that GPCRs arose from a

unique and common ancestor and through genetic duplication and other evolutionary mechanisms, reached the diversity and complexity that this superfamily presents nowadays.

#### I.1.4 GPCR ligands and constitutive activation

Upon ligand interaction, GPCR undergo conformational changes that enable the transition of an inactive state of the receptor towards an active state, creating a balance between these two states. Sometimes, GPCR can present a constitutive activation in absence of ligands due to the unbalance of this equilibrium towards the active state of the receptor (*Seifert and Wenzel-Seifert, 2002*). Consequently, the exchange of the GDP to GTP and the activation of the downstream G-protein machinery promote a basal activation of the signalling pathway without the interaction with a ligand (*Costa and Herz, 1989*).

GPCR can be found with multiple conformations, implying different responses in each situation. These conformations are stabilised by different ligands, being the most responsive conformation of the receptor promoted by the interaction with a full agonist. In turn, partial agonists show less efficiency in stabilising the most active conformation, thus promoting a lower exchange of GDP to GTP and a lower activation of the signalling pathway. Other ligands, known as inverse agonists, stabilise the inactive state of the receptor, gradually reducing the basal or constitutive activation of the GPCR. Finally, antagonists do not alter the equilibrium between active and inactive states, while blocking other ligands to interact with the receptor (Figure 4).

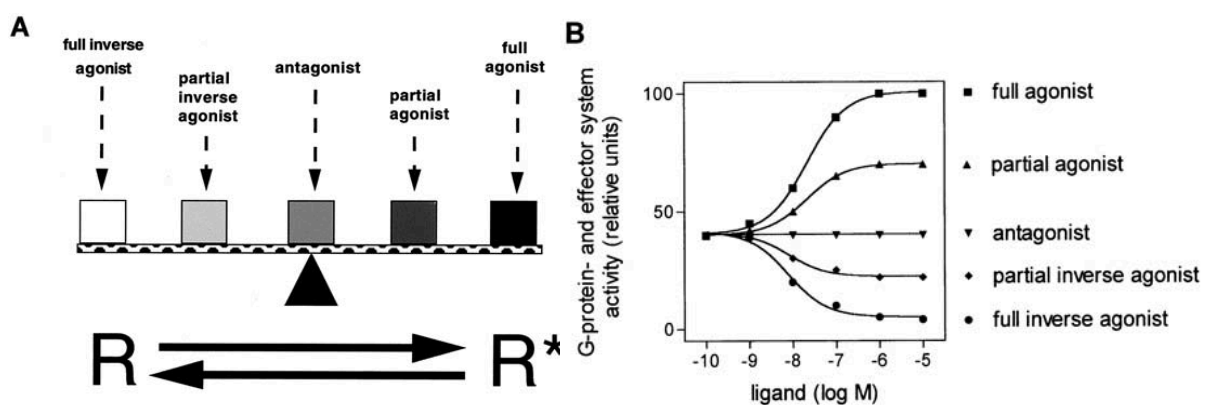


**Figure I4. GPCR activation according to the two-state model.** A) Two-state model assumes the isomerization of a receptor in the inactive R and active R\* states. B) Action of different ligands on GPCR constitutive activity (*Seifert and Wenzel-Seifert, 2002*).

Agonists and antagonists interact with the orthosteric site of the GPCR. This site is where the endogenous ligands physically interact with the receptor (*Neubig et al., 2003*). However, GPCR may contain multiple allosteric domains, where modulatory compounds can interact to regulate the response of the receptor to specific agonists. (*Bridges and Lindsley, 2008*;



## INTRODUCTION

*Leach and Gregory, 2017; May et al., 2007).*

Even though the agonist, inverse agonist and antagonist nomenclature for GPCR ligands had a great consensus, it should be revised as the concept of biased agonism is growing and having more adepts among pharmacologists. Hitherto, the fact that different ligands could stabilise a receptor in different conformations, promoting the activation of certain signalling pathways in detriment of others, was not taken into account (*Costa-Neto et al., 2016*). According to this new paradigm, a molecule could potentially be a full agonist for a given signalling pathway and at the same time, act as an antagonist when analysed in another (*van der Westhuizen et al., 2014*). Moreover, the biased agonism concept includes interactions affecting the subcellular localisation of the receptor (*Costa-Neto et al., 2016*) (Figure 5). Nowadays, the hot-topic within the biased agonism field relies on how the ligand efficiencies for a given signalling pathway should be calculated (*Kenakin, 2014; van der Westhuizen et al., 2014*).

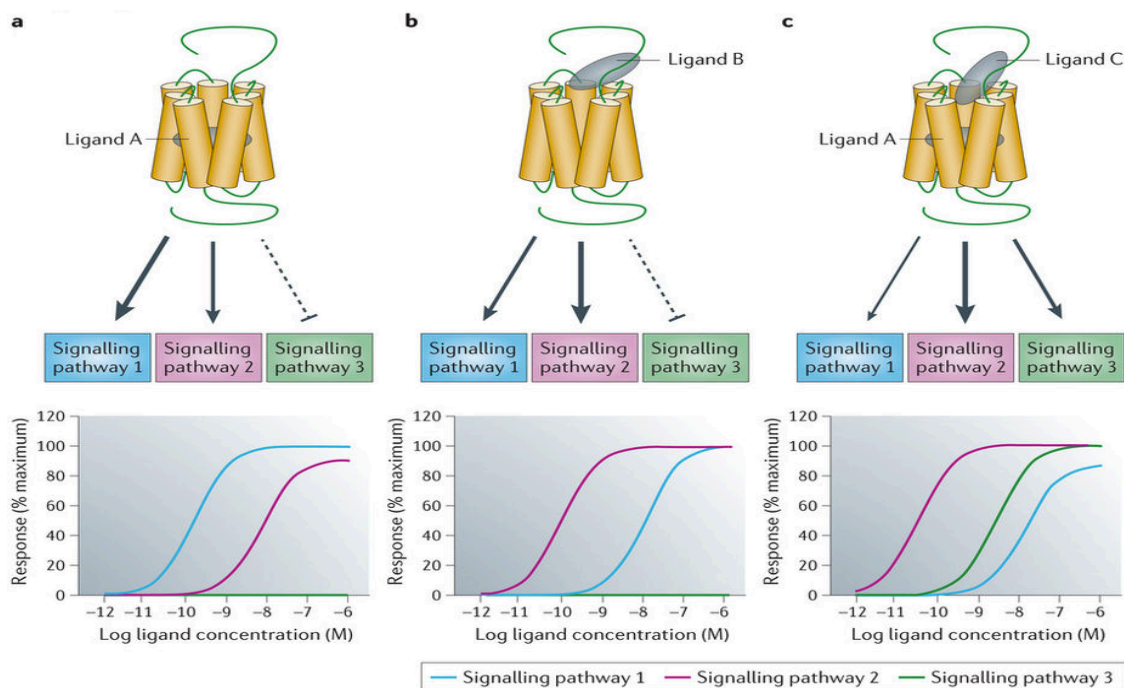


**Figure 15. Example of biased signalling showing the shift in efficiency of an agonist.** A) Ligand A presents a high efficiency and acts as full agonist for signalling pathway 1, lower potency towards signalling pathway 2, acting as partial agonist, and has no effects in pathway 3. B) Allosteric B ligand presents a higher potency for signalling pathway 2 than the pathway 1. C) Even with compound A bound at the orthosteric domain of the receptor, binding of the allosteric modulator C induces a biased signalling promotes the activation of signalling pathways 2 and 3, diminishing the activation of pathway 1 (*Wooten et al., 2013*).

### I.1.5 GPCR activation and signalling pathways

GPCR owe their name to the capacity to interact, modulate and regulate the function of heterotrimeric G-proteins constituted of  $\alpha$  (39-46 kDa),  $\beta$  (37 kDa) and  $\gamma$  (8 kDa) subunits. Upon ligand activation, conformational changes are transmitted through the receptor that

enables it to act as a guanine nucleotide exchange factor (GEF), provoking a substitution of a GDP to GTP in the  $\alpha$  subunit of the G-protein (*Syrovatkina et al., 2016*). It is accepted that the  $G_{\alpha}$ -GTP destabilises the G-protein heterotrimer, separating then the  $G_{\alpha}$  and the  $G_{\beta\gamma}$  subunits. Both  $G_{\alpha}$  and  $G_{\beta\gamma}$  subunits are signalling molecules able to interact with different effector proteins and activate or inhibit a wide range of second messengers. The signal terminates when the intrinsic GTPase activity of  $G_{\alpha}$  subunit hydrolyses the GTP producing GDP + phosphate (*Bourne et al., 1991*). The hydrolysis of the GTP catalysed by the  $G_{\alpha}$  subunit is slow, but it can be accelerated with the interaction of RGS proteins (*Syrovatkina et al., 2016*). The  $G_{\beta\gamma}$  activity ends when the subunits interact again with the  $G_{\alpha}$ -GDP subunit.

Sixteen different genes code for twenty-one  $G_{\alpha}$  subunits, while six different  $G_{\beta}$  subunits are coded by five genes, and there are nine  $G_{\gamma}$  subunits (*Downes and Gautam, 1999*). In mammals, the different  $G_{\alpha}$  subunits were classified in four groups according to their sequence homology and the signal cascade they activate (*Milligan and Kostenis, 2006*) (Figure 4).  $G_{\alpha_s}$  and  $G_{\alpha_i}$  families regulate the effector protein adenylyl cyclase (AC) activity. While the first is in charge to stimulate the AC, the latter inhibits its catalytic activity. The AC conducts the conversion of ATP to cAMP, which is one of the most relevant second messengers. cAMP is able to activate the Ser/Thr protein kinase A (PKA), which in turn phosphorylates different proteins, from ion channels and receptors to transcriptional factors that modulate and regulate cell function. On the other hand,  $G_{\alpha_{q/11}}$  activates Phospholipase C  $\beta$  (PLC $\beta$ ) that hydrolyses membrane phosphoinositol, generating the second messengers inositol-1,4,5 triphosphate (IP<sub>3</sub>) and diacylglycerol (DAG). DAG activates Ser/Thr protein kinase C (PKC), while IP<sub>3</sub> leads to increases in the calcium intracellular levels, another significant second messenger. Finally,  $G_{\alpha_{12/13}}$  families activate Rho proteins.

Many GPCR responses are not mediated by conventional second messengers, but are result of the integration of different signalling networks and cascades, among which we can find MAPK or JNK Ser/Thr kinases. It has been described that MAPK activation involve a *Brodetella Pertussis* toxin sensitive G-protein ( $G_{\alpha_i}$ ), being strongly dependent of  $G_{\beta\gamma}$  complexes (*Faure et al., 1994; Koch et al., 1994; McKay and Morrison, 2007*). Moreover, it was deduced that in the absence of tyrosine kinase receptors (RTK) ligands, GPCR activation could stimulate



INTRODUCTION

RTK, generating mitogenic signals in a process called transactivation (Figure 6). Upon transactivation, RTK initiates its own the signalling cascade, via Ras, Raf, MEK and ERK 1/2 pathway. The process is triggered by Sos recruitment towards the membrane by  $G_{\beta\gamma}$  subunits. Sos promotes the Ras exchange of GDP to GTP, being this last protein the link between GPCR activation and ERK phosphorylation (Chaplin et al., 2017; Marinissen and Gutkind, 2001; Paradis et al., 2015). Other pathways can activate Ras in a transactivation-independent manner, being dependent on  $G\alpha_q$ -mediated variation in intracellular calcium concentration.

Phosphorylation of two serine and threonine residues separated by just one amino acid is required for ERK1/2 activation. The highly specialised enzyme MEK is the only enzyme that can phosphorylate these two residues, being considered a rate-limiting step in ERK activation. Ras-independent mechanisms can also activate MEK. These mechanisms include B-Raf, which is a kinase activated by Rap, which in turn is under the control of PKA and  $G\alpha_s$ -GPCR. Activated ERK1/2 could be transferred to the nucleus where regulates, via phosphorylation, other kinases and transcription factors (Davis, 1995).

Recently, evidence of heterotrimeric G-proteins independent GPCR signalling, as well as RTK-transactivation independent mechanisms have been revealed (Luttrell and Lejkowitz, 2002; Ranjan et al., 2016). These signalling implicate direct union of Src and/or  $\beta$ -arrestins to the receptors (DeWire et al., 2008).

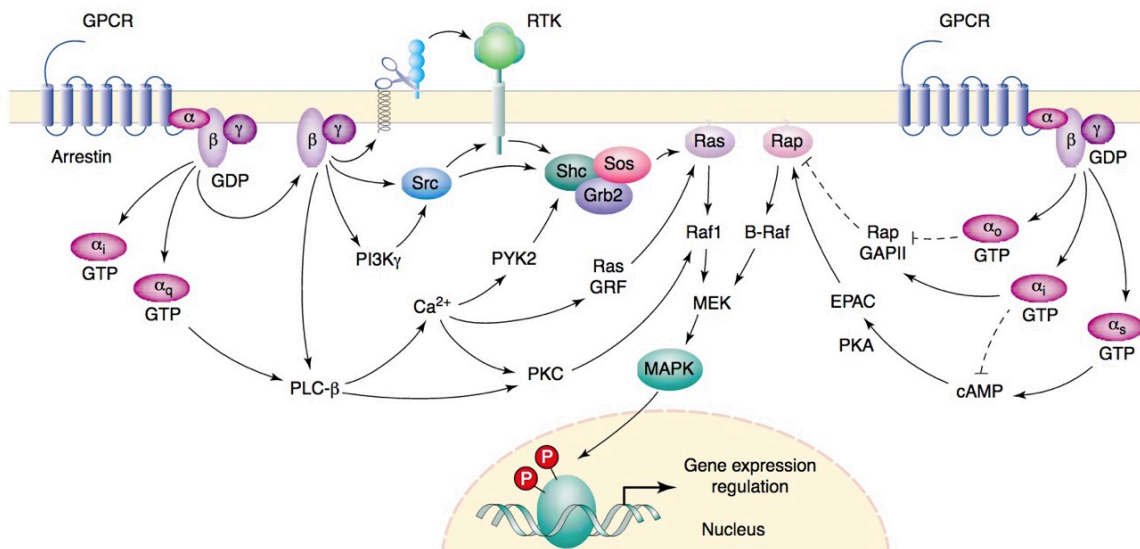


Figure I6. Representation of some GPCR signals connecting with MAPK activation (Marinissen and Gutkind, 2001).

### I.1.6 Regulation of GPCR activity

Exposure of GPCR to ligands often results in a rapid attenuation of receptor responsiveness, impeding overstimulation of the signalling pathway and possible side effects of a persistent response. The process, named desensitisation, could be done in three different mechanisms: i) receptor uncoupling the G-protein due to receptor phosphorylation (*Ferguson, 2001; Golan et al., 2009; Hausdorff et al., 1989*); ii) receptor internalisation to intracellular compartments (*Ferguson, 2001; Moore et al., 2007*) and iii) down-regulation of the number of receptors in the cell. The time-span of these processes range from seconds in the case of phosphorylation, to minutes for internalisation, and hours in the case of the receptor down-regulation. The achievement of the latter mechanism is through the reduction of mRNA and protein synthesis, as well as degrading the existing receptors in lysosomes (*Jockers et al., 1999; Pak et al., 1999*). Moreover, the desensitisation could be complete, which implies the abolition of the receptor signalling, as observed in olfactory systems, or result in an attenuation of the maximal response of the receptor, which is the case for  $\beta_2$  adrenergic receptor (*Thomsen et al., 2016*).

Regarding the first desensitisation mechanism mentioned, phosphorylation of serine and threonine residues of the ICL and the C-terminal domains of GPCR promote the uncoupling of the G-protein. This rapid covalent modification is done by second messenger-activated kinases (kinases A and C) and GRK (*Hilger et al., 2018; Krupnick and Benovic, 1998; Lefkowitz et al., 1993*). Second messenger-activated kinases phosphorylate ligand-activated GPCR, but also indiscriminately non ligand-exposed GPCR as well. In contrast, GRK family just phosphorylates agonist-activated receptors, enabling the binding of  $\beta$ -arrestins, which are cytosolic proteins that uncouple G-proteins (*Kang et al., 2014; Kelly et al., 2008; Ranjan et al., 2016*).

In the internalisation process,  $\beta$ -arrestins enables the interaction of GRK-phosphorylated GPCR with clathrin-mediated endocytosis (*Ranjan et al., 2016*) (Figure 7). Upon activation of the receptor,  $\beta$ -arrestins are translocated towards the cell membrane, interacting with GPCR and blocking the receptor capacity to interact with G-proteins (*Kang et al., 2015*) and engaging the clathrin-mediated endocytosis; altogether reducing the signalling capacity of the receptor (*Kang et al., 2014*). However, recent works suggest the capacity of family B of GPCR to interact simultaneously with G-proteins and  $\beta$ -arrestins (*Wehbi et al., 2013*), then enabling the receptor to continually promote a signal throughout all the internalisation process (*Thomsen et al., 2016*).



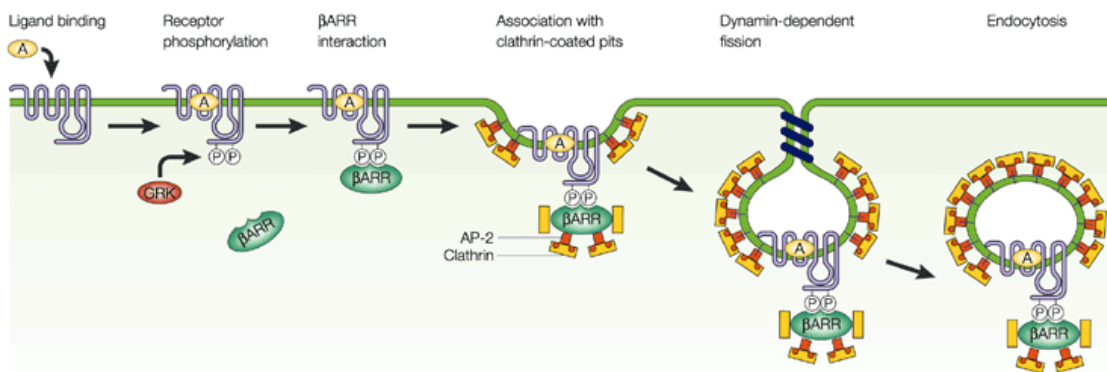


**Figure 17. GPCR desensitisation and recycling mechanisms** (Pierce and Lefkowitz, 2001).

$\beta$ -arrestins- and clathrin-independent internalisation processes of GPCR exist. This mechanism involves the receptors found in cholesterol-rich plasma membrane domains named caveolae (Navarro *et al.*, 2014a; Parton and del Pozo, 2013). These caveolae could constitute another ligand-mediated internalisation mechanism (Kong *et al.*, 2007; Navarro *et al.*, 2014a; Wu *et al.*, 2008). Moreover, caveolae are domains that enable GPCR-signalling proteins specific interactions, acting as signalling domains (Ostrom and Insel, 2004; Villar *et al.*, 2016).

Finally, desensitisation and internalisation processes to internal compartments enable GPCR to signal through G-protein independent pathways (Daaka *et al.*, 1998; Lefkowitz, 1998).  $\beta$ -arrestins do not act only in the molecular switch required for GPCR desensitisation and internalisation, but also function as scaffolds to transduce and compartmentalise the alternative signals. In fact,  $\beta$ -arrestins have the ability to interact with endocytic and signalling proteins like c-Src (Luttrell, 2005), MAPK and Raf (DeFea *et al.*, 2000). The endocytosis, indeed, could promote the de-phosphorylation of the receptor by phosphatases, either triggering the recycling of the GPCR back to the cell surface or leading the receptor towards the degradation pathway (Métayé *et al.*, 2005).

Besides the regulation of GPCR due to the internalisation and desensitisation processes, GPCR topology enables the heptaspanning-membrane receptors to interact with a wide range of proteins. Characteristics like subcellular localisation, conformation or signalling pathways are GPCR properties liable to be modified and regulated upon protein-protein interactions. Moreover, these interactions could result in complex structures able to promote and integrate functions (J Gingell *et al.*, 2016; Kenakin and Miller, 2010). Cytoskeletal proteins, signalling proteins, ion channels and other receptors are partners of GPCR in these supramolecular structures (Franco *et al.*, 2005).

The interactions could involve extracellular domains of the receptor. When the length of ECLs is short, the extracellular-GPCR interactions target the receptor N-terminal

sequences. Growing evidence show that these extracellular interactions modify the pharmacological properties of the receptor. An example are the receptor activity-modifying proteins (RAMPs) (*J Gingell et al., 2016*). To date, three RAMPs have been discovered (*Sexton et al., 2009*), that affect the signalling and the pharmacology of GPCR like CRF<sub>1</sub>R (*Wootten et al., 2013*) or the glucagon (*Weston et al., 2015*) receptors.

At the cytoplasmic side, the large C-terminal domain and the 3<sup>rd</sup> ICL are the main targets for cytosolic proteins involved in signalling, subcellular localisation or cellular trafficking. The cytosolic protein calmodulin (CaM) provides two examples. Due to a short peptide, this calcium sensor protein is able to interact with the intracellular domains of GPCR allowing a calcium-dependent receptor signalling. In the case of the CaM- A<sub>2</sub>A adenosine receptor, the C-terminal domain of the receptor is involved, while for the interaction with the dopamine D<sub>2</sub> receptor, the 3<sup>rd</sup> intracellular loop of the GPCR is involved (*Bofill-Cardona et al., 2000; Navarro et al., 2009*).

Finally, many GPCR oligomers have been described at plasma membrane level (*Franco et al., 2016; George et al., 2002; Herrick-Davis et al., 2015; Moreno et al., 2011, 2017; Navarro et al., 2008, 2010a*). Nowadays, the capacity to form homodimers, heterodimers and oligomers of higher order is accepted as a common trait in GPCR biology (*Bonaventura et al., 2015; Bouvier, 2001; Cordoní et al., 2015; Ferré et al., 2009; Franco et al., 2003, 2016; Guitart et al., 2014; Navarro et al., 2013*). Oligomerization could modify the functional properties of the receptor, as well as generating new ones. These mechanisms could explain the diverse pharmacology and complex signalling of neurotransmitter/neuroregulator receptors.

## I.2 GPCR OLIGOMERIZATION

### I.2.1 GPCR Interaction

Traditionally, ligand-binding and signal-transduction mechanisms of GPCR were based on the presumption that these receptors were monomers that acted with a 1:1 stoichiometry with G-protein. However, since the nineties, many studies have demonstrated GPCR oligomerization, being relevant for their regulation.

Indirect pharmacological evidence, like complex binding competition results, were interpreted for the scientific community as proofs of a cooperativity only explained by the formation of dimers or oligomer complexes (*Franco et al., 1996; Wreggett and Wells, 1995*). Maggio and collaborators were able to describe the dimerization of M<sub>3</sub> muscarinic receptors



## INTRODUCTION

and the  $\alpha_2$ -adrenergic receptors by the use of chimeras. These chimeras, consisted in the first five transmembrane domains of one receptor and the last two of the other, and were able to perform co-immunoprecipitation and complementation studies when transfected together. Moreover, independently transfected chimeras were not able to bind ligands or to signal, but when co-transfected, a rescue in the ligand binding and signal-transduction was obtained (Maggio *et al.*, 1993). Hence, GPCR oligomerization is not limited to the physical interaction of identical receptors, known as homomerization, but it also embraces the interaction of different receptors, named heteromerization. Traditionally, dimers, which are the result of the union of two monomers, have been considered the simplest functional oligomeric units. Nowadays, crystal structures and signal-particle tracking and imaging breakthroughs, have provided powerful and more precise tools to unravel oligomer's stoichiometry (Kasai and Kusumi, 2014). In this regard, new oligomeric models have been proposed, and the one involving a tetramer is the most reliable to date (Cordomi *et al.*, 2015).

Oligomerization of G-protein coupled receptors might partially explain the wide variety and the high diversity of the brain functions. Additionally, this phenomenon is important for some GPCR functions like biogenesis (Ferré, 2010; Kim *et al.*, 2009). In some cases, dimerization is essential for the functionality of the receptor due to the conformation changes provoked by the dimerization process, which enables ligand binding at the receptor (Zhang *et al.*, 2014).

A higher level of organization, formed by GPCR oligomers and other proteins able to modulate the receptors' activity, has been described. These supramolecular complexes interact through and across the membrane in horizontal and vertical interactions, being distributed and rearranged in clusters when activated by hormones or neurotransmitters. In these clusters, receptors could be then directly regulated by other receptors, enzymes or proteins that physically interact with them, but also being indirectly modulated by other non-physically interacting cluster proteins, providing a higher regulation of GPCR function (Franco *et al.*, 2003; Thomsen *et al.*, 2016).

The new challenges in G-protein receptor oligomers field lie in deciphering the functional role of these complexes and in understanding the formation and destruction of the homo-heterodimers, how are these processes regulated, and in identifying new interacting-partners.

Noteworthy, GPCR oligomerization introduces a grievous concern. Nowadays, most of the drugs against GPCR have been designed under the premise of a monomeric function of the receptors (Franco *et al.*, 2013). The discovery of homodimerization and heterodimerization

casts doubts about the efficiency of the existing drugs and the need of a reevaluation taking into account the possible interactions of the targeted receptors.

### **I.2.2 Architecture of GPCR heteromers**

To explain the GPCR dimerization or oligomerization processes, two different considerations should be taken. In case of direct interactions, a physical contact between the two receptors is required, while in indirect interactions; some bridge-proteins, like cytosolic proteins, are needed to fulfil the oligomerization process.

Regarding to the latter, the GPCR-intracellular domains are responsible of the interaction with a wide range of cytosolic proteins. Some of these proteins have been proposed as scaffolding proteins that contribute to create a macromolecular organization, enabling the interaction of different receptors and also interactions between GPCR and signalling proteins that modulate the receptor function (*Magalbaes et al., 2012; Walther and Ferguson, 2015*).

In the case of direct interactions, diverse theories have been proposed. On one hand, some researchers suggested that the formation of GPCR oligomers took place in the endoplasmic reticulum of the cell. In this case, oligomers would not necessarily be modulated ligand, leaving the oligomeric regulation of the GPCRs up just to ontogeny and degradation processes (*Bouvier, 2001; Van Craenenbroeck et al., 2014*). However, Bouvier and collaborators already suggested that given the structural complexity of GPCR superfamily, think about just a single interaction mechanism would not be recommended (*Bouvier, 2001*). On the other hand, some oligomer-formation theories defend the presence of the receptor at plasma membrane, where depending of the cell conditions, the ligand binding, post-traductional modifications or the plasma membrane region they are located, are going to be found in equilibrated monomeric or oligomeric forms (*Baltoumas et al., 2016*). Baltoumas and collaborators hypothesised about GPCR dimerization could happen due to receptor accumulation in cholesterol-rich plasma membrane hot spots. In the same line and defending the occurrence of receptor dimerization at the cell surface, some authors defend that oligomerization formation is due to hydrophobic disarrangements between the width of the hydrophobic plasma membrane and the length of the hydrophobic part of the receptor's transmembrane domains. Then, if the hydrophobic part of the protein surpasses the width of the plasma membrane, oligomerization processes reduce the exposure of the receptor hydrophobic domains (*Gabbauer and Böckmann, 2016*). Finally, direct interactions between transmembrane domains or intracellular domains could be mediated by covalent interactions like disulphide



bonds, or non-covalent interactions, due to electrostatic and hydrophobic forces (Figure 8).

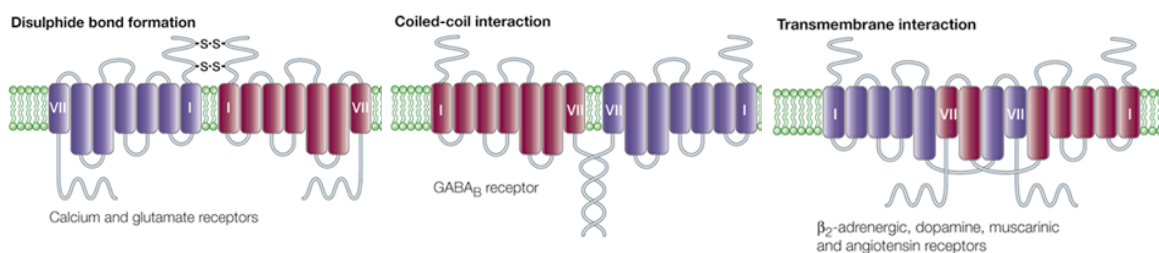


**Figure I8. Molecular determinants of GPCR dimerization** (Bouvier *et al.*, 2001).

Different type of intermolecular interactions are involved in the formation of GPCR homo- and heterodimers. In the family C of GPCR, the large and cysteine residues-containing N-terminus domain could contribute to the dimerization of the receptors by establishment of disulphide bonds with the cysteine residues of the partner receptor or protomer (Miura *et al.*, 2005; Romano *et al.*, 1996, 2001). In some family A receptors such angiotensin II receptor (Miura *et al.*, 2005), the serotonin 5-HT<sub>4</sub>R receptor (Berthouze *et al.*, 2007) or the acetylcholine M<sub>3</sub> muscarinic receptor (Hu *et al.*, 2012) disulphide-bonds interactions also take place in the N-terminus domain. In another type of interaction the C-terminus domain is fundamental, as presented in the homodimerization of the  $\beta_2$ -adrenergic receptor (Salahpour *et al.*, 2004), or in the coiled-coil of the GABA<sub>B1</sub> and GABA<sub>B2</sub> dimers (Margeta-Mitrovic *et al.*, 2000). Finally, direct interactions could be mediated by ionic or hydrophobic interactions between the extracellular, intracellular and transmembrane domains of the receptors. The implication of transmembrane domains has been proposed for dopamine D<sub>2</sub> receptors homodimerization (Guo *et al.*, 2008; Ng *et al.*, 1996), for  $\mu$ -opioid receptors (Manglik *et al.*, 2012), the  $\beta_1$ -adrenergic (Huang *et al.*, 2013) and the  $\beta_2$ -adrenergic receptors (Parmar *et al.*, 2017). However, all the interaction mechanisms proposed indicate that multiple domains could be implicated in the stabilisation and ensemble of GPCR dimers.

Nowadays, structure and crystallisation advances combined with the computational modelling have allowed three-dimensional models that explain the G-protein coupled receptor dimerization. GPCR crystal structure analyses have revealed that monomers mainly interact through their transmembrane domains, in head-to-head structures between the two receptors. The domains taking part of these interactions are the TM1, TM4, TM4/5 or TM5/6 of each receptor (Gonzalez *et al.*, 2014). Thus, in the case of TM1 interactions, the TM1 of one receptor will face the TM1 of the other partner of the dimer. Likewise, in the TM4 interactions, the fourth transmembrane domain of a receptor will face the fourth transmembrane domain of the partner, and for TM4/5 or TM5/6 interactions, the TM4 of a

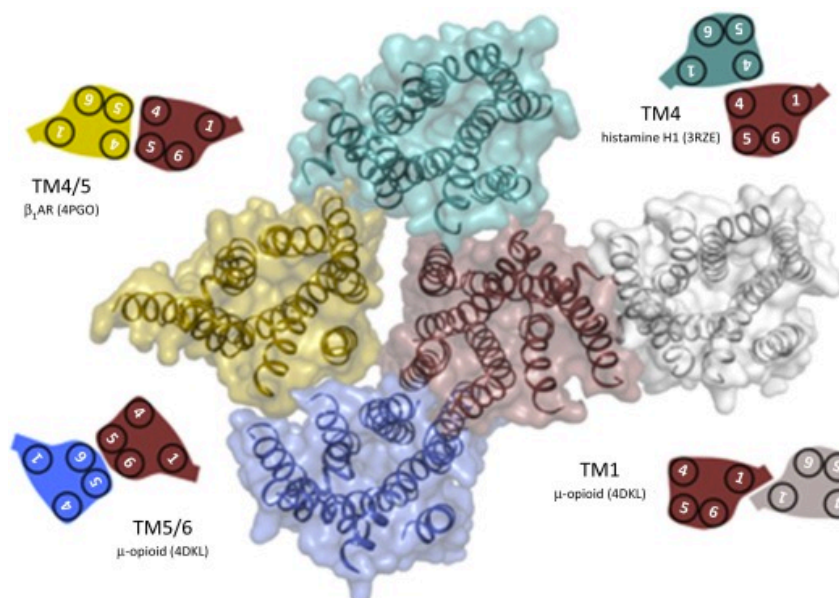


**Figure 19. Three-dimensional model of GPCR of homodimer formation.** Extracellular view of the overlapped receptor pairs of the central red receptor. The regions involved in the dimer formation are: TM1 (white), TM4 (grey), TM4/5 (yellow) or TM5/6 (blue) (Cordomi *et al.*, 2015).

receptor will interact with the TM5 of the other GPCR and vice versa, being two transmembrane domains of each receptor involved in the interactions. Similarly, in TM5/6 interactions, both TM5 and TM6 of both interacting receptors are involved in the architecture arrangements of the dimer. It seems that the interactions between TM1 and TM4/5 are the most appearing interactions in crystal structures, therefore, being the most plausible in dimeric models (González *et al.*, 2014) (Figure 9). However, when the structure of the G protein is taken into account, very few possible structures allow GPCR operation. In this regard, the dimeric model involving TM5/6 domains would impede the receptor conformational changes that trigger G-protein signalling, suggesting that dimers involving these transmembrane domains would not conform functional units (Cordomi *et al.*, 2015). Similarly, in the TM4 interactions and according to the stoichiometric accepted model, the coupling of the  $\alpha$  subunit would not be compatible, due to the fact that the G-protein subunit would collide with the partner receptor of the dimer (Cordomi *et al.*, 2015). These new models have raised scepticism in the previous oligomer stoichiometric beliefs, and nowadays, is accepted within the scientific community that the stoichiometry of GPCR dimers is 2:1 (receptor: G-protein) (Jastrzebska *et al.*, 2013). Moreover, many authors defend that the minimum GPCR functional unit would be formed for two equal receptors and a G-protein (Banères and Parello, 2003; Franco *et al.*, 2013; Jastrzebska *et al.*, 2013).

The dimeric models proposed by Cordomi and collaborators explain, indeed, how would receptors interact in order to form higher order oligomers. The most simple structures





would be the head-to-head interaction of two dimers, generating a tetramer (Cordomi *et al.*, 2015). According to the 2:1 receptor/G-protein stoichiometry, the tetramer structure would potentially admit two G-proteins, both in the inner and outer protomers of the complex, allowing the in-in, in-out and out-out combinations (Cordomi *et al.*, 2015).

### I.2.3 Techniques used to identify GPCR oligomers

One of the first evidence of GPCR dimerization was obtained using pharmacologic assays. Complex binding competition curves in radioligand binding assays suggested a possible oligomerization of GPCR. Cooperativity, which is a change in the intrinsic properties of a receptor upon interaction with a ligand, and in the case of GPCR is mostly negative, could be explained by ligand binding to a receptor forming homodimers, thus upon ligand binding to a protomer of the dimer, the regulation of the affinity characteristics of the partner receptor are triggered (Franco *et al.*, 1996; Hirschberg and Schimerlik, 1994; Limbird *et al.*, 1975; Mattera *et al.*, 1985; Wreggett and Wells, 1995). In addition, some results based on radioligand binding assays in membrane preparations expressing two investigated receptors, could be more easily explained if the receptors were interacting. In these cell membrane preparations, where the downstream signalling machinery of receptors was not present, the modulation of ligand-binding capacity of a receptor can only be given by conformational changes in the receptors upon direct or indirect receptor interaction (Franco *et al.*, 2007, 2008). In many cases, these interactions have been detected in native tissue, being interpreted as an evidence of *in vivo* receptor heteromers occurrence (González-Maeso *et al.*, 2008; Marcellino *et al.*, 2008a).

Another biochemical assay to study GPCR dimerization is co-immunoprecipitation. In 1996, Hebert and collaborators used this technique to investigate the dimerization of  $\beta_2$ -adrenergic receptor (Hebert *et al.*, 1996). Since then, the glutamate metabotropic mGlu<sub>5</sub>R (Romano *et al.*, 1996), the  $\delta$ -opioid (Cvejić and Devi, 1997) or the serotonin 5-HT<sub>2C</sub> (Herrick-Davis *et al.*, 2004) receptor dimers have been described using similar strategies. In addition, co-immunoprecipitation assays have been useful to investigate heterodimerization processes. The interaction of GABA<sub>B1</sub> and GABA<sub>B2</sub> receptors (Jones *et al.*, 1998; Kaupmann *et al.*, 1998) or the interaction of  $\delta$  and  $\kappa$  opioid receptors (Jordan and Devi, 1999) were demonstrated with co-immunoprecipitation analyses. Likewise, interaction of receptors for different neurotransmitters like adenosine A<sub>1</sub>R and dopamine D<sub>1</sub>R (Ginés *et al.*, 2000), the adenosine A<sub>2A</sub>R and metabotropic glutamate mGlu<sub>5</sub> (Ferré *et al.*, 2002) or the cannabinoid CB<sub>1</sub> and dopamine D<sub>2</sub> (Kearn *et al.*, 2005) heterodimers were described with this technique.

Despite its historical relevance in detecting interacting proteins, co-immunoprecipitation assays have some drawbacks, specially in the case of membrane proteins, that must be solubilised with detergents. Highly hydrophobic proteins like GPCR could form aggregates upon incomplete solubilisation that lead to false positive results. Therefore, the general acceptance of these complexes awaited a direct confirmation of GPCR dimerization by the use of biophysical methods based on light resonance energy transfer.

In 1948, Theodor Förster formulated the theory of resonance energy transfer that postulated the phenomenon of a non-radioactive energy transfer from a chromophore in excited state (donor) to a close molecule that absorbs it (acceptor). Based in this concept, resonance energy transfer techniques could be performed in living cells expressing fusion proteins of the GPCR fused to donor and acceptor proteins. If both donor and acceptor proteins are fluorescent molecules, we will refer to this technique as Förster Resonance Energy Transfer (FRET) technique, meanwhile if the donor is bioluminescent and the acceptor is fluorescent, we will refer to it as Bioluminescent Resonance Energy Transfer (BRET).

Two requisites must be fulfilled in order to achieve energy transfer. The first one is that the emission spectrum of the donor and the excitation spectrum of the acceptor must be overlapped, allowing part of the emitted energy from the donor excite the fluorescent molecule of the acceptor protein. The other requisite is the close proximity of donor and acceptor in space ( $<100 \text{ \AA}$  or 10 nm). The efficiency of energy transfer decreases with the sixth potency of distance (*Sheng and Hoogenraad, 2007; Stryer, 1978*).

FRET assays use different mutated variants of the Green Fluorescent Protein (GFP). Mutations of a given donor or acceptor have led to proteins with different excitation and emission spectrum. The most common fluorescent proteins used are the GFP<sup>2</sup>, which is excited at 400 nm and emits at 510 nm, and the Yellow Fluorescent Protein (YFP), which is excited at 485 nm and emits at 530 nm. When these proteins are fused to the studied receptors and co-expressed at the same time, and in case that the distance between GPCRs is less than 10 nm, an energy transfer between the two receptors will take place, and the YFP-specific emission at 530 nm will be measured (*Gandía et al., 2008; Navarro et al., 2010a; Pflieger and Eidne, 2005*) (Figure 10).

The BRET approach takes advantage of the luminescence phenomenon occurring naturally in marine animals such as jellyfishes like *Aequorea victoria* or the sea pansy *Renilla reniformis*. From this last one, Renilla luciferase (*Rluc*) was isolated. This protein can oxidize a substrate to produce light. The substrate Coelenterazine H, when catalytically oxidised, emits



## INTRODUCTION

at 480 nm, which allows the excitation of the YFP. In turn, the substrate Deep Blue C emits at 400 nm, enabling the excitation of the GFP<sup>2</sup>. According to the fluorescent proteins and substrate used, two variants of BRET exist. When YFP and the substrate coelenterazine H are used, it is named BRET<sub>1</sub>, and when the chosen acceptor and the substrate are GFP<sup>2</sup> and Deep Blue C respectively, it is named BRET<sub>2</sub> (Figure 11).

The use of resonance energy transfer (RET) techniques has served to reveal several protein complexes. Many researchers took advantage of the phenomenon to study the

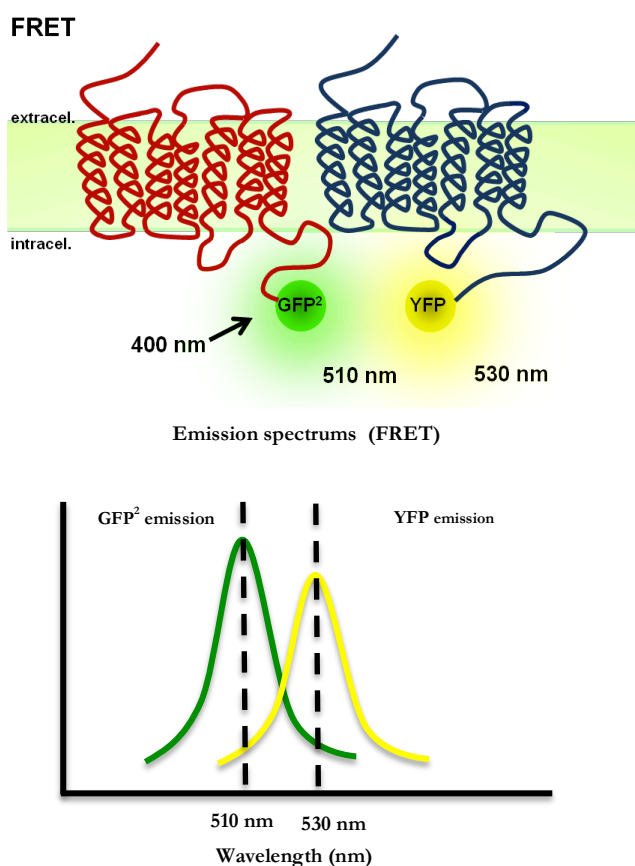


**Figure I10.** Schematic representation of FRET assay with the corresponding fluorescent protein wavelengths.

homodimerization processes of adenosine A<sub>2A</sub> receptors (Canals *et al.*, 2004), the  $\delta$ -opioid receptor (Johnston *et al.*, 2011), or the  $\beta_2$ -adrenergic (Parmar *et al.*, 2017) receptor. At the same time, an increasing number of heteromers have been identified or confirmed using these techniques, e.g. the adenosine A<sub>1</sub>R and A<sub>2A</sub>R heterodimers (Ciruela *et al.*, 2006), the dopamine D<sub>1</sub>R and D<sub>3</sub>R dimers (Marcellino *et al.*, 2008a), the dopamine D<sub>1</sub> and D<sub>2</sub> receptor heterodimers (Pei *et al.*, 2010), cannabinoid CB<sub>1</sub>R and CB<sub>2</sub>R heterodimers (Callén *et al.*, 2012), dopamine D<sub>1</sub> and CRF<sub>2</sub> receptor heterodimer (Fuenzalida *et al.*, 2014) or the A<sub>2A</sub>-D<sub>2</sub> receptor heterodimer (Bonaventura *et al.*, 2015).

Despite the efficiency of these techniques in address GPCR dimerization, new strategies based on the RET have been developed lately, including photobleaching FRET or time-resolved FRET. In the latter, the use of fluorochromes with longer life-spans enable acceptor excitations without a persistent and external excitation of the donor, obtaining the energy transfer between the two receptors but increasing the signal-to-noise ratio (Pfleger and Eidne, 2005). With these strategies, Vilardaga and collaborators were able to describe a cross-talk between  $\alpha_2$ -adrenergic and  $\mu$ -opioid receptors, where morphine binding to  $\mu$ -opioid receptor entails a conformational change that

impedes the signalling of the norepinephrine through the  $\alpha_2$ -adrenergic receptor (Vilardaga *et al.*, 2008).

The techniques described above enable the detection of two interacting proteins. However, the CNS complexity required the development of more advanced techniques. In this regard, Carriba and collaborators developed the sequential resonance energy transfer (SRET). This approach takes advantage of BRET and FRET techniques to perform a BRET<sub>2</sub> assay, where *Rluc* capable to excite a GFP<sup>2</sup> protein, and use this excited GFP<sup>2</sup> as a donor to consecutively excite a YFP, therefore sequentially performing a BRET<sub>2</sub> and a FRET. The principal advantage of SRET is that enables the study of

trimeric complexes (Carriba *et al.*, 2008). The discovery of new mutations and development of new fluorescent proteins has increased the SRET possibilities, allowing a sequential BRET<sub>1</sub> and a FRET between the YFP and a DsRed protein (that is excited at 530 nm and emits at 590 nm), or directly two sequential FRET, the first between GFP<sup>2</sup> and YFP, and the latter between YFP and DsRed.

In turn, molecular complementation strategies, like the bimolecular fluorescent complementation (BiFC) or the bimolecular luminescence complementation (BiLC), are based

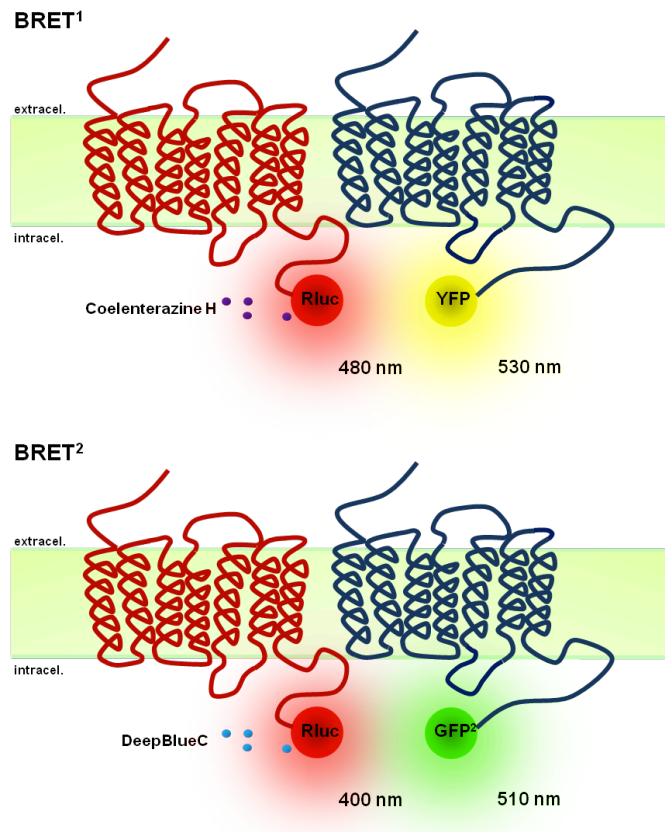


Figure I11. Schematic representation of BRET<sup>1</sup> and BRET<sup>2</sup> techniques.

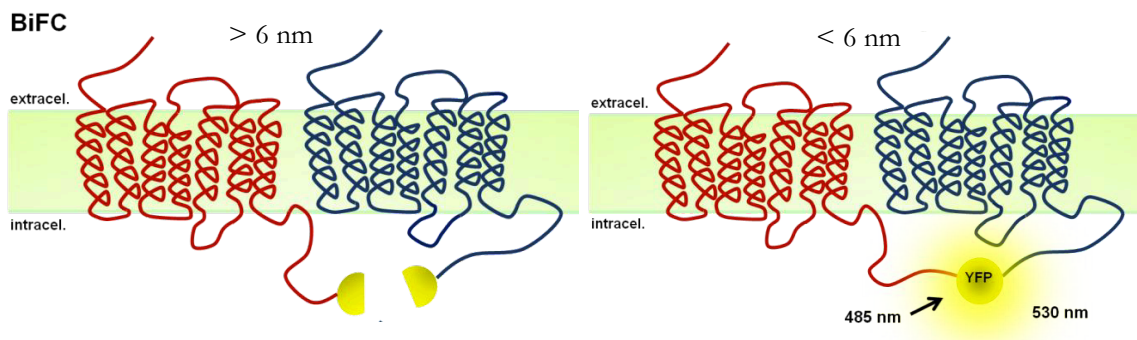


Figure I12. Schematic representation of Bimolecular Fluorescence Complementation technique



## INTRODUCTION

on the reconstitution of the fluorescent sYFP or Venus (nYFP and cYFP) or the bioluminescent RLuc8 protein. These proteins are constituted by two different fragments, that upon interaction, can generate fluorescence in the case of sYFP or Venus, or have enzymatic activity in the case of RLuc8 (Hu *et al.*, 2002; Paulmurugan and Gambhir, 2003). The reconstitution of the protein fragments just can happen if the distance between them is less than 6 nm (Figure 12). Despite BiFC and BiLC enable the detection of dimeric structures, the study of tetramer structures is possible upon the simultaneously use of BiFC and BiLC techniques (Bonaventura *et al.*, 2015).

Nowadays, technical advances have also reached the microscopy field. Such breakthroughs have brought along the development of the Total Internal Reflection Fluorescence (TIRF) technique. This microscopy technique takes advantage of the optical properties of light for, upon employing the appropriate settings, illuminate and obtain information of thin focal planes (Poulter *et al.*, 2015). Depending on the settings utilised, focal planes of <200 nm width can be observed with this microscope. This provides a better signal-to-noise ratio that enables the study of membrane protein diffusion or focal adhesion phenomenon, among others. In this line, several studies have put their focus on study the GPCR properties (Delgado-Peraza *et al.*, 2016; Gidon *et al.*, 2016). Noteworthy, TIRF techniques can be applied to heteromer studies providing stoichiometry details of the receptor oligomers and the diffusion properties of the oligomers. Upon employing fluorescently labelled GPCR, and photobleaching the fluorescent particles of a given focal plane, it is possible to infer how many the fluorescent particles are present in a given cluster of protomers. After the utilisation of proper algorithms the stoichiometry of the heteromer could be known (Navarro *et al.*, 2016a). Interestingly, it is also possible to record the trajectories of the receptors change and whether they change upon heteromerization. For instance, it may occur that a given receptor with Brownian diffusion in the cell surface gets a confined movement upon heteromer formation. These relevant aspects of GPCR biology could be addressed with TIRF microscopy (Navarro *et al.*, 2016a).

The major drawback of the techniques presented above is that are used in heterologous expression systems. Hence, new strategies are needed to study protein-protein interactions in native tissue. In this regard, the most relevant approach available is the *in situ* Proximity Ligation Assay (PLA), developed by Fredriksson and collaborators. This technique requires primary antibodies directed against the proteins of interest. Once the antibodies are bind to their targets, two PLA probes are added. These PLA probes are secondary antibodies that contain an oligonucleotide. With the use of a ligase, the nucleotides linked to the

antibodies can form a circular DNA chain that, thanks to a polymerase and labelled nucleotides, can be amplified (*Fredriksson et al., 2002*). The resulting punctuation of the protein-protein interactions could be analysed, then, with the use of a fluorescence microscope (Figure 13). This may occur if the two receptors are very close; in fact, if the positive red punctuation of a positive PLA is obtained, it is assumed that the two receptors are directly interacting.

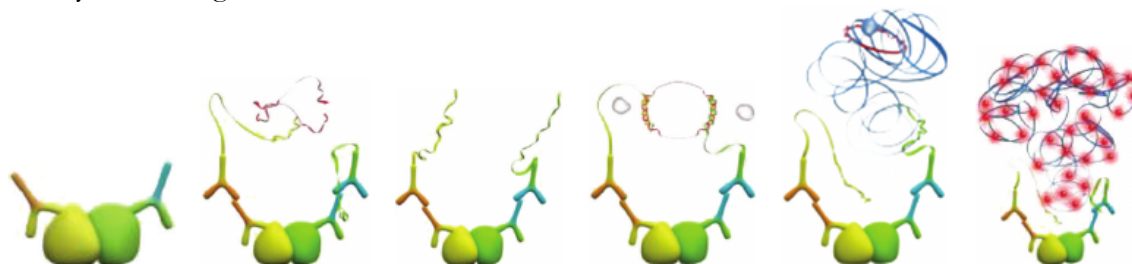


Figure I13. Schematic view of the PLA technique procedure (abnova.com).

#### I.2.4 Functional consequences of GPCR oligomerization

Receptor dimerization has been found to play a key role in regulation at several levels, including traffic to the cell surface or even conferring to the receptors new pharmacological and signalling properties. Although the physiological relevance of all the oligomerization processes is not fully understood, the studies performed in heterologous systems have provided interesting clues. For instance, dimerization could be implicated in GPCR ontogenesis, having a role in controlling protein folding and targeting newly synthesised receptors to the cell surface. Likewise, oligomerization could interfere in the endocytosis, recycling and/or degradation of GPCR. Regarding agonist binding, oligomerization can confer new pharmacological properties, since ligand binding to a receptor could influence the ligand binding to the second receptor of the dimer (*Ferré et al., 2007; Franco et al., 2008*). Finally, another aspect worth to be mentioned is that oligomerization processes can modify the signalling pathways of a receptor, since ligand activation of one receptor could lead to an allosteric modulation of the other partner of the complex, due to conformational changes in the heteromer signalling that may be potentiated, attenuated or even skewed towards the coupling of a non-cognate G-protein.

Metabotropic GABA<sub>B</sub>R heterodimers provide a compelling example of how GPCR oligomerization might be important in receptor folding and transport to the cell surface. In 1998, three simultaneous studies (*Jones et al., 1998; Kaupmann et al., 1998; White et al., 1998*) demonstrated that co-expression of the two GABA<sub>B</sub> receptor isoforms, GABA<sub>B1</sub> and GABA<sub>B2</sub>, were required for a functional GABA<sub>B</sub>R formation at the cell surface. The GABA<sub>B1</sub>



## INTRODUCTION

isoform is unable to reach the cell surface, being retained at the endoplasmic reticulum as an immature glycoprotein. Contrarily, the GABA<sub>B2</sub> isoform is expressed at the cell plasma membrane, but unable to neither bind ligands nor to signal. Only when the two receptors were co-expressed, heteromers are formed and found at cell surface showing their characteristic function. In fact, GABA<sub>B2</sub> acts as an essential chaperone for the correct folding and for targeting of GABA<sub>B1</sub> isoform at cell membrane. Moreover, GABA<sub>B1</sub> is unable to signal when expressed alone, suggesting that the functional unit of the receptor should be the heterodimer (*Margeta-Mitrovic et al., 2000*).

Oligomerization also has a key role in maturation or targeting to the cell membrane of vasopressin V<sub>2</sub> receptor homodimers or the chemokine receptor CCR5 dimers. Truncated forms of the receptors retained the corresponding homodimers at intracellular level, leading to insipid nephrogenic diabetes (*Benkirane et al., 1997*) or a slow appearing of AIDS effects (*Zhu and Weiss, 1998*). Moreover, it is assumed that biogenesis of many oligomers and receptor-receptor interactions of family A of GPCRs already occur in the early stages of receptor folding and processing at the ER or the Golgi apparatus, and then traffic as dimers to the plasma membrane. This could constitute a quality checkpoint for the newly synthesised receptors (*Herrick-Davis et al., 2006*). Once in the membrane, the GPCR heteromers form functional entities able to couple G-protein and signal, exhibiting pharmacological and functional properties that differ from the ones displayed by the receptors in monomeric state (*Bulenger et al., 2005; Franco et al., 2013*).

In the same line, oligomerization may also affect GPCR internalisation and desensitisation. This is the case of somatostatin receptors. SSTR<sub>1</sub> possesses resistance to agonist-induced internalization; however, thanks to the interaction with SSTR<sub>5</sub>, internalisation of the heterodimer occurs upon ligand activation of the receptors (*Rocheville et al., 2000*).

Oligomerization might also regulate the signalling properties of the receptors. The modulation  $\kappa$ - and  $\delta$ -opioid receptor dimer was the first case described. Upon heterodimerization and combined agonist treatment, the functional properties of the receptor change and result in a synergic potentiation of the receptors' signalling (*Gomes et al., 2000*).

The case of the  $\kappa$  and  $\delta$  opioid receptor heteromers was the first described with different properties compared with the receptors in monomeric state. Since then, multiple studies have suggested diverse modulation mechanisms where properties of a given GPCR change upon ligand binding in the other receptor of the oligomer. Dopamine and adenosine receptor heteromers provide multiple examples for negative cooperativity between receptors. In the case of the Adenosine A<sub>1</sub> and Dopamine D<sub>1</sub> heteromer, adenosine receptor agonists

inhibit the action of dopamine D<sub>1</sub> receptor agonists (Fuxe *et al.*, 2007), promoting the disappearance of the high affinity state of the D<sub>1</sub>R (Ginés *et al.*, 2000). Similarly, in the A<sub>2A</sub>R-D<sub>2</sub>R heteromer, agonist binding to the A<sub>2A</sub> receptor reduces the affinity the dopamine D<sub>2</sub> receptor presents for its agonists and its ability to couple and signal through G<sub>i</sub> protein (Fuxe *et al.*, 2007). In the heterodimer formed by adenosine A<sub>2A</sub> receptors and cannabinoid CB<sub>1</sub> receptors (Carriba *et al.*, 2007) the activation of the adenosine receptor reduces the activity of the CB<sub>1</sub>R (Ferreira *et al.*, 2015). Another interesting example is the one provided by adenosine A<sub>1</sub> and A<sub>2A</sub> receptor dimers. Activation of the A<sub>2A</sub> receptor diminishes the affinity of the A<sub>1</sub> receptor for its ligands and inhibits the signalling (Ciruela *et al.*, 2006). Taking into account that the A<sub>1</sub>R affinity for adenosine is higher than the A<sub>2A</sub>R affinity, low concentrations of adenosine preferentially activated the A<sub>1</sub> receptor. Thus, and acting through A<sub>1</sub> receptor downstream machinery, low adenosine concentrations will inhibit glutamate release in the striatum. Contrarily, when the adenosine levels are high, A<sub>2A</sub> receptors will be activated and the function of A<sub>1</sub> receptors will be blunted. Consequently, high adenosine levels promote the release of glutamate in the striatum (Ciruela *et al.*, 2006). Taken together, A<sub>1</sub>-A<sub>2A</sub> heteromer acts as an on-off switch for the glutamate release at the striatum depending on the adenosine concentration in the striatal intersynaptic space.

Another characteristic derived from G-protein receptor dimerization is the possibility of a change in the G-protein coupled beneath the receptors. Lee and collaborators successfully described that the dopamine D<sub>2</sub> and D<sub>1</sub> receptor heteromer in transfected cells couple to a non-cognate G-protein (Lee *et al.*, 2004). While in monomeric state the D<sub>2</sub>R signals through a G $\alpha_i$  protein and the D<sub>1</sub>R interacts with a G $\alpha_s$ ; upon dimerization of both receptors, a G $\alpha_i$  is found beneath the heteromer (Hasbi *et al.*, 2014; Perreault *et al.*, 2016). Also involving the D<sub>2</sub>R, a switch in the signalling is observed in the D<sub>2</sub>R-CB<sub>1</sub>R heteromer compared to the monomeric receptors. Both GPCR are coupled to G $\alpha_i$  proteins when expressed alone, but the heteromer signals through a G $\alpha_s$  when the two are simultaneously activated (Kearn *et al.*, 2005).

The coupling of G proteins to dimers and the stoichiometry of receptor dimer and G-proteins has become a controversial subject. Some studies demonstrated in 2005 that just one protomer or receptor of the dimer could interact with a G-protein (Goudet *et al.*, 2005; Hlavackova *et al.*, 2005). However, posterior studies employing nanodisc technology suggested that  $\beta_2$ -adrenergic receptors,  $\mu$ -opioid receptor or the rhodopsin receptor could function as monomeric entities (Bayburt *et al.*, 2007; Kuszak *et al.*, 2009; Whorton *et al.*, 2007). Experiments with nanodiscs arose a debate within the field for two reasons. On the one hand, models using nanodiscs are far from being physiological, without considering multiple cell factors that





## INTRODUCTION

modulate GPCR. On the other hand, this model does not allow, due to steric hindrance, the occurrence of receptor dimers. Adding an argument in favour the dimer hypothesis, El Moustaine and collaborators showed that monomers of family C GPCR were able to interact with their ligands, but the activation of the receptor and signalling through G-protein required a dimeric state (*El Moustaine et al., 2012*). However, confirmation of whether GPCR dimers can only couple one G protein or, in contrast, if each receptor of the dimer is capable of binding a G protein is yet to be revealed.

The new strategies and approaches available, ranging from TIRF microscopy tools or crystallography, to the use of interacting peptides that disrupt the dimer formation, have become fundamental tools for the study of GPCR (*Jastrzebska et al., 2015; Moreno et al., 2017*). The use of such methodology has provided a more detailed insight in G coupled receptor oligomers their functional consequences, and future progress and advances in the available researchers tool-kit will increase the knowledge within the GPCR field, and for instance, help to shed some light in questions like the stoichiometry relationship between receptors and G proteins.

## 1.3 THE ENDOCANNABINOID SYSTEM

### 1.3.1 Components of the endocannabinoid system

The consumption of cannabis plant (*Cannabis sativa*) has been widely described in literature. The medicinal use of the marijuana dates back to the ancient Chinese medicine, where first uses of the plant to treat pains were compiled in medical books. Similarly, papyrus found in Egypt describe the use and the benefits of the plant to treat psychiatric disorders, several pains or even for gynaecological treatments in the ancient Egyptian culture. In occidental medicine, it was not until 1839 that the cannabis plant was used in a strictly medical purpose, and since then, the research on the molecular basis of the medical and the psychotropic effects of the plant has gained ground. The first, of more than 70 phytocannabinoid compounds contained in the plant, were isolated, but remarkably, it was in 1964 that Mechoulam and Gaoni identified and synthesised the main psychotropic component of the *Cannabis sativa*, the  $\Delta^9$ -tetrahydrocannabinidiol ( $\Delta^9$ -THC). Thereafter, discovery of endogenous cannabinoid-like components i.e. of compounds able to activate the receptor for  $\Delta^9$ -THC were achieved later.

The endocannabinoid system has an important neuromodulatory role within the CNS, regulating neural development, neural plasticity or neuroinflammation processes (*Lu and Mackie, 2016*). Additionally, endocannabinoids participate in the regulation of body temperature and a variety of physiological processes like hunger, sleep, cellular proliferation, reproduction or immune response (*Makrjannis, 2014*). Noteworthy, the capacity of cannabinoid receptors of oligomerizing with other GPCR, gives them the opportunity to indirectly modulate other physiological responses not necessary linked to the endocannabinoid system.

The endocannabinoid system is formed by cannabinoid receptors, the endogenous ligands or endocannabinoids and the enzymes for their synthesis and degradation. Regarding the receptors, despite some controversy, CB<sub>1</sub>R and the CB<sub>2</sub>R are the only two G-protein coupled receptors included in the system, while the transient receptor potential cation channel subfamily V type 1 or Vanilloid receptor 1 (TRPV1) (*Di Marzo et al., 2001*) that binds capsaicin is the other receptor included. In 1990 Matsuda and collaborators cloned and molecularly characterised the CB<sub>1</sub>R (*Matsuda et al., 1990*), and three years later, Munro and collaborators did the same with the CB<sub>2</sub>R (*Munro et al., 1993*). The expression levels of the cannabinoid receptors is comparable to GABA, glutamate or dopamine receptor levels at striatum, predicting an important role of cannabinoid receptor in the synapses (*Herkenham et al., 1990*). Moreover the conservation of these expressions among species suggests a conserved physiological role of the whole endocannabinoid system.

Other components of the system are the synthesis and degradation enzymes. The precursors of endocannabinoids are membrane phospholipids that upon action of the enzymes N-arachidonyl-transferase (NAT), N-acyl-phosphatidyletanolamine phospholipase D (NAPE-PLD) or the diacylglycerol lipase (DAG-lipase) produce the principal endogenous cananbinoids: anandamide (AEA) and the 2-arachidonoylglycerol (2-AG) (Figure 14). In 1992 Devane and collaborators identified AEA (*Devane et al., 1992*), and three years later, 2-arachynodilglycerol (2-AG) was discovered and found to be 200 times more abundant than anandamide (*Sugiura et al., 1995*). Noladin ether (*Hanus et al., 2001*), virodhamin or N-arachinodoyldopamine (*Huang et al., 2002*) are also endocannabinoid ligands found in lower concentrations. Finally, the Fatty Acid Amides Hydrolase (FAAH) and the monoacylglycerol lipase (MAGL) enzymes degrade the endocannabinoids.

The synthesis of endocannabinoids is mainly on-demand, and the produced compounds are not being stored in vesicles. Characteristically, in the CNS the synthesis of endocannabinoids is preceded by the activation of the post-synaptic neuron. The generated



## INTRODUCTION

endocannabinoids present in the synaptic cleft can diffuse and activate receptors expressed in the pre-synaptic neuron, regulating the neurotransmitter release. This phenomenon is known as retrograde signalling. Nonetheless, retrograde activation can be complemented by the cannabinoid-compound modulation of post-synaptic neurons through action on the CB<sub>1</sub>, CB<sub>2</sub> or TRPV1 receptors expressed in these cells.

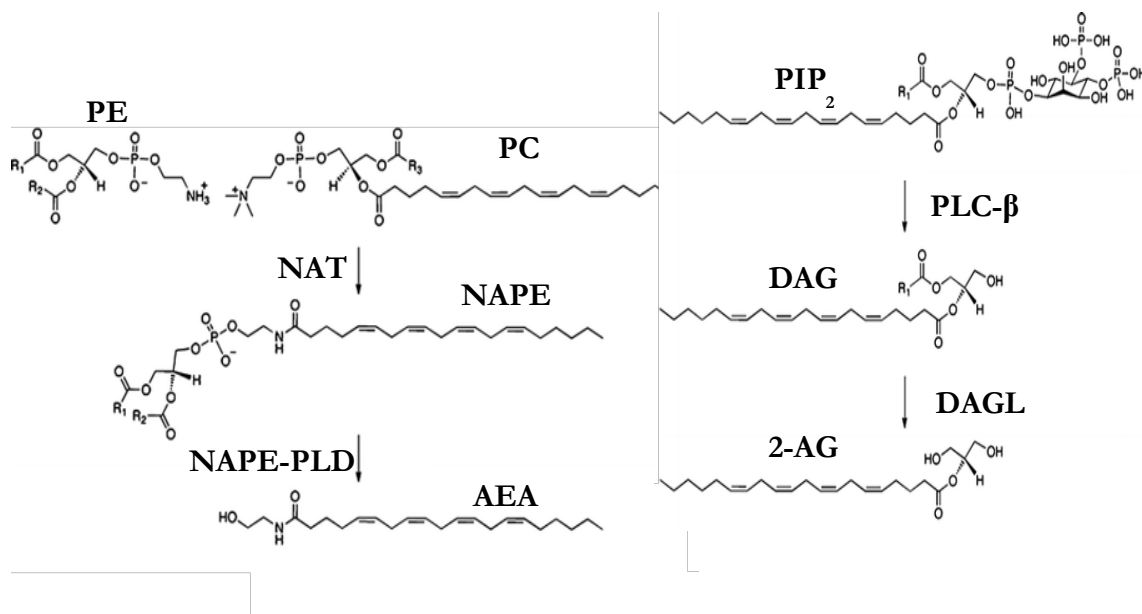


**Figure I14. Schematic representation of Anandamide and 2-arachidonylglycerol synthesis.** At left, membrane phospholipids Phosphatidylethanolamine (PE) or Phosphatidylcholine (PC) are converted to N-arachidonyl-phosphoethanolamine (NAPE) by action of the N-acyl-transferase (NAT). Then NAPE is converted to Anandamide (AEA) by the enzyme N-arachidonyl-phosphatidylethanolamine (NAPE-PLD). At right, membrane phospholipid Phosphatidylinositol-bisphosphate (PIP<sub>2</sub>) are converted to diacylglycerol (DAG) by the action of phospholipase C- β (PLC-β). Finally, the action of diacylglycerol lipase (DAGL) synthesise 2-arachidonylglycerol (2-AG). Modified from Hermanson and Marnett, 2011.

However, all the actions and responses produced by cannabinoids could not be explained by activation of CB<sub>1</sub> and CB<sub>2</sub> receptors or the TRPV1 channels. Further research within the field showed that some orphan receptors can bind cannabinoid compounds. GPR55 (Ryberg *et al.*, 2007) and GPR18 (Gantzer *et al.*, 1997; Kobno *et al.*, 2006) orphan G-protein coupled receptors are some examples of classified as non-cannabinoid receptors that are able to bind cannabinoids. Although full consensus is still lacking, it seems that lysophosphatidylinositol (LPI) is the endogenous ligand of GPR55 (Oka *et al.*, 2007), and the N-arachidonylglycine (NAGly) is the endogenous ligand of GPR18 (Kobno *et al.*, 2006). However, upon interaction with cannabinoids, these receptors are able to signal, generate physiological responses and modulate the CNS activity, and even though not being considered cannabinoid receptors, increasing the versatility of responses and actions produced by endocannabinoids or cannabinoid compounds in the body.

### I.3.2 Cannabinoid receptors

- I.3.2.1 CB<sub>1</sub> Receptor

The CB<sub>1</sub>R is coded, in humans, by a gene located in chromosome 6, at the 6q14-q15 position (Caenazzo *et al.*, 1991; Hoebe *et al.*, 1991). The protein contains 472 amino acids, with a conserved homology between mice, rats and humans. Recent research has obtained crystal structures of the receptor bind to the specific antagonist AM6538 (Hua *et al.*, 2016) or to the inhibitor taranabant (Shao *et al.*, 2016). The receptor belongs to family A of GPCR and it can be glycosylated in three different residues at the N-terminal domain (Figure 15). The receptor is densely distributed in GABAergic and glutamatergic synapses of basal ganglia, hippocampus, cerebral cortex and cerebellum and with a lower expression in the diencephalon, the brain stem or the spinal cord (Glass *et al.*, 1997; Herkenham *et al.*, 1990; Lu and Mackie, 2016). Apart from this widespread distribution, CB<sub>1</sub>R is considered the most expressed G-protein coupled receptor in the CNS (Katona and Freund, 2008). In all these structures CB<sub>1</sub>R is mainly located in the axonal terminals of neurons, with a lower distribution at the post-synaptic level (Laprairie *et al.*, 2012). Lately, the presence of the receptor in glial cells has been reported, playing an important role in modulating neuroinflammation (Bilkei-Gorzo, 2012; Mecha *et al.*, 2015).

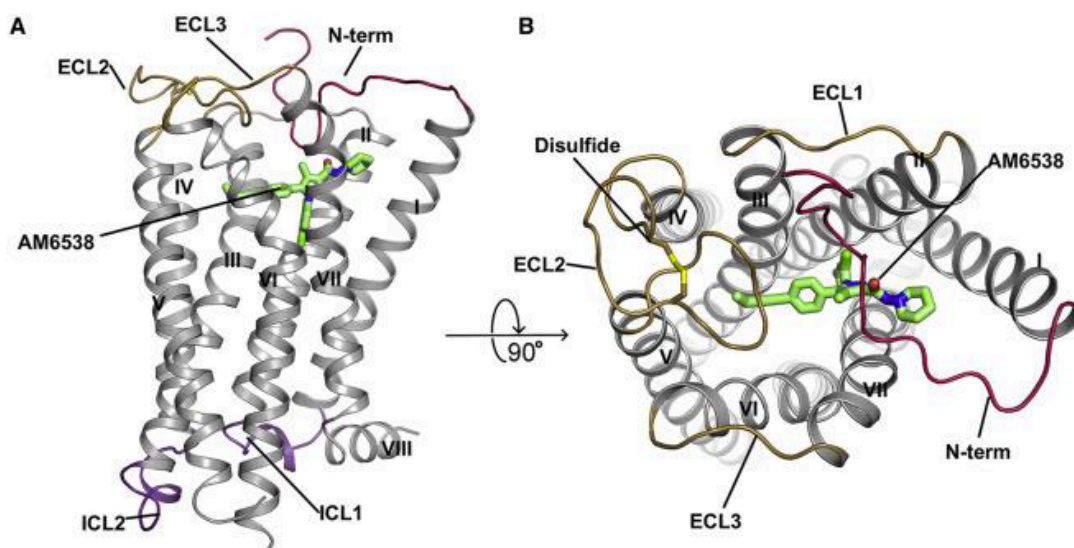


**Figure I15. Crystal structure of CB<sub>1</sub>R bound to the antagonist AM6538.** A) Parallel view of the receptor across the membrane. B) Perpendicular to the membrane view of the receptor from the extracellular domain (Hua *et al.*, 2016).

The CB<sub>1</sub> receptor signalling is mainly mediated by G $\alpha_i$  coupling, thus inhibiting the action of adenylyl cyclase and decreasing cAMP levels (Howlett *et al.*, 1986). However, CB<sub>1</sub>R is considered a promiscuous G-protein coupling receptor due to its ability to switch the G $\alpha$  subunit underneath the receptor. Upon treatment with PTX (Bonhaus *et al.*, 1998) or due to oligomerization processes like in D<sub>2</sub>R-CB<sub>1</sub>R (Jarrabian *et al.*, 2004; Kearn *et al.*, 2005), CB<sub>1</sub>R



signals through a  $G\alpha_s$ . In the latter case, both  $CB_1$  and  $D_2$  receptors signal through a  $G\alpha_i$  subunit, but co-activation with dopamine and endocannabinoids leads to a  $G\alpha_s$  activation, with the subsequent increase of cAMP levels promoted by AC (Scotter *et al.*, 2010). Further research has suggested that some residues at the second intracellular loop were determinant for the  $G\alpha_s$  coupling to the  $CB_1R$  (Chen *et al.*, 2010).

Thanks to their location at pre-synapse and the activation of a  $G\alpha_i$  pathway,  $CB_1R$  exert the well-known retrograde signalling that controls neurotransmitter release from the pre-synaptic terminals. Upon activation of the post-synaptic neuron with the consequent calcium increases, endocannabinoids are produced. The generated ligands can act as retrograde molecules and activate pre-synaptic  $CB_1$  receptors, leading to the inhibition of calcium influx in pre-synaptic neurons (Wilson and Nicoll, 2002). Moreover,  $CB_1R$  can modulate the action of different ion channels. Voltage gated calcium channels (VGCC) (Castillo *et al.*, 2012), as well as a N type and P/Q calcium channels are inhibited by  $CB_1R$ , while the rectifying potassium channels are activated by  $CB_1R$  activity (Lu and Mackie, 2016; McAllister and Glass, 2002). Altogether, and due to this retrograde signalling mechanism and the modulation of channel ions, cannabinoids acting on  $CB_1R$  reduce the neurotransmitter release from the pre-synaptic terminals and can regulate multiple physiological responses within the brain: the motor control, involving receptors present at both indirect and direct motor pathways of the basal ganglia (Laprairie *et al.*, 2012; Valdeolivas *et al.*, 2017); learning, cognition and long-term depression (LTD) memory processes occurring at the hippocampus (Wang *et al.*, 2017); or the regulation of neural plasticity at the cerebral cortex, amygdala and mesolimbic reward pathways being implicated in drug addiction (Lu and Mackie, 2016).

However,  $CB_1R$  is also found at post-synaptic neurons. Thus, autocrine endocannabinoid signalling is equally important, leading to a regulation of the post-synaptic signalling. In this regard, it is remarkable the cannabinoid modulation of GABAergic neurons present in the indirect motor pathways exerted upon interaction with different GPCR like adenosine  $A_{2A}R$  or the  $D_2R$  (Carriba *et al.*, 2007; Marcellino *et al.*, 2008b; Navarro *et al.*, 2008).

- I.3.2.2  $CB_2$  Receptor

Shortly after the discovery of  $CB_1R$ , Munro and collaborators identified the  $CB_2$  receptor (Munro *et al.*, 1993). Located in the chromosome 1 (1p36.11) in humans, the  $CNR2$  gene codes for a 360 amino acid protein, with an overall homology of 44% with the  $CB_1R$ , that increases to 68% when the ligand-binding domain is considered, (Brown *et al.*, 2002; Griffin *et al.*, 2000; Montero *et al.*, 2005; Munro *et al.*, 1993). Despite the crystal structure of the receptor

has not been obtained, several three-dimensional models of the cannabinoid receptor 2 based in the crystal structures available of CB<sub>1</sub>R have been published (Feng *et al.*, 2014; Morales *et al.*, 2016; Ragusa *et al.*, 2015) (Figure 16).

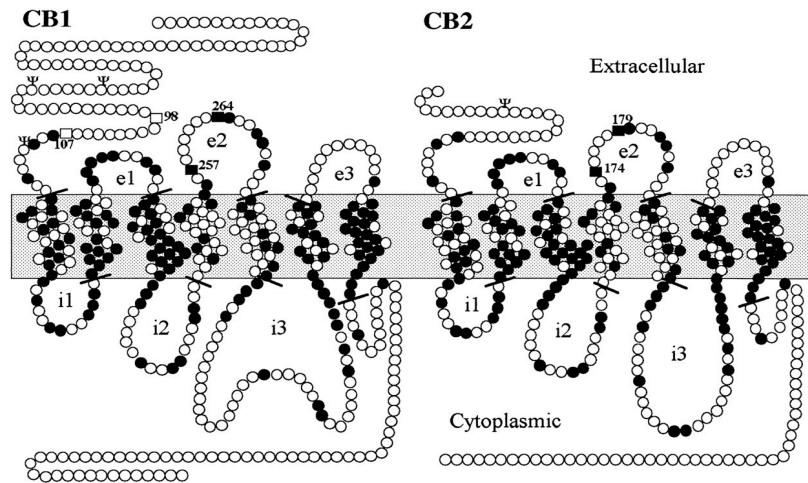


**Figure I16. Structure of human CB<sub>1</sub> and CB<sub>2</sub> receptors.** In black are represented the conserved amino acids in both CB<sub>1</sub>R and CB<sub>2</sub>R.  $\psi$  are used to mark the glycosylated sites (Shire *et al.*, 1996).

Initially, the CB<sub>2</sub>R was thought to be a peripheral receptor due to the high expression in macrophages, mononuclear blood cells, lymphocytes B and other cells of the immune system (Galiègue *et al.*, 1995; Howlett *et al.*, 2002). Moreover, besides immune and hematopoietic cells, CB<sub>2</sub>R is found in liver, endocrine tissues, muscle, pancreatic cells, heart and bladder (Atwood and Mackie, 2010). However, with the advance of methodologies and techniques, the presence of CB<sub>2</sub>R in CNS was proved. Several researchers have detected the receptor expression in glial cells (Cabral and Marciano-Cabral, 2005; Fernández-Ruiz *et al.*, 2007; Mecha *et al.*, 2015; Navarro *et al.*, 2016b), while Lanciego and collaborators showed the expression of CB<sub>2</sub>R in primate (*Maccacca fascicularis*) neurons of different brain regions (Lanciego *et al.*, 2011). The most relevant neuronal immunohistochemical labelling for CB<sub>2</sub>R was obtained in Purkinje cells of the cerebellum and pyramidal neurons of hippocampus (Li and Kim, 2015; Rodríguez-Cueto *et al.*, 2014), and with lower immunoreactivity in olfactory bulb, cortex, striatum, brain stem, pineal gland, thalamus, hypothalamus, amygdala and substantia nigra *pars reticulata* (Atwood and Mackie, 2010). In striking contrast with the CB<sub>1</sub>R, the subcellular localisation of the CB<sub>2</sub>R in hippocampal, cortex and substantia nigra neurons is mainly post-synaptic (Brusco *et al.*, 2008).

Ligand binding to CB<sub>2</sub>R leads to a G $\alpha_{i/o}$  coupling. Therefore, AC and PKA pathways are inhibited after CB<sub>2</sub>R activation. Stimulation of the receptor could activate different MAPK (Lu and Mackie, 2016). At the same time, mTOR and PI3K/Akt signalling pathways have been



linked to CB<sub>2</sub>R (*Palazuelos et al., 2012*), implicating the receptor in neural survival and proliferation. Moreover, the presence of the receptor in neural progenitor cells confirms the role of the receptor in neural proliferation (*Díaz-Alonso et al., 2017; Galve-Roperh et al., 2013*). However, activation of the receptor in tumour cells induces the activation of apoptotic pathways while inhibits the cancer cell growth (*Fernández-Ruiz et al., 2007; Wang et al., 2018*).

Due to the high expression in macrophages and lymphocytes, CB<sub>2</sub>R has always been related to a regulatory role in the immune system. In this regard, it has been seen that inflammatory processes promote, in the periphery, an increase of the endocannabinoid production and an increase of the available ligand for CB<sub>2</sub>R. Meanwhile, activation of the receptor leads to anti-inflammatory responses and lower production of pro-inflammatory chemokine (*Pacher and Mechoulam, 2011*). Similarly, recent findings show that CB<sub>2</sub>R expression is increased in brain in neuroinflammatory processes. Inflammation markers have been reported in neurodegenerative diseases like Parkinson disease (PD), Alzheimer disease (AD) or Huntington disease (HD), and in other pathologies like schizophrenia (*Atwood and Mackie, 2010; Navarro et al., 2016b; Pacher and Mechoulam, 2011*). Therefore, due to the anti-inflammatory and neuroprotective role of CB<sub>2</sub>R in immune system cells, and to the increased presence of the receptor in CNS under inflammatory conditions, CB<sub>2</sub>R is a promising target to counteract the effects of neurodegenerative diseases.

### I.3.3 Cannabinoid receptor heteromers

Cannabinoid receptors, like other GPCR, can be subject to oligomerization processes that modulate their pharmacology, signalling properties and general characteristics. Both CB<sub>1</sub> and CB<sub>2</sub> receptors form homodimers and heterodimers with multiple GPCR (*Boroto-Escuela et al., 2014*).

In 2000, Mukhopadhyay and collaborators co-immunoprecipitated CB<sub>1</sub>R homomers in solubilized rat tissue preparations (*Mukhopadhyay et al., 2000*). Other authors confirmed the CB<sub>1</sub>R homomerization in posterior studies (*Mackie, 2005; Wager-Miller et al., 2002; Xu et al., 2005*), even in human tissue (*De Jesús et al., 2006*). Similarly, in 2004 Filppula and collaborators successfully identified the CB<sub>2</sub>R homomers (*Filppula et al., 2004*). Nonetheless, the pharmacological and functional consequences of cannabinoid receptors heteromerization are more relevant than the homodimerization ones.

Both CB<sub>1</sub> and CB<sub>2</sub> receptors can form heterodimers with multiple partners. Interestingly, one of the interactions could occur between both cannabinoid GPCR receptors. Thus, in 2012 Callén and collaborators identified the CB<sub>1</sub>R-CB<sub>2</sub>R in heterologous cells

heteromer, in neuroblastoma SHSY5Y cells and in rat tissue (*Callén et al., 2012*). In this study, heteromerization led to a negative cross-talk and a cross-antagonism phenomenon in Akt signalling pathway, resulting in lower neurite growth in SHSY5Y cells. In the same line, other authors demonstrated a reduction of CB<sub>1</sub>R and CB<sub>2</sub>R mRNA expression and a reduction of CB<sub>1</sub>-CB<sub>2</sub> receptor heteromer presence in *globus pallidus* neurons of parkinsonian monkeys, result of a chronic treatment with levodopa (*Sierra et al., 2015*). These results indicated the existence of the heteromer in native tissue of different species, as well as possible physiological and pathological consequences of the interaction.

Interestingly, CB<sub>1</sub>R can heteromerize with GPR55 receptor. Upon interaction, GPR55-mediated ERK1/2 phosphorylation and signalling through NFAT and SRE factors is reduced (*Kargl et al., 2012*). In turn, the ability of the CB<sub>2</sub>R to interact with GPR55 was described simultaneously by two research groups. In 2014, Balenga and collaborators focused their study in determine the functional consequences of the CB<sub>2</sub>R-GPR55 heteromerization. The results showed that the expression of a receptor influences the characteristic signalling of the partner receptor in the heteromer. Thus, presence of CB<sub>2</sub> receptor lead to a diminished transcription factor response after GPR55 activation, and an increase in the MAPK signalling. Similarly, GPR55 could alter the CB<sub>2</sub>R signalling, demonstrating the existence of a cross-talk between both receptors (*Balenga et al., 2014*). The other study focused their efforts on demonstrate the role of the CB<sub>2</sub>R-GPR55 heteromer in tumor progression. The study shows that due to the negative cross-talk between CB<sub>2</sub>R and GPR55, high doses of  $\Delta^9$ -THC can prevent or induce a slower tumour growth, while low doses of  $\Delta^9$ -THC do not affect the tumoral growth (*Moreno et al., 2014*). Similarly, the CB<sub>2</sub>R is capable to interact with another cannabinoid-related GPCR, GPR18. The CB<sub>2</sub>R-GPR18 heteromer seems to be involved in microglia migration, and a cross-talk between the receptors is suggested (*Franklin and Stella, 2003; McHugh et al., 2008*).

Besides the heteromers CB<sub>1</sub> and CB<sub>2</sub> receptors could form with other cannabinoid related GPCR, both receptors are implicated in many other oligomerization processes. Worth mention are the interactions of CB<sub>1</sub>R with adenosine and dopamine receptors.

In striatal medium spiny neurons, endocannabinoids through their action on pre-synaptic CB<sub>1</sub>R lead to the inhibition of glutamate release. At these pre-synaptic neurons, CB<sub>1</sub>R might form heteromers with adenosine A<sub>2A</sub> receptors (*Ferré, 2010*). In this context, A<sub>2A</sub>R inhibits CB<sub>1</sub>R-mediated synaptic effects, probably occurring at cAMP/PKA pathway (*Martire et al., 2011*). The CB<sub>1</sub>R-A<sub>2A</sub>R heteromers have also been reported at post-synaptic level (*Carriba et al., 2007; Navarro et al., 2008; Tebano et al., 2009*), but with different physiological





consequences of the interaction. In line, and due to the expression of the dopamine D<sub>2</sub> receptor in the striatal medium spiny neurons, and the close relationship of CB<sub>1</sub>R and A<sub>2A</sub>R receptors with the dopamine receptor, it is not surprising that the D<sub>2</sub>R-CB<sub>1</sub>R heteromer was described (Kearn *et al.*, 2005; Khan and Lee, 2014). In this case, the functional consequence of the interaction implies a switch in the G-protein coupling after the co-activation of the CB<sub>1</sub>-D<sub>2</sub> receptor heteromer (Glass and Felder, 1997; Jarrabian *et al.*, 2004; Kearn *et al.*, 2005; Marcellino *et al.*, 2008b). The close relationship of A<sub>2A</sub>R, CB<sub>1</sub>R and D<sub>2</sub>R arose hypothesis about the possibility of the three receptors forming a macromolecular complex. It was not until 2008, that Navarro and collaborators identified the interaction of the three receptors (Navarro *et al.*, 2008) adding complexity to the regulation of these motor pathways in physiological and pathological conditions (Bonaventura *et al.*, 2014; Pinna *et al.*, 2014).

Other CB<sub>1</sub>R-containing heteromers have been described, with important implications in CNS or peripheral functions. The CB<sub>1</sub>R and serotonin 5HT<sub>2A</sub> receptor heteromer is involved in the deleterious effects of cannabis in memory (Viñals *et al.*, 2015), and the interaction between the CB<sub>1</sub> receptor with  $\delta$ ,  $\kappa$  and  $\mu$ -opioid receptors could have consequences in alcohol consumption and addiction or in neurite formation processes (Busblin *et al.*, 2012; Fujita *et al.*, 2014; Hojo *et al.*, 2008; López-Moreno *et al.*, 2010; Rozenfeld *et al.*, 2012). CB<sub>1</sub>R could influence the food intake and appetite, as well as waking-sleep states through the heteromerization with orexin OX<sub>1</sub> receptor (Ellis *et al.*, 2006; Jäntti *et al.*, 2014; Pertwee, 2010), or be involved in angiotensin related pathogenesis in the liver through AT<sub>1</sub>R-CB<sub>1</sub>R heteromers (Rozenfeld *et al.*, 2011).

On its behalf, CB<sub>2</sub>R-containing heteromers have been less studied. However, and in line with the above indicated CB<sub>2</sub>-GPR55 receptor heteromer, which can have implications in tumoral growth, Coke and collaborators have described a role for the CB<sub>2</sub>R-CXC<sub>4</sub>R in tumour progression, thus being the heteromer suggested as a relevant target in metastasis (Coke *et al.*, 2016). Moreover, other studies attribute a neuroprotective role for cannabidiol in hypoxic and ischemic episodes through their action on CB<sub>2</sub>R-5HT<sub>2A</sub>R heteromers (Pazos *et al.*, 2013).

#### **I.3.4 Cannabinoids role in neuroinflammation process**

Neuroinflammation can be described as the inflammatory response that the CNS undergoes when is threatened by harmful elements. The process can involve multiple actors ranging from microglia and astrocytes to lymphocytes or macrophages, and pursues the objective of eliminate the insult and to repair the damaged tissue. However, a sustained neuroinflammatory response can derive in negative consequences that contribute to the

disease progress. In this regard, cannabinoids have always been related to a protective function within the CNS, and many researchers have determined the neuroprotective role of exogenous and endogenous cannabinoids in in vitro and in vivo models of excitotoxicity and neurodegeneration (*van der Stelt and Di Marzo, 2005*).

Excitotoxicity is the pathological process in which excessive neuronal activation, due to the action of excitatory neurotransmitters like glutamate, promote the consequently increase in intracellular calcium that can lead to metabolic damage and eventually, to the cell death. Many evidence in literature suggest a pivotal role for excitotoxicity in the beginning of the degeneration processes concomitant in Alzheimer's disease, Parkinson's disease, Amyotrophic Lateral Sclerosis (ALS) or Multiple Sclerosis (MS). In the AD, PD or even HD: motor disorders implicating motor pathways, the over-stimulation of the pathways comes from the cortical glutamate release. The excessive concentration of this stimulatory neurotransmitter produces the increase of calcium levels in the post-synaptic neurons that triggers the activation of caspases and is followed by neuronal death (*Kermer et al., 1999*). In this context, cannabinoid administration could establish a neuroprotective effect by diminishing either the glutamate release at the pre-synaptic neuron and the activation tone of the glutamate over-stimulated neurons, as several excitotoxicity and neurodegenerative models have determined (*Mechoulam et al., 2002; van der Stelt et al., 2002*). Moreover, the levels of the endocannabinoids 2-AG and anandamide are notably increased after neuronal damage (*Berger et al., 2004; Franklin et al., 2003; Muthian et al., 2004*).

Neuronal function is supported by the action of different cell types that contribute to the CNS homeostasis. In this regard, astrocytes are involved in, among other functions, energy supply, in the clearance of ions or neurotransmitters like glutamate from the synaptic cleft preventing the neurotoxic effects of excessive neuronal activation, and in the synthesis of antioxidant compounds and trophic factors that exert a neuroprotective role. However, in certain pathological situations, astrocytes can produce pro-inflammatory cytokines that will contribute to the neuroinflammatory process (*Zorec et al., 2018*). The presence of CB<sub>1</sub> and CB<sub>2</sub> receptors has been demonstrated in this cell type (*Duarte et al., 2012; Sheng et al., 2005*), and its activation leads to a reduced pro-inflammatory cytokine release in neuroinflammatory conditions (*Molina-Holgado et al., 2002*). Moreover, it has been seen that endocannabinoids could be regulating the glutamate up-take of astrocytes helping to reduce the excitotoxicity generated by this neurotransmitter (*Shivachar, 2007*).



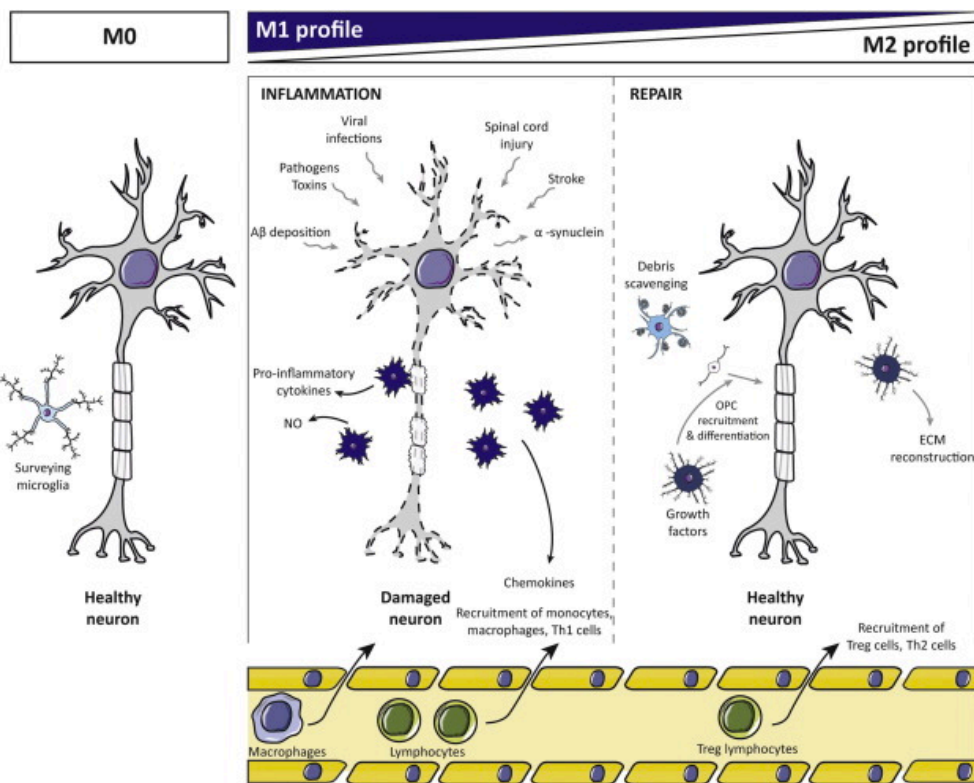


**Figure I17. Microglial phenotypes in inflammation contexts.** In homeostatic conditions, surveillant M0 phenotype monitors the nervous system. After injury, stroke, toxins or neurodegenerative damage, M1 microglial profile secretes inflammatory mediators and chemokines triggering monocytes and Th1 cell recruitment. These peripheral cells will amplify the inflammatory context and increase the neuronal damage. Contrarily, M2 microglial phenotype through segregation of growth factors could promote a reparative and neuroprotective effects in the CNS. Recruitment of Treg and Th2 lymphocytes will be necessary to the restore of the CNS homeostasy (Mecha et al., 2016).

Endocannabinoids have another important role in neuroprotection due to their implication in modulate microglial activation. Microglial cells sense the neural environment and quickly respond to threats and neuron malfunctions. After a brain injury and bacterial or viral infection, microglial cells are able to detect the threat and undergo phenotypic changes. Thus, in first instance, microglia acquires a reactive M1 pro-inflammatory phenotype, promoting an acute inflammation that ensures the clearance of the insult. Subsequently, microglial cells acquire an M2 anti-inflammatory phenotype, that tries to repair the tissue and restore the homeostatic conditions (Franco and Fernández-Suárez, 2015; Mecha et al., 2016; Walker and Lue, 2015). However, in neurodegenerative diseases, the persisting insult promotes the microglial M1-phenotype and chronifies the pro-inflammatory environment, generating a worst outcome and increasing the neurodegeneration process (Figure 17). In this context endocannabinoids could play an important role. Both CB<sub>1</sub> and CB<sub>2</sub> receptors have been detected in microglial cells (Malek et al., 2015) and, indeed, the CB<sub>2</sub>R expression is highly increased under pro-inflammatory conditions (Ashton and Glass, 2007; Concannon et al., 2016;

*Maresz et al., 2005*). Interestingly, it seems that endocannabinoids have a role in driving the acquisition of inflammatory phenotypes of microglial cells (*Mecha et al., 2015*). Therefore, CB<sub>1</sub> and CB<sub>2</sub> receptors are potential targets for therapies trying to unbalance microglia towards a more reparative M2 inflammatory phenotype (*Navarro et al., 2016b*).

## I.4 CALCIUM SENSOR PROTEINS

### I.4.1 Relevance of calcium in neuron physiology

Calcium ion is a second messenger of vital importance for cell behaviour. It participates in multiple functions like signal transduction, cell division, differentiation or apoptosis (*Carafoli, 2002; Orrenius et al., 2003*) and its intracellular concentration oscillates from submicromolar to millimolar concentrations (*Ghosh et al., 2017; Tsien and Tsien, 1990*). Small changes in calcium intracellular levels will regulate different processes, although these changes will also depend on the specific velocity, the frequency or the magnitude of the signal (*Zampese and Pizzzo, 2012*).

At CNS, the role of calcium presents even greater importance. The calcium-mediated signalling, characterised by dynamic gradients called Ca<sup>2+</sup> waves are fundamental for neuron communication (*Berridge, 1998*). Neuronal transmission is a refined process requiring a rapid and local increase of calcium concentration at pre-synaptic and post-synaptic level. The entrance of calcium at the pre-synapse allows the release of neurotransmitter vesicles, and at the post-synapse, as well as helping to propagate the signals to other neurons, will contribute to the short and long-term plasticity (*Catterall and Few, 2008; Mochida et al., 2008*). Not only calcium is in charge of these processes, but also is involved in the control of the development, maturation and refinement of the synapse (*Greer and Greenberg, 2008*). In order to regulate the intracellular levels of this ion, cells possess a wide range of calcium-binding proteins that modulate and restring the spatial and temporal impact of calcium as second messenger. Therefore, these proteins play an important role in the calcium induced signalling (*Di Donato et al., 2013*).

Three different groups of calcium binding protein exist, with many proteins differing in subcellular and tissue distribution in each group. Buffer proteins, like S100G or parvalbumin, form the first one. These proteins are characterised by having a high affinity for calcium and by not suffering big conformational changes, therefore, acting mainly as chelates (*Schröder et al., 1996; Schwaller, 2009*). The second group is formed by proteins like thermolysin,



which require to bind calcium ions for being stabilised (*Buchanan et al., 1986*) and finally, the third group contains the calcium sensor proteins. These proteins have a low affinity for calcium, but suffer important conformational changes upon the calcium binding, triggering the interaction with different effector proteins. The second and third groups bind the calcium ions through EF-hand domains (*Mikhaylova et al., 2011*). This domain, present in 122 proteins, consists in 29 amino acids with a characteristic structure formed by two  $\alpha$ -helix separated by a connecting loop (*Burgoyne, 2007*).

In this chapter we are going to focus on the study of calcium sensor proteins in CNS. Calcium sensor proteins are characterised by suffering conformational changes upon binding calcium ions. The conformational rearrangement permits the interaction of the sensors with different effectors, enabling the transmission of information through phosphorylation or gene expression changes (*Hashimoto and Kudla, 2011*). Altogether provokes, in the last resort, the modulation of neuronal activity (*McCue et al., 2010a*). The common ancestor of these proteins is calmodulin (CaM) (*Mikhaylova et al., 2011*). According to their evolution and the history of their discovery, the calcium sensor proteins of the CaM superfamily have been divided in the Neuronal Calcium Sensor (NCS) family and the neuronal calcium-binding proteins (nCaBP) family, that contains Caldendrin and Calneuron calcium-binding proteins (*Mikhaylova et al., 2011*). The members of the two families have a similar structure, derived from its common ancestor. The sensors contain four calcium-binding EF-hand domains, even though not all of them are functional (*Mikhaylova et al., 2011*). In spite of the structural homology with CaM, NCS and nCaBP present multiple differences at amino acid sequence level and at the functional implications of their interactions (*Burgoyne, 2007; Ikura and Ames, 2006*).

#### **I.4.2. Calmodulin**

Calmodulin (CaM) is one of the most important EF-hand domain-containing proteins, being an essential calcium sensor protein. In humans, three different genes (CALM1-3) code for an identical protein (*Sorensen et al., 2013*). Noteworthy, the homology of the protein among vertebrate species is maintained, not having been described any amino acid changes between mammals (*Friedberg and Rboads, 2001*). The CaM structure is formed by 148 amino acids, containing a  $\alpha$ -helix structure with two globular domains at the N- and C-terminal domains. These domains contain two EF-hand domains each (*Sorensen et al., 2013*). Altogether results in a protein with an affinity for calcium of 5-10 microMolar ( $\mu\text{M}$ ) (*Mikhaylova et al., 2011*). The two globular (N- and C-terminal) domains present different calcium binding kinetics, increasing the versatility of the sensor (*Tadross et al., 2008*). Upon the interaction with calcium

ions (one in each of the four EF-hand domains present in CaM), CaM suffers conformational changes that enable specific interactions with, reported to date, more than 120 proteins (enzymes, ion channels, transcription factors or cytoskeletal proteins). Thus, the protein acts as a sensor and as a signal transducer (Marcelo *et al.*, 2016). Extracellular stimuli like insulin, hormones or adipogenic signals are going to trigger intracellular calcium increases. Afterwards, CaM will bind the calcium ions and interact with multiple kinases and downstream machinery that will promote cell growth, regulation of energy homeostasis, protein synthesis or regulation of gene expression among others (Marcelo *et al.*, 2016) (Figure 18).

CaM is present in all eukaryotic cells, but its expression is remarkable in heart and brain, with a subcellular localisation at plasma membrane, endoplasmic reticulum or mitochondria. Its widespread distribution, allows the sensor being involved in process related to metabolism (Marcelo *et al.*, 2016), apoptosis (Berchtold and Villalobo, 2014; Özcan and Tabas, 2010), inflammation and in the immune system (Ainscough *et al.*, 2015; Racioppi and Means, 2008), cell proliferation and autophagy (Berchtold and Villalobo, 2014), long term memory (Limbäck-Stokin *et al.*, 2004) or nervous system development (Ghosh and Greenberg, 1995). Moreover, CaM has been related to cancer processes, as increases of this protein have been described in tumour cells (Berchtold and Villalobo, 2014).

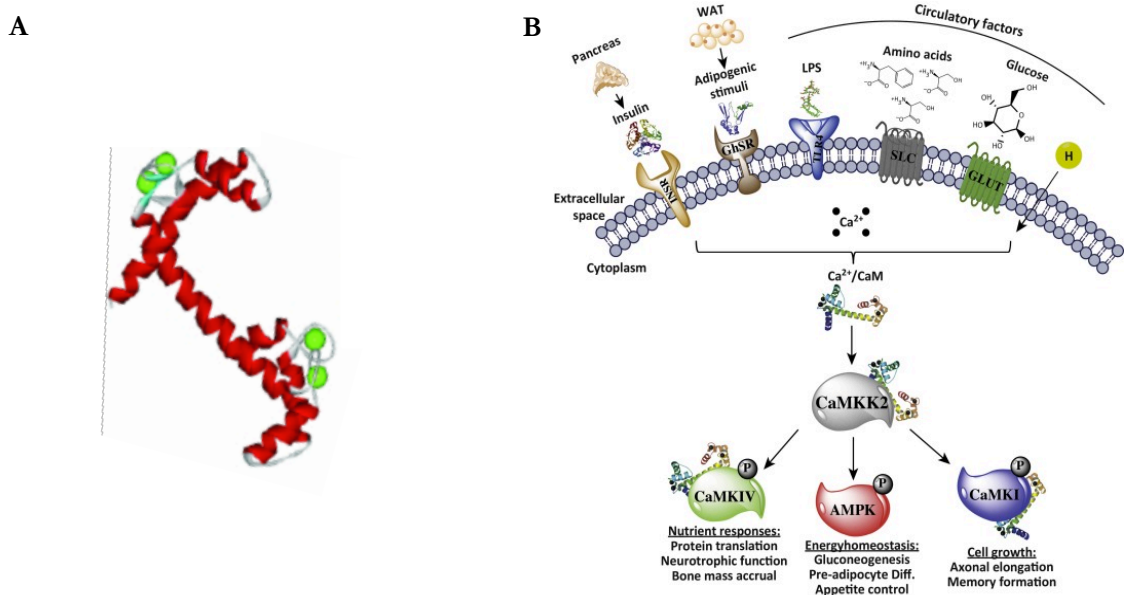


**Figure I18. Calmodulin.** A) Structural representation of CaM bound to 4 calcium ions (green circles) (McCue *et al.*, 2010). B) Representation of the different signalling cascades mediated by CaM (Marcelo *et al.*, 2016).



### I.4.3. Neuronal calcium-binding Proteins

Neuronal calcium-binding proteins (nCaBP) family members were classified together due to their close relationship, even though, some phylogenetic analysis suggested that two different subfamilies could be divided from nCaBP (McCue *et al.*, 2010b). Both subfamilies could have arisen at the same time during vertebrate evolution, being the Caldendrin/CaBP subfamily and the Calneuron subfamily (Haeseleer *et al.*, 2002; McCue *et al.*, 2010b; Mikhaylova *et al.*, 2006).

Five different genes code for CaBP subfamily proteins, being Caldendrin the first identified (Seidenbecher *et al.*, 1998). All the proteins of the subfamily exhibit some differences in amino acid substitutions, or deletions in some cases, respect CaM; but present a higher similarity with CaM than the NCS family or Calneurons (McCue *et al.*, 2010a; Seidenbecher *et al.*, 1998). The structure of CaBP proteins is maintained among the subfamily members, with a C-terminus domain containing the four EF-hand domains but a N-terminal domain that varies in length and structure (Mikhaylova *et al.*, 2006). This N-terminal domain variability is suggested to play an important role in the subcellular distribution and function of the subfamily proteins (Mikhaylova *et al.*, 2011). Caldendrin is the member of the subfamily most prominently distributed in the brain, whereas the rest of the proteins are only highly expressed in retina or ear (Mikhaylova *et al.*, 2006). The existing differences in the structure (Figure 19A), give to these proteins different affinities for calcium ions. In the case of the caldendrin, the affinity for calcium is 2.5  $\mu\text{M}$  (Mikhaylova *et al.*, 2006).

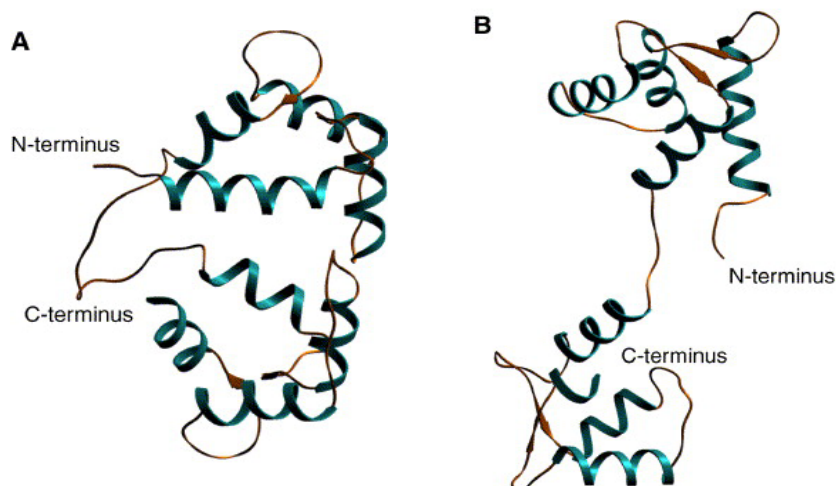


**Figure I19. Predicted structures of nCaBP family proteins.** A) Structure predicted with Swiss Modeler Service for Caldendrin. B) Predicted structure of Calneuron-1 using the same technology (Mikhaylova *et al.*, 2006)

CaBP and CaM could interact with the same proteins, although implying different regulation of the target. For instance, calmodulin and caldendrin interact with the post-synaptic voltage-gated  $\text{Ca}_v1.2$  (L-type) calcium channels, but the regulation will differ according to which is the sensor interacting with the protein. While calmodulin prevents the activation of the channel and the  $\text{Ca}^{2+}$  influx, caldendrin facilitates the calcium currents to the post-synaptic neuron (Zhou *et al.*, 2004)

On the other hand, the second subfamily is formed by two proteins, calneuron-1 and calneuron-2. These proteins are very similar to each other, with an overall identity of 63% and a sequence of, respectively, 219 and 215 amino acids (Mikbaylova *et al.*, 2006). Differing from the other calcium sensor proteins, calneurons have a C-terminal 38-amino acid transmembrane extension that enables them to be anchored to the membrane (McCue *et al.*, 2010b). Both proteins harbour four EF-hand domains, however only two are functional. Nonetheless, calneurons can bind calcium with high affinity (440 nM) (Mikbaylova *et al.*, 2011). The two non-functional EF-hand domains, placed at the C-terminus, seem to be important for the interaction specificity and the dynamics of the calneurons (Figure 19B).

Despite some studies attribute to calneuron-1 and calneuron-2 a regulatory role in the phospholipid synthesis and in membrane trafficking in the Golgi (Hradsky *et al.*, 2015; Mikbaylova *et al.*, 2009) or an allosteric modulatory effect in the  $\text{A}_{2\text{A}}$ - $\text{D}_2$  receptor heteromer signalling (Navarro *et al.*, 2014b), little is known about their function at the CNS.

#### I.4.4. Neuronal Calcium Sensor

In 1995 Nef and collaborators named Neuronal Calcium Sensors (NCS) the family of calcium binding and structurally similar proteins that embraced the visinin, the S-modulin, the recoverin, the visinin-like-1 protein (VLP-1) and the frequenin/NCS-1 (Nef *et al.*, 1995). Since then, the family has expanded, being frequenin the family's common ancestor (McCue *et al.*, 2010a). Frequenin was firstly found in *Drosophila Melanogaster* (Pongs *et al.*, 1993), but after it was discovered in human neuronal cells and other species, the

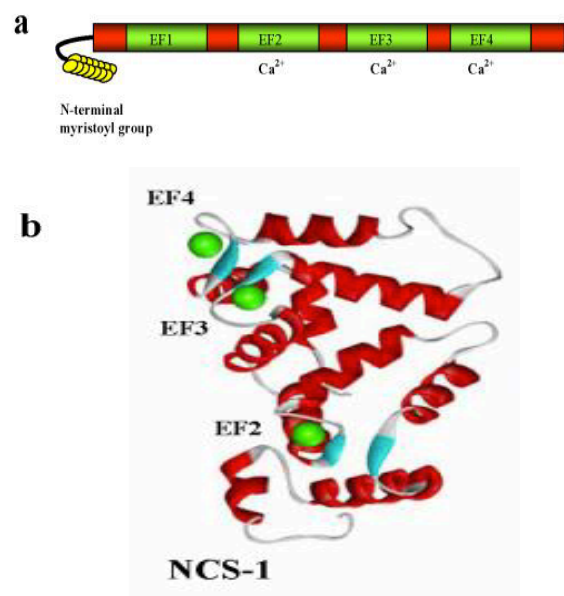


**Figure I20. Crystal structure of NCS-1 calcium sensor.** A) Schematic representation of NCS-1 protein showing the EF-hand domains involved in calcium binding. B) Crystal structure of NCS-1 with calcium ions bound (green spheres) (Adapted from McCue *et al.*, 2010).





name of Neuronal Calcium Sensor 1 (NCS-1) was coined. Finally, some studies demonstrated the localization of NCS-1 in other cells than neurons, even though the expression was lower than in neurons (*Blasiolo et al., 2005; Kapp-Barnea et al., 2003; McFerran et al., 1998*).

NCS proteins share low homology with CaM (*Burgoyne, 2007*). Structurally, NCS proteins contain four EF-hand domains, however just two or three of them are functional (*Mikhaylova et al., 2011*). In NCS-1, the four EF-hand form a single globular domain, with three of them able to bind calcium ions. Interestingly, NCS-1 is myristoylated at the N-terminal domain, modification that helps the protein to be anchored to membrane structures. This modification seems to happen constitutively, however there are researchers that advocates that the myristoylation is added after that the specific N-terminal domain residues are exposed upon the conformational changes occurring after calcium binding (*Ames et al., 1997*). This protein can also interact with  $Mg^{2+}$  ions, which may vary the overall affinity for  $Ca^{2+}$ . In absence of  $Mg^{2+}$ , NCS-1 displays an affinity of 90 nM for  $Ca^{2+}$ , while in presence of  $Mg^{2+}$  it is of 440 nM (*Mikhaylova et al., 2011*) (Figure 20).

Upon interaction with calcium, NCS proteins can modulate multiple cellular processes. It has been suggested that NCS sensors are involved in neurotransmission (*Pongs et al., 1993*), exocytosis (*Haynes et al., 2005; McFerran et al., 1998*), learning processes (*Gomez et al., 2001*), regulation of ion channels (*Weiss et al., 2000*), synaptic plasticity (*Sippy et al., 2003*), neuronal surviving (*Nakamura et al., 2006*) or receptor endocytosis (*Kabbani et al., 2012*). Moreover, several mental and neurological diseases like epilepsy, schizophrenia, Alzheimer disease or even cancer have been linked with these proteins (*Braunewell, 2005*). Increased levels of NCS-1 have been found in brain of schizophrenic or bipolar patients (*Kob et al., 2003*), being suggestive of involvement of NCS-1 in increased neuronal excitability.

#### **I.4.5. Calcium sensor proteins as regulators of GPCR activity**

One of the interacting targets of calcium-binding EF-hand domain-containing sensors are GPCR. The first evidence of the GPCR-calcium sensor protein interaction came in 2001 when El Far and collaborators identified a C-terminal domain motif of the metabotropic glutamate receptor 7 able to interact with CaM. Interestingly, the domain was coincident to the motif involved in  $\beta\gamma$  subunit interaction (*El Far et al., 2001*). In the same line, CaM has been linked to other GPCR, implicating a regulation of the receptors. CaM can also interact with the third intracellular loop of the  $\mu$ -opioid receptor or the serotonin 5-HT<sub>1A</sub> receptors (*Turner et al., 2004; Wang et al., 1999*). Upon interaction with the calcium-binding protein, the

ability of the receptor to couple the cognate G-protein is diminished, suggesting a competition between the sensor and G-protein for the receptor interaction (*Wang et al., 1999*). On the other hand, calmodulin interacts with the N-terminal domain of the third intracellular loop of the D<sub>2</sub>R, compromising the interaction of the receptor with the G-protein (*Bofill-Cardona et al., 2000*). Further studies have demonstrated that the activation of the receptor increased the colocalization of CaM and D<sub>2</sub>R in heterologous model system and primary cultures of neurons (*Liu et al., 2007*). CaM can interact with the C-terminus of GPCR, as it has been shown in the CaM-A<sub>2A</sub>R interaction (*Woods et al., 2008*). After the discovery of the CaM-A<sub>2A</sub>R interaction, it was suggested a role of CaM in the A<sub>2A</sub>R-D<sub>2</sub>R heteromer. In this regard, Navarro and collaborators demonstrated the interaction and a calcium-dependent CaM modulatory role in the A<sub>2A</sub>-D<sub>2</sub> receptor heteromer (*Navarro et al., 2009*).

Regarding the D<sub>2</sub>R but involving the other families of calcium sensors, the interaction with NCS-1 has been widely described. In 2005, a compelling ultrastructural work of Negyessy and Goldman-Rakic showed the colocalization of the NCS-1 and D<sub>2</sub>R at pre-synaptic and post-synaptic level of primate prefrontal cortex (*Negyessy and Goldman-Rakic, 2005*). Moreover, NCS-1 protein mediates the D<sub>2</sub>R desensitization (*Kabbani et al., 2002*), making this interaction a good target for anti-psychotic drugs (*Kabbani et al., 2012*). Recent studies employing fluorescence spectroscopy and nuclear magnetic resonance described the stoichiometry of the D<sub>2</sub>R-NCS-1 interaction as 2:1, implying that a dimer of the GPCR would be interacting with a NCS-1 monomer (*Lian et al., 2011*). In the same line, Pandalaneni suggested that NCS-1 could be interacting at the same time with the D<sub>2</sub>R and G-protein Receptor Kinase 1 (GRK1), acting as a scaffolding protein for the kinase recruitment to the receptor (*Pandalaneni et al., 2015*). However, results from another study have suggested that a D<sub>2</sub>R dimer was able to interact with two NCS-1 molecules (*Woll et al., 2011*).

Leaving the interaction with the D<sub>2</sub>R aside, in 2012 Navarro and collaborators described the interaction of NCS-1 with A<sub>2A</sub>R. In addition, the calcium sensor could be modulating the A<sub>2A</sub>R function in a calcium dependent manner, and differently than the previous reported CaM-A<sub>2A</sub>R interaction regulation (*Navarro et al., 2012*). Finally, further investigations showed the interaction, not only of NCS-1, but also of calneuron-1, with the A<sub>2A</sub>-D<sub>2</sub> receptor heteromer (*Navarro et al., 2014b*). Interestingly, in this study, an allosteric modulation of the heteromer signalling was proposed according to the intracellular calcium levels and the differential interaction of the sensors to the receptor oligomer.

In summary, regulation of GPCR activity could be carried out by calcium sensor proteins. Therefore it is necessary to further investigate the relationships between G-protein



coupled receptors and calcium sensor proteins, specially in the CNS where calcium ion is a key player.

### I.5 COCAINE ADDICTION

#### I.5.1 The reward system

The reward system or mesocorticolimbic pathway is a set of neuronal pathways of vital importance. Upon obtaining pleasure and wellness, the system reinforces the subjects to repeat the beneficial actions that have activated the pathway. Food ingestion, drinking water in thirsty moments, establishing social connections with other people or having sex, will promote, then, through activation of the system, the motivation of the subject to further repeat the actions, and in last resort ensure the individual's survival.

Anatomically, the pathway is formed by the ventral tegmental area (VTA), the nucleus Accumbens (NAcc), and the prefrontal cortex. Altogether creating an ensemble that connects motivation processes and motor activity (*Soares-Cunha et al., 2016*). Although the mesolimbic pathway has dopamine as the principal neurotransmitter of the pathway, glutamate and GABA participate in the mesolimbic system (*Steketee and Kalivas, 2011*).

The VTA consists in an heterogeneous neuron pools (*Phillipson, 1979*) placed next to the substantia nigra (*Oades and Halliday, 1987*). Approximately, 60% of the neurons of the VTA are dopaminergic (*German and Manaye, 1993*), and project to different areas of the brain like NAcc and prefrontal cortex (*Bariselli et al., 2016; Morales and Margolis, 2017*). Upon a rewarding action, the ventral tegmental area is activated and dopamine and glutamate are released at the NAcc and the prefrontal cortex (*McClure et al., 2003; Tecuapetla et al., 2010*), promoting the behavioural adaptations and neuroplasticity to establish an association between the reward and the action (*Jay, 2003*). The ventral tegmental area could be regulated by the different projection neurons that innervate this structure. Moreover, the expression of different GPCR like the corticotropin-releasing factor receptor (CRF-R) involved in stress responses, the orexin receptor (Ox-R) involved in food intake or the sleep-wake cycles, the ghrelin receptor (GHS-R) or the sigma-1 and sigma-2 receptors make this structure highly adjustable to different signals besides to the dopaminergic, glutamatergic and GABAergic signals that intrinsically regulate the reward pathway.

The NAcc projects GABAergic neurons to the VTA, generating a negative feedback in order to modulate the system (*Steketee and Kalivas, 2011*). In turn, besides VTA afferences,

NAcc also receives neural connections from structures like amygdala, hypothalamus or hippocampus, which are related with emotions and memory, and also from the cortex (*Di Ciano et al., 2001; Steketee and Kalivas, 2011*). Altogether will promote refined responses and the preservation of the behaviours that have brought the positive feeling.

The last region of the reward pathway is the prefrontal cortex. This area receives dopaminergic neurons from the VTA and NAcc projection neurons, and in turn, this structure is innervating the motor cortex, the VTA and the NAcc (*Joffe et al., 2014*) (Figure 21). The prefrontal cortex is in charge of the decision-making processes and in shaping social behaviours (*Yang and Raine, 2009*). Moreover the coordination of thoughts and actions according to the inner goals (*Miller et al., 2002*), as well as the modulation of the intensity of the subject responses are carried out in this brain region (*Bush et al., 2002*).

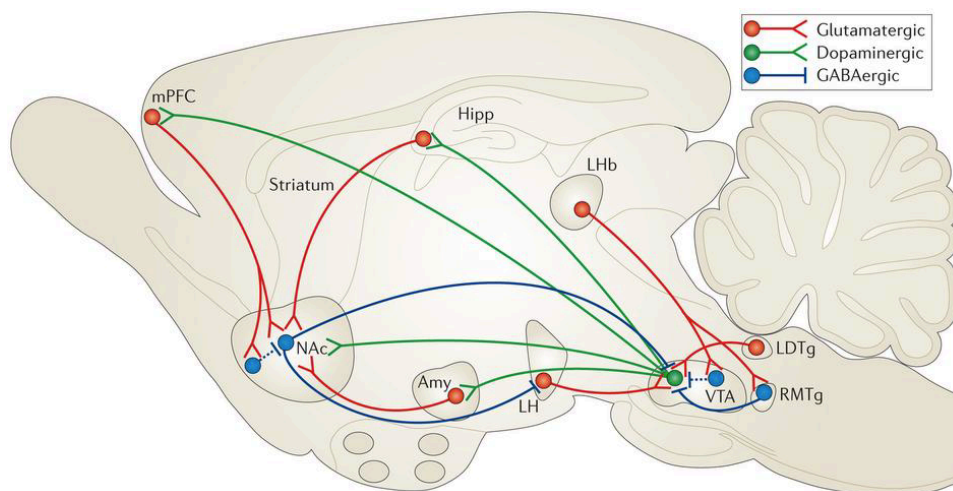


**Figure I21. Schematic representation of the dopaminergic, glutamate and GABAergic connections of the reward system in a rodent brain (Russo and Nestler, 2013).**

Substances of abuse alter the reward system functionality. For instance, there are multiple evidence linking cocaine consumption with increases of dopamine and an unbalance of the mesolimbic pathways and prefrontal cortex function (*Belin and Everitt, 2008; Pettit and Justice, 1991; Roberts et al., 1977; Will et al., 2016*). In fact, the involvement of these brain areas and their deregulation is what makes cocaine, and other drugs of abuse, substances of a high addictive potential.

### I.5.2 Drug addiction development

Drug addiction is a chronic disease defined by the compulsive seek and consumption of psychostimulant substances, leading to an uncontrolled ingestion of the drug of abuse and the appearance of negative emotional states in the patients. Not only consumers of the drug suffer the negative effects of the consumption, but also affect the family, anyone akin to the



patient and the whole society. The National Institute on Drug Abuse (NIDA) estimates in 700 dollar billions regarding health care, low productivity and crimes, the cost of tobacco, alcohol and illegal drugs consumption in the American society.

Often, addiction correlates the psychoactive compound consumption with the unbalance of chemical equilibrium of the brain and the subsequently alteration of neuronal function (*Joffe et al., 2014*). More precisely, these compounds affect the brain reward system, altering the motivation, behaviour, mood, memory and other related pathways (*Joffe et al., 2014*). The substances that produce those effects are, among others, alcohol, tobacco, cannabinoids, opioids, psychostimulants, hallucinogens or synthetic drugs (*Joffe et al., 2014*). Nonetheless, some behaviours that not imply substance consumption could be catalogued as addictive, like sex or gambling, to name but a few (*DiLeone et al., 2012*). Moreover, addiction implies the incapacity of the consumer to abstain himself from the ingestion of the addictive compound or the repetition of the behaviours even the detrimental effects of that consumption or action.

Establishment of chronicity is characterised by the cyclic progression through consumption, withdrawal and relapse phases (*Koob and Volkow, 2016*). At the beginning of the condition, the drug ingestion is motivated by the positive reinforcements of the substance (euphoria, pleasure...) but upon addiction progression, the drug consumption is driven by the urge of relieve the negative reinforcements produced by the abstinence syndrome during the withdrawal phase. Once this point is achieved, compulsive behaviours in order to obtain new doses and multiple changes in the patient's brain happen, and affected individuals are more prone to future relapses. Uncontrolled addiction will lead the subject to shorter consumptions time-spans, with more time, to forget the basic needs of water and food ingestion and, in the last term, to the death.

### **I.5.3 Cocaine mechanism of action**

Cocaine is a purified compound of the originally South-American *Erythroxylum coca* plant. Chew or make infusions of coca plant leaves was common in ancient Andean cultures, to produce euphoria or reduce hunger, thirst, fatigue and pain or even used to treat altitude sickness. In 1860 Albert Neiman isolated cocaine form the plant, and since then utilisation and consumption of the drug has dramatically increased. Initially, the substance was included in wines, in Coca-Cola or even in mouthwashes, being widely used. Years later appeared the first evidence of cocaine detrimental effects, provoking a reduction, little by little, of its employment in legal products. The efforts of the governments to forbid the seeding,

distribution and use of the drug have not prevented cocaine being consumed worldwide. Moreover, some reports reflect a tendency for cocaine consumption to be increasing, raising awareness not only to the detrimental effects provoked to health but also to the social and criminal problems associated to the distribution and consumption of this drug of abuse.

Cocaine is classified as a psychostimulant substance. Like caffeine, nicotine or any other psychostimulant, its consumption leads to increased motor and cognitive activity, reinforcing the waking state, attention and awareness. However, contrarily to caffeine and nicotine, cocaine is considered a drug of abuse. Together with other psychostimulant drugs like methamphetamine or ecstasy, it is a regulated substance. Nevertheless, in 2014 was estimated that 250 million people consume cocaine (2016 WHO report on drugs).

Evidence shows that cocaine inhibits the uptake of monoamine neurotransmitters like norepinephrine (*Ross and Renyi, 1967*), dopamine (*Heikkila et al., 1979; Moore and Gudelsky, 1977; Ritz et al., 1987*) or serotonin (*Moore and Gudelsky, 1977*). Posterior studies attributed the behavioural (*Colpaert et al., 1978; De Wit and Wise, 1977; Miczek et al., 1982*) and motor (*Giros et al., 1996*) effects of cocaine to its action on the dopamine transporter more than into the serotonin or norepinephrine transporters. The proposed mechanism of action was the blockade of the transporter, preventing the dopamine recapture from the synaptic cleft to the neuron cytosol. In this line, Di Chiara and Imperato presented, in 1988, microdialysis-based evidence of increased dopamine levels in Nucleus Accumbens after cocaine administration (*Di Chiara and Imperato, 1988*). Thanks to the molecular modelling of Beuming and collaborators, in 2008, the dopamine transporter (DAT) domains involved in the interaction with cocaine were elucidated. According to this study, the TM  $\alpha$ -helix 1, 3, 6 and 8 of the transporter are in charge of the interaction with the psychotropic substance (*Beuming et al., 2008*). These domains are also responsible of the interaction with dopamine, and in case cocaine is already interacting with them, dopamine reuptake will be inhibited (Figure 22).

The above described is one of the cocaine's mechanisms of action, however, not all the dopamine increases promoted by the drug are explained by its action on DAT. Several studies have suggested that the phasic activity of the dopaminergic neurons of ventral tegmental area (VTA) could generate learning signals upon unexpected rewards (*Schultz et al., 1997*). The purpose of the signal is to promote the learning of the actions that have implied a reward and motivate the subject to repeatedly seek them. However, when the reward is predictable, the dopaminergic neurons are not activated and the learning signals cease (*Lüscher, 2016*). In this context, the pharmacological potency of the drug of abuse create an inappropriate learning process that promotes the seek and consumption of the drug at



## INTRODUCTION

expense of forgetting the rest of the physiological behaviours (Lüscher, 2016). Based on this model, cocaine addiction should be considered a disease of the dopaminergic system, whose function has been altered and increased. The confirmation of the model came with the Adamantidis and collaborators work of 2011, where animals optogenetically stimulated in VTA dopaminergic neurons showed a place preference, without involving the DAT (Adamantidis *et al.*, 2011). Self-stimulation of these neurons promotes a positive reward that lead the animals to continuously repeat the actions needed to obtain the reward (Pascoli *et al.*, 2015). Interestingly, the injection of a drug of abuse produces the same effect as the self-stimulation, the cease of the continued actions needed to obtain the reward (Pascoli *et al.*, 2015). Similarly, some studies with knockout animals deficient in monoamine transporters or dopamine transporters, have failed in prevent the self-administration of the drug of the animals or the place preference observed in behavioural studies (Hnasko *et al.*, 2007; Rocha, 2003), thus demonstrating the existence of other mechanisms of action of cocaine besides the blockade of the DAT.

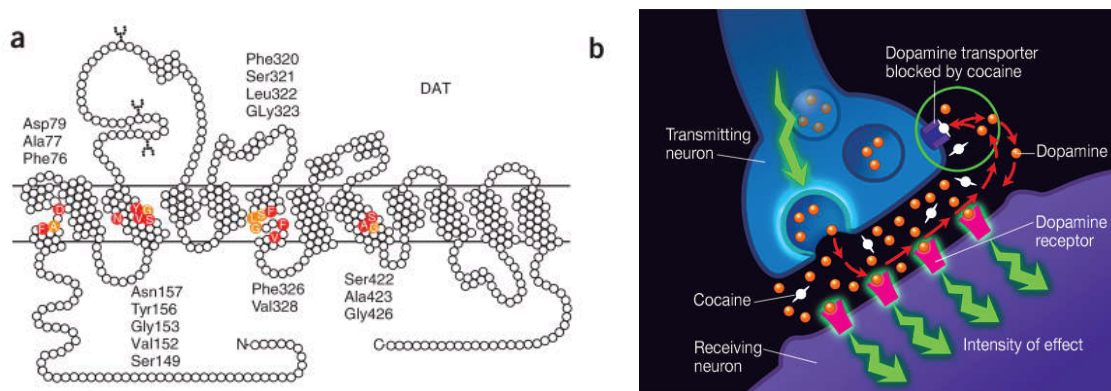


**Figure I22. Cocaine effects on dopamine transporter.** A) Representation of the dopamine transporter DAT. In red are represented the interacting residues between cocaine and the transporter (Beuming *et al.*, 2008). B) Cocaine classic mechanism of action. Through the interaction with DAT, dopamine levels in the synaptic cleft are increased (Obtained from the National Institute of Drug Abuse, NIDA)

Another relevant aspect still in study is the cocaine's mechanism of action promoting behavioural changes. After exposition to the drug, excitability and hyperactivity appear, often in form of aggressiveness and irritability in first instance, and in erratic and compulsive behaviour later. The hypothetic mechanism driving those chronic cocaine consumption effects is the synaptic plasticity alteration. This changes leave the addict more vulnerable, being prone to relapses (Wolf, 2016). Different changes in dendrites after cocaine consumption have been associated with behavioural changes (Christian *et al.*, 2017; Robinson and Kolb, 1999; Robinson *et al.*, 2001; Zhu *et al.*, 2016). These changes implied neurofilament, cytoskeletal or gap junction proteins, being these proteins involved in stabilisation and integration of the

receptors in synapses or in the deregulation of neuronal excitability mechanisms (*Creed et al., 2016*).

Noteworthy, studies in non-neuronal cell models without expressing DAT showed some effects of cocaine. This fact arose the question of what mechanisms could be behind this response to cocaine. Further studies described the interaction of the drug with different elements, and nowadays is accepted that cocaine could interact at physiological concentrations with, for instance, sigma receptors (*Mésangeau et al., 2008*). There are two sigma receptors, sigma-1 and sigma-2, which are now considered as potential targets to combat cocaine addiction.

### **I.5.4 Sigma receptors and their relationship with cocaine**

Sigma-1 receptors were originally described as opioid receptors, due to their ability to bind an opioid-like mimetic, the SKF-10,047. This ligand cannot interact with  $\kappa$  or  $\mu$ -opioid receptors, but its interaction with sigma-1 receptors was enough to classify these receptors as members of the opioid receptor subfamily (*Martin et al., 1976*). Nonetheless, the action of the receptor was not blocked by naloxone or naltrexone, two opioid antagonists, with the consequent classification of sigma-1 as non-opioid orphan receptor (*Vaupel, 1983*). It was not until 1996 that the sigma-1 receptor was cloned, confirming it was neither a opioid-receptor nor a GPCR (*Hanner et al., 1996*). Sigma-1 receptor does not present similarities with any other human protein. More recently, Schmidt and collaborators were able to obtain its three-dimensional structure (*Schmidt et al., 2016*). The crystal presents a trimeric structure with protomers containing one transmembrane domain and a C-terminal hydrophobic domain in contact with the lipid membrane (Figure 23). Sigma-1 receptor is widely distributed in peripheral tissues (*Stone et al., 2006*) as well as in different CNS areas, mainly in brain regions devoted to memory, emotions, sensory and motor functions (*Guitart et al., 2004*). Looking into the subcellular localization of the receptor, it can be found in endoplasmic reticulum performing chaperone functions (*Hayashi and Su, 2007*) although it also may be located in the plasmatic, mitochondrial and nuclear membranes (*Alonso et al., 2000*). Sigma-1 is able to bind different compounds, among which stands out the, haloperidol, steroids like progesterone or cocaine (*Hayashi and Su, 2005*). However, its endogenous ligand has not been discovered yet. Define this compounds as agonists or antagonists of the receptor is difficult due to the inability to signal and the structure of the receptor, with no resemblance to the GPCR or channel receptors. In spite this fact, the sigma-1 ligand PRE-084 has been classified as agonist, and haloperidol as antagonist. PRE-084 dissociates in a dose-dependent manner sigma-1





## INTRODUCTION

receptor from the binding immunoglobulin protein/78 kDa glucose-regulated protein (BiP/GRP-78) (Hayashi and Su, 2007), while haloperidol inhibits this disassociation.

Despite not having signalling downstream machinery, in presence of agonists, sigma-1 receptor interacts with several proteins (Su et al., 2010). These interactions enable sigma-1 receptor to modulate the activity of GPCR and ion channels (Aguinaga et al., 2018; Kim, 2017; Navarro et al., 2013; Wu and Bowen, 2008). It is hypothesised that, through these wide range of interactions, sigma-1 receptor might have a role in disorders like depression, neuropathic pain or cardiovascular diseases (Schmidt et al., 2016; Su et al., 2010). Likewise, it has been described a mutation in this receptor responsible of the juvenile amyotrophic lateral sclerosis development and/or progression (Al-Saif et al., 2011; Mavlyutov et al., 2013).

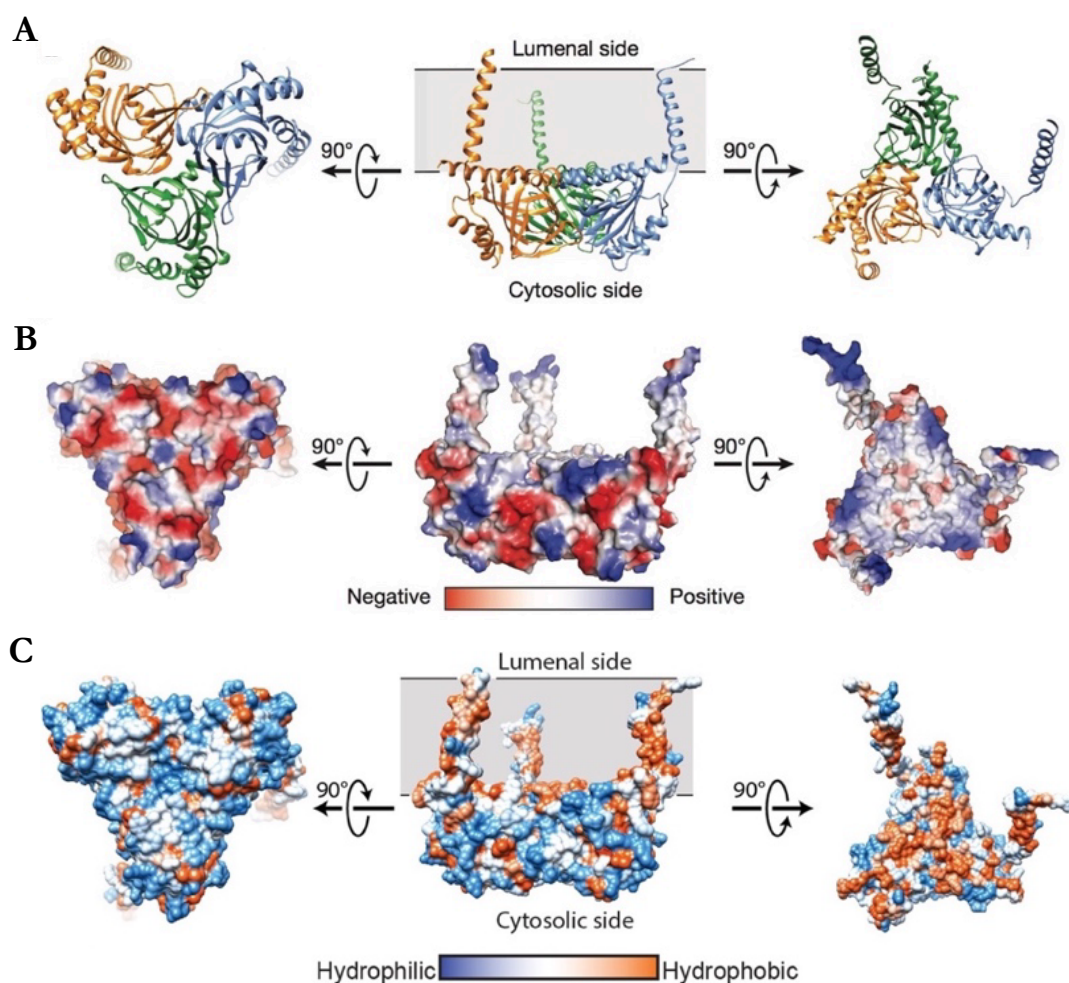


**Figure I23. Crystal structure of sigma-1 receptor.** A) Perpendicular to the plasmatic membrane image. In a lateral view, the receptor presents a plain surface associated with the membrane. B) Coloured model according to the electrostatic potential, revealing a cytosolic polar surface (left) and a non-polar surface that interacts with the membrane and it is surrounded by positive charges. C) Structure of sigma-1 receptor shows a hydrophilic surface (in blue) in the cytosolic face (left), while the transmembrane domains and the surface in contact with the membrane are hydrophobic (in orange and at right). The plasmatic membrane is shown in grey (Schmidt et al., 2016).

Focusing on the role of sigma-1 receptor in cocaine addiction, Matsumoto and collaborators demonstrated the capability of this receptor to bind cocaine at assumable

concentrations in vivo (*Matsumoto et al., 2001*). Indeed, cocaine showed a moderate affinity for sigma-1 receptors in radioligand binding assays (*Matsumoto et al., 2003*). However, previous results, even though without address the interaction between the drug and the receptor, had already suggested a role of sigma-1 receptor in different aspects of cocaine consumption like hyperlocomotion (*Barr et al., 2015; Menkel et al., 1991*), sensitization (*Ujike et al., 1996*), reward mechanisms (*Romieu et al., 2000, 2002*) or even in convulsions and lethality (*Matsumoto et al., 2001*). In fact, the reduction of sigma-1 receptor levels in the brain with antisense oligonucleotides diminished the convulsive and locomotive effects of cocaine consumption (*Matsumoto et al., 2001, 2002*) and antagonists contribute to reduce cocaine lethality in animal models (*Matsumoto et al., 2004*), while agonists of sigma-1 receptor enhanced the toxicity of the drug of abuse (*Matsumoto et al., 2002, 2003*).

In the same line, sigma-1 receptor interacts and modulates different GPCR somehow involved in cocaine or drug addiction. It has been demonstrated that upon cocaine binding, sigma-1 receptor is able to disrupt the interaction of CRF1 and OX<sub>1</sub> receptor (*Navarro et al., 2015*) expressed in the VTA and characterised by a negative crosstalk in cAMP and MAPK signalling levels. With the disruption of the interaction, the negative crosstalk disappears and stress conditions could lead to cocaine seek and to relapses (*Navarro et al., 2015*). Similarly, interactions of sigma-1 receptor with the dopamine receptors have also been described. On one hand, upon the binding of cocaine, sigma-1 receptor is able to interact and enhance the D<sub>1</sub>R cAMP and ERK functionality (*Navarro et al., 2010b*), while, on the other hand sigma-1 receptor can potentiate MAPK phosphorylation and inhibit cAMP production of the D<sub>2</sub>R (*Navarro et al., 2013*). These results, altogether, show that the opposite signalling pathways activated by D<sub>1</sub>R and D<sub>2</sub>R are differently and fine regulated by cocaine-bound sigma-1 receptor. Overall, these results also suggest a molecular mechanism through which cocaine could generate addiction and molecularly predispose the brain to relapses and future cocaine consumption, while it also could explain the locomotive effects of the drug (Figure 24). Moreover, recent studies of Aguinaga and collaborators have demonstrated that cocaine regulates D<sub>1</sub>R activity upon time, involving an interaction of sigma-1 receptor and D<sub>1</sub>R in acute cocaine intakes and an interaction of the sigma-2 receptor and D<sub>1</sub>R in chronic drug consumption (*Aguinaga et al., 2018*). Therefore, suggesting that D<sub>1</sub>R is going to be differently regulated by sigma-receptor depending on the stage of the cocaine addiction.



On its behalf, the first evidences of the sigma-2 receptor existence came from radioligand studies which the sigma-1 receptor was blocked (*Hellewell et al., 1994*), but it was not until 2011 when Xu and collaborators identified the progesterone receptor membrane component-1 (PGRMC-1) as the potential sigma-2 receptor (*Xu et al., 2011*). Mass spectrophotometry and radioligand assays confirmed the results, however, the determined molecular weights of PGRMC-1 were 22 and 28 kDa, while the value obtained for sigma-2 receptor was 21.5 kDa (*Hellewell et al., 1994*). Despite that post-transcriptional modifications or alternative splicing could explain these weight differences, some researchers put in doubt the identification done by Xu's laboratory due to the divergence in the molecular weights. In any case, PGRMC-1 belongs to the membrane-associated progesterone receptors family (*Cabill, 2007; Mifsud and Bateman, 2002*), although it cannot bind progesterone by itself (*Min et al., 2005*) and does not have any homology with any nuclear steroid receptor (*Mifsud and Bateman, 2002*). The sigma-2 receptor is distributed in the lungs, liver, brain, liver, heart, muscles and pancreas (*Gerdes et al., 1998; Krebs et al., 2000*), while it is, at subcellular level, expressed in endoplasmic reticulum, mitochondria, cell membrane and lysosomes, with the notable

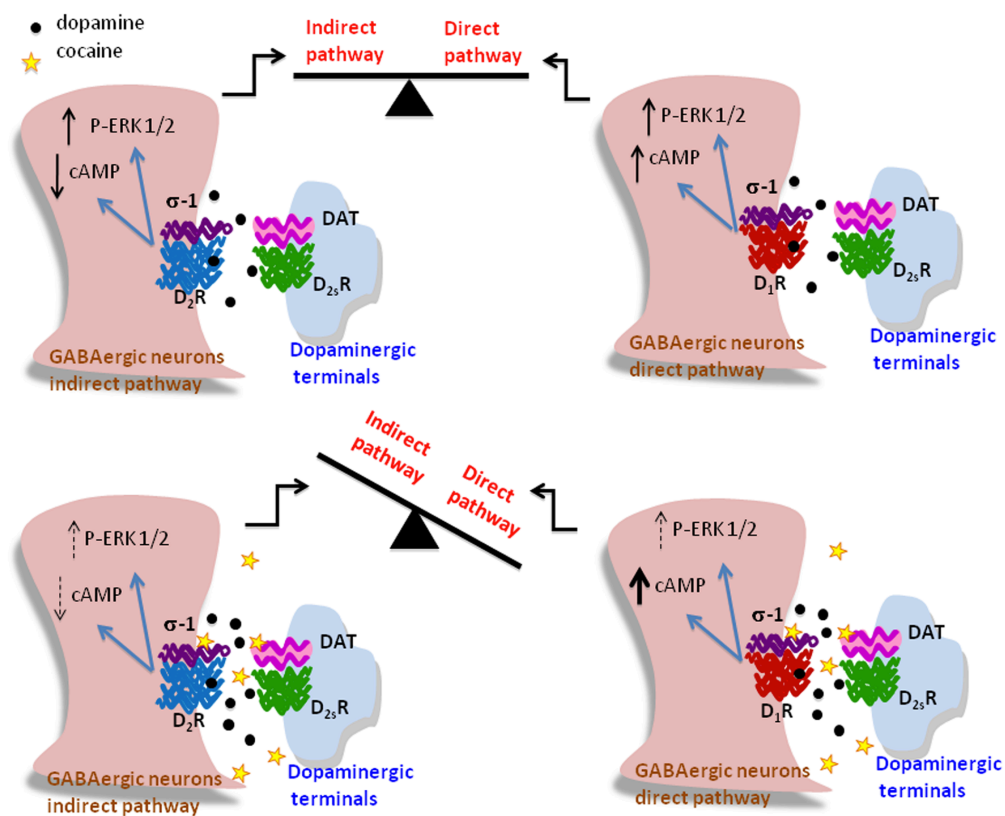


**Figure I24. Representative scheme of cocaine and sigma-1 receptor regulation of D<sub>1</sub>R and D<sub>2</sub>R in striatal pathways.** Direct and indirect pathways promote a balanced regulation of movement by the opposite effects of dopamine through D<sub>1</sub>R and D<sub>2</sub>R (Above). In presence of cocaine, and the increase of dopamine due to DAT blocking, cocaine-bound sigma-1 receptor enhances D<sub>1</sub>R activity in GABAergic neurons of the direct pathway, while inhibits the D<sub>2</sub>R function in the indirect pathway, unbalancing the movement control (*Navarro et al., 2013*).

exception of the nucleus (Zeng *et al.*, 2007).

The role of sigma-2 receptor has not been well established yet. However, some studies suggest that this receptor is involved in cell proliferation and cholesterol biosynthesis (Abmed *et al.*, 2010; Robe *et al.*, 2009). Moreover, it has been defined as a proliferation biomarker for some tumours (van Waarde *et al.*, 2015). In fact, both sigma-1 and sigma-2 receptors have been linked to quick proliferation and are expressed in cancer cells. Particularly interesting is the case of sigma-2 receptor, which is 10-folds more expressed in proliferative than quiescent cancer cells (van Waarde *et al.*, 2010), and its activation could lead to cancer cell death (Berardi *et al.*, 2009; Cramford and Bowen, 2002) by apoptotic or non-apoptotic cell death mechanisms (Mach *et al.*, 2013; Zeng *et al.*, 2014). Paradoxically, PGRMC-1 agonists (Colabufo *et al.*, 2004) and sigma-2 receptor antagonists (Abmed *et al.*, 2010; Jonbete *et al.*, 2010) could inhibit tumour progression. These apparently contradictory results could be explained by the difficulty to determine any sigma receptor ligand as agonist or antagonist. In this line, some previous agonist-classified sigma-2 receptor ligands turned out to be antagonists and vice versa (Zeng *et al.*, 2014).

Nowadays, the relevance of sigma-2 receptor in apoptosis and programmed cell death is drawing the attention of many researchers, however, the role of this receptor in cocaine and drug of abuse studies is also gaining ground (Garvés-Ramírez *et al.*, 2011). In 2007, it was observed that cocaine-induced behavioural effects were attenuated after a sigma-2 receptor antagonist treatment (Matsumoto *et al.*, 2007), and posterior studies revealed that sigma-2 receptor antagonists reduced the hyperlocomotive effects provoked by cocaine in mice (Lever *et al.*, 2014).

Regarding the molecular level and similarly to sigma-1 receptors, sigma-2 receptors interact with components of the dopaminergic system. In this line, cocaine could modulate the dopaminergic neurotransmission in the VTA by interacting with either sigma-1 or sigma-2 receptors. Moreover, a recent study indicates that D<sub>1</sub>R-sigma-1 receptors interaction is more relevant in acute cocaine consumption, while the D<sub>1</sub>R-sigma-2 receptor interaction plays a predominant role in chronic consumption of the substance (Aguinaga *et al.*, 2018).

In summary, the results suggest a role for both sigma-1 receptor and sigma-2 receptor in cocaine addiction, and part of the reason lies in the potential of these receptors to interact with GPCR. Nonetheless, further studies are required to confirm the potential of sigma receptors as targets to fight cocaine addiction and to define the best therapeutic approach, i.e. whether to use agonist or antagonists of these receptors.



### I.5.5 Ghrelin, ghrelin receptors and the control of food intake

Ghrelin is an orexigenic peptide hormone. This peptide acts as a signal to predispose the subject to ingest, giving reasons to those who consider ghrelin as the ‘hunger hormone’. The gene codifying for ghrelin is placed in the third chromosome (3p25-26), and generates a peptide of 117 amino acids named preproghrelin. Posterior enzymatic cleavages enable the obtain of the proghrelin and the anorexigenic peptide obestatin (*Schellekens et al., 2010*) (Figure

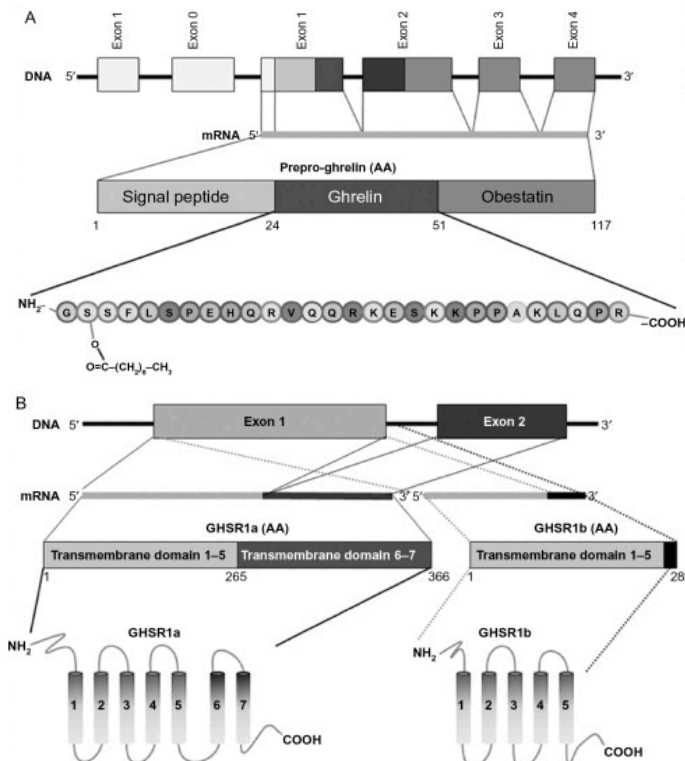


**Figure I25. Human ghrelin and GHS-R1 receptor gene structure.** A) The human ghrelin gene codes for 117 amino acid preproghrelin which is enzymatically cleaved to proghrelin and a C-terminal peptide obestatin. A posterior acylation of serine-3 is necessary for the mature conformation of the peptide. B) The two exons of GHS-R gene codify for the full-length GHS-R1a or the splicing alternative GHS-R1b lacking the second intron (*Schellekens et al., 2009*).

25A). A final step for ghrelin synthesis is the acylation of a serine residue of the peptide (*Yang et al., 2008*). This final process confers ghrelin its ability to activate its receptors and to be functional. In plasma, ghrelin is found in either acylated (just 10% of the circulating ghrelin) or deacylated forms (the 90% of the ghrelin found in plasma). The differential forms of the peptide found in blood are explained by the fact that the acylated form of the peptide has a life span in blood of only 8 minutes (*Kojima et al., 1999*). Ghrelin is mainly synthesized at the oxyntic cells of the stomach and then liberated to the plasma, while small production occurs in the brain at the arcuate nucleus of the hypothalamus. Ghrelin is the only peptide hormone with a post-transcriptional modification involving acetylation, and its expression in plasma fluctuates during the day, following a circadian rhythm (*Silver and Balsam, 2010*). Therefore, the levels of ghrelin are increased before ingest, while they diminish after eating (*Cabral et al., 2017*). This peptide is characterised indeed, for its ability to cross the blood-brain barrier, even though the mechanism through which this is achieved is still unknown. Once in the brain, ghrelin can act in the ghrelin receptors localized in hypothalamus, amygdala, hippocampus, in

dopaminergic regions of the mesencephalon and striatum, and in the VTA (Mason *et al.*, 2014) (Figure 26).

Ghrelin can act either in peripheral tissues or the CNS. In the periphery, its action promotes the motility and the gastric secretion of HCl, as well as modulates the endocrine function of the pancreas and it is related to the glucose metabolism. Moreover, ghrelin seems to be involved in different cardiovascular diseases (Lilleness and Frishman, 2016), and promotes the proliferation of adipocytes of the white adipose tissue (Lanfranco *et al.*, 2010; Wells, 2009). Regarding the ghrelin actions in the CNS, it can stimulate appetite through its action on the hypothalamus, as well as promoting the release of Growth hormone in the hypophysis.

Growth hormone can be released from hypophysis or pituitary gland upon action of peptides known as growth hormone secretagogues. Ghrelin is one of them, and in fact, the ghrelin receptor was first identified as the Growth Hormone Secretagogue Receptor (GHS-R). This receptor was cloned in 1996 by Howard and collaborators (Howard *et al.*, 1996), and encodes a 366 amino acid and 41 kDa protein (Howard *et al.*, 1996) that belongs to the GPCR family A, and is known as GHS-R1a. However, an alternative splicing of the gene enables the transcription of the receptor known as GHS-R1b (Schellekens *et al.*, 2010) (Figure 25B). Despite that it has been described that the receptor GHS-R1a, a full containing 7-TM domain receptor, upon binding of ghrelin activates  $G\alpha_q$  subunit, promoting the increase of  $IP_3$  and the release of intracellular calcium storages, activation of  $G\alpha_i$  or even  $G\alpha_s$  has been described in certain situations (Damian *et al.*, 2015; Holst *et al.*, 2005). On its behalf, GHS-R1b lacks the sixth and seventh transmembrane domains of GHS-R1a. The absence of this two domains, prevents the receptor from neither binding the ghrelin peptide nor to couple G-protein, therefore not being capable of activate or promote a downstream signalling (Mary *et al.*, 2013). Recent studies have started to shed some light into the role of GHS-R1b. It has been described, that GHS-R1a and GHS-R1b might be co-expressed in the same cells, and that the two proteins are able to form homodimers and also to heterodimerizate between them, existing a negative regulation of GHS-R1b towards GHS-R1a (Mary *et al.*, 2013). Two different modulation mechanisms have been proposed. In the first, the inability of GHS-R1a to reach the plasma membrane is overcome upon the interaction with GHS-R1b, thus just upon heterodimerization with GHS-R1b, is GHS-R1a able to reach the plasma membrane (Chow *et al.*, 2012). The second mechanism proposes a negative allosteric modulation from GHS-R1b towards the GHS-R1a, preventing the functional ghrelin receptor to signal upon interaction with the truncated ghrelin receptor (Mary *et al.*, 2013). These two mechanisms would not be, necessarily, excluding each other, enabling the possibility of happen at the same



time (Mary *et al.*, 2013).

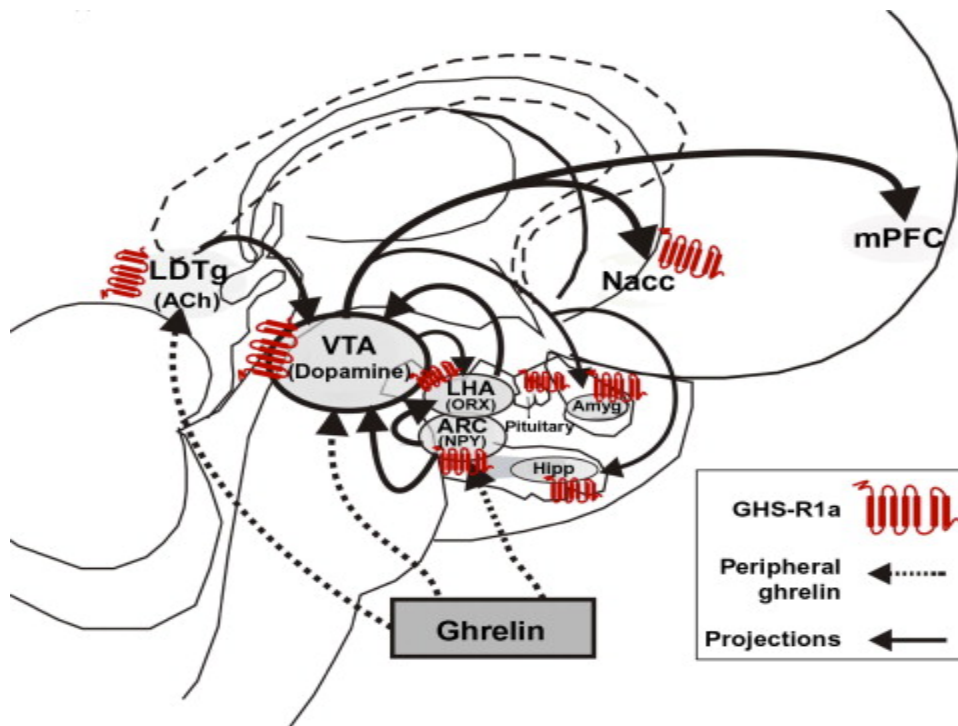


**Figure I26. Ghrelin signalling in the mesolimbic reward circuitry in human brain.** Schematic representation of ghrelin-mediated regulation of homeostatic food intake and reward in human brain. GHS-R1a expression is found at amygdala, arcuate nucleus, laterodorsal tegmental area, lateral hypothalamic area, the hippocampus and the medial prefrontal cortex (indicated in red). Peripheral ghrelin can directly activate VTA dopaminergic neurons that project to NAcc. Moreover, ghrelin modulation of VTA projections to other brain regions like amygdala or hippocampus has been suggested (Schekellens *et al.*, 2013).

### I.5.6 Ghrelin in the reward pathway and its involvement in addiction processes

Despite that ghrelin is mainly synthesised at the stomach, the majority of its actions take place at the brain. It has been demonstrated that intracerebroventricular administrations of the peptide can stimulate, independently, food ingest and growth hormone segregation (Howick *et al.*, 2017; Shintani *et al.*, 2001), therefore being a regulator of both systems. However, the expression of ghrelin receptors in VTA, amygdala or different dopaminergic brain areas suggests that the hormone could be influent, somehow, to reward system (Zigman *et al.*, 2006).

Activation of GHS-R1a present at the VTA could have a role in motivating the seek of palatable food and the subsequent obtain of reward (Wise, 2002). Reward pathway is activated with the experience, reward expectations and/or exposure to delightful stimulus (Richardson and Gratton, 1998). In this regard, many authors have proposed a role of ghrelin in modulating the reward system, regulating the appetite, anticipating the food ingestion feelings, triggering expectations and creating a positive reinforcement. In this line, administration of ghrelin antagonists in the VTA or NAcc, or the use of animals deficient in the receptor could i) block the orexigenic effects of peripheral administration of ghrelin (Abizaid and Horvath, 2008;

*Abizaid et al., 2006; Jerlhag et al., 2006; Skibicka et al., 2011*), and ii) modify the time spent in conditioned place preference zones where animals receive a food reward (*Egecioglu et al., 2010; Perello et al., 2010*). Moreover, looking into the molecular details, it has been demonstrated a crosstalk between ghrelin and dopamine, with the peptide hormone amplifying the dopamine produced signalling thanks to the formation of a GHS-R1a-D<sub>1</sub>R heteromer (*Jiang et al., 2006*). These results evidence the role of ghrelin in the reward system, suggesting that this peptide hormone could influence subjects to seek and to consume food in order to obtain the reward that palatable ingestions bring along.

According to the evidence and the relationship between ghrelin and the reward system, it is not difficult to hypothesise that the ghrelinergic system might be involved in drug addiction. In this line, Jerlhag and collaborators demonstrated the requirement of ghrelin signalling to generate alcohol addiction, suggesting ghrelin and its receptors as good targets to tackle alcohol addiction (*Jerlhag et al., 2009*). Similarly, it is worth considering a role of ghrelin in cocaine addiction. In fact, one of the effects derived from cocaine consumption is the reduction of the hunger feeling. Moreover, ghrelin receptors are co-expressed with dopamine receptors or sigma receptors in multiple brain regions, and even can heteromerize with them (*Jiang et al., 2006*). Cocaine addiction dramatically alters the dopaminergic pathways in the brain. To date, it has been seen the relationship of ghrelin and the motivation to seek palatable food, as well as the link between cocaine and reward pathways or the reduction of hunger after cocaine consumption. According to this background, it is tempting to speculate about a molecular mechanism linking cocaine addiction and the ghrelinergic system. However, further research has to be done in order to reveal such interaction and its possible physiological consequences or its involvement in addiction processes.







## **II. AIMS**



## II. AIMS

G protein coupled receptors are responsible of several functions within the Central Nervous System in both physiological and pathological conditions. Thus, the modulation of GPCRs, through homo- or heteromerization processes, through interaction with non-GPCR proteins, or regulation of the intrinsic characteristics of the GPCR through allosterism, can have implications in either addiction or neuroinflammation. GPCR actively participate and regulate both phenomena, making of great importance to disclose the biochemical and molecular characteristics of the receptors implicated. In this frame, *the General Aim of this thesis is to investigate the relevant molecular and functional G-protein coupled receptor interactions in neuroinflammation and addiction.* To reach this overall goal, four particular aims were formulated.

First, the Thesis is focused on the endocannabinoid system and its two receptors. CB<sub>1</sub>R and CB<sub>2</sub>R are GPCR with a fundamental role in homeostatic control of body temperature, neurotransmission or immune response. Regarding the latter, accumulation of  $\beta$ -amyloid in Alzheimer's Disease or  $\alpha$ -synuclein in Parkinson's Disease, bring about neuroinflammatory processes in which microglial cells participate. Microglial cells express both CB<sub>1</sub> and CB<sub>2</sub> receptors, and endogenous or exogenous cannabinoids acting through its receptors, may influence the establishment of pro-inflammatory or neuroprotective microglial phenotypes. In order to shed some light into the role of cannabinoid receptors when microglial cells are activated in conditions mimicking neuroinflammation, the first specific aim was:

**Aim I – To investigate the role of CB<sub>1</sub> and CB<sub>2</sub> receptors and the CB<sub>1</sub>-CB<sub>2</sub> receptor heteromer in different activation microglial phenotypes.**

Interaction with non-GPCR proteins could modulate the activity of a given GPCR. Despite the potential of calcium sensor proteins as GPCR regulator, very few interactions between members of these two protein families have been described. Upon binding calcium ions at their EF-hand domains, calcium sensors suffer conformational changes that enable them to interact and modulate the function of different proteins of the signal transmission



machinery. The role of calcium is very relevant in enkephalinergic GABAergic neurons of the motor pathway in which the CB<sub>1</sub>R is expressed. In this context, the second aim of the Thesis was:

**Aim 2 – To identify interactions between CB<sub>1</sub>R and EF-hand domain-containing calcium proteins and their functional consequences.**

GPCRs play a key role in the control of the reward pathway thus impacting on plasticity events related to drug addiction. The role of the reward pathway is ensuring survival thus leading to consumption of food or water, and to promote behaviours like sex that are both necessary for survival and pleasant. Among the different neurotransmitters and compounds acting on the system, the orexigenic peptide hormone ghrelin contributes to trigger the food seeking behaviour. The molecular actions of ghrelin rely on the growth hormone secretagogue receptor 1 (GHS-R1a) which is a GPCR. However, due to alternative splicing, there is a truncated isoform of the receptor named GHS-R1b. This truncated receptor, lacking the transmembrane domains 6<sup>th</sup> and 7<sup>th</sup> cannot bind the hormone and does not interact with any G protein. It has been demonstrated that both ghrelin receptors can heteromerise, however, the role and function of the truncated GHS-R1b receptor is not fully understood. Accordingly, the third aim of the Thesis was:

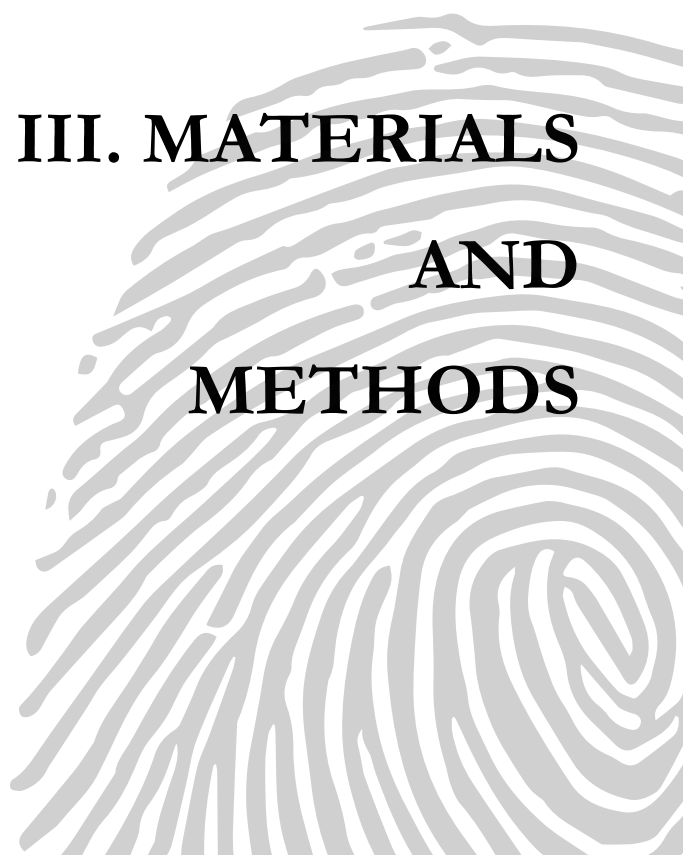
**Aim 3 – To give insight into the functional role of the alternatively-spliced truncated form of the ghrelin receptor gene product.**

Due to its involvement on the mechanisms underlying motivation to consume food, alterations in ghrelin receptors signalling have been proposed as relevant in food intake disorders like obesity. Interestingly, the consumption of cocaine, a drug of abuse, leads to a loss of appetite and a reduction of food seeking. The actions of cocaine are mainly mediated by the blockade of dopamine transporters and the subsequently increase in the dopamine available to pre- and post-synaptic dopamine receptors. However, cocaine also binds, at physiologically relevant levels, to the non-opioid sigma-1 and sigma-2 receptors. Although the physiological role of sigma receptors is not known yet, they can interact with GPCRs. Taking

together all this information we hypothesised that sigma and ghrelin receptors could be closely involved in the anorexigenic effect of cocaine. To test this hypothesis, the fourth aim of the Thesis was:

**Aim 4 – To investigate direct and indirect interactions between sigma-1 receptor and ghrelin receptor and to determinate the modulatory role of cocaine on the function of sigma-1-ghrelin receptor complexes.**





**III. MATERIALS  
AND  
METHODS**





### **III. MATERIALS AND METHODS**

#### **III.1 Expression vectors and fusion proteins**

Several fusion proteins were constructed in order to perform the different assays reported in the different chapters of the thesis.

The cDNAs for the human version of the cannabinoid CB<sub>1</sub> receptor without containing the stop codons was obtained by PCR and subcloned into a RLuc-containing vector using sense and antisense primers harbouring unique restriction sites for HindIII and BamHI. Also, with the use of sense and antisense primers containing the unique restriction sites for BamHI and KpnI, the receptor was cloned into the pEYFP-containing vector. Overall, vectors containing the sequence for CB<sub>1</sub>R-RLuc and CB<sub>1</sub>R-YFP were generated.

To obtain the CB<sub>2</sub>R-containing fusion proteins, the cDNA of the human CB<sub>2</sub>R was amplified by PCR without containing the stop codon. Using sense and antisense primers harbouring the HindIII and BamHI restriction enzymes, and BamHI and KpnI, the receptor was subcloned into, respectively, a pRLuc-N1 vector or the pGFP<sup>2</sup>-N1-containing vector. Overall, vectors containing the sequence for CB<sub>2</sub>RRluc and CB<sub>2</sub>RGFP<sup>2</sup> fusion proteins were generated.

For preparing the D<sub>1</sub>R fusion protein, the dopamine D<sub>1</sub> receptor was amplified by PCR without its stop codon to then, subclone the receptor into a p-GFP<sup>2</sup>-containing vector with the use of sense and antisense primers containing KpnI and BamHI restriction enzymes. The result of this procedure was a vector containing the sequence of D<sub>1</sub>-GFP<sup>2</sup> fusion protein.

As described in Navarro and collaborators study (*Navarro et al., 2014*), pcDNA3.1 vector encoding for the Calneuron-1 calcium sensor was amplified without its stop codons using sense and antisense primers harbouring BamHI and HindII or BamHI and KpnI restriction sites to subclone Calneuron1 into pRLuc-N1 or pEYFP-N1 vectors. The resulting vectors contained the sequences for Calneuron1-RLuc and Calneuron1-YFP fusion proteins.

Similarly, the cDNA encoding for Caldendrin in pcDNA3.1 vector was subcloned into a pEYFP-N1 vector using sense and antisense primers harbouring EcoRI and BamHI restriction sites in order to obtain Caldendrin-YFP fusion protein, as it is indicated in Navarro et al., 2014.

The NCS1 calcium sensor the protocol used was similar, thus amplifying pcDNA3.1 encoding for NCS1 without its stop codons, and subcloning it into the pRLuc-N1 and

pEYFP-N1 vectors using the XhoI and BamHI restriction sites, NCS1-Rluc and NCS1-YFP fusion proteins were obtained (Navarro *et al.*, 2014).

Human cDNA for GHS-R1a was amplified by PCR without its stop codon using sense and antisense primers with EcoRI and KpnI restriction sites to be subcloned into pRluc-N1 and pGFP<sup>2</sup>-N1 vectors to obtain GHS-R1a-Rluc and GHS-R1a-GFP<sup>2</sup> fusion proteins.

For GHS-R1b, the receptor was amplified without stop codon and harbouring the EcoRI and KpnI restriction sites to subclone the receptor in pRluc-N1 and pEYFP-N1 vectors, consequently obtaining the vectors encoding for GHS-R1b-Rluc and GHS-R1b-YFP fusion proteins.

Sigma-1 receptor ( $\sigma_1$ -R) fusion proteins  $\sigma_1$ -R-Rluc and  $\sigma_1$ -R-YFP were obtained after amplifying the cDNA for the receptor without stop codons and harbouring the EcoRI and KpnI restriction sites, to then subclone the receptor into the pcDNA3.1-RLuc and pEYFP-N1 vectors.

The same approach and restriction sites were employed in order to subclone the sequence of the CRF1 receptor in the pRluc-N1 and pEYFP-N1 vectors. The resulting vectors contained the sequence for CRF1R-Rluc and CRF1R-YFP fusion proteins. In turn, to subclone the A<sub>2A</sub>R into pGFP<sup>2</sup>-N1 vector, the amplification by PCR of the receptor without stop codon and required the incorporation of HindIII and BamHI restriction sites.

Sequences encoding amino acid residues 1-155 and 155-238 of the Venus variant of yellow fluorescent protein (Venus) were subcloned in the pcDNA3.1 vector to obtain complementary N- and C- hemiproteins (pcDNA3.1-nVenus and pcDNA3.1-cVenus). Then cDNAs for GHS-R1b and GHS-R1a and  $\sigma_1$ -R were subcloned (using the above described restriction sites) to pcDNA3.1-nVenus or pcDNA3.1-cVenus, to provide plasmids expressing the receptors fused to each part of the n-and-cYFP Venus hemiprotein on the C-terminal domain (GHS-R1b-nYFP, GHS-R1a-nYFP, GHS-R1a-cYFP and  $\sigma_1$ -R-cYFP). The same protocol was used with cDNA for GHS-R1b, which was subcloned into the pcDNA3.1-nRluc8 to obtain the GHS-R1b-nRluc8 fusion protein, while sequences for GHS-R1a and adenosine A<sub>1</sub> receptors (using HindIII and BamHI restriction sites in the case of A<sub>1</sub>R) were subcloned into pcDNA3.1cRluc8 vector to obtain GHS-R1a-cRluc8 and A<sub>1</sub>-cRluc8.

### III.2 Directed mutagenesis

Two different sequences of the CB<sub>1</sub>R were mutated by site-directed mutagenesis approach. To obtain a C-terminal truncation of the CB<sub>1</sub>R sequence, PCR was used to remove

the last 40 amino acids from the CB<sub>1</sub>R sequence. To produce a mutation in the 3<sup>rd</sup> intracellular loop of the receptor, the sequence <sub>321</sub>TSEDGKVQVT<sub>330</sub> placed in the third intracellular loop of the CB<sub>1</sub>R was mutated to <sub>321</sub>AAEDGKVQVT<sub>330</sub> in order to obtain the CB<sub>1</sub><sup>A321-A322</sup> receptor. Then, sequences encoding for those mutants were subcloned as above described into pEYFP-containing vector to create vectors encoding CB<sub>1</sub><sup>ΔCT</sup>-YFP or the CB<sub>1</sub><sup>A321-A322</sup>-YFP receptors (named CB<sub>1</sub>R<sup>ΔICL3</sup>-YFP in the following sections of the thesis).

Constructs of Calneuron-1 with the C-terminal domain truncated (Calneuron1<sup>ΔCT</sup>) and the N-terminal myristoylation-deficient NCS-1 mutant (NCS1<sup>Δmyristoylated</sup>) obtained as described elsewhere (*Hradsky et al., 2011*) were kindly provided by M. Kreutz laboratory. Then, the sequences encoding for these mutations were subcloned into pEYFP-N1 vector pEYFP-N1 using HindIII and BamHI restriction sites to obtain NCS1<sup>Δmyristoylated</sup>-YFP and calneuron1<sup>ΔCT</sup>-YFP fusion proteins (*Navarro et al., 2014*).

### III.3 Cell lines and culture conditions

Human Embryonic Kidney -293 T (HEK-293T) and the immortalised microglial-murine N9 cell lines were used.

HEK-293T cells were grown in Dulbecco's Modified Eagle's Medium (DMEM) (Gibco; Paisley, Scotland, UK) supplemented with 2 mM of L-glutamine (Invitrogen; Paisley, Scotland, UK), 5% of 56°C inactivated Foetal Bovine Serum (FBS) (Gibco; Paisley, Scotland, UK), MEM non-essential amino acids solution (1/100) (Invitrogen; Paisley, Scotland, UK) and 100 units/ml penicillin/streptomycin (P/S) antibiotic (Invitrogen; Paisley, Scotland, UK). When the cells were 90-100% confluent, trypsin was used to detach cells from plates. The enzyme was inactivated with the use of DMEM supplemented with 5% FBS, P/S, L-glutamine and MEM non-essential amino acids. Then, cells were diluted (1/10) and seeded in new plates. Cells were discarded after 20 passages.

N9 cell line was harvested in Roswell Park Memorial Institute (RPMI) 1640 (Gibco; Paisley, Scotland, UK) medium supplemented with 2 mM of L-glutamine, 10% of 56°C inactivated Foetal Bovine Serum (FBS), MEM non-essential amino acids solution (1/100) and 100 units/ml penicillin/streptomycin (P/S) antibiotic. When the confluence arrived to 100%, the cells were splitted as above described. Cells were discarded after 8 passages.

All cell lines were maintained in a 5% CO<sub>2</sub> humid atmosphere and at a temperature of 37°C.

### III.4 Primary cell cultures

Mice striatal primary microglial cultures were obtained after removing the brain from C57BL/6 mice of 2 to 4 days of age. The brains were mechanically dissected and the meninges removed, digesting the striatal tissue with 0,25% trypsin for 20 minutes. Trypsinization was stopped by the addition of an equal volume of DMEM-F12 culture medium supplemented with 10% foetal bovine serum, 100U/ml P/S and 0.5 µg/ml amphotericin B and 160 mg/ml of deoxyribonuclease I. Then, cells were brought to a single cell suspension by repeated pipetting followed by passage through a 100 µm-pore mesh and pelleted for 7 min at 200 g. The glial cells pellet was resuspended in medium and seeded at 3.5 x 10<sup>5</sup> cells/ml in poly-D-lysine coated 6-well plates. The cultures were maintained at 37°C in humidified 5% CO<sub>2</sub> atmosphere, being the medium replaced once a week. Microglial cell cultures were then obtained from 19-21 day glial cultures by mild trypsinization (0.05-0.12% trypsin) process and seeded as it follows: 500,000 cells/well in poly-D-lysine coated 6-well plates, 50,000 cell/well in 96-well plates or 75,000 cells/18mm coverslip. Cells were used 24 hours after plating.

The striatal primary neurons were obtained either from foetal Sprague Dawley rats or C57BL/6 mice of 19-20 days. After mechanically removing meninges from brain, striatal tissue was digested in 0.25% trypsin for 20 minutes. Trypsinization process was stopped by the addition of equal volume of DMEM-F12 culture medium (Gibco; Paisley, Scotland, UK) supplemented with 10% foetal bovine serum, 100U/ml P/S and 0.5 µg/ml amphotericin B and 160 mg/ml of deoxyribonuclease I. After passage through a 100 µm-pore mesh and pelleting (7 min at 200 g), neurons were resuspended in DMEM-F12 supplemented medium and seeded in poly-D-lysine coated 6-well plates at 500,000 cells/well, 50,000 cell/well in 96-well plates or 75,000 cells/18mm coverslip. 24 hours later, the medium was replaced and cells were maintained in Neurobasal medium (Gibco; Paisley, Scotland, UK) supplemented with 5% FBS, 2 mM L-glutamine, 100 U/ml P/S and 2% (v/v) B27 supplement. The cells were maintained at 37°C in humidified 5% CO<sub>2</sub> atmosphere for 12 days before utilisation of the cultures, being the medium replaced once a week.

### III.5 Cell viability

Cell survival rate was calculated by counting alive and dead cells in a Countless II FL automated cell counter (Thermo Fisher Scientific-Life Technologies) after diluting (1:1 v/v) of the samples with Trypan blue (Thermo Scientific; Waltham, MA, USA).

### III.6 Cell transfection

For HEK-293T and N9 cell lines, the PolyEthylenImine (PEI) (Sigma-Aldrich, St Louis, MO, United States) transfection protocol was employed. To carry out this methodology, each cDNA were diluted in a 150 mM NaCl solution, whereas 40 mM PEI was diluted 1/20 with 150 mM NaCl in a total volume equal than the DNA-NaCl solution. The two equal volume solutions were gently mixed. After 10 minutes, the mix was added to the cells in serum-starved DMEM or RPMI medium. Previous to proceed to replace the medium by supplemented DMEM or RPMI, cells were incubated for 4 hours at 37°C, 5% CO<sub>2</sub> and humid conditions. Experiments were performed 48h after the transfection (unless otherwise indicated).

The other transfection methodology, which was Lipofectamine 2000 transfection method, was used for primary cell cultures. Lipofectamine 2000 reagent (Invitrogen; Paisley, Scotland, UK) was diluted in Opti-MEM medium according to manufacturer's recommendations, and each cDNA diluted in the same volume of Opti-MEM than the Lipofectamine 2000-Opti-MEM preparation. Then, the two solutions were mixed by gentle pipetting. After 30 minutes, the complexes formed between Lipofectamine 2000 and the cDNA were added to the cells growing in serum-starved medium, and after 4 hours medium was removed and replaced for DMEM or Neurobasal supplemented medium. 48 hours after this procedure, the experiments were carried out.

### III.7 Generation of Parkinson's disease (PD) Model

For the development of the disease, male Wistar rats were used. The experiments were carried out in accordance with European Union directives (2010/63/EU and 86/609/CEE) and were approved by the Ethical committee of the University of Santiago de Compostela.

The animals were divided into three different groups: non-lesioned, 6-hydroxydopamine (6-hydroxy-DA) lesioned animals receiving vehicle, and 6-hydroxy-DA-lesioned rats receiving a chronic treatment with levodopa. After anaesthesia with ketamine/xylazine (1%ketamine, 75 mg/kg; 2% xylazine, 10 mg/kg), and placement in a David Kopf stereotaxic apparatus, the animals received a unilateral injection in the right

medial forebrain bundle of 12 µg of 6-hydroxy-DA prepared in 4 µl of sterile saline medium containing 0.2 % of ascorbic acid. The stereotaxic coordinates were 3.7 mm posterior to bregma, -1.6 mm lateral to midline, and 8.8 mm ventral to the skull at the midline, in the flat skull position. The solution was injected at 1 µl/min with a 5-µl Hamilton syringe coupled with a motorized injector; the cannula was left in situ for 2 minutes after the injection. Three weeks after the procedure, post-surgery efficacy of the lesion was evaluated by the amphetamine rotation test and the cylinder test. The extent of the lesion was verified by tyrosine hydroxylase (TH) western blot analysis, and the correct nigrostriatal lesion was confirmed by the loss of TH immunohistochemistry staining. Amphetamine-induced rotation was tested in a bank of eight automated rotamer bowls by monitoring full (360°) body turns in either direction. Right and left full body turns were recorded over 90 min following an injection of D-amphetamine (2.5 mg/kg intraperitoneal) dissolved in saline medium. Rats that displayed more than six full body turns/min ipsilateral to the lesion were included in the study (this rate would correspond to an over 90% depletion of the dopamine striatal fibers in the striatum). The cylinder test was employed to evaluate the spontaneous forelimb movements. Rats individually placed in a glass cylinder (20 cm of diameter) were evaluated by a blinded observer to the animals' identity, who scored the number of left or right forepaw contacts and presenting left (impaired) touches in percentage of the total touches. A control animal would thus receive an unbiased score of 50%, whereas lesion usually reduces performance of the impaired paw to less than 20% of the total wall contacts.

### III.8 Treatment with levodopa and dyskinesia assessment of PD model animals

PD animal models were chronically treated with levodopa; receiving a subcutaneous injection of levodopa methyl ester (6 mg/kg) plus benserazide (10 mg/kg) performed daily for 3 weeks. This treatment may lead to reliably dyskinetic movements. In order to discriminate between non-dyskinetic and dyskinetic animals, the manifestation of levodopa-induced abnormal involuntary movements (AIMs) was evaluated according to the rat dyskinesia scale described in detail elsewhere (*Benito et al., 2003; Farré et al., 2015*). In brief, the severity of each AIM subtype (limb, orolingual and axial) was assessed using scores from 0 to 4: 1 being occasional, 2 present 50% of the time, 3 being continuous but interrupted by strong sensory stimuli and 4 showing continuous movement that was not interrupted by strong stimuli. Hence, rats were classified as 'dyskinetic' if they displayed a 2 score per monitoring period on at least two AIM subtypes. Animals classified as 'non-dyskinetic' exhibited either no AIMs or

very mild and occasional ones. Animals with low scores, for example, without performing neither non-dyskinetic nor dyskinetic treats, were discarded.

### III.9 APP transgenic mouse model of Alzheimer's disease (AD)

APP<sub>Sw,Ind</sub> transgenic mice (line 9; C57BL/6 background) expressing human APP695 harbouring the FAD-linked Swedish (K670 N/M671 L) and Indiana (V717 F) mutations under the PDGF $\beta$  promoter were obtained by crossing APP<sub>Sw,Ind</sub> to non-transgenic (WT) mice as described by Mucke and collaborators (Mucke et al., 2000).

### III.10 A $\beta$ -oligomer production

A $\beta$ -oligomer preparation was carried out by placing a lyophilized A $\beta$ 1-42 in 1,1,1,3,3,3-hexafluoro-2-propanol (HFIP) to a concentration of 0.5 mg/ml. After evaporation of the HFIP, the peptide film was stored at -80°C. 24 hours prior to its use, the peptide film was dissolved in dimethylsulfoxide (DMSO), sonicated, brought to a 50  $\mu$ M concentration with F12 medium, and kept for oligomerization at 4°C for 24 hours. Fresh A $\beta$ 1-42 oligomer preparations were used in each experiment, and the quality of the preparations was validated by SDS-PAGE (10% tricine gels) and subsequent immunoblotting using antibodies detecting the N-terminus of A $\beta$  peptide.

### III.11 Cocaine treatment

Male Sprague-Dawley rats weighing 200-220 grams were selected for the experiments. Rats were kept in controlled environment with 12 hour light-dark cycle at 21°C room temperature, with food and water provided *ad libitum*. The Ethics Committee of the Faculty of Biological Science of the Pontifical Catholic University of Chile approved all the experimental procedures, which fulfilled all the international guidelines and rules (NIH Guide for the Care and Use of Laboratory Animals).

The animals taking place in the study were divided in two groups of experimental series with their respective controls (cocaine versus saline): of chronic-treated rats and acute-treated cocaine rats. The chronic administration protocol consisted of 15 mg/kg intraperitoneal cocaine injections twice a day for 14 days, whereas the acute cocaine treatment protocol consisted of two intraperitoneal injections of 15 mg/kg cocaine, being one in the morning and the second in the afternoon.



### III.12 Fixation procedure

The male Sprague-Dawley rats employed in the cocaine treatment were deeply anesthetized the day after the last cocaine injection. Ketamine-xylazine (50 mg/kg and 5 mg/kg respectively) was used as anaesthesia. Rats were intracardially perfused with 50 ml of saline followed by 500 ml of 4% paraformaldehyde (PFA) in phosphate buffer. Then the animals were sacrificed and the brains post-fixed with 4% PFA for 2 hours and left in 20% sucrose during 2 days.

### III.13 RealTime (RT)-PCR assay

To assay the levels of receptors RNA transcripts, cells were lysed with 1 ml of Trizol Reagent. After addition of 200 µl of chloroform and gentle mixing, cells were centrifuged for 15 minutes at 12000 g and 4°C. The aqueous phase containing RNA was recovered and mixed with an equal volume of icecold 2-propanol and left O/N at -80°C. After discarding the supernatants and a washing step with 70% ethanol, the pellets were resuspended in H<sub>2</sub>O. All DNA of the samples was eliminated by the use of a RQ1 RNase free DNase (Promega). The RNA was quantified with the use of a Nano Drop ND-1000 spectrophotometer (Thermo Scientific; Whaltam, MA, USA) and the quality assessed with the Bioanalyzed 2100 system. Total RNA (1 µg) was reversely transcribed by random priming using Moloney Murine Leukemia Virus (M-MLV) reverse transcriptase, RNase H minus, point mutant, following the protocol of 'Two-Step RT-PCR' provided by Promega. The resulting single-stranded cDNA was used to perform the PCR amplification of the receptors of interest and an internal control.

The primers employed for RT-PCR assays are summarised in Table 1:

Gene of interest	Forward	Reverse
GADPH	5'-CATCCTGCACCACCAACTGCTTAG-3'	5'-GCCTGCTTCACCACCTTCTTGATG-3'
GHS-R1a	5'-GCTCTTCGTGGTGGGCATCT-3'	5'-GAGAAGGATTCAAATCCTAGCA-3'
GHS-R1b	5'-GCTCTTCGTGGTGGGCATCT-3'	5'-TCAGCGGGTGCCAGGACTC-3'
CB <sub>1</sub> R	5'-CATCCAGTGTGGGAGAAT-3'	5'-TATGGTCCACATCAGGAAA-3'
CB <sub>2</sub> R	5'-CATCACTGCCTGGCTCACT-3'	5'-AGCATAGTCCTCGGTCCTCA-3'

**Table 1. Sequences of Forward and Reverse primers used in RT-PCR assays**

### III.14 Immunocytochemistry

To proceed with immunocytochemical assays, cells were fixed in 4% PFA for 15 min, followed by several washings with PBS buffer containing 20 mM glycine to quench the aldehyde groups. After permeabilization of the membranes with PBS-20 mM glycine- 0,05% Triton X-100 buffer for 5 minutes, cells were treated with PBS- 20 mM glycine- 1% bovine serum albumin for 1 hour. Then, cells were incubated with the respective primary antibodies for 1 hour at room temperature or over-night at 4°C. After removing the primary antibody and several washing procedures with PBS- 20 mM glycine buffer, cells were incubated for 1 hour with specific secondary antibodies. The nuclei of the cells were stained with Hoechst and the samples were mounted with Mowiol at 30% for the posterior observation in a Leica SP2 confocal microscope (Leica Microsystems; Mannheim, Germany).

The primary antibodies employed are summarised in the Table 2 and the secondary antibodies are listed in the Table 3.

**Table 2. Primary antibodies used in the different assays.**

<b>Epitope</b>	<b>Specie</b>	<b>Manufacturer</b>	<b>Dilution</b>
Anti-Rluc	Mouse	Millipore	1/200
Anti-Iba1	Rabbit	Sigma Aldrich	1/100
Anti-CB <sub>2</sub> R	Goat	Santa Cruz Biotechnology	1/50
Anti-CB <sub>1</sub> R	Rabbit	Cayman Chemical	1/100
Anti- MHC ClassII	Rabbit or Mouse	Abcam	1/100
Anti-Tubulin	Mouse	Sigma-Aldrich	1/2000
Anti-YFP	Rabbit	Santa Cruz Biotechnology	1/1000
Anti- ERK1/2	Rabbit	Sigma-Aldrich	1/40000
Anti-PhosphoERK	Mouse	Sigma-Aldrich	1/2500
Anti-Calneuron-1	Rabbit	Abcam	1/100
Anti-NCS1	Rabbit	Abcam	1/100
Anti-sigma1-R	Goat	Santa Cruz Biotechnology	1/100
Anti-GHS-R1a	Mouse	Abcam	1/100



**Table 3. List of secondary antibodies employed**

<b>Epitope</b>	<b>Specie reactivity</b>	<b>Manufacturer</b>	<b>Dilution</b>
Alexa Fluor 488	Anti-Goat	Invitrogen	1/200
Cy-3	Anti-Rabbit	Jackson ImmunoResearch	1/200
Cy-3	Anti-Mouse	Jackson ImmunoResearch	1/200
IRDye 800	Anti-Mouse	Sigma-Aldrich	1/10000
IRDye 680	Anti-Rabbit	Sigma-Aldrich	1/10000

### III.15 Western Blotting

The determination of protein expression levels by immunoblotting was usually carried out in transfected HEK-293T cells. After treatment of cells to isolate the appropriate protein preparation, equivalent amounts of cell protein (10 µg) were separated by polyacrylamide gel electrophoresis on denaturing conditions (10% SDS). Proteins in gels were transferred into PVDF membranes, which were then treated with a blocking solution and PBS (1:1 v/v) for 1 hour. Primary antibodies diluted in PBS buffer were added and kept over-night at 4°C. After removal of the primary antibody and several washes, membranes were incubated for 1 hour with the secondary antibodies. Membranes were dried after several washes and quantification was performed using an Odyssey infrared scanner. Band densities were quantified using the scanner software.

### III.16 Biotinylation of cell surface proteins

Living cells washed three times with a borate buffer containing 10 mM H<sub>3</sub>BO<sub>3</sub>, 150 mM NaCl and pH 8.8 were incubated with 50 µg/ml sulfo-NHS-LC-Biotin in borate buffer for 5 minutes. Three washing steps with the borate buffer were followed by the addition of 13 mM NH<sub>4</sub>Cl for 5 minutes to quench the remaining biotin. Then, cells were washed with PBS and disrupted with three 10-s strokes in a Polytron. After that, cells were centrifuged at 16,000 x g for 30 minutes. The pellet was solubilised in ice-cold lysis buffer (50 mM Tris-HCl, 1% Triton X-100, 0.2% SDS, 100 mM NaCl, 1 mM EDTA and 0.5% sodium deoxycholate) for 30 minutes and centrifuged at 16000 g for 20 minutes. The supernatant was incubated at 4°C with 80 µl of streptavidin-agarose beads for 1 hour with constant rotation. Beads were washed three times with ice-cold lysis buffer and liquid was aspirated to dryness with a 28-gauge needle. Subsequently, 50 µl of SDS-PAGE sample buffer (8 M urea, 2% SDS, 100 mM

dithiothreitol and 375 mM Tris; pH 6.8) were added to each sample. After heating at 37°C for 2 hours, proteins were dissociated and resolved by SDS-polyacrylamide gel electrophoresis in 10% gels and immunoblotted as described above.

### III.17 In situ Proximity Ligation Assays

Cells or tissue preparations placed on glass coverslips were fixed in 4% PFA for 15 minutes and washed three times with PBS containing 20 mM glycine to quench aldehyde groups. Then cells were permeabilised with PBS- 20 mM Glycine and 0.05% Triton X-100 for 5 minutes. After this process, cells were incubated for 1 hour at 37°C with the blocking solution provided by the Duolink InSitu Probemaker Kit (Sigma-Aldrich, St Louis, MO, United States). Cells were treated O/N at 4°C with specific primary antibodies (conjugated or not with the complementary +/- PLA probes). When necessary, PLA probes against the primary antibodies were used. The ligation of the complementary probes and the amplification steps were performed following the manufacturer's indications. In brief, ligase enzyme was diluted in ligation buffer and cells were incubated with the mix at 37°C for 1 hour. Subsequently, cells were treated, for 100 minutes at 37°C, with a mixture of a polymerase and an amplification buffer and with Hoechst to stain the cell nuclei. All steps were performed avoiding the exposure of samples to light. Coverslips were mounted in 30% Mowiol and samples were observed in a Leica SP2 confocal microscope with an apochromatic 63x oil-immersion objective (N.A. 1.4). 405 and 594 nm laser lines were used to detect nuclei and the red spots of interacting complementary PLA probes. For each field of view a stacks of the two channels and several stacks of 0.5  $\mu\text{m}$  width step size were acquired. The number of cells containing one or more red spots versus total cells (blue nucleus) and, in cells containing spots, the ratio  $r$  (number of red spots/ cell) were determined by means of the Duolink image tool software (Sigma-Aldrich, St Louis, MO, United States).

### III.18 ERK1/2 phosphorylation

Two different approaches to determine ERK1/2 phosphorylation have been used. In the first method, the culture medium of the cells was substituted by serum-starved medium 4 hours before treating the cells with the ligands of interest for 7 minutes and at 37°C and in a humid atmosphere. Then, cells were placed in ice to abruptly stop the metabolism and cells were washed once with ice-cold PBS. Subsequently, ice-cold lysis buffer (50 mM Tris-HCl pH 7.4, 50 mM NaF, 150 mM NaCl, 45 mM-glycerophosphate, 1% Triton X-100, 20  $\mu\text{M}$  phenylarsine oxide, 0.4 mM  $\text{NaVO}_4$  and protease inhibitor) was added. Cellular debris was removed

by centrifugation at 13000 g for 10 minutes at 4°C and the protein levels were quantified by the bicinchonic acid method, using bovine serum albumin dilutions as standard. Equivalent amounts of the protein (10 µg) were separated, immunolabelled using specific antibodies (see antibodies table) and processed for immunoblotting as described in III.15 (Western-blotting).

For the second methodology used for ERK1/2 Phosphorylation determination, 40000-50000 cells were seeded in 96 well transparent plates, kept 48h in an incubator at 37°C, and 5% CO<sub>2</sub> humid atmosphere. Then, medium was changed to serum-free medium 4 hours previous to add the desired ligands diluted in non-supplemented medium (10 minutes for the antagonists and 7 minutes for the agonists). After ligand activation, cells were washed twice with cold PBS before treatment with 30 µl of lysis buffer for 20 minutes. 10 µl of the supernatants were placed in a white ProxiPlate 384-well microplates and ERK1/2 phosphorylation was determined using AlphaScreen® SureFire® kit (Perkin Elmer; Wellesley, MA, United States) and the EnSpire® Multimode Plate Reader.

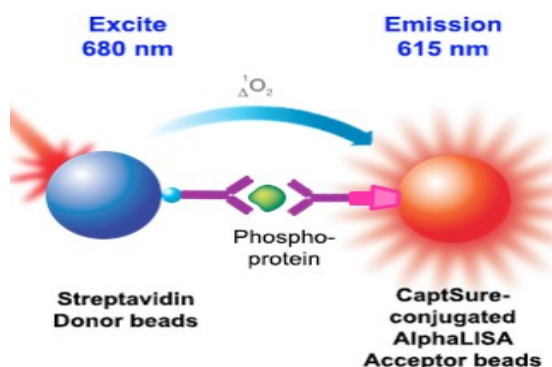


**Figure M1. Schematic representation of AlphaScreen ERK phosphorylation assay principle** (Obtained from perkinelmer.com).

### III.19 Resonance energy transfer assays

Different variations of RET techniques have been employed. For bioluminescence resonance energy transfer BRET<sup>1</sup> and BRET<sup>2</sup> assays, cells were co-transfected as previously described with constant amounts of the cDNA encoding for the Rluc-containing fusion protein, and increasing amounts of cDNA encoding the acceptor protein. 48 hours after transfection, cell medium was removed and replaced for 0.1% glucose supplemented Hank's Balanced Salt Solution (HBSS) buffer ( 140 mM NaCl, 5 mM KCl, 1.2 mM CaCl<sub>2</sub>, 0.4 mM MgSO<sub>4</sub>-7H<sub>2</sub>O, 0.5 mM MgCl<sub>2</sub>-6H<sub>2</sub>O, 0.3 mM Na<sub>2</sub>HPO<sub>4</sub>, 0.4 mM KH<sub>2</sub>PO<sub>4</sub> and 4 mM NaHCO<sub>3</sub>). After collecting the cells, protein concentration was determined using the Bradford assay kit (Bio-rad; Munich, Germany), using bovine serum albumin dilutions as standards. To quantify fluorescence, cells were plated in 96-well black and transparent bottom microplates

and fluorescence measured in a Fluostar Optima Fluorimeter (BMG Lab technologies; Offenburg, Germany). For BRET<sup>1</sup> measurements, 20 µg of cell suspensions were distributed in 96-well white microplates and 5 µM of Coelenterazine H was added before BRET signal acquisition using a Mithras LB 940 reader (Berthold Technologies; Germany). Rluc expression was also quantified by reading luminescence 10 minutes after the coelenterazine H addition, using once again, the Mithras LB 940. In the case of BRET<sup>2</sup>, the transference of energy between the proteins was measured 30 seconds after the addition of 5 µM of DeepBlue C, while, similarly to BRET<sup>1</sup>, the quantification of Rluc expression was performed 10 minutes after the 5 µM coelenterazine H addition. Net BRET was defined as  $((\text{long-wavelength emission})/(\text{short-wavelength emission})) - C_r$ , where  $C_r$  corresponds to  $((\text{long-wavelength emission})/(\text{short-wavelength emission}))$  of the Rluc protein expressed individually.

For SRET assays, cells were co-transfected with constant amounts of Rluc and GFP<sup>2</sup>-containing fusion proteins and increasing amounts of YFP-containing fusion proteins. After replacing the medium for 0.1% glucose supplemented HBSS and collecting the cells, different determinations were performed. 20 µg of protein were placed in appropriate 96-well plates. To quantify fluorescence, cells were plated in 96-well black and transparent bottom microplates and fluorescence measured in a Fluostar Optima Fluorimeter, and to quantify Rluc expression luminescence was read 10 minutes after the coelenterazine H addition, using once again, the Mithras LB 940. The SRET signal, however, was obtained measuring the long wavelength (530 nm) and short wavelength (410nm) using a Mithras LB 940 reader, after the addition 5 µM of Deep Blue C. By analogy with BRET, SRET is defined as  $((\text{long-wavelength emission} / \text{short-wavelength emission})) - C_r$ , being  $C_r$  the  $(\text{long-wavelength emission} / \text{short-wavelength emission})$  of cells expressing Rluc and GFP<sup>2</sup> proteins. For SRET quantification, linear unmixing was done, taking into account the spectral signature to separate the two fluorescence emission spectra, and values were expressed as milliSRET units (mSU; net SRET 1000).

### III.20 Bimolecular Complementation Assays

Bimolecular fluorescence complementation (BiFC) assays and bimolecular luminescence complementation assays (BiLC) techniques have been employed. When performed individually, cDNA of the fluorescent or bioluminescent hemiproteins were co-transfected in constant amounts. Cells were placed into the appropriate plates, thus, to read fluorescence by the BiFC black 96-well plates with transparent bottom were used and for

BiLC assays, white 96-well plates were employed. Fluorescence or bioluminescence values were read with Fluostar Optima Fluorimeter or the Mithras LB 940 reader.

Using a combination of the two Bimolecular Complementation Assays, a tetramer structure could be detected. In this case, cells were co-transfected with constant amounts of cDNA for Rluc hemiprotein-containing fusion proteins and increasing amounts of cDNA of fluorescent hemiprotein-containing fusion proteins. The values due to RET complemented YFP Venus or Rluc8 expression and BRET values were determined as described before.

### **III.21 Determination of intracellular calcium levels using a calmodulin-based assay**

For determining the intracellular calcium release cells were co-transfected with cDNA of the proteins of interest and 3  $\mu\text{g}$  of the GCaMP6 calcium sensor, which upon  $\text{Ca}^{2+}$  binding, emits fluorescence. 48 hours after transfection, cell culture medium was replaced by  $\text{Mg}^{2+}$ -free Locke's buffer (154 mM NaCl, 5.6 mM KCl, 3.6  $\text{NaHCO}_3$ , 2.3  $\text{CaCl}_2$ , 5.6 mM glucose, 5 mM HEPES, pH 7.4) supplemented with 10  $\mu\text{M}$  glycine. 150000 cells were plated in 96-well black, clear-bottom microtiter plates and incubated with the desired ligands. Fluorescence emission intensity of the GCaMP6 was recorded for 150 seconds (30 flashes/ well) at 515 nm upon excitation at 488 nm on the EnSpire<sup>®</sup> Multimode Plate Reader (Perkin Elmer; Wellesley, MA, United States).

### **III.22 Nitric Oxide (NO) production**

50,000 cells plated in transparent 96-well microplates (100  $\mu\text{l}$ /well) were cultured for 48 hours at 37°C and 5%  $\text{CO}_2$  in a humid atmosphere and treated with different concentrations of pro-inflammatory condition triggering reagents like Lipopolysaccharides (LPS) or interferon- $\gamma$  (INF- $\gamma$ ) or vehicle. A fraction of 50  $\mu\text{l}$  of the supernatants were collected and distributed in 96-well black microplates with transparent bottom. Then NO production was analysed by the use of Griess reagent System (Promega; Madison, WI, United States). Briefly, supernatants were incubated with 50  $\mu\text{l}$  sulphanilamide solution for 15 minutes, previous to adding 50  $\mu\text{l}$  N-1-naphthylethylenediamine dihydrochloride (NED) solution under acidic conditions. After 15 minutes and within the next 30 minutes, the NO production was measured at 540 nm using Multiskan Ascent spectrophotometer (Thermo Lab Systems).

### III.23 cAMP determination

Two hours before initiating the assay, cell culture medium was substituted by serum-starved medium. Then, cells were detached and resuspended in serum-starved medium containing 50  $\mu\text{M}$  zardaverine (a phosphodiesterase inhibitor), 0.1% BSA and 5 mM HEPES. Cells were plated in 384-well microplates (1,000 to 3,000 cells/well) and treated with the corresponding ligands. In case antagonists were required, a pre-treatment of 15 minutes with antagonists was applied before agonist activation for 15 minutes. Finally, if the Gi-mediated signalling was addressed, cells were stimulated for 15 minutes with forskolin. Samples were subsequently treated with donor and acceptor probes of the Lance Ultra cAMP kit (Perkin Elmer; Wellesley, MA, United States) that used homogeneous time-resolved fluorescence (HTRF) energy transfer methodology to measure intracellular cAMP production. The fluorescence readings (at 665 nm) were performed using a PHERAstar Flagship microplate reader (BMG Lab technologies; Offenburg, Germany) equipped with a HTRF optical module.

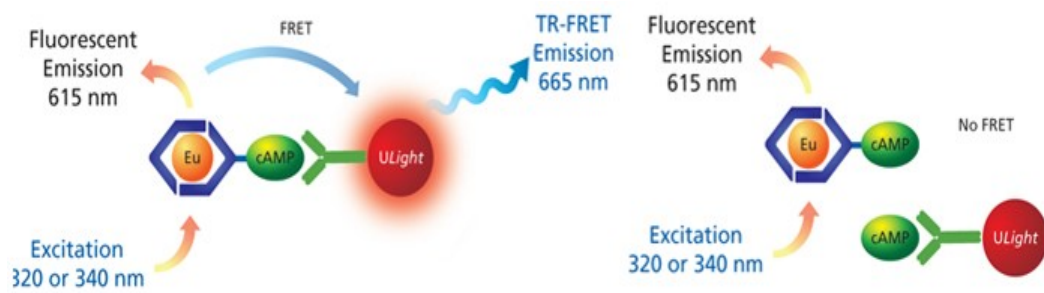


**Figure M2.** Schematic representation of the cAMP determination principle (Obtained from perkinelmer.com).

### III.24 Dynamic Mass Redistribution (DMR) label-free assays

The cell dynamic redistribution induced upon receptor activation was detected by illuminating with a polychromatic light the underside of a biosensor and measuring the changes in the wavelength of the reflected monochromatic light, which is a sensitive function of the index of refraction. The magnitude of this wavelength shift, expressed in picometers, is directly proportional to the amount of DMR.

The assays starts with the cells being seeded into 384-well sensor microplates (10000 cells/well), generating a 80% confluent monolayer in the well bottom. Previous to the assay, cells were washed twice with the assay buffer (HBSS with 20 mM HEPES, pH 7.15) and incubated for 2 hours at room temperature with assay buffer containing 0.1% DMSO (40  $\mu\text{l}$ /well). Then the sensor plate was scanned and a baseline optical signature recorded for 10 minutes before adding 10  $\mu\text{l}$  of the ligand/reagent dissolved in the experimental buffer. In case antagonists were required, 10  $\mu\text{l}$  antagonist treatment and 30 minutes lecture of DMR



response, followed by the 10  $\mu\text{l}$  agonist activation, was performed. The DMR responses were monitored for, at least, 5,000 seconds in an EnSpire Multimode Plate Reader (Perkin Elmer; Wellesley, MA, United States), and the results were analysed using the EnSpire Workstation Software v4.10.

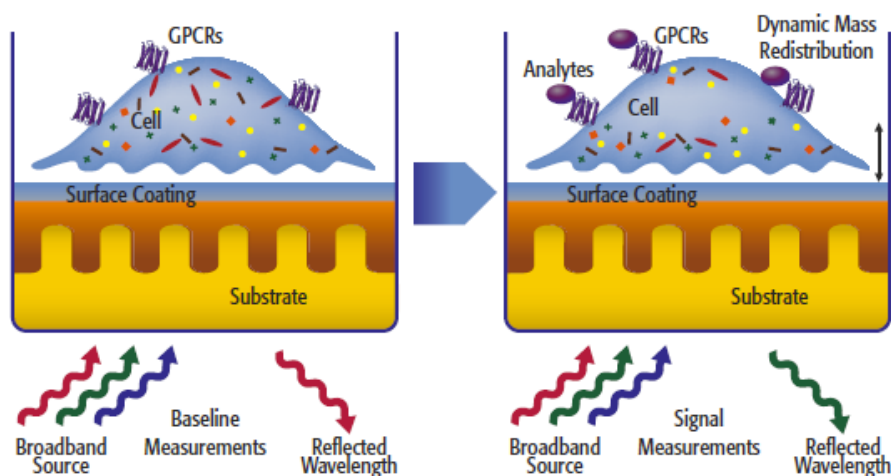


Figure M3. Schematic representation of the DMR principle. (Obtained from perkinelmer.com)

### III.25 Computational modelling

Structure of sigma-1 receptor was modelled based on the recently crystal structure (PDB id 5HK1). The inactive conformation of human GHS-R1a (UniProt: Q92847) was built using crystal structures of the neurotensin 1 receptor (PDB id 4XES for all parts of the receptor, and PDB id 3ZEV for the C-terminal part of the TM7 and helix 8). Human neurotensin 1 receptor and GHS-R1a share 33% of sequence identity and 51% of sequence similarity. The 'active-like' form of GHS-R1a was modelled by incorporating the active features present in the crystal structure of the  $\beta_2$ -adrenergic receptor in complex with  $G\alpha_s$  (PDB id 3SN6). The 'active-like' model of GHS-R1a contains  $G\alpha_i$  (PDB id 1AGR). The GHS-R1a homodimer was constructed based on the symmetric TM5/6 protein-protein interface observed in the crystal structure of the  $\mu\text{OR}$  (PDB id 4DKL). The GHS-R1a – sigma-1 receptor complex was constructed using protein-protein docking with HADDOCK, under the imposed experimental restrains that TM 1 and 2 of GHS-R1a contract the single TM of sigma-1 receptor.

### III.26 Ligands, Expression Vectors and Reagents

#### Ligands and reagents

Lipopolysaccharides (LPS) (Sigma-Aldrich; St Louis, MO, United States)  
 2-arachidoloylglycerol (Tocris Bioscience; Bristol, UK)  
 Anandamide (Tocris Bioscience; Bristol, UK)  
 Rimonaban (Tocris Bioscience; Bristol, UK)  
 JWH133 (Tocris Bioscience; Bristol, UK)  
 AM630 (Tocris Bioscience; Bristol, UK)  
 Arachidonyl-2'-chloroethylamide (ACEA) (Tocris Bioscience; Bristol, UK)  
 Interferon- $\gamma$  (Sigma-Aldrich; St Louis, MO, United States)  
 $^3\text{H}$ -WIN 55,212-2 (PerkinElmer; Wellesley, MA, United States)  
 Cannabidiol (CBD) (Tocris Bioscience; Bristol, UK)  
 WIN 55,212-2 mesylate (Tocris Bioscience; Bristol, UK)  
 SR144528 (Tocris Bioscience; Bristol, UK)  
 PRE-084 (Tocris Bioscience; Bristol, UK)  
 Ghrelin (Tocris Bioscience; Bristol, UK)  
 YIL-781 (Tocris Bioscience; Bristol, UK)  
 Cocaine-chlorhydrate (Spanish *Agencia del Medicamento*; Ref n $^{\circ}$ : 2003C00220)  
 Zardaverine (Tocris Bioscience; Bristol, UK)  
 Trizol Reagent (Sigma-Aldrich, St Louis, MO, United States)  
 1-bromo-3-chloropropane (Sigma-Aldrich, St Louis, MO, United States)  
 Mowiol (Calbiochem; Darmstad, Germany)  
 Ionomycin Calcium Salt from *Streptomyces conglubatus* (Sigma-Aldrich, St Louis, MO, USA)  
 DeepBlue C (Molecular Probes; Eugene, OR, USA)  
 Coelenterazine H (PJK GmbH; Kleinblittersdorf, Germany)  
 Paraformaldehyde 10% (Electron Microscopy Sciences, Hatfield, PA, USA)  
 DMSO (Sigma-Aldrich, St Louis, MO, USA)

#### Expression Vectors and Genetic Engineering Reagents:

pRLuc-N1 plasmid vector (Perkin Elmer; Wellesley, MA, United States)  
 pEYFP-N1 (Clontech; Heidelberg, Germany)  
 p-GFP $^2$  (Clontech; Heidelberg, Germany)  
 SNAP-tagged human CB $_2$ R plasmid vector (Cisbio Assays, Codolet, France)  
 pcDNA3.1-cRluc8 vector (Perkin Elmer; Wellesley, MA, United States)

## MATERIALS AND METHODS

pcDNA3.1-nRluc8 vector (Perkin Elmer; Wellesley, MA, United States)

pcDNA3.1-nVenus vector (Perkin Elmer; Wellesley, MA, United States)

pcDNA3.1-cVenus vector (Perkin Elmer; Wellesley, MA, United States)

Restriction Enzymes (Promega; Madison, WI, United States)

TaqDNA polymerase (Promega; Madison, WI, United States)

Moloney Murine Leukemia Virus Reverse Transcriptase (Promega; Madison, WI, USA)

Site-Directed mutagenesis kit (Clontech; Heidelberg, Germany)



**IV. RESULTS  
AND  
DISCUSSION**



## **IV. RESULTS AND DISCUSSION**

### **Chapter 1**

#### IV.1 Modulation of the expression and signalling of cannabinoid CB<sub>1</sub>, CB<sub>2</sub> and CB<sub>1</sub>-CB<sub>2</sub> receptor heteromers in activated microglia.

The endocannabinoid system is an important system for the homeostatic control of body temperature, neurotransmission or immune response. Regarding the latter, many researchers have determined the neuroprotective role of exogenous and endogenous cannabinoids (*van der Stelt and Di Marzo, 2005*). This fact is based on the implication of microglial cells in sensing the neuronal environment together with the pathological changes produced by the onset of neurodegenerative diseases. The characteristic accumulation of  $\beta$ -amyloid in Alzheimer's Disease (AD) and  $\alpha$ -synuclein in Parkinson's disease (PD) bring about inflammation processes within the CNS, that are mediated by activated microglia, whose can evolve into two different phenotypes. The M1 pro-inflammatory phenotype, commonly present in acute responses against pathogenic insults, promotes the release of pro-inflammatory cytokines and the clearance of the threat. In physiological states, after the clearance of the insult, microglia may adopt a M2 reparative phenotype, having a tissue-repairing and homeostatic role (*Mecha et al., 2015*). However, persistence of the inflammatory threat in neurodegenerative diseases, provokes a chronic M1 phenotype, enhancing the pro-inflammatory environment that ends up increasing the detrimental effects on the neurodegenerative disease progression (*Malek et al., 2015*). In this regard, it has been shown that endocannabinoids, through action on cannabinoid receptors, could be regulating the microglial phenotype. Therefore cannabinoid receptors are potential targets for therapies attempting to direct microglial activation towards a reparative M2 phenotype (*Mecha et al., 2016; Navarro et al., 2016*).

As it has been previously described, CB<sub>1</sub>R and CB<sub>2</sub>R are GPCR (*Lu and Mackie, 2016*) co-expressed coincides in microglia (*Bilkei-Gorzo, 2012; Mecha et al., 2015*). Moreover, a direct interaction between both receptors has been described in HEK293T and SHSY5Y cells, with implications regarding the receptors signalling (*Callén et al., 2012*). However, the possible interaction of CB<sub>1</sub>R and CB<sub>2</sub>R in microglial cells and the consequences of such receptor-



receptor interaction have never been studied.

Thus, in this chapter 1, the role of the CB<sub>1</sub>R, CB<sub>2</sub>R and the CB<sub>1</sub>-CB<sub>2</sub> receptor heteromer in different activation microglial phenotypes was investigated to meet the **AIM I** of the Thesis.

In this chapter, the author of this Thesis, Edgar Angelats, provided part of the results obtained in N9 microglial cell line and performed the quantitative PCR assays in primary cultures of microglia. These and other results by members of the laboratory and in collaboration with other laboratories, led to the paper entitled **'Receptor-heteromer mediated regulation of endocannabinoid signalling in activated microglia. Role of CB<sub>1</sub> and CB<sub>2</sub> receptors and relevance for Alzheimer's disease and levodopa-induced dyskinesia'** G. Navarro, D. Borroto-Escuela, E. Angelats, I. Etayo, I. Reyes-Resina, M. Pulido-Salgado, A.I. Rodríguez-Pérez, E.I. Canela, J. Saura, J.L. Lanciego, J.L. Labandeira-García, C.A. Saura, K. Fuxe, R. Franco. The paper is published in *Brain, Behaviour and Immunity* 67 (2018) 139-161, and I. Reyes-Resina and I. Etayo, who are co-authors of the publication have included this work on their thesis.

#### IV.1.1 N9 microglial cell activation

In order to study whether the CB<sub>1</sub>-CB<sub>2</sub> receptor heteromer formation may occur in resting and activated microglia, we firstly focused our research on inducing an activated phenotype to microglial-derived N9 cells using LPS and INF- $\gamma$ . Initially, a dose response assay, with a range of 0.1-5  $\mu$ M of LPS plus a constant amount of 200 U/mL of INF- $\gamma$  was carried out. The NO production was measured as surrogate marker of the cell activation. Results shown in Figure R1A led to select the 1  $\mu$ M dose of LPS as a sufficient concentration to produce cell activation. In parallel, a time response assay was performed, challenging N9 cells with 1  $\mu$ M LPS and 200 U/mL of INF- $\gamma$  within a range of 2 to 96 hours. Once again, cell NO production was measured, with the 48 h treatment being selected for further studies (Figure R1B).

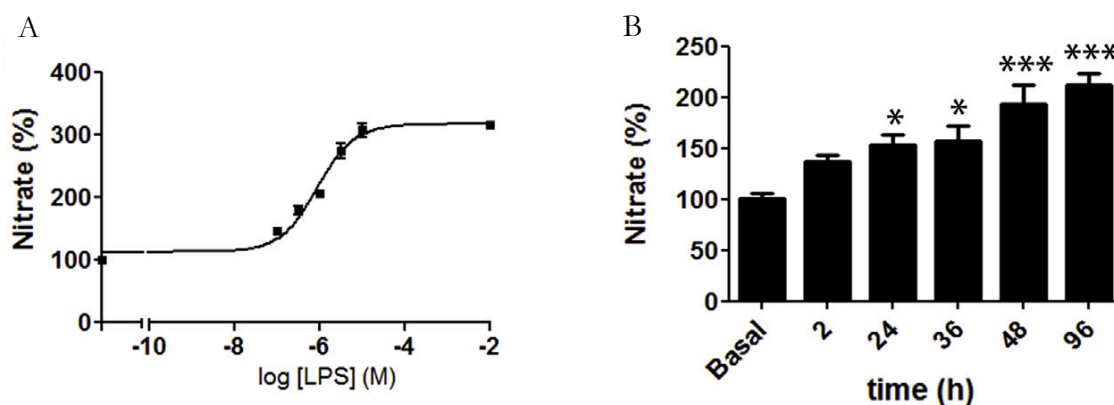


**Figure R1. NO production in N9 cell line.** A) N9 cell line was treated for 48 h with different concentrations of LPS in presence of 200 U/ml INF- $\gamma$ . B) N9 cells were treated for different times (2, 24, 36, 48 and 96 h) with 1  $\mu$ M LPS and 200 U/ml INF- $\gamma$ . In both A and B, NO production was measured in cell-free growth culture medium. Values are the mean  $\pm$  S.E.M. of 6 different experiments in triplicates. One-way ANOVA followed by a Bonferroni's multiple comparison *post hoc* test were used for statistical analysis (\* $p$ <0.05; \*\*\* $p$ <0.001 versus basal conditions).

#### IV.1.2 Identification of CB<sub>1</sub>-CB<sub>2</sub> receptor heteromers in N9 microglial cell type

To address whether CB<sub>1</sub> and CB<sub>2</sub> receptors are forming heteromers in microglial cells, BRET assays were performed. On one hand, N9 cell line was transfected with a constant amount of cDNA for CB<sub>1</sub>R-Rluc (0.7  $\mu$ g) and increasing amounts of cDNA for CB<sub>2</sub>R-GFP<sup>2</sup> (0.2-1  $\mu$ g) providing readouts in a 1000-12000 fluorescence unit range. In co-transfected cells a saturated BRET curve was obtained (BRET<sub>max</sub> of  $46 \pm 2$  mBU and BRET<sub>50</sub> of  $4 \pm 1$ ), indicating the existence of CB<sub>1</sub>R-CB<sub>2</sub>R heteromeric complex in N9 cells (Figure R2). As negative control, cells were transfected with the same amount of cDNA for CB<sub>1</sub>R-Rluc (0.7





$\mu\text{g}$ ) and increasing amounts of cDNA for  $\text{D}_1\text{R-GFP}^2$  (0.3-1.5  $\mu\text{g}$ ) providing readouts in a 1000-12000 fluorescence unit range. Lack of interaction was confirmed by a linear signal, which reflects inspecificity. On the other hand, N9 cells co-expressing similar amounts of the  $\text{CB}_1\text{R-Rluc}$  and  $\text{CB}_2\text{R-GFP}^2$  than control cells, were treated for 48 h with 1  $\mu\text{M}$  LPS and 200 U/mL of  $\text{INF-}\gamma$  previous to perform BRET assays. Once again, a saturation curve was obtained, being higher in this condition than in resting cells (Figure R2). These results indicate that neuroinflammation-like conditions potentiate  $\text{CB}_1\text{-CB}_2$  receptor heteromer formation by increasing the number of heteromers and/or rearranging the quaternary structure of the heteromer.

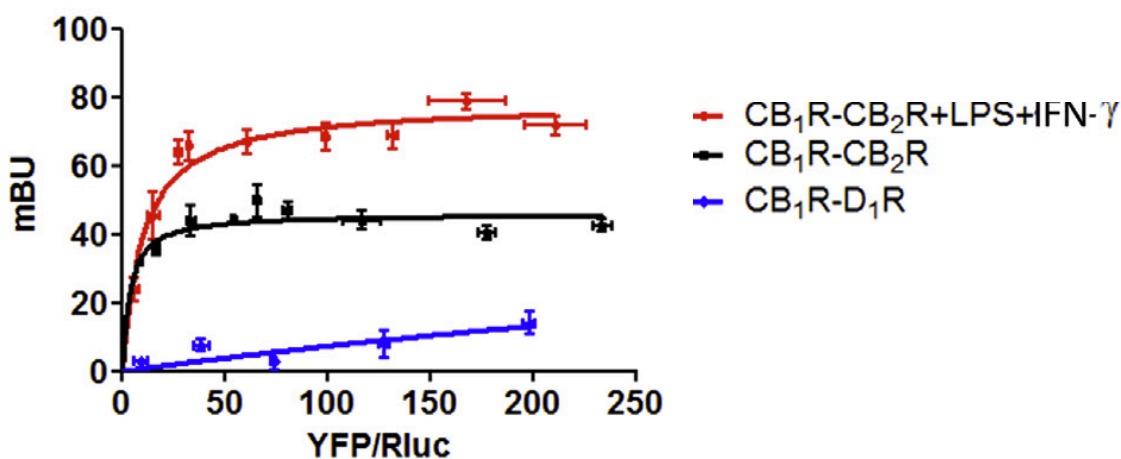


**Figure R2. Heteromerization of  $\text{CB}_1$  and  $\text{CB}_2$  receptors in resting and activated microglial N9 cells.** BRET assays were performed in N9 cells transfected with a constant amount of cDNA for  $\text{CB}_1\text{R-Rluc}$  (0.7  $\mu\text{g}$ ) and increasing amounts of cDNA for  $\text{CB}_2\text{R-GFP}^2$  (0.2-1  $\mu\text{g}$ ) and treated (red line) or not (black line) with 1  $\mu\text{M}$  LPS and 200 U/ml  $\text{INF-}\gamma$  (48 h treatment). As negative control, N9 cells were transfected with constant amounts of  $\text{CB}_1\text{R-Rluc}$  (0.7  $\mu\text{g}$ ) and increasing amounts of cDNA for  $\text{D}_1\text{R-GFP}^2$  (0.3-1.5  $\mu\text{g}$ ). Values are the mean  $\pm$  S.E.M. of 8 different experiments in quadruplicates.

To evaluate the endogenous expression of cannabinoid receptors in N9 cells, we performed immunocytochemistry assays using specific antibodies against  $\text{CB}_1$  and  $\text{CB}_2$  receptors and fluorescence was detected in a confocal microscopy.  $\text{CB}_1\text{R}$  expression was relatively high, while  $\text{CB}_2\text{R}$  expression was low ( $520 \pm 30$  and  $150 \pm 20\%$  increase over basal, respectively) (Figure R3A). However, when cells were treated for 48 h with 1  $\mu\text{M}$  LPS and 200 U/mL of  $\text{INF-}\gamma$ ,  $\text{CB}_1\text{R}$  expression was similar than in resting state, whereas  $\text{CB}_2\text{R}$  expression markedly increased ( $580 \pm 40$  and  $290 \pm 30\%$  increase over basal, respectively) (Figure R3A). Proximity Ligation Assays (PLAs) are used as complementary technique to observe protein-protein interactions in heterologous or native tissue. When this technique was used to detect changes in the number of  $\text{CB}_1\text{-CB}_2$  receptor heteromers, the results showed that the treatment

of N9 cells with LPS and  $\text{INF-}\gamma$  markedly increased the number of red clusters/spots (Figure R3B), which were due to proximity of the receptors. Absence of the anti- $\text{CB}_1\text{R}$  primary antibody, showed a negligible number of red clusters in all imaging fields, was used as negative control. Differences in percentage of spot-containing cells and in the number of red spots per cell were statistically significant when compared to those in resting N9 cells (Figure R3C). Taken together BRET, immunocytochemistry and PLA assays, it may be concluded that activation of microglial-derived N9 cells led to a significant increase in the expression of the  $\text{CB}_2\text{R}$  and in the amount of  $\text{CB}_1\text{-CB}_2$  heteromers.

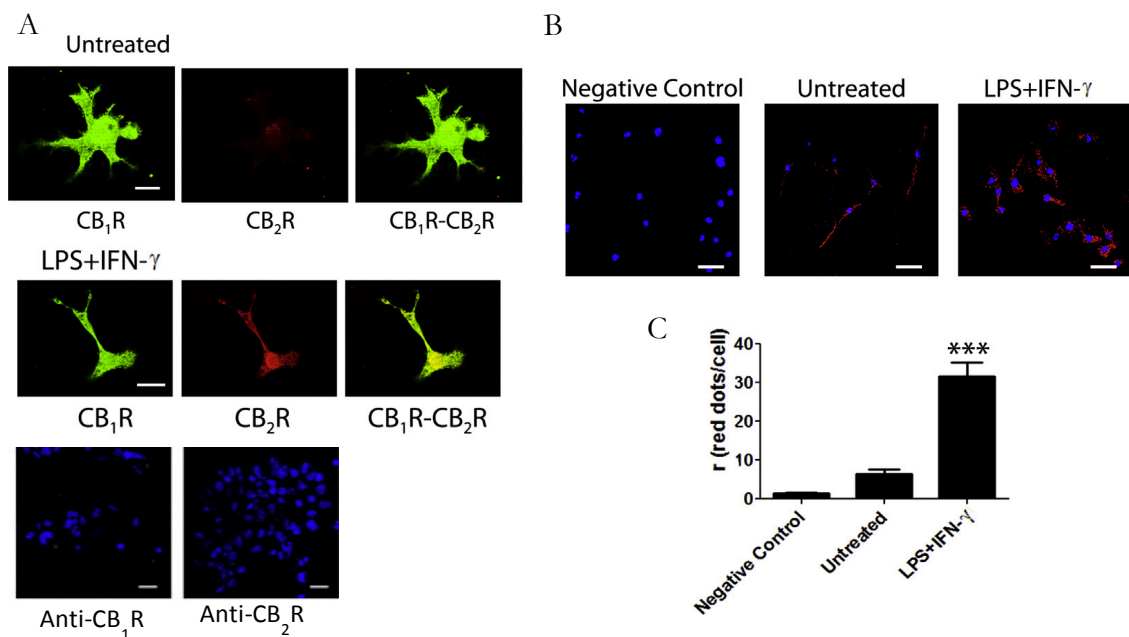


**Figure R3. Evaluation of expression and heteromerization levels of cannabinoid receptor in N9 cells.** A) Immunocytochemistry assay was performed in N9 cells. Specific antibodies against  $\text{CB}_1\text{R}$  (green) and  $\text{CB}_2\text{R}$  (red) were used. Co-localisation is shown in yellow. Controls without the use of the primary antibody were performed to ensure antibody specificity. Scale bar: 5  $\mu\text{m}$ . Fluorescence was quantified by Fiji-Image J software. B) Proximity Ligation Assays (PLA) in N9 cells were performed by the use of the specific antibodies against  $\text{CB}_1\text{R}$  and  $\text{CB}_2\text{R}$ . Cell nuclei were stained with Hoechst (blue) and heteromers appear as red clusters/dots. Representative images corresponding to stacks of 4 sequential planes are shown. Scale bar: 15  $\mu\text{m}$ . C) Quantification of visualised clusters. In the y-axis the number of clusters/spots in spot-containing cells is displayed. Values are the mean  $\pm$  S.E.M of 5 different experiments. One-way ANOVA and Bonferroni's multiple comparison *post hoc* test were used for statistical analysis (\*\*\*)  $p < 0.001$  versus control).

#### IV.1.3 LPS and $\text{INF-}\gamma$ action on primary microglial cultures

Then, we moved to a more physiological model, which consisted of primary cultures of microglia from mouse striatum. In these cells we first addressed the production of NO after a treatment with LPS and  $\text{INF-}\gamma$  to confirm the potential of these cells to become activated. The primary cultures were treated for 48 h with 1  $\mu\text{M}$  LPS and 200 U/mL of  $\text{INF-}\gamma$  and the NO production in treated cells was significantly higher than in non-activated ones



(Figure R4A). The microglial nature of the culture was assayed using an antibody against a specific marker, namely Ionized calcium binding adaptor molecule 1 (Iba1). In immunostaining experiments using anti-Iba1 antibody it was observed that microglial cells grouped when subjected to LPS and INF- $\gamma$  treatment, while untreated cells were spread over the fields of observation (Figure R4B). Cell death measured in cell cultures for 48 h was moderate: 9% in cells treated with LPS and INF- $\gamma$  versus 4% in non-stimulated cells (Figure R4C).

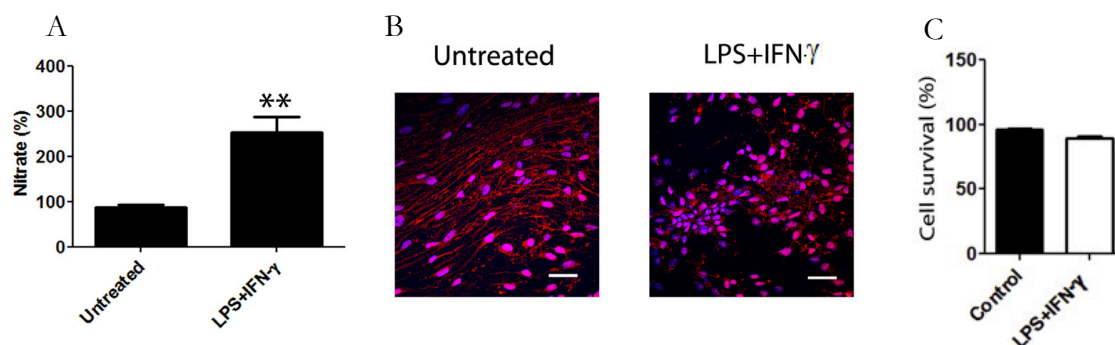


**Figure R4. Evaluation of combined LPS and INF- $\gamma$  treatment in microglial primary cultures.** A) Primary cultures of striatal microglia were stimulated with 1  $\mu$ M LPS and 200 U/mL INF- $\gamma$  for 48 h and nitrate production was determined. Values are the mean  $\pm$  S.E.M. of 6 different experiments in triplicates. One-way ANOVA and Bonferroni's multiple comparison *post hoc* test were used for statistical analysis (\*\* $p$ <0.01 versus control). B) Immunocytochemical assays were performed in primary cultures of striatal microglia incubated for 48h with 1  $\mu$ M LPS and 200 U/mL INF- $\gamma$ . Staining against the microglial marker Iba-1 was performed with a primary antibody against the protein and a Cy3 secondary antibody. Scale bar: 30  $\mu$ m. C) Analysis of cell survival of microglial striatal primary cultures after 48 h stimulation with 1  $\mu$ M LPS and 200 U/mL INF- $\gamma$ . After diluting the cells 1:1 v/v in Trypan Blue, cells were counted and expressed as percentage of cell survival.

Then, we wanted to analyse the presence of CB<sub>1</sub>R and CB<sub>2</sub>R in microglial primary cultures, and quantify, by RT-PCR, the relative expression of transcripts for both receptors in presence of vehicle, LPS or LPS and INF- $\gamma$ . The results obtained shown a two-fold increase in the expression of CB<sub>1</sub>R mRNA under LPS or LPS and INF- $\gamma$  treatments, while for CB<sub>2</sub>R mRNA, the expression increased 12-fold in LPS treated cells and 21-fold in LPS and INF- $\gamma$  treated cells (versus medium-treated cells) (Figure R5A and B). Furthermore, we performed immunocytochemistry assays using specific antibodies against CB<sub>1</sub>R and CB<sub>2</sub>R that showed similar results to those found in N9 cells, i.e. a marked increase in fluorescent CB<sub>2</sub>R staining (from 280  $\pm$  20 to 520  $\pm$  30% over basal), and a moderate increase in CB<sub>1</sub>R staining (from 200  $\pm$  10 to 270  $\pm$  30 over basal) (Figure R5C) after activation of the microglial cells. Apart from a marked CB<sub>1</sub> and CB<sub>2</sub> receptor co-localisation, PLA assay images in Figure R5D showed a pronounced increase in the amount of heteromers per cell when cells were treated with LPS and INF- $\gamma$  (26 spots/spot-containing cell in LPS/INF- $\gamma$ -treated cells versus 2.3 in non-

activated cells). These results complement those obtained using N9 cells and show a marked increase of CB<sub>1</sub>-CB<sub>2</sub> heteromeric complexes when microglia was activated.

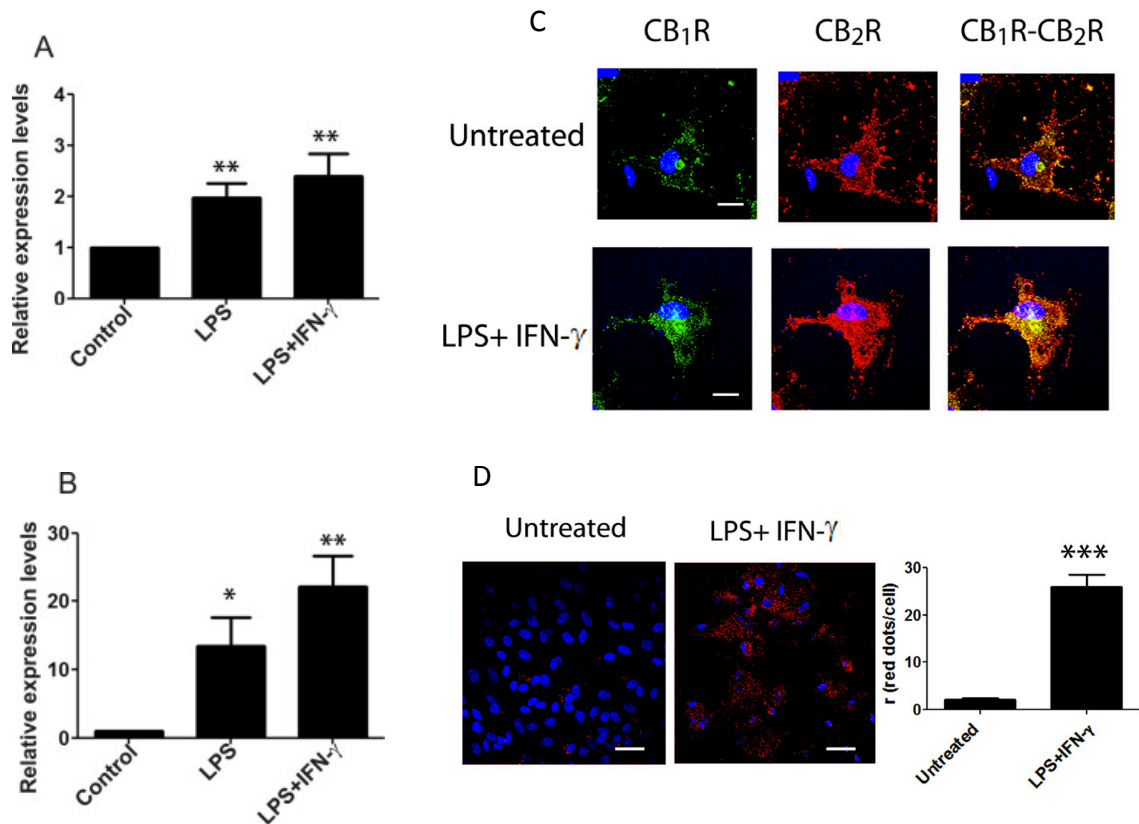


**Figure R5. Effects of LPS and INF- $\gamma$  treatment on cannabinoid receptors of primary microglial cultures.** Microglial primary cultures underwent a 48 h treatment of 1  $\mu$ M LPS, 1  $\mu$ M LPS and 200 U/mL INF- $\gamma$  or vehicle previous to extract the mRNA of CB<sub>1</sub>R (A) and CB<sub>2</sub>R (B). Transcripts were retrotranscribed to DNA and a RT-PCR was performed. Values are the mean  $\pm$  S.E.M. of 3 different experiments in triplicates. One-way ANOVA and Bonferroni's multiple comparison *post hoc* test were used for statistical analysis (\* $p$ <0.05; \*\* $p$ <0.01 versus control). C) Immunocytochemical assays were performed in primary cultures of striatal microglia treated or not with 1  $\mu$ M LPS and 200 U/mL INF- $\gamma$  for 48 h. Using anti-CB<sub>1</sub>R (green) and anti-CB<sub>2</sub>R (red) antibodies, expression of both receptors was detected. Colocalisation is shown in yellow. Scale bar: 5  $\mu$ m. D) PLA assays were performed as described in Methods in microglial primary cultures incubated in presence or absence of 1  $\mu$ M LPS and 200 U/mL INF- $\gamma$  for 48 h. Representative images corresponding to stacks of 4 sequential planes are shown. Cell nuclei were stained with Hoechst (Blue) and receptor complexes appear as red spots. Scale bar: 30  $\mu$ m. Values are the mean  $\pm$  S.E.M. of 5 different experiments. One-way ANOVA followed of a Bonferroni's multiple comparison *post hoc* test were used for statistical analysis (\*\* $p$ <0.001 versus control).

#### IV.1.4 Cannabinoid receptor signalling in activated microglia

Nowadays, it is widely accepted that signalling pathways assigned to a specific GPCR may change in heteromeric contexts. To elucidate the properties of CB<sub>1</sub>-CB<sub>2</sub> heteromers we measured forskolin-induced intracellular cAMP levels, ERK1/2 phosphorylation and Dynamic Mass Redistribution (DMR) signal (upon receptor activation). DMR is a label-free technique used in GPCR research as it measures the rearrangement of cell components, leading to a mass redistribution, that is mostly mediated by G protein activation (*Simon et al.*,



2016). When N9 cells were treated with ACEA (200 nM), the CB<sub>1</sub>R selective agonist, a significant decrease in the 0.5 μM forskolin-induced cAMP levels confirmed the G<sub>i</sub> coupling of this cannabinoid receptor. Treatment of N9 cells with the selective CB<sub>2</sub>R agonist JWH133 (100 nM), had no significant effect on the forskolin-induced cAMP levels. However, when N9 cells were treated with both ACEA and JWH133, no effect was observed, thus indication that even at low expression levels, CB<sub>2</sub>R activation blocks CB<sub>1</sub>R function. Also, anandamide and 2-AG treatment induced weak effects showing capability of CB<sub>2</sub>R to inhibit CB<sub>1</sub>R function (Figure R6A). Moreover, when N9 cells were pre-treated with a selective antagonist of CB<sub>1</sub>R, rimonabant (1 μM), not only the CB<sub>1</sub>R but also the CB<sub>2</sub>R selective agonist effect was blocked. Also, AM630 (1 μM), the selective antagonist of CB<sub>2</sub> receptors, reduced the CB<sub>1</sub> receptor-mediated decrease of forskolin-induced cAMP levels (Figure R6A). Similar results were observed in ERK1/2 phosphorylation assays, showing little ERK activation upon treatment with JWH133 or ACEA and JWH133 co-treatment (Figure R6B). Moreover, the cross-antagonism phenomenon was, once again, evident since CB<sub>2</sub>R antagonist AM630 was able to reduce ACEA-induced ERK1/2 phosphorylation and rimonabant the activation of the cell signalling produced by JWH133 (Figure R6B). In DMR assays, the results obtained were in agreement with cAMP and ERK1/2 phosphorylation assay results, thus showing a marked cell mass redistribution upon ACEA treatment, while cell response to JWH133 addition was lower. Once again, negative cross-talk and cross-antagonism phenomenon were observed (Figure R6C).

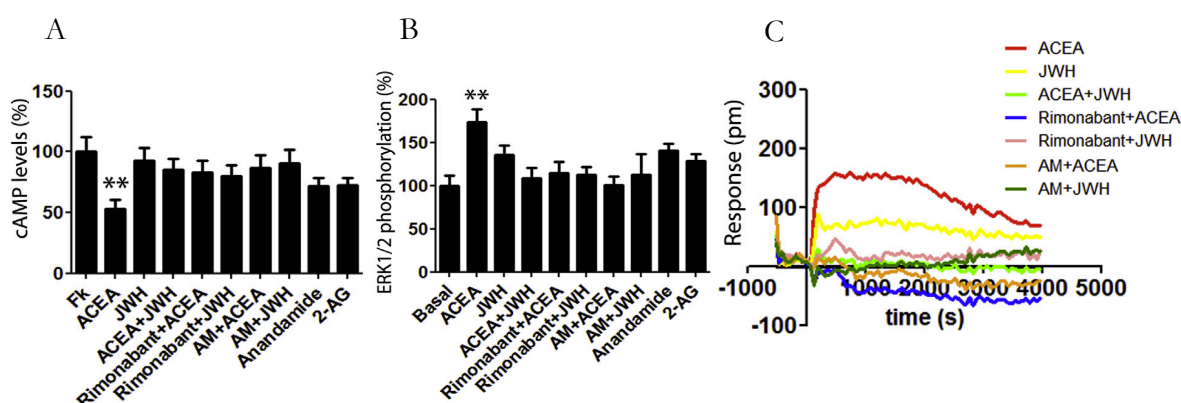


**Figure R6. Endocannabinoid signalling in resting N9 cells.** Cells pre-treated with selective receptor antagonists (1 μM rimonabant for CB<sub>1</sub>R or 1 μM AM630 for CB<sub>2</sub>R) were subsequently treated with selective agonists (200 nM ACEA for CB<sub>1</sub>R and 100 nM JWH133 for CB<sub>2</sub>R) alone or in combination, or with the endocannabinoids (200 nM anandamide or 200 nM 2-AG). In A, Forskolin-induced cAMP levels were determined 15 min after 0.5 μM forskolin addition (8 nM cAMP, which corresponds to a 280% increase over basal levels). In B, ERK1/2 phosphorylation was analysed using an AlphaScreen SureFire Kit (Perkin Elmer). In C, DMR tracings represent the picometer shifts of reflected light wavelength (in pm) over time. In A and B, values are the mean ± S.E.M. of 8 different experiments in triplicates. In all cAMP accumulation and MAPK signalling, one-way ANOVA followed by Bonferroni's multiple comparison post hoc test were used for statistical analysis (\*p<0.05, \*\*p<0.01, \*\*\*p<0.001; versus forskolin treatment in cAMP determinations or versus untreated cells in ERK phosphorylation).

When the experiments were repeated in cells previously treated with 1  $\mu\text{M}$  LPS and 200 U/mL of  $\text{INF-}\gamma$  for 48 h, cAMP N9 signalling after the addition of  $\text{CB}_1\text{R}$  agonist ACEA reflected similar results than in untreated cells, whereas the selective  $\text{CB}_2$  receptor agonist JHW133 produced an important decrease (55% approximately) of the forskolin-induced cAMP levels (Figure R7A). Taking into account the above-described results from immunocytochemistry assays, it appears that  $\text{CB}_2\text{R}$  by themselves become functionally relevant under conditions mimicking neuroinflammation. Remarkably, the effect on cAMP levels when N9 cells were simultaneously treated with the two agonists (ACEA plus JHW133) was additive. Moreover, treatment with endocannabinoids (anandamide or 2-AG) disclosed the seemingly paradoxical effect, i.e. the negative cross-talk in resting cells turned into being positive in cells treated with LPS and  $\text{INF-}\gamma$  (Figure R7A). Cross-antagonism was more robust in activated cells as pre-treatment with any of the two selective receptor antagonists abolished  $\text{CB}_1$  and/or  $\text{CB}_2$  receptor activation (Figure R7A). ERK1/2 phosphorylation and DMR were measured in cells activated with 1  $\mu\text{M}$  LPS and 200 U/mL of  $\text{INF-}\gamma$  for 48 h. The results showed a very high potency of JHW133. The  $\text{CB}_2$  receptor-selective compound increased by 5-fold the basal level of ERK1/2 phosphorylation (Figure R7B) and by 2-fold the label-free signal (Figure R7C). Also noteworthy was the additive effect when cells were simultaneously treated with ACEA and JHW133. These differential agonistic effects in resting (negative cross-talk) and activated (positive cross-talk) microglial cells contrasted with the cross-antagonism found in all conditions.

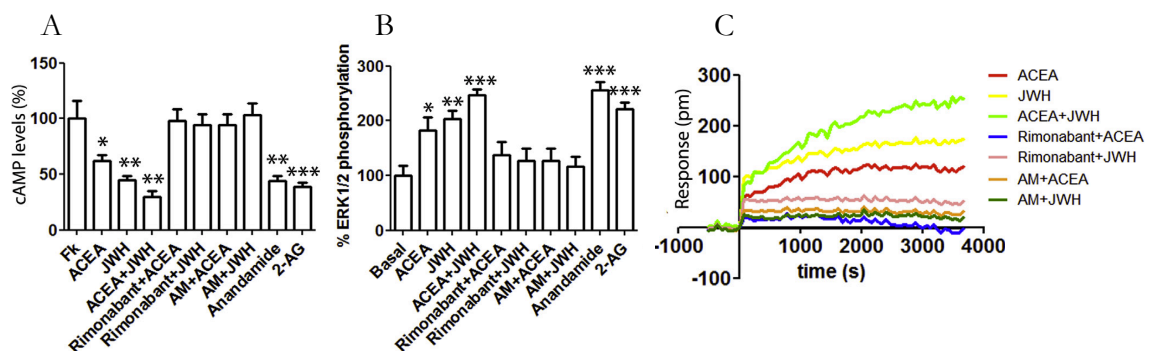


**Figure R7. Combined LPS and  $\text{INF-}\gamma$  treatment affects cannabinoid receptor signalling in N9 cells.**

N9 cells were incubated for 48 h in presence of 1  $\mu\text{M}$  LPS and 200 U/ml  $\text{INF-}\gamma$ . Then, N9 cells were pre-treated with selective receptor antagonists (1  $\mu\text{M}$  rimonabant for  $\text{CB}_1\text{R}$  or 1  $\mu\text{M}$  AM630 for  $\text{CB}_2\text{R}$ ) and subsequently treated with selective agonists (200 nM ACEA for  $\text{CB}_1\text{R}$  and 100 nM JWH133 for  $\text{CB}_2\text{R}$ ) alone or in combination, or with the endocannabinoids (200 nM anandamide or 200 nM 2-AG). In A, Forskolin-induced cAMP levels were determined 15 min after 0.5  $\mu\text{M}$  forskolin treatment (8 nM cAMP, which corresponds to a 280% increase over basal levels). In B, ERK1/2 phosphorylation was analysed using an AlphaScreen SureFire Kit (Perkin Elmer). In C, DMR tracings represent the picometer shifts of reflected light wavelength (in pm) over time. In A and B, values are the mean  $\pm$  S.E.M. of 8 different experiments in triplicates. In all cAMP accumulation and MAPK signalling, one-way ANOVA followed by Bonferroni's multiple comparison *post hoc* test were used for statistical analysis (\* $p < 0.05$ , \*\* $p < 0.01$ , \*\*\* $p < 0.001$ ; versus forskolin treatment in cAMP determinations or versus untreated cells in ERK phosphorylation).

#### IV.1.5 Agonistic and antagonistic modulation of intracellular pathways in microglial primary cultures

Signalling experiments similar to those above described for cell lines were performed in primary cultures of striatal microglia. As expected, CB<sub>1</sub>R specific agonist ACEA (200 nM) induced a characteristic decrease in cAMP accumulation, while the CB<sub>2</sub>R agonist JWH133 was not able to decrease the cAMP levels. Similarly to what happened in N9 microglial cell line, co-treatment with both agonists led to a negative cross-talk phenomenon. Upon activation of microglia with LPS and INF- $\gamma$ , CB<sub>2</sub>R activation was robust and simultaneous treatment with the selective agonists showed an additive effect. Finally, when cells were treated with amyloid  $\beta$  aggregates, which is one of the hallmarks of Alzheimer's disease, the results were similar to those in activated microglial cells (Figure R8A). Likewise, when ERK1/2 phosphorylation was analysed, CB<sub>2</sub>R showed more response in LPS and INF- $\gamma$  treated cells, and the negative cross-talk after co-activation with ACEA and JWH133 in basal conditions switched to an additive effect of both ligands upon the activation of the cells with LPS and INF- $\gamma$  or in presence of amyloid  $\beta$  aggregates (Figure R8B).

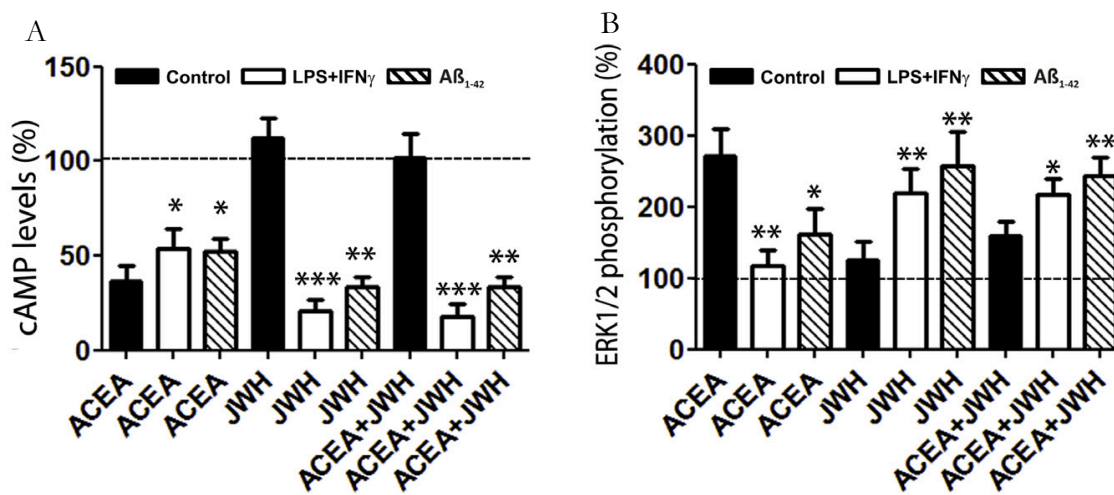


**Figure R8. Combined LPS and INF- $\gamma$  treatment modifies cannabinoid receptor function in primary microglial cultures from mouse striatum.** Primary cultures of mouse microglia were incubated for 48 h in presence (white bars) or absence (black bars) of 1  $\mu$ M LPS and 200 U/ml of INF- $\gamma$ , or in presence of 500 nM A $\beta$ <sub>1-42</sub> (striped bars), and subsequently treated with ACEA (200 nM), JWH133 (100 nM) or both. Forskolin-induced cAMP levels (5 nM forskolin, corresponding to a 320% increase over basal levels) (A) and ERK1/2 phosphorylation (B) were determined as described in Methods. Values are the mean  $\pm$  S.E.M. of 7 different experiments in triplicates. In both cases, one-way ANOVA followed by a Bonferroni's multiple comparison *post hoc* test were used for statistical analysis (\*p<0.05, \*\*p<0.01, \*\*\*p<0.001; versus forskolin treatment in cAMP determinations or versus untreated cells in pERK assays).

Finally, DMR recordings in resting and activated cells provided results that were similar to those obtained in cAMP and MAP kinase activation pathways (Figure R9). However, a difference was found in activated cells in which the positive cross-talk was not

found (Figure R9B). The label-free signal induced either by agonist was already marked and very high for primary cultures. Mass redistribution was therefore maximal using ACEA or JWH133, and this may be the reason that DMR technology was not able to detect the positive cross-talk detected in cAMP and pERK1/2 assays. Results in N9 and in primary cultures indicate that microglial activation leads to a very marked qualitative and quantitative change in cannabinoid receptor-mediated effects that at least in part, seem to be mediated by CB<sub>1</sub>-CB<sub>2</sub> receptor heteromers.

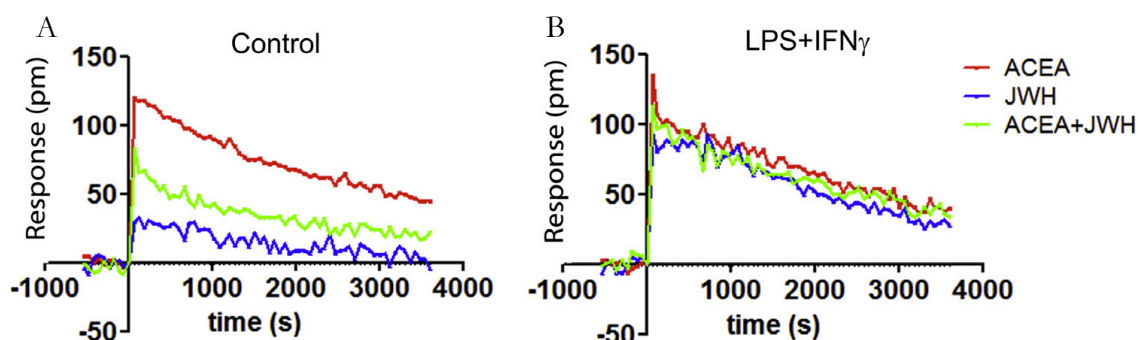


**Figure R9. Dynamic Mass Redistribution (DMR) assays in primary microglial cultures.** Primary cultures of striatal microglia were incubated in presence (B) or absence (A) of 1  $\mu$ M LPS and 200 U/ml of INF- $\gamma$  for 48 h and subsequently treated with ACEA (200 nM, red line), JWH133 (100 nM, blue line) or both (green line). Values are the mean  $\pm$  S.E.M. of 6 different experiments.

#### IV.1.6 CB<sub>1</sub>-CB<sub>2</sub> receptor heteromer expression in dyskinetic animals

The 6-hydroxy-DA rat model of Parkinson disease, prepared by unilateral neurotoxin injection on the right hemisphere, courses with microglial activation and neuroinflammation (*Aron Badin et al., 2013*). Specific primary antibodies against CB<sub>1</sub> and CB<sub>2</sub> receptors and DNA probes linked to rabbit and goat secondary antibodies were used to perform PLA assays. Using selective probes, proximity between the two receptors was detected by confocal microscopy as punctuate red fluorescence signals. In naïve rats we detected that 8% of the cells were PLA positive and displayed around 2 red clusters/cell (Figure R10A). The non-lesioned (left) hemisphere in lesioned animals showed a 9.2% of labelled cells with a bit less than 2 red spots/cell, while the level of receptor complexes in the lesioned (right) hemisphere was significantly higher (18.7%) with 2.4 red spots/cell. The result indicates that lesioned animals displayed a significant increase in the level of striatal CB<sub>1</sub>-CB<sub>2</sub> receptor complexes (Figure R10B).





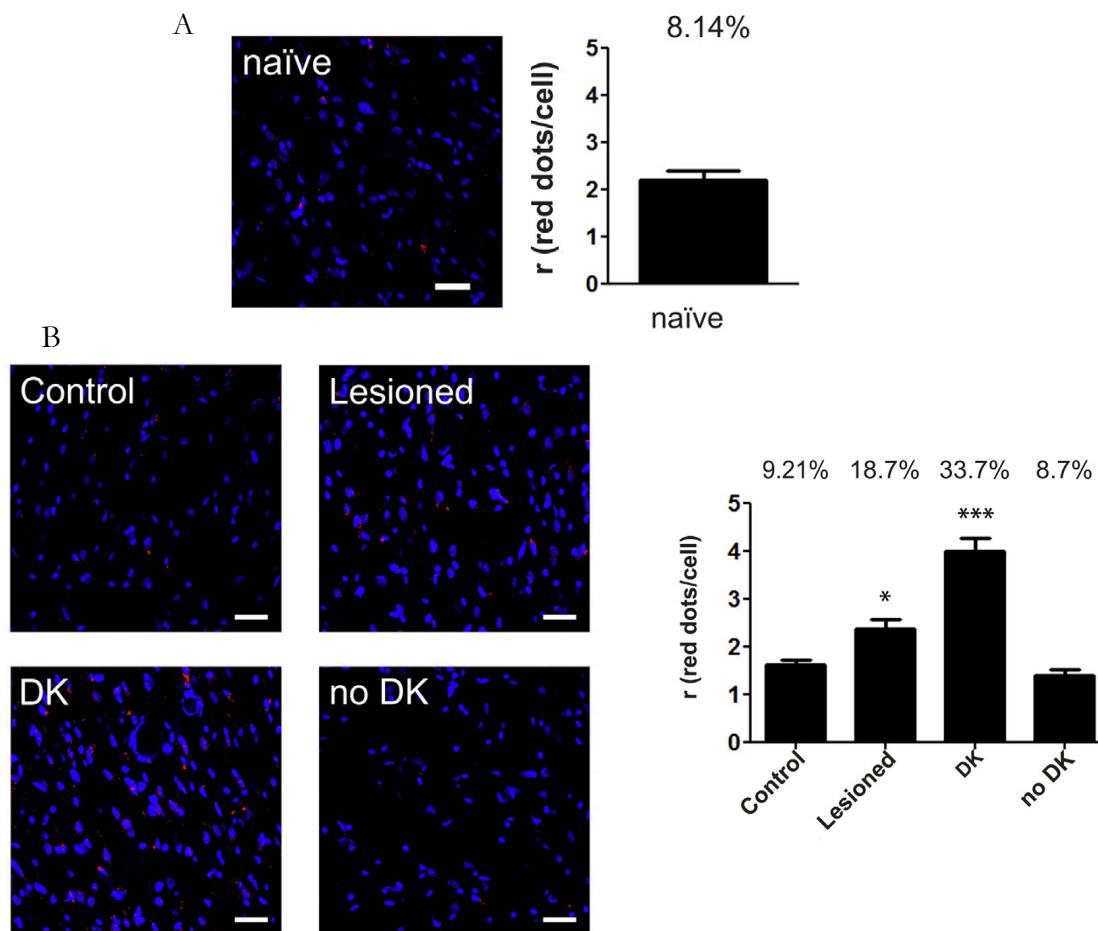


**Figure R10. CB<sub>1</sub>-CB<sub>2</sub> receptor complex expression in the rat model of Parkinson's disease.** PLA assays were performed in striatal sections from non-lesioned (naïve) (A) or hemistriatal sections from lesioned rats as well as in levodopa-treated rats displaying (DK) or not (no DK) dyskinesia (B). In B, control corresponds to sections of the non-lesioned (left) side, whereas lesioned 'DK' and 'no DK' corresponds to sections from the lesioned (right) side. Confocal microscopy images (4 superimposed sections) are shown; heteromeric complexes appear as red clusters surrounding Hoechst-stained nuclei in blue. Panels showing the r ratio (number of red spots/spot-containing cell) and percentage of cells containing one or more red spots are shown in the graphs. Data (ratio or percentage of positive cells) are the mean  $\pm$  S.E.M. of counts in 6-8 different fields from every brain sample of non-lesioned (naïve), lesioned (control), and levodopa treated rats displaying (DK) or not (no DK) dyskinesia (n=3 in each group). Two-way ANOVA analysis showed significant inter-group differences on ratio and percentage of positive cells. \*p<0.05, \*\*\*p<0.001 (respect to naïve) after Bonferroni's *post hoc* test. Scale bars: 30  $\mu$ m.

In equivalent sections we assayed the occurrence of activated microglia (using an antibody against a rat MHC class II activation marker). Unlike in control animals, a high number of activated cells was found in lesioned and in levodopa-treated rats (both dyskinetic and non-dyskinetic) (Figure R11). However, inter-group differences in the number of activated microglial cells in the 6-hydroxy-DA-lesioned animals were not statistically significant. Interestingly, in rats rendered dyskinetic by the chronic levodopa treatment, the percentage of cells (in the lesioned hemisphere) showing red clusters increased to 33.7% with an average of 4 red spots/cell. In contrast, the levodopa treatment in rats not displaying

dyskinesia showed similar results as in the naïve animals or as in the left hemisphere in lesioned animals (8.7% and 1.3 red spots/cell) (Figure R10B). These results indicate that the dyskinetic animals have an important increase of cannabinoid CB<sub>1</sub>-CB<sub>2</sub> receptor complexes.

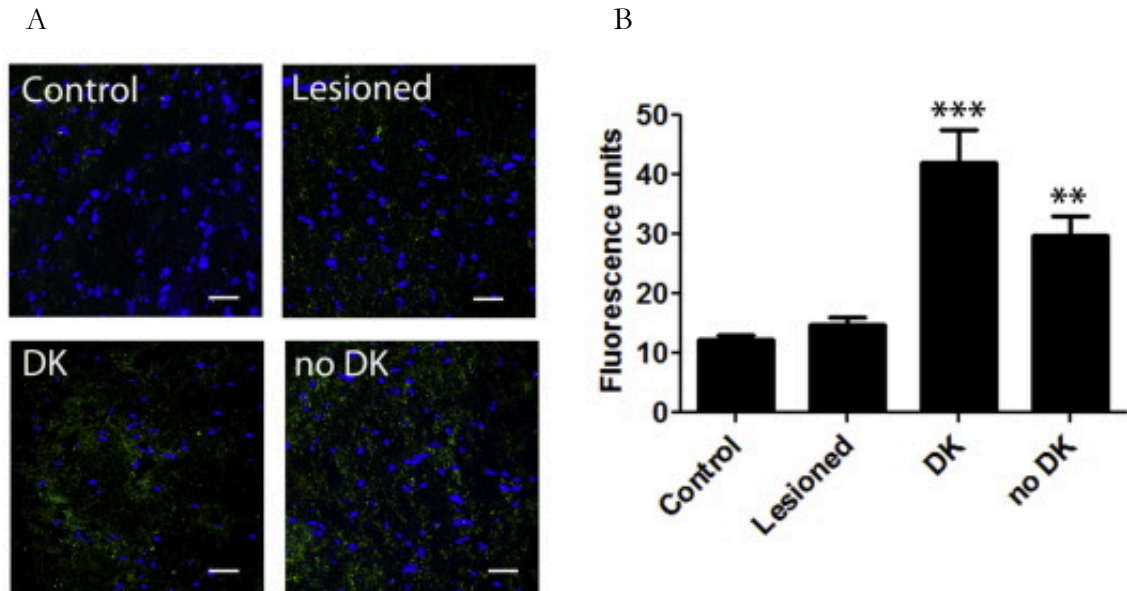


**Figure R11. Evaluation of microglial activation in a rat model of Parkinson's disease.** A) MHC class II labelling (green) in striatal sections of lesioned rats as well as levodopa-treated rats displaying (DK) or no (no DK) dyskinesia. Confocal images (4 superimposed images) are shown with the Hoechst-stained nuclei in blue. Scale Bar 30  $\mu$ m. B) Mean values of the fluorescence intensity (of MHC class II labelling)  $\pm$  S.E.M. of different fields from every brain sample of non-lesioned (naïve), lesioned (control), and levodopa treated rats displaying (DK) or not (no DK) dyskinesia (n=3 in each group). One-way ANOVA analysis showed significant inter-group differences on ratio and percentage of positive cells. \*\*p<0.01, \*\*\*p<0.001 (respect to the control) after Bonferroni's *post hoc* test.

#### IV.1.7 CB<sub>1</sub>-CB<sub>2</sub> heteromer expression and function in the APP<sub>Sw,Ind</sub> transgenic mouse model of Alzheimer's disease

Alzheimer's disease is a pathology that courses with neuroinflammation. It is also known that receptors that are important in neuroinflammatory processes are downregulated in human resting microglia but are markedly expressed in samples from AD patients. Examples are adenosine A<sub>2A</sub> receptors, which appear in glial cells in the hippocampus and the cerebral cortex of AD patients (Angulo *et al.*, 2003) and cannabinoid CB<sub>2</sub>R, whose levels are upregulated together with those of glial markers in the frontal cortex of AD patients (Solas *et al.*, 2013). Although no transgenic model appropriately reflects the many sides of the human AD condition (Medina and Avila, 2014), neuroinflammation has been described in the APP<sub>Sw,Ind</sub> mouse, including the occurrence of reactive astrocytes and microglia displaying an activated phenotype (Mucke *et al.*, 2000; Saura *et al.*, 2005). Hippocampus from two-day-old pups obtained from APP<sub>Sw,Ind</sub> x WT mouse crossings were individually genotyped and classified as



non-transgenic (control) and heterozygous APP transgenic mice, which in adulthood display amyloid plaques, neuroinflammatory responses, including reactive microglia and cognitive deficits (Mucke *et al.*, 2000). Primary hippocampal cultures of microglia were prepared and PLA assays were developed to detect expression changes in CB<sub>1</sub>-CB<sub>2</sub> receptor complexes. While only 5% of the cultured cells of non-transgenic control samples were stained, the number of cells displaying red clusters in cells from APP<sub>Sw,Ind</sub> transgenic mice increased to 83%. Moreover the number of red dots/cell significantly increased from 1.5 to 6 (Figure R12A). These notable results made us wonder whether the microglial cells from phenotypically ‘normal’ pups could already display an activated phenotype. Indeed, using an antibody against a mouse MHC class II activation marker, an activated microglial phenotype was found in cultures from heterozygous animals but not in those from control ones (Figure R12B).

Then, endocannabinoid signalling was addressed in microglial primary cultures of non-transgenic and APP<sub>Sw,Ind</sub>. Cultures of hippocampal microglia were pretreated with forskolin

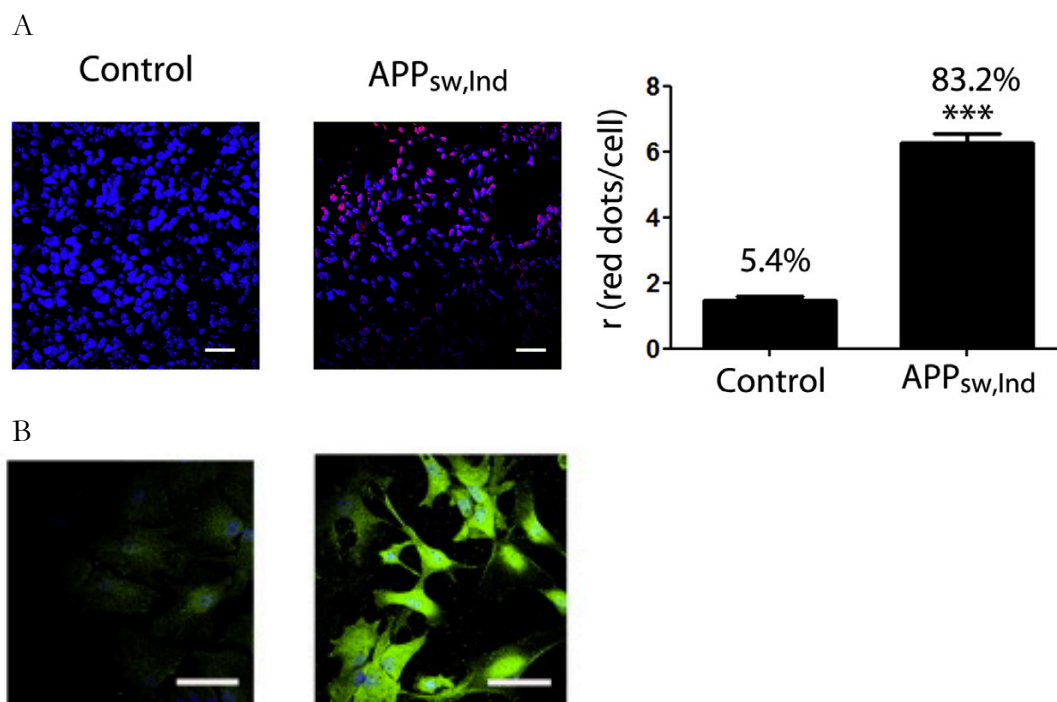


**Figure R12. CB<sub>1</sub>-CB<sub>2</sub> heteromer expression in the APP<sub>Sw,Ind</sub> mouse model of Alzheimer's disease.**

A) Primary microglia cultures from hippocampus of two-day-old non-transgenic (control) and APP<sub>Sw,Ind</sub> mice were analysed by PLA, which was performed using primary antibodies against CB<sub>1</sub> or CB<sub>2</sub> receptors. Confocal microscopy images (stacks of 4 consecutive planes) show heteroreceptor complexes as red clusters in Hoechst-stained nuclei (blue). Scale bar: 30  $\mu$ m. At right, the graph shows the number of red dots/dot-containing cell; the number above each bar indicates the percentage of cells presenting red clusters. Values are the mean  $\pm$  S.E.M. of 6 different experiments. In all cases, one-way ANOVA analysis followed by Bonferroni's multiple comparison *post hoc* test were used for statics analysis (\*\**p*<0.001 versus the control). B) Immunocytochemical assays performed in primary microglia cultures from hippocampus of two-day-old non-transgenic (control) and APP<sub>Sw,Ind</sub> mice using an antibody against MHC class II (green) and showing the activation of the cells. Scale bar: 30  $\mu$ m.

and subsequently treated with selective agonists of the cannabinoid receptors, ACEA or JWH133, or with the endocannabinoids, 2-AG or anandamide, and cAMP levels were determined. CB<sub>1</sub>R activation in control mice mildly decreased cAMP levels (approximately 20%) while the CB<sub>2</sub>R selective agonist had no significant effect. In contrast, in samples from APP<sub>Sw,Ind</sub> mice, the decrease of cAMP levels was higher (approximately 40%), and similar after CB<sub>1</sub> or CB<sub>2</sub> receptor activation (Figure R13A). Simultaneous activation of the two receptors lead to a negative cross-talk in the control animals that turned into positive in cells from APP<sub>Sw,Ind</sub> mice (Figure R13A). Interestingly, endocannabinoids also produced a higher signal in the cells obtained from APP<sub>Sw,Ind</sub> mice. When label-free assays were performed, in control cells, CB<sub>2</sub>R stimulation showed a small effect while co-administration of ACEA and JWH133 resulted in a negative cross-talk. However, once again, in microglia from APP<sub>Sw,Ind</sub> pups, CB<sub>2</sub> agonist-stimulation had a significant effect and potentiated CB<sub>1</sub>R signalling (Figure R13A and B). Common trends in activated microglial cells are an increase in the expression of the CB<sub>1</sub>-CB<sub>2</sub> receptor heteromer and a qualitative and quantitative change in the cannabinoid receptor signalling.

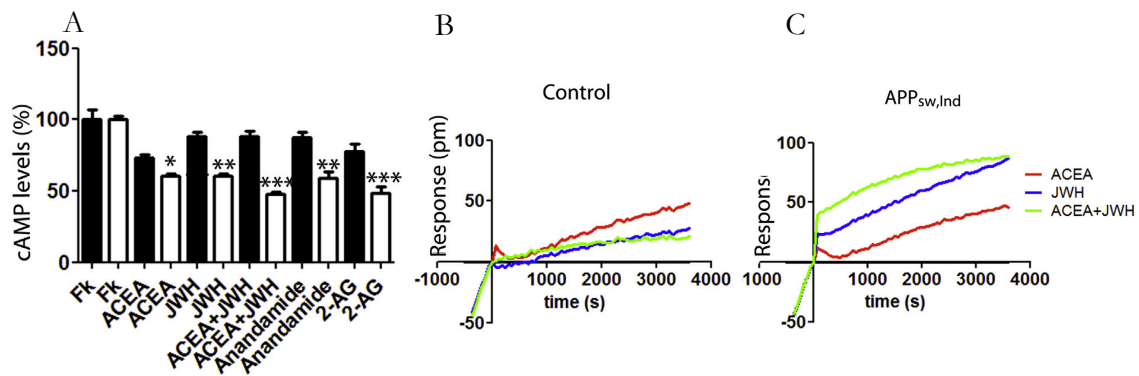


**Figure R13. CB<sub>1</sub>-CB<sub>2</sub> heteromer function in the APP<sub>Sw,Ind</sub> mouse model of Alzheimer's disease.** A) Hippocampal primary cultures of microglia of two-old-day non-transgenic mice (black bars in A) and APP<sub>Sw,Ind</sub> (white bars) were stimulated with 200 nM ACEA, 100 nM JWH133 or both, or with anandamide (200 nM) or 2-AG (200 nM) followed by a 15 min treatment of forskolin (500 nM). cAMP levels were determined and the values are the mean  $\pm$  S.E.M. of 4-6 different experiments in triplicates. In all cases, one-way ANOVA followed by Bonferroni's multiple comparison *post hoc* test was used for statistics analysis (\* $p < 0.05$ , \*\* $p < 0.01$ , \*\*\* $p < 0.001$  versus forskolin treatment). B) and C) DMR curves obtained using the primary microglia cultures from the hippocampus of control (B) and APP<sub>Sw,Ind</sub> (C) pups stimulated with ACEA (200 nM, red line), JWH133 (100 nM, blue line) or both (green line).



#### IV.1.8 Discussion

The effect of anandamide on NO release in activated microglia is mainly mediated via CB<sub>2</sub>R although a functional cross-talk with GPR55 or GPR18 has been suggested (*Malek et al., 2015*). The results described in this chapter, including BRET, PLA and signalling studies, indicate that CB<sub>2</sub>R mediated effects in activated microglia are modulated, at least in part, by a direct interaction between the two cannabinoid receptor types. As deduced from the partial cross-antagonism, resting microglia expresses CB<sub>1</sub>R that seem to be partly forming heteromers with CB<sub>2</sub>R, whose expression is small and whose coupling to G proteins was not evident. The scenario is different when N9 cells or primary cultures are activated using LPS and INF- $\gamma$ . Apart from a marked increase in its expression, CB<sub>2</sub>R were robustly coupled to the signalling machinery. Taken together, the results in activated cells fit with cannabinoid receptors occurring mainly as heteromeric complexes whose quaternary structure composition is different from that of heteromeric complexes occurring in resting cells. In fact, BRET results indicated that the distance between BRET donor and acceptor is significantly different in CB<sub>1</sub>R-CB<sub>2</sub>R heteromers in resting versus activated microglial cells. The full cross-antagonism in activated microglia is also consistent with preponderance of CB<sub>1</sub>-CB<sub>2</sub> receptor heteromer expression. In summary, CB<sub>1</sub>-CB<sub>2</sub> heteromers are expressed in activated microglia and, accordingly, they may be considered as potential targets of endocannabinoids, phytocannabinoids or synthetic molecules acting on cannabinoid receptors.

The differential receptor expression and signalling, which was identified in all assayed models, and occurrence of CB<sub>1</sub>-CB<sub>2</sub> heteromers, may explain the myriad of results reported for CB<sub>1</sub> and CB<sub>2</sub> receptor role in immune modulation, microglial activation and potential to combat neuroinflammation (*Kaplan, 2013; Stella, 2010*). Cannabinoid action on CB<sub>1</sub>-CB<sub>2</sub> heteromer-containing activated microglia may explain, in full or in part, the anti-inflammatory and psychotropic-free effects elicited by ultra-low concentrations of tetrahydrocannabinol in LPS-treated mice (*Fisbhein-Kaminietsky et al., 2014*), the higher susceptibility of CB<sub>1</sub>R knockout mice to neurodegeneration (*Fowler et al., 2010*) and the neuroinflammation regulatory role of CB<sub>1</sub>R (*Zoppi et al., 2011*) underscored using genetic (knockout mice) and pharmacological approaches. They could also explain results that were attributed to be cannabinoid-receptor-independent (*Ribeiro et al., 2013*).

There is consensus on the relevant role of the endocannabinoid system in regulating neurodegeneration. Microglia and microglial endocannabinoid system have attracted attention to afford neuroprotection in diseases coursing with neuroinflammation e.g. PD, AD and Huntington's chorea (*Fernández-Ruiz et al., 2015; Leonelli et al., 2009; Mecha et al., 2016; Navarro*

*et al.*, 2016). Indeed, targeting CB<sub>1</sub>R with agonists at non-psychoactive doses or targeting CB<sub>2</sub>R are considered beneficial in experimental models of AD because this treatment induce repair mechanisms and afford protection against tau phosphorylation and A $\beta$  action (*Aso and Ferrer, 2014*). Selective CB<sub>2</sub>R ligands have potential in diseases having neuroinflammatory factors, from brain ischemia (*Bu et al.*, 2016) to AD (*Campbell and Gowran, 2007*). Microglial enzymes that degrade endocannabinoids and/or microglial CB<sub>2</sub>R are now considered a better target option than CB<sub>1</sub>R, which have a marked expression in neurons and whose activation provokes psychotropic effects (*Cabral and Griffin-Thomas, 2009; De Filippis et al., 2009; Fagan and Campbell, 2014; Galve-Roperb et al., 2008; de Lago and Fernández-Ruiz, 2007; Navarro et al., 2016*). Both CB<sub>2</sub>R and fatty acid amide hydrolase (FAAH), the enzyme that degrades anandamide, are up-regulated in glia surrounding plaques in the brain of AD patients (*Benito et al., 2003*). Interestingly, animals resulting from crossing a transgenic AD line, 5xFAD, and FAAH null mice have less amyloid burden, reduced neurite plaque number and decreased gliosis (*Vázquez et al., 2015*). Finally, anti-inflammatory effects of nicotine in microglia exposed to A $\beta$  are mediated by CB<sub>2</sub>R (*Jia et al., 2016*).

CB<sub>1</sub>R is the most abundant GPCR in the central nervous system. Its expression is more abundant in neurons than in glia but results in this chapter show that it is upregulated in activated microglia in which it reportedly exerts a neuroprotective role. Although CB<sub>2</sub>R expression in neurons is restricted to some specific brain areas, we found low expression in resting microglia and an upregulation in activated microglia and, overall, the results indicate that cannabinoid receptor expression in activated microglia correlates with an increase of CB<sub>1</sub>-CB<sub>2</sub> receptor heteromers and fit with emission tomography-based evidence (*Janssen et al., 2016*) showing that CB<sub>2</sub>R expression in microglia may be negligible unless neuroinflammation occurs and microglia is activated. Expression of CB<sub>2</sub>R in the brain from patients suffering AD is higher than in the brain from similar-age controls and correlates with two relevant AD molecular markers such as senile plaque scores and A $\beta$ <sub>42</sub> levels (*Solas et al., 2013*). Similar results have been described in animal models of the disease. For instance, PET radiotracer studies in amyloid-bearing mice show that CB<sub>2</sub>R selective ligands may be used as neuroinflammation biomarkers (*Savonenko et al., 2015*). The results in primary cultures showed activated microglia and a marked CB<sub>2</sub>R expression in APP<sub>Sw,Ind</sub> mice. This finding correlates with the observation that, in primary cultures of microglia from control mice, treatment with A $\beta$ <sub>1-42</sub> led to a cannabinoid receptor signalling similar to the one exerted in cells treated with LPS and INF- $\gamma$  (Figure R8). The expression of CB<sub>1</sub>-CB<sub>2</sub> receptor heteromers was also higher



in microglia from APP<sub>Sw,Ind</sub> mice. Overall, it is tempting to speculate that the higher expression of CB<sub>2</sub>R receptors in activated microglial phenotypes underlies the neuroprotective effect of cannabinoids. According to this hypothesis, the notable expression increase of CB<sub>1</sub>-CB<sub>2</sub> heteromers in activated microglia, make these complexes a possible target to further explore their potential to regulate microglial polarisation. For instance, it would be necessary to determine how cannabinoids in activated microglia regulate the levels of cytokine/chemokines and other factors that are key in converting the pro-inflammatory M1 to the neuroprotective M2 phenotype (Franco and Fernández-Suárez, 2015).

PD is another disease coursing with a neuroinflammatory component. Overexpression of CB<sub>2</sub>R is detected in either 6-hydroxy-DA-lesioned rats or LPS-treated mice, and correlates with microglial activation (Aron Badin *et al.*, 2013; Barnum *et al.*, 2008; Concannon *et al.*, 2015; Muñoz *et al.*, 2014). In contrast, endocannabinoid levels are more elevated in the inflammation-driven than in the neurotoxic model (Concannon *et al.*, 2015). Of note, the non-selective cannabinoid receptor agonist, WIN-55,212-2, or the CB<sub>2</sub>R selective agonist JWH015, afford neuroprotection in the MPTP neurotoxic PD model, which courses with a significant microglial activation plus overexpression of CB<sub>2</sub>R in midbrain (Price *et al.*, 2009). The results in this chapter showing the expression of CB<sub>1</sub>-CB<sub>2</sub> heteromers in microglia would explain why non-selective cannabinoid receptor agonists were neuroprotective in a MPTP model and why selective CB<sub>1</sub>R antagonists prevented nigral neuroprotection and reduced NADPH oxidase activity, reactive oxygen species production and DNA damage of microglial cells (Chung *et al.*, 2011). The CB<sub>1</sub>R-mediated effects were not due to neuronal receptors, as neuroprotection against the MPTP insult was not evident in neuron-enriched cultures but in mesencephalic co-cultures of neurons and microglia (Chung *et al.*, 2011). We found that the percentage of cells expressing the CB<sub>1</sub>-CB<sub>2</sub> receptor complexes significantly increased (from 9.2 to 18.7) in the lesioned hemisphere of the 6-hydroxy-DA-treated rats. This result is consistent with activation of microglia in this PD model (He *et al.*, 2001). Remarkably, heteromer complex expression returned to normal in rats receiving chronic levodopa treatment that did not exhibit dyskinesia, whereas both, number of cells containing the heteromer (up to 33.7% of the cells) and heteromer expression level, increased in dyskinetic rats (Figure R10). Such findings may be due to a compensatory mechanism in which cannabinoid receptor activation could be neuroprotective or, alternatively, the overexpression of receptors could trigger the manifestation of dyskinetic movements. These results not correlating with increased microgliosis, constitute a base to propose CB<sub>1</sub>-CB<sub>2</sub> receptor heteromer as targets to either combat or prevent involuntary movements in patients undertaking a dopamine replacement

therapy and to reduce inflammation by suppressing activated-microglia production of pro-inflammatory molecules.

As pointed out by Rom and Persidsky (*Rom and Persidsky, 2013*), the discovery of therapeutic agents targeting CB<sub>2</sub>R is hampered by their complex signalling pathways. The hydrophobic nature of cannabinoids and functional selectivity are further sources of complexity. Biased agonism and GPCR heteromerization may cause functional selectivity, being, the first, more useful for drug discovery, and the latter, useful for discovering the physiological relevance of cannabinoid signalling in health and disease. Even using the same selective agonists, JHW133 and ACEA, functional selectivity was evident when comparing within-heteromer allosteric interactions. In fact, in all cell models, and also when comparing data in homozygous versus heterozygous transgenic AD animals, the negative allosteric receptor-receptor interactions became positive in activated conditions. Our BRET data in naïve and LPS plus INF- $\gamma$  treated cells show that the differential allosteric mechanisms correlated with structural change within the CB<sub>1</sub>-CB<sub>2</sub> heteromer. Taken together, the results in this chapter suggest an active conformation in the CB<sub>1</sub>-CB<sub>2</sub> heteromer that would be the real target of endogenous or synthetic cannabinoids in reactive microglia. Drug discovery should take into account the occurrence of this heteromer as well as the dynamics of the allosteric receptor-receptor interactions within these complexes in activated microglia due to the fact that the enhanced CB<sub>1</sub>-CB<sub>2</sub> receptor-receptor interactions may be regulating the endocannabinoid function.







## Chapter 2.

### IV. 2 Identification of a neuronal calcium- cAMP signalling cross-talk at cannabinoid CB<sub>1</sub>R mediated by interactions with EF-hand calcium sensors

Heteromerization of GPCR could modulate the receptors' activity in many aspects. Nonetheless, other interactions modulating the GPCR action have been described. Among them, neuronal calcium-binding proteins may interact with cell surface receptors. Calcium sensors, upon binding calcium ions at their EF-hand domains, suffer a conformational change that enables them to interact and modulate different proteins of the signal transmission machinery. In fact, the regulation of D<sub>2</sub>R, A<sub>2A</sub>R or the D<sub>2</sub>R-A<sub>2A</sub>R heteromer by calmodulin, calneuron1 and NCS1 has been reported (Navarro *et al.*, 2009, 2014). In enkephalinergic GABAergic neurons of the motor pathway, A<sub>2A</sub>R and D<sub>2</sub>R form heteromers, and are co-expressed with CB<sub>1</sub>R. It is not known, however, whether cannabinoid receptors may interact with calcium sensors and are regulated by calcium ions.

In this second chapter the potential interaction of CB<sub>1</sub>R with different EF-hand-containing calcium sensor proteins was studied and the functional consequences derived of such interactions were investigated to fulfil the **AIM II** of the Thesis.

In this chapter, the author of the Thesis, Edgar Angelats performed the experiments with participation of the undergraduate student M. Requesens in BRET assays, and of D. Aguinaga in the isolation of primary cultures. These results obtained using reagents from Prof. Kreutz, led to the paper entitled '**Cross-talk of calcium-and-cAMP signalling at cannabinoid CB<sub>1</sub> receptor mediated by interactions with the EF-hand calcium sensors**' whose authors are: E. Angelats, M. Requesens, D. Aguinaga, R. Franco, M.R. Kreutz, G. Navarro. The paper has been accepted (in June 2018) for publication in *Frontiers in Cell and Developmental Biology*.



### IV.2.1 Identification of calcium sensors able to interact with CB<sub>1</sub>R

To determine whether CB<sub>1</sub>R, which belongs to the superfamily of G protein-coupled receptors, could form heteromeric complexes with calcium-binding proteins, an immunocytochemistry assay was first developed to assess whether CB<sub>1</sub>R and three calcium sensors of relevance in neurons, may co-localise in co-transfected cells. To do so, the heterologous HEK-293T cell-expression system was used. Cells were transfected with cDNAs for CB<sub>1</sub>R-Rluc, and either calneuron1-YFP, NCS1-YFP or caldendrin-YFP. Calcium-binding protein expression was detected by YFP's own fluorescence while CB<sub>1</sub>R fused to Rluc was detected by the use of an anti-Rluc antibody and a Cy3-conjugated secondary antibody. As observed in Figure R14, in cells transfected with CB<sub>1</sub>R-Rluc and calcium-sensor fused to YFP, all calcium-sensors were found in different cell locations while CB<sub>1</sub>R was expressed mainly in the cell membrane level. These localisations were similar to those observed when cells were transfected with only one fusion protein (Figure R14). Moreover, signs of co-localisation were observed for the CB<sub>1</sub>R-Rluc and calneuron1-YFP or NCS1-YFP (Figure R15). Indeed, co-localisation does not prove a direct interaction; hence, to demonstrate potential physical interaction between receptor pairs, a bioluminescence resonance energy transfer (BRET) approach was used.

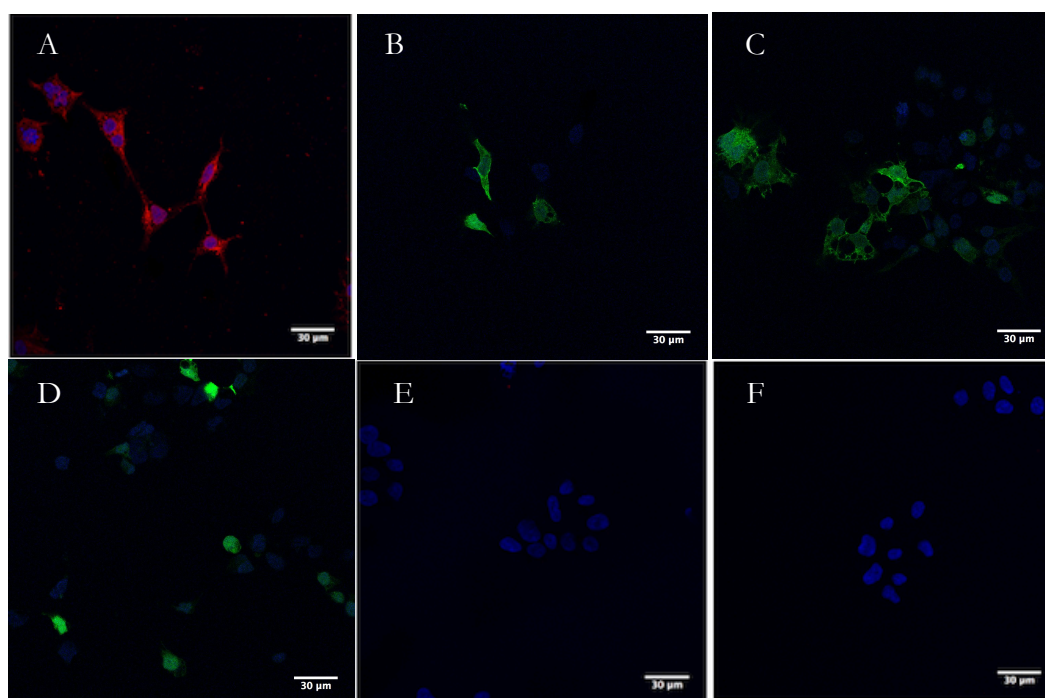


**Figure R14. CB<sub>1</sub>R and calcium-binding proteins expression.** For immunocytochemical assays HEK-293T cells were transfected with CB<sub>1</sub>R (1.5 μg; A, E and F) and calneuron1-YFP (2 μg; B), NCS1-YFP (2 μg; C) and caldendrin-YFP (3 μg; D). The YFP was detected by its own fluorescence while CB<sub>1</sub>R was detected with a primary antibody against Rluc and a Cy3-antiMouse secondary antibody. In E and F CB<sub>1</sub>R cDNA was transfected in HEK-293T cells but in absence of primary (E) or secondary (F) antibodies. Scale bar: 30 μm



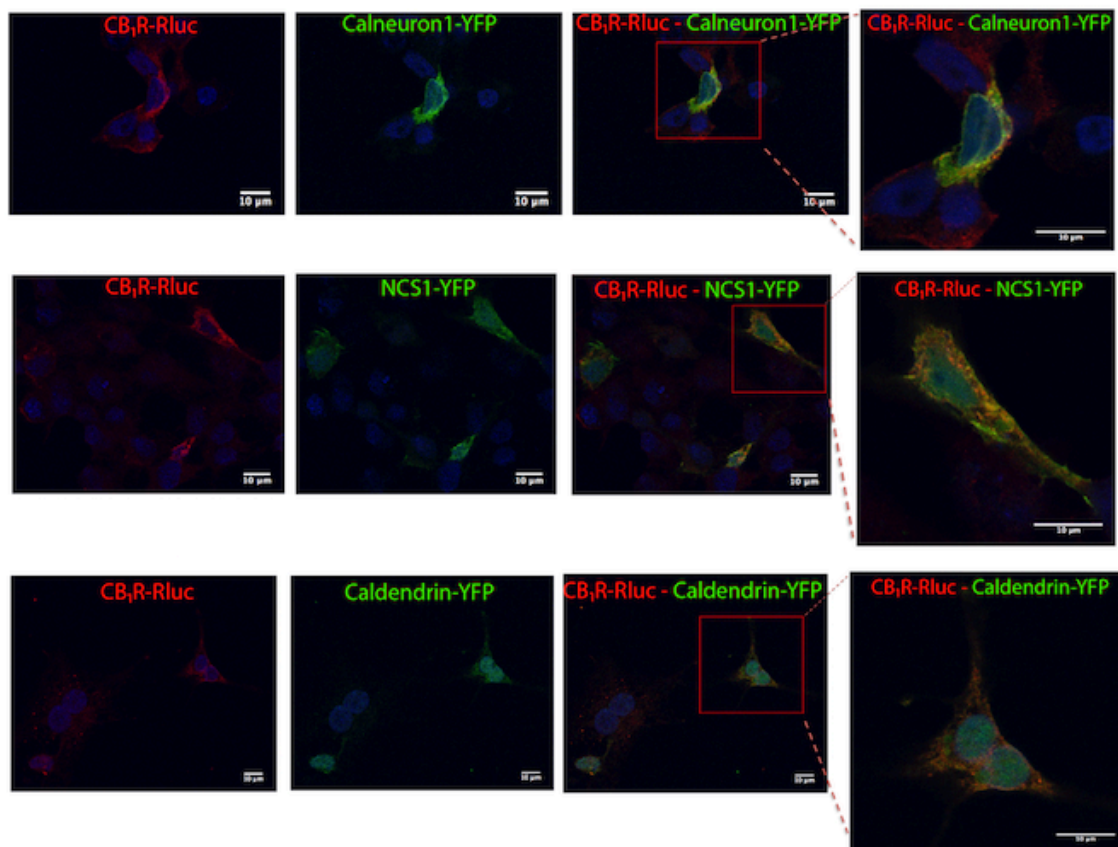


**Figure R15. Co-localisation of CB<sub>1</sub>R and calcium-binding proteins in HEK-293T transfected cells.** For immunocytochemical assays HEK-293T cells were co-transfected with CB<sub>1</sub>R (1.5 µg) and calneuron1-YFP (2 µg), CB<sub>1</sub>R (1.5 µg) and NCS1-YFP (2 µg) and with CB<sub>1</sub>R (1.5 µg) and caldendrin-YFP (3 µg). Left images show the localisation of CB<sub>1</sub>R-Rluc of each co-transfection. Fluorescence of each sensor-YFP is shown in central images and the merge of both proteins is shown in right images, with an amplification of boxed cells. Scale bar: 10 µm

BRET was undertaken in HEK-293T cells expressing a constant amount of cDNA for CB<sub>1</sub>R-Rluc (0.75 µg) and increasing amounts of cDNAs for calneuron1-YFP (0.25 to 1.75 µg), NCS1-YFP (0.25-2 µg) or caldendrin-YFP (0.5-2.5 µg). For calneuron1-YFP and NCS1-YFP, a saturation BRET curve was obtained, thus indicating a specific interaction between CB<sub>1</sub>R-Rluc and those two proteins. BRET parameter values were: BRET<sub>max</sub> 30 ± 3 mBU and BRET<sub>50</sub> 10 ± 3 for the interaction with calneuron1, and BRET<sub>max</sub> 170 ± 20 mBU and BRET<sub>50</sub> 70 ± 10 for the interaction with NCS1 (Figure R16A and B). Interestingly, the increase of intracellular Ca<sup>2+</sup> concentration by pre-incubation for 30 min with ionomycin did not modify the degree of interaction (Figure R16A and B). In contrast, an unspecific linear signal was obtained between CB<sub>1</sub>R and caldendrin-YFP, indicating the lack of interaction between these proteins (Figure R16C). Actually, these results constitute a proper negative control of the assay. In summary, the results indicate that at basal or increased Ca<sup>2+</sup> intracellular levels, CB<sub>1</sub>R may interact with calneuron1 or NCS1 but not with caldendrin.



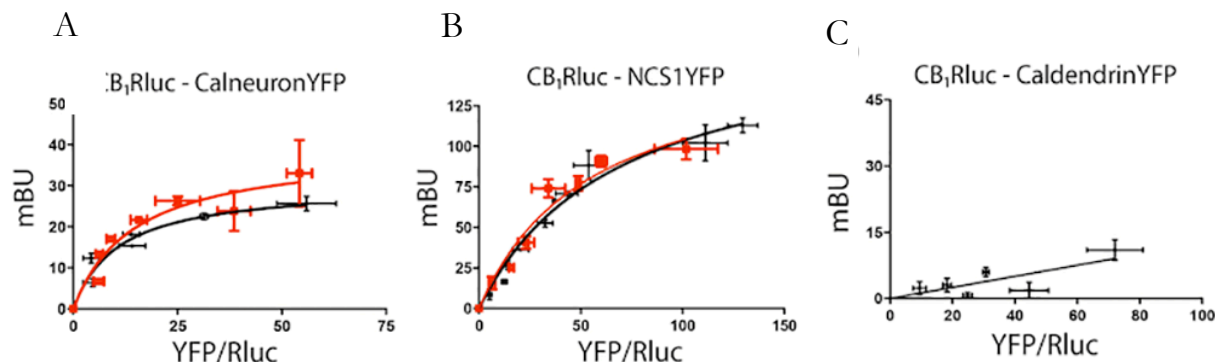


**Figure R16. Study of the interaction of CB<sub>1</sub>R with calcium-binding proteins.** BRET assays were performed transfecting HEK-293T cells with a constant amount of CB<sub>1</sub>R-Rluc (1.5 μg) and increasing amounts of calneuron1-YFP (0.25 to 2 μg) (A), NCS1-YFP (0.5 to 2.5 μg) (B) and caldendrinYFP (1 to 3 μg) (C) in the presence (red lines) or in the absence (black lines) of 1 μM ionomycin and 1.24 mM of CaCl<sub>2</sub>. Values are the mean ± S.E.M. of 10 different experiments in duplicates.

#### IV.2.2 Mapping the interaction motives

Taking into account previous data on motives in the structure of calcium sensors and the general organization of heptaspanning GPCR. BRET assays were undertaken using different mutated versions of CB<sub>1</sub>R and calneuron1 or NCS1. As indicated in Material and Methods, plasmids containing the sequence of mutant forms in the third intracellular loop and the C-terminal domain of CB<sub>1</sub>R were used (see details in Methods). For calcium sensors, NCS1 was mutated deleting the myristoylation site in the N-terminal domain of NCS1 and a part of the C-terminal end of the calneuron1 was deleted to prevent membrane anchoring. BRET assays using Rluc or YFP fusion proteins containing these mutated forms led to the results displayed in Figure R17. On the one hand, the BRET results show that mutated calneuron1 and mutated NCS1 cannot interact with the CB<sub>1</sub>R (Figure R17A and D). On the other hand, the mutated form in the third intracellular loop of the CB<sub>1</sub>R abolished the interaction with both calcium sensor proteins (Figure R17C and F). Finally, mutations in the C-terminal domain led to unspecific signal when NCS1-YFP was used (Figure R17E) but did not significantly altered the direct interaction established between calneuron1-YFP and the cannabinoid receptor (Figure R17B). These results suggest that NCS1 directly interact with the C-terminal tail and the third intracellular loop of the CB<sub>1</sub>R, while calneuron1 only interact with the C-terminal tail of the receptor.



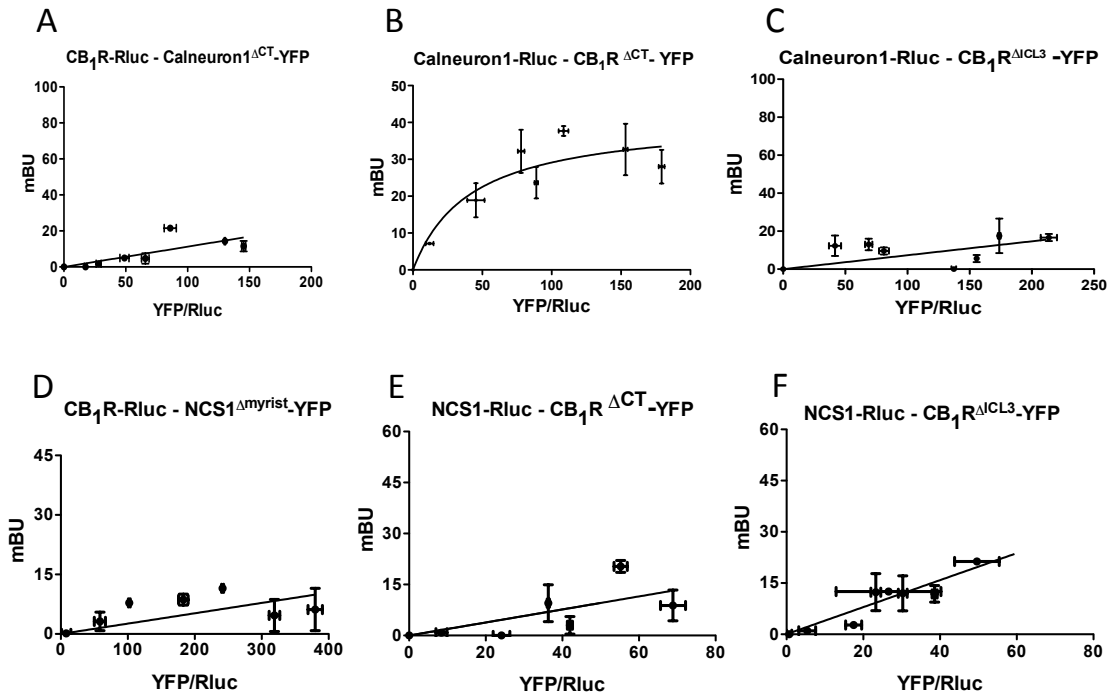


**Figure R17. Determination of interacting domains of CB<sub>1</sub>R-calneuron1 and CB<sub>1</sub>R-NCS1 interactions.** HEK-293T cells transfected with a constant amount of cDNA for CB<sub>1</sub>R-Rluc (1.5 μg) and increasing amounts of calneuron1<sup>ΔCT</sup>-YFP (1 to 3 μg) (A), calneuron1-Rluc (3 μg) and CB<sub>1</sub>R<sup>ΔCT</sup>-YFP (0.25 to 1.5 μg) (B), calneuron1-Rluc (3 μg) and CB<sub>1</sub>R<sup>ΔICL3</sup>-YFP (0.5 to 2 μg) (C), CB<sub>1</sub>R-Rluc (1.5 μg) and NCS1<sup>Δmyrist</sup>-YFP (1 to 3 μg) (D), NCS1-Rluc (2.5 μg) and CB<sub>1</sub>R<sup>ΔCT</sup>-YFP (0.25 to 1.5 μg) (E), and NCS1-Rluc (2.5 μg) and CB<sub>1</sub>R<sup>ΔICL3</sup>-YFP (0.5 to 2 μg) (F). Values are the mean ± of 8 different experiments in duplicates.

#### IV.2.3 Calneuron1 and NCS1 compete for interacting with CB<sub>1</sub>R

The above-described results concerning the CB<sub>1</sub>R-calcium sensors interaction indicated that NCS1 and calneuron1 could form heteromers with the CB<sub>1</sub>R, and possibly, be competing between each other for the interaction with the receptor. To confirm such hypothesis we performed BRET competition assays by expressing the CB<sub>1</sub>R-Rluc and one sensor fused to the YFP in the presence of increasing amounts of the second calcium sensor. The BRET assays were performed in cell treated or not with ionomycin and the results are presented in the Figure R18. Results using constant amounts of the cDNA for CB<sub>1</sub>R-Rluc and calneuron1-YFP increasing amounts of NCS1 indicated that the latter protein was able to dose-dependently reduce the BRET signal between CB<sub>1</sub>R-Rluc and calneuron1-YFP, therefore competing for the binding of calneuron1 to the CB<sub>1</sub>R; such competence disappeared in the presence of elevated intracellular concentrations, indicating that in higher calcium concentrations, NCS1 was not able to decrease the CB<sub>1</sub>R-Rluc – calneuron1-YFP BRET signal (Figure R18A). Just the opposite was found when using increasing amounts of cDNA



for calneuron1. In these case, increasing amounts of calneuron1 did compete with NCS1-YFP for the binding to the receptor when concentrations of intracellular  $\text{Ca}^{2+}$  were elevated, while in basal conditions, calneuron1 did not significantly affect the  $\text{CB}_1\text{R-Rluc} - \text{NCS1-YFP}$  BRET signal (Figure R18B).

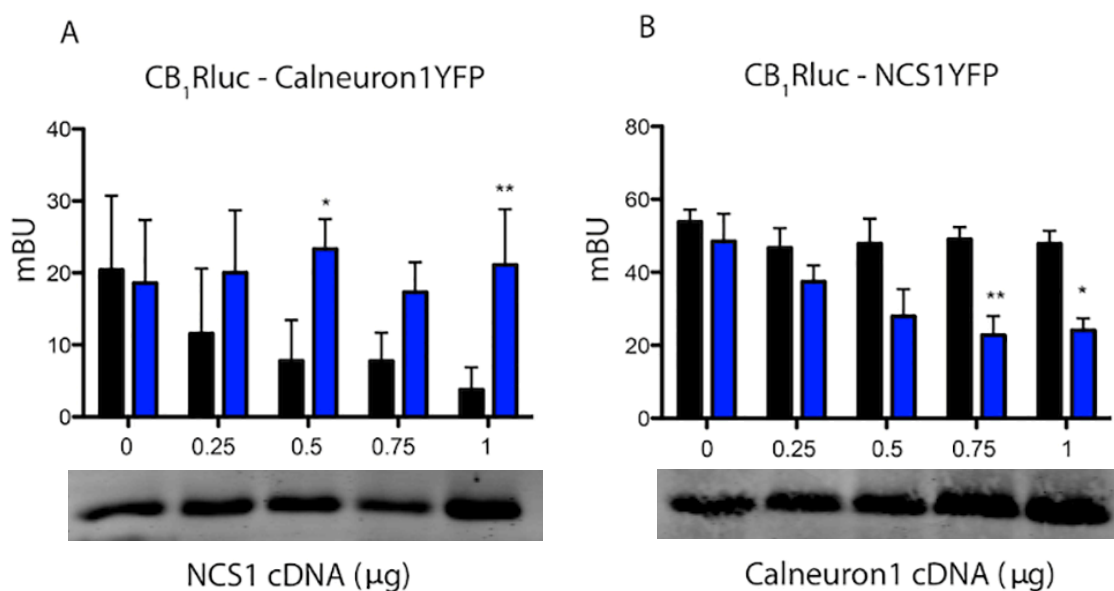


**Figure R18. Calneuron and NCS1 competition for  $\text{CB}_1\text{R}$  interaction.** BRET assays were performed in HEK-293T cells transfected with constant amounts of  $\text{CB}_1\text{R-Rluc}$  (1.5  $\mu\text{g}$ ) and calneuron1-YFP (2  $\mu\text{g}$ ) and increasing amounts of NCS1 (0 to 1  $\mu\text{g}$ ) (A) or constant amounts  $\text{CB}_1\text{R-Rluc}$  (1.5  $\mu\text{g}$ ) and NCS1-YFP (1.5  $\mu\text{g}$ ) and increasing amounts of calneuron1 (0 to 1  $\mu\text{g}$ ) in presence (blue bars) or absence (black lines) of 1  $\mu\text{M}$  ionomycin and 1.24 mM of  $\text{CaCl}_2$ . Representative western blots of the NCS1 and Calneuron1 increasing expression are shown. Values are the mean  $\pm$  S.E.M. of 10 different experiments in duplicates and a one-way ANOVA followed by a Dunnett's post-hoc test was used for statistical comparison of the influence of Ionomycin and calcium concentration levels on each DNA concentration (\* $p < 0.05$ ; \*\* $p < 0.01$ ).

#### IV.2.4 Occurrence of receptor-calcium sensor complexes in natural sources

Mouse striatal samples were chosen to prepare cultures of neurons, which endogenously express all the proteins under study, and look for interactions between the cannabinoid receptor 1 and calneuron1 or NCS1. In order to detect receptor-sensor complexes in primary cultures of neurons, PLA assays were carried out in cells treated or not with ionomycin. Red dot/clusters indicating the occurrence of the receptor-calneuron1 and receptor-NCS1 complexes were found in all conditions (Figure R19A). The absence of the primary anti- $\text{CB}_1\text{R}$  or anti-sensor antibodies led to a marked reduction of the PLA signal (Figure R19A). The number of cells containing one or more red spots versus total cells (blue nucleus) and, in cells containing spots, the ratio  $r$  (number of red spots/cell), were determined by means of the Duolink Image tool software. Significant differences were found in both basal conditions and in treated with ionomycin. In absence of ionomycin, the number of cells



expressing CB<sub>1</sub>R-calneuron1 complexes and the relative amount of clusters was lower than the number of cells expressing CB<sub>1</sub>R-NCS1 and of spots/cell. The results were totally opposite when neurons were treated with ionomycin, which led to a marked reduction in the percentage of cells expressing CB<sub>1</sub>R/NCS1 complexes (and in the spot/cell ratio) and a marked increase in the percentage of cells expressing CB<sub>1</sub>R/calneuron1 complexes (and in the spot/cell ratio) (Figure R19B). As the calcium-binding proteins assayed seemingly compete for the binding to CB<sub>1</sub>R, the results indicate that low calcium concentrations favour the interaction with NCS1, whereas CB<sub>1</sub>R is mainly bound to calneuron1 when intracellular Ca<sup>2+</sup> levels increase.

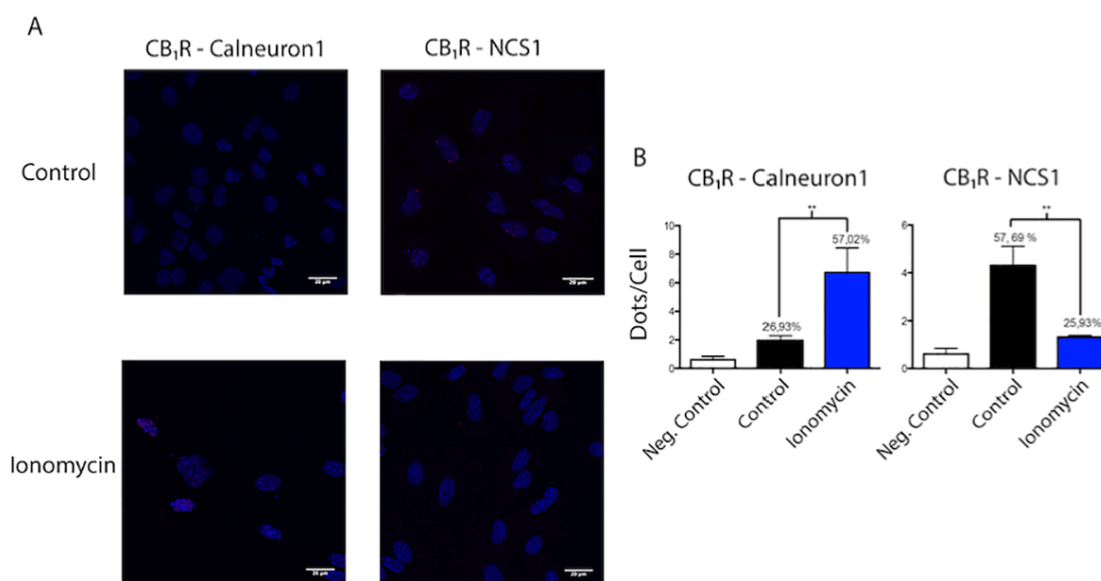


**Figure R19. Determination of CB<sub>1</sub>R interaction with calcium-binding proteins in mice primary cell cultures.** In situ PLA assay was performed to detect CB<sub>1</sub>R-calneuron1 and CB<sub>1</sub>R-NCS1 interaction was performed as described in Materials and Methods using primary antibodies against CB<sub>1</sub>R and calneuron1 or CB<sub>1</sub>R and NCS1 in presence or absence of 1  $\mu$ M Ionomycin and 2.4 mM of CaCl<sub>2</sub>. Interactions were detected as red spots in Hoechst-stained nuclei in the confocal microscopy images (superimposed sections of 0.5  $\mu$ m width). Scale bar: 20  $\mu$ m (A). Dots (number of red spots) per cell and percentage of red-spots containing cells are shown in the bar graphs. Data are the means  $\pm$  S.E.M. of counts of 8 different fields for every condition. A one-way ANOVA followed by a Tukey's multiple comparison test was performed for the statistical analysis (\* $p$ <0.05; \*\* $p$ <0.01) (B).

Taking into account the differential interaction of calneuron1 or NCS1 with CB<sub>1</sub>R, we wanted to analyse if there were any changes under the canonical signalling pathway of CB<sub>1</sub>R. Thus, we addressed the intracellular cAMP levels of striatal neuron cultures of mice in presence or absence of ionomycin. In those cells in basal conditions, the CB<sub>1</sub>R-agonist ACEA produced a decrease in the forskolin-induced cAMP levels, fact that was blocked upon a previous treatment with the CB<sub>1</sub>R antagonist rimonabant (Figure R20). However, in cells incubated with ionomycin, ACEA did not decrease the cAMP signalling of the CB<sub>1</sub>R. Moreover, the results obtained for the CB<sub>1</sub>R agonist ACEA under basal or ionomycin





treatment differed significantly (Figure R20), disclosing and suggesting a different modulation of the CB<sub>1</sub>R upon interaction with NCS1 or calneuron1.

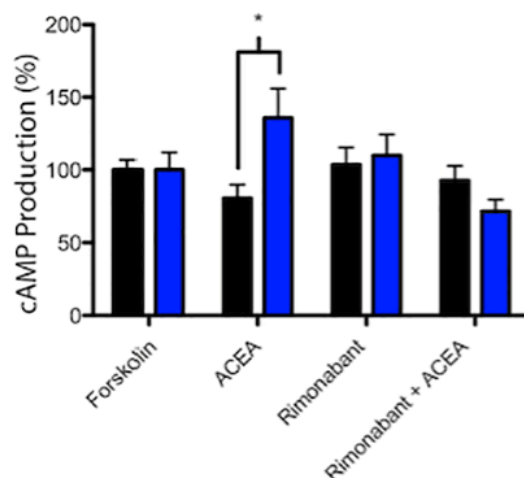


**Figure R20. CB<sub>1</sub>R signalling in striatal cell cultures of mice.** cAMP levels induced by CB<sub>1</sub>R stimulation were assessed in striatal mice neurons activated with the CB<sub>1</sub>R agonist ACEA (100 nM) with or without a previous treatment of CB<sub>1</sub>R antagonist Rimonabant (1  $\mu$ M) upon stimulation with Forskolin (0.5  $\mu$ M) in presence (blue bars) or absence (black bars) of 1  $\mu$ M of Ionomycin and 2.4 mM CaCl<sub>2</sub>. A one-way ANOVA followed by a Dunnett's post-hoc test was used for statistical comparison of the influence of Ionomycin and calcium concentration in each treatment (\* $p$ <0.05).

#### IV.2.5 Discussion

At the molecular level, GPCR-mediated signalling not only depends on the coupled G protein but on other molecules able to interact with the receptor and/or components of the signalling machinery. Calmodulin was the first calcium-binding protein that was identified as modulator of GPCR with relevance for neurotransmission (Ferré, 2010; Navarro *et al.*, 2009; Woods *et al.*, 2008). However, little is known about the action of other calcium sensors expressed in neurons and their effects on GPCR function (Mikhaylova *et al.*, 2011).

Recently, it has been demonstrated that NCS1 can interact with dopamine D<sub>2</sub>R (Woll *et al.*, 2011) and adenosine A<sub>2A</sub>R (Navarro *et al.*, 2012). In turn, calneuron-1 can also establish interactions with the A<sub>2A</sub>-D<sub>2</sub> heteroreceptor complexes (Navarro *et al.*, 2014). Taking into account the close relationship between A<sub>2A</sub>, D<sub>2</sub> and CB<sub>1</sub> receptors in GABAergic striatopallidal neurons, we wanted to investigate if these calcium sensors could be regulating the cannabinoid CB<sub>1</sub> receptor. Hence, in this chapter, we selected three abundantly expressed calcium sensors (NCS1, calneuron1 and caldendrin) with known function and targets in the brain. Caldendrin is highly enriched at synaptic sites (Seidenbecher *et al.*, 1998) and binds various synaptic proteins (Dieterich *et al.*, 2008; Gorny *et al.*, 2012; Seidenbecher *et al.*, 2004). NCS1, that



seems to be involved in several neuronal functions like neurotransmission (*Pongs et al., 1993*), exocytosis (*Haynes et al., 2005*) or regulating ion channels (*Weiss et al., 2000*) and the synaptic plasticity (*Sippy et al., 2003*), and calneuron1, which has a described role in phospholipid synthesis and in membrane trafficking in the Golgi (*Hradsky et al., 2015; Mikbaylova et al., 2009*). To date, no interaction of calcium sensors had been described for CB<sub>1</sub>R, however, the results presented in this chapter show that, the three calcium sensors employed displayed some co-localisation when co-transfected with the CB<sub>1</sub>R in HEK-293T cells. However, when BRET assays were carried out, just NCS1 and calneuron1 were able to form specific interactions with the receptor.

The interfaces through which CB<sub>1</sub>R might interact with different proteins are partially characterised. Intracellular loops (particularly the 2<sup>nd</sup> and the 3<sup>rd</sup>) are involved in coupling to heteromeric G proteins and also to other scaffolding and/or signalling proteins (*Khan and Lee, 2014*). Also the C-terminal domain of GPCR arise as important for directing signalling to different pathways (*Navarro et al., 2018; Stadel et al., 2011*). It has been also suggested that structural features in the 2<sup>nd</sup> intracellular loop may be responsible for a change of coupling from the cognate Gi to a Gs protein (*Chen et al., 2010*) and that the third intracellular loop is important for the constitutive activation (*Abadji et al., 1999*). Based on preliminary and our previous experiments, we tested CB<sub>1</sub>R that were mutated in amino acids that are responsible for interactions with other proteins (*Navarro et al., 2010a*). Plasmids were prepared containing the CB<sub>1</sub>R in which two conserved residues of the third intracellular loop that are susceptible of phosphorylation (thus acquiring negative charges) were mutated to Ala (CB<sub>1</sub>R<sup>ΔICL3</sup>). A truncation of the C-terminal domain, responsible of some CB<sub>1</sub>R interactions, was done (CB<sub>1</sub>R<sup>ΔCT</sup>). One of the remarkable findings was the asymmetric interaction mode with calcium sensors; whereas mutations in the third intracellular loop abolished binding to both calneuron1 and NCS1 calcium-binding proteins, mutations in the C-terminal domain abolished interaction with NCS1 but not with calneuron1. In summary, our results disclosed structural differences in the interaction between the CB<sub>1</sub>R and calneuron-1 or NCS1.

The capacity of calcium sensor proteins to interact and modulate GPCR activity had been previously demonstrated. Implications on the A<sub>2A</sub>R-mediated signalling upon heteromerization with NCS1 were demonstrated by Navarro and collaborators (*Navarro et al., 2012*), and furthermore, capacity of calneuron1 and NCS1 to differently interact and regulate GPCR signalling depending on the calcium concentration levels was demonstrated for the A<sub>2A</sub>R-D<sub>2</sub>R heteromer (*Navarro et al., 2014*). In this chapter, we provide data indicating that the CB<sub>1</sub>R is also alternatively interacting with calneuron1 or NCS1 in a calcium-dependent



fashion. Moreover, the signalling studies suggest that this differential intracellular calcium concentration-related NCS1/calneuron1-CB<sub>1</sub>R interaction implies a modulation and a fine regulation of the receptor signalling. In this line, it had been previously shown that a calcium-binding sensor protein like calmodulin could not only regulate, but also compete with G-proteins, for the interaction motifs of the 3<sup>rd</sup> intracellular loop of the  $\mu$ -opioid receptor, hence preventing the interaction of G<sub>i</sub> proteins with the receptor and diminishing the receptor signalling (*Wang et al., 1999*). Accordingly to the structural interaction and signalling data obtained, it cannot be discarded that calneuron1 interacting domains with the CB<sub>1</sub>R could be overlapped with the G protein-CB<sub>1</sub>R interacting motifs, hence preventing G<sub>i</sub> proteins, the canonical signalling pathway of CB<sub>1</sub>R, to interact with the receptor. Taken together, the evidence points to Ca<sup>2+</sup>, acting through calneuron-1 and NCS1 calcium-binding sensors, to be a relevant regulator of the CB<sub>1</sub>R function, adding complexity to the cumbersome signalling of this GPCR.



### Chapter 3.

#### IV.3 Determination of the functional role for the truncated Ghrelin receptor GHS-R1b

GHS-R1a is the receptor that mediates the action of ghrelin. This GPCR has a truncated version, GHS-R1b, which lacks transmembrane domains 6 and 7. GHS-R1b is unable to interact with ghrelin or to couple any G-protein. Thus, the exact role of GHS-R1b remains unknown.

In 2012, Chow and collaborators (*Chow et al., 2012*) started to shed some light into the matter, suggesting that the role of GHS-R1b was to negatively regulate the GHS-R1a upon heteromerization. Once the interaction was established, trafficking to the plasma membrane of GHS-R1a was reduced, retaining the functional receptor in inner compartments of the cell. However, a year later, Mary and collaborators (*Mary et al., 2013*) demonstrated that GHS-R1b allosterically modulated GHS-R1a. Upon interaction with the truncated form, GHS-R1a acquired a conformation that prevented the functional receptor neither to couple a G-protein nor to signal.

Thus, the objective in chapter 3, was to determine the role of the truncated isoform of the ghrelin receptor and better understand the functional changes of ghrelin receptors upon heteromerization, fulfilling the **aim III** of the Thesis.

In this chapter, the author of the Thesis, Edgar Angelats, provided results related to the modulatory role of GHS-R1b on the GHS-R1a function and on the dopamine D<sub>1</sub>-GHS-R1a heteroreceptor function. The experimental approach and results were designed and performed in the laboratory of the University of Barcelona, and led to the paper '**A significant role of the truncated Ghrelin receptor GHS-R1b in Ghrelin-induced signalling in neurons**' Navarro G., Aguinaga D., Angelats E., Medrano M., Moreno E., Mallol J., Cortés A., Canela E.I., Casadó V., McCormick P.J. Lluís C., Ferré S. The paper is published in *J.Biol. Chem* 2016 June 17 291(25): 13048-13062, and D. Aguinaga, co-author of this manuscript, has included this work in his thesis.



### IV.3.1 GHS-R1b-mediated modulation of GHS-R1a expression at the plasma membrane

The role of GHS-R1b on GHS-R1a expression in the plasma membrane was first evaluated by immunocytochemistry in HEK-293T cells transfected with cDNA of GHS-R1a fused to YFP (GHS-R1a-YFP, 1  $\mu$ g), GHS-R1b fused to Rluc (GHS-R1b-Rluc, 0.5  $\mu$ g) or both. Both GHS-R1a-YFP (Figure R21, identified by its own fluorescence) and GHS-R1b-Rluc (Figure R21, identified by anti-Rluc and secondary Cy3 antibodies), when expressed alone, could be detected in intracellular structures and at the plasma membrane level. Some degree of co-localisation could be observed upon GHS-R1a-YFP and GHS-R1b-Rluc co-transfection (Figure R21). As shown in figure R22, the fused receptors retained the same degree of functionality than non-fused receptors.

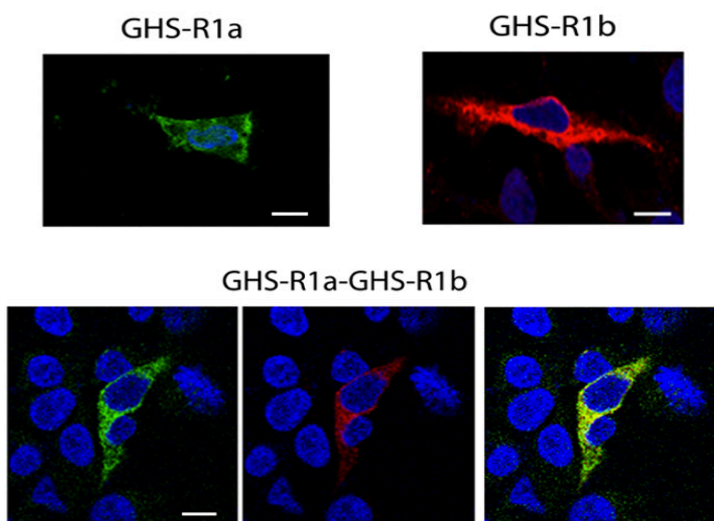


**Figure R21. Evaluation of ghrelin receptors expression.** Confocal microscopy images of HEK-293T cells transfected with GHS-R1a-YFP (1.5  $\mu$ g), GHS-R1b-Rluc (0.5  $\mu$ g) or both receptors. YFP was detected by its own fluorescence (green), while Rluc was detected with a monoclonal anti-Rluc primary antibody and a Cy-3 secondary antibody (red). Co-localisation of both receptors is shown in yellow. Cell nuclei were stained with Hoechst (blue). Scale bars= 10  $\mu$ m.

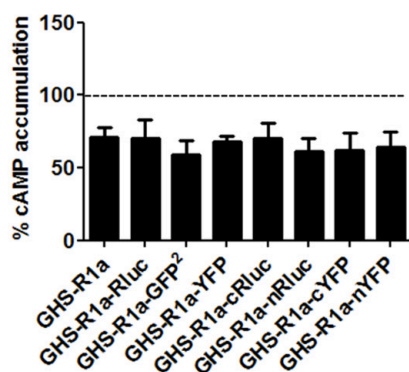


**Figure R22. Functionality of Ghrelin-receptor fusion proteins.** cAMP values determined in HEK-293T cells transfected with cDNA (1.5  $\mu$ g) from the indicated receptors or fusion proteins. Cells were treated with ghrelin (100 nM) or vehicle for 15 min prior to 15 min incubation with forskolin (0.5  $\mu$ M). Values are the mean  $\pm$  S.E.M. of three or four experiments and expressed as decreases (percent) versus forskolin alone (100%, dotted line). No statistical differences between differently transfected cells were found by ANOVA followed by Bonferroni's corrections ( $p > 0.05$ ).

To provide a more accurate determination of receptor expression at the plasma membrane, biotinylation experiments using a non-membrane permeable biotin were performed. Thus, HEK-293T cells were co-transfected with GHS-R1a-YFP cDNA (1  $\mu$ g) and increasing amounts of GHS-R1b-Rluc (0, 0.1, 0.2, 0.3, or 0.6  $\mu$ g) or only with GHS-R1b-Rluc cDNA (0.3  $\mu$ g). Total expression of GHS-R1a-YFP (YFP fluorescence, 20000  $\pm$  2000 units) did not significantly change by the expression of GHS-R1b-Rluc (Rluc

luminescence, 10000 to 300000 units). To determine the relative expression of GHS-R1b with respect to GHS-R1a (GHS-R1b/GHS-R1a) in transfected cells, we performed parallel experiments in which HEK-293T cells were transfected with increasing amounts of the cDNA for GHS-R1a-YFP (up to 1.5  $\mu\text{g}$ ) or GHS-R1b-YFP cDNA (up to 0.6  $\mu\text{g}$ ), and the relative total expression of receptors was calculated by Western blotting using an anti-YFP antibody. Linearity of transfected cDNA *versus* the Western blotting signal or versus fluorescence was obtained in both cases (transfected cDNA in micrograms versus fluorescence values in arbitrary units gave linear plots with slopes of 0.885 and 0.099, respectively), which allowed the accurate determination of the relative GHS-R1b/GHS-R1a expression ratio. Co-transfection with 1  $\mu\text{g}$  of GHS-R1a-YFP and 0, 0.1, 0.2, 0.3, or 0.6  $\mu\text{g}$  of GHS-R1b-YFP gave GHS-R1b/GHS-R1a ratios of 0, 0.25, 0.5, 1.4 and 5, respectively. Biotinylation experiments demonstrated that transfected GHS-R1a was always present in the plasma membrane, with or without co-transfection with GHS-R1b, and that co-transfection with GHS-R1b resulting in GHS-R1b/GHS-R1a ratio from 0.25 to 5 led to an inverted U shape in the relative expression of GHS-R1a in the plasma membrane (Figure R23A). As negative control, no changes in GHS-R1a expression at the plasma membrane were detected upon co-transfection with increasing amounts of CB<sub>1</sub>R-Rluc cDNA (Figure R23B, the corresponding CB<sub>1</sub>R/GHS-R1a expression ratio was calculated as above using the slope value of 0.139 corresponding to linear plots of transfected CB<sub>1</sub>R-YFP cDNA in micrograms versus

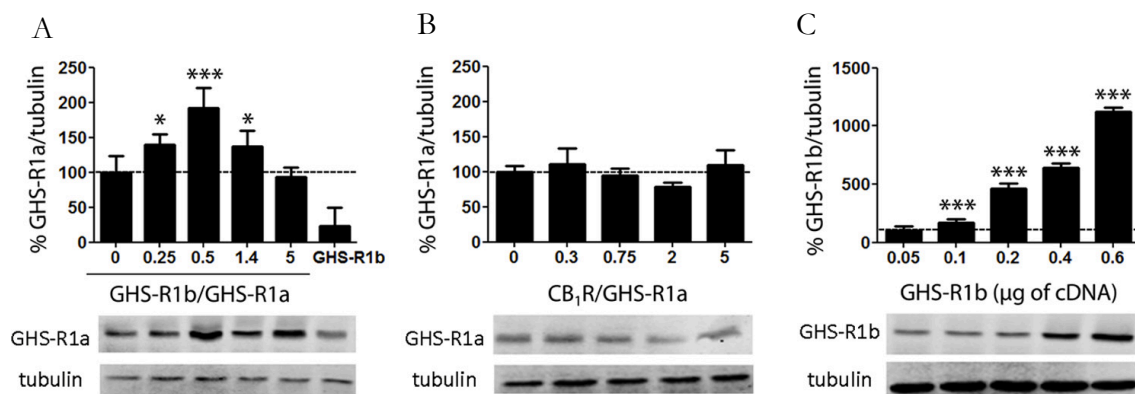


**Figure R23. Biotinylation experiments in HEK-293T transfected cells.** HEK-293T cells co-transfected with GHS-R1a-YFP (1  $\mu\text{g}$ ) and increasing amounts of GHS-R1b-Rluc cDNA (0-0.6  $\mu\text{g}$ ) or GHS-R1b-Rluc alone (0.5  $\mu\text{g}$ ) (A), with GHS-R1a-YFP (1  $\mu\text{g}$ ) and increasing amounts of CB<sub>1</sub>R-Rluc (0-1  $\mu\text{g}$ ) (B) or transfected with increasing amounts of GHS-R1b-Rluc (0.05-0.6  $\mu\text{g}$ ) (C) were treated as described in Materials and Methods. Quantification of immunoreactive bands from four to six independent experiments is shown. Values represent the mean  $\pm$  S.E.M. of the percentage of GHS-R1a-YFP membrane expression versus control cells (cells not expressing GHS-R1b-Rluc or CB<sub>1</sub>R-Rluc) (A and B) or the percentage of GHS-R1b-Rluc membrane expression *versus* control cells (non-transfected cells) (C). Statistical differences of differently transfected cells were analysed by ANOVA followed by Bonferroni's corrections (\*,  $p < 0.05$ ; \*\*\*,  $p < 0.001$  compared with control cells). Representative Western blotting analyses are shown in the bottom panels.

fluorescence in arbitrary units). Furthermore, biotinylation also demonstrated a linear increase in the plasma membrane expression of GHS-R1b upon increasing amounts of GHS-R1b-YFP (Figure R23C). These data indicate that GHS-R1b differentially modulates GHS-R1a expression at the plasma membrane level as function of GHS-R1b/GHS-R1a expression ratio.

#### **IV.3.2 GHS-R1b-mediated modulation of GHS-R1a signalling in transfected HEK-293T cells**

The role of GHS-R1b on GHS-R1a signalling was evaluated in HEK-293T cells expressing the same amount of GHS-R1a-YFP (fluorescence,  $20000 \pm 2000$ ) and increasing amounts of GHS-R1b-Rluc (0 to 5 GHS-R1b/GHS-R1a ratio). First, the effect of GHS-R1b on GHS-R1a signalling was determined with a DMR label-free assay. Ghrelin (10, 30 and 100 nM) induced dose- and time-dependent signalling in cells only transfected with GHS-R1a-YFP, which was inhibited by the GHS-R1a antagonist YIL781 (Figure R24A). Ghrelin-induced DMR was completely blocked by pertussis toxin (PTX) but not by cholera toxin (CTX) or the  $G_q$  inhibitor YM254890 (Figure R24B), indicating a predominant ghrelin-mediated  $G_{i/o}$  protein coupling to GHS-R1a in HEK-293T cells. As expected, ghrelin did not produce any significant effect in cells only expressing GHS-R1b-Rluc (Figure R24C). The ghrelin-mediated DMR signal was then analysed upon three different GHS-R1b/GHS-R1a expression ratios: 0.5, 1.4 and 5. At GHS-R1b/GHS-R1a expression ratio of 0.5, ghrelin was significantly more efficient than when the cells were only transfected with GHS-R1a (Figure R25A). Taking also into account the results of biotinylation experiments, these results suggest that low relative GHS-R1b expression potentiates ghrelin-induced  $G_{i/o}$  protein-mediated signalling by facilitating GHS-R1a trafficking to the plasma membrane. However, progressive increases of the relative expression of GHS-R1b led to a progressive decrease in signalling that went down to an almost complete lack of effect of ghrelin on cells expressing the GHS-R1b/GHS-R1a ratio of 5 (Figure R25C). This switch from facilitation to inhibition of ghrelin-induced  $G_{i/o}$  protein-mediated signalling cannot be explained by GHS-R1b-mediated modulation of GHS-R1a trafficking because plasma membrane expression of GHS-R1a was the same at the highest GHS-R1b/GHS-R1a expression ratio than in cells not co-transfected with GHS-R1b (Figure R23A).

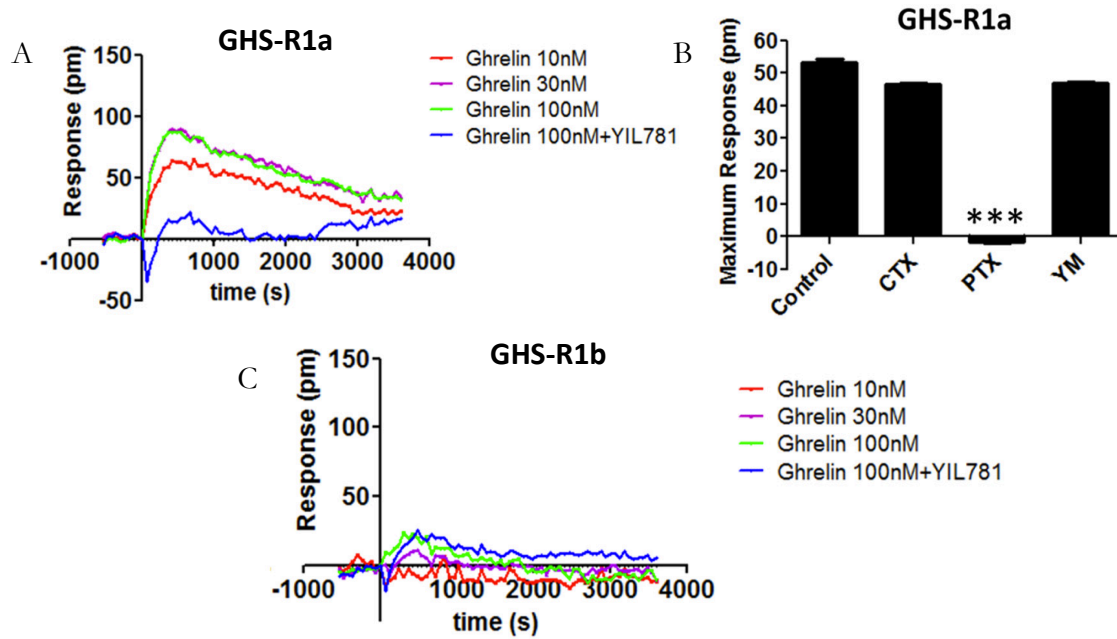


**Figure R24. DMR analysis of GHS-R1a mediated signalling.** HEK-293T cells transfected with GHS-R1a-YFP (1  $\mu$ g) (A and B) or GHS-R1b-Rluc (0.4  $\mu$ g) (C) were treated with 10 nM (red lines), 30 nM (Purple lines) or 100 nM (green lines) of ghrelin with or without a previous treatment with GHS-R1a antagonist YIL-781 (30 min) (blue lines), and the DMR signal analysed (A and C). In B, cells were pretreated overnight with PTX (10 ng/ml), CTX (100 ng/ml) or the  $G\alpha_q$  inhibitor YM254890 (YM, 1  $\mu$ M). Maximum responses of ghrelin (30 nM) at 500 s are derived from the corresponding picometer shifts of reflected light wavelength *versus* time curves. Statistical differences of the effect of ghrelin between cells treated with PTX compared with vehicle-treated cells were analysed by ANOVA followed by Bonferroni's corrections (\*\*\*,  $p < 0.001$ ).

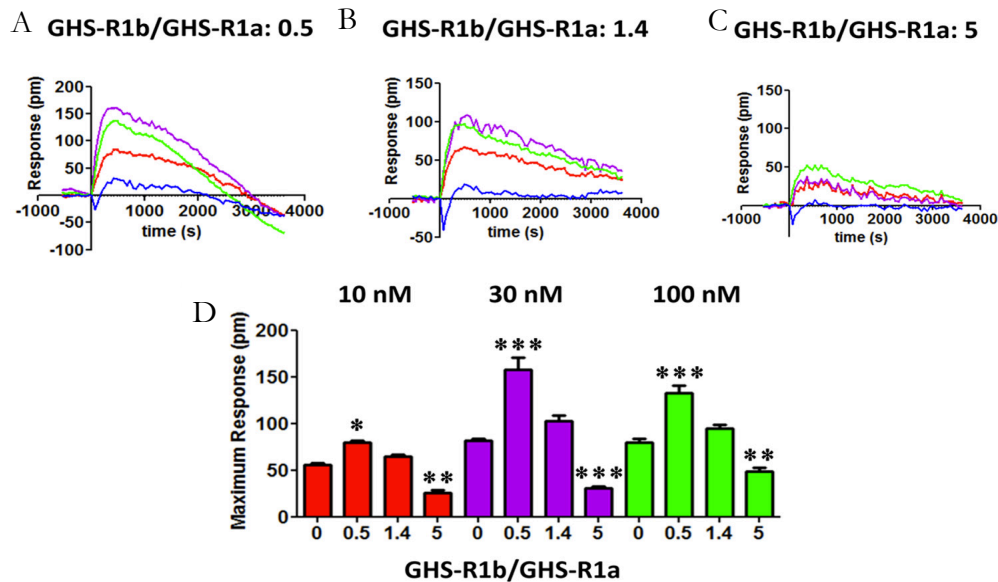


**Figure R25. GHS-R1b modulation of GHS-R1a signalling detected by DMR in HEK-293T cells.** DMR signals were determined in HEK-293T cells co-transfected with GHS-R1a-YFP (1  $\mu$ g) and increasing amounts of GHS-R1b-Rluc (0.05 to 0.6  $\mu$ g) to obtain a 0.5 (A), 1.4 (B) or 5 (C) GHS-R1b/GHS-R1a ratio. Cells were activated with increasing concentrations of ghrelin (10, 30 and 100 nM). Representative picometer (pm) shifts of reflected wavelength versus time curves are shown in A, B and C, each curve representing the mean of an optical trace experiment carried out in triplicate. In D, maximal responses at 500 s induced by different ghrelin concentrations are compared for GHS-R1b/GHS-R1a ratios from 0 to 5. CA values are derived from the A, B and C curves. Statistical differences of the effect of ghrelin in cells transfected with different GHS-R1b/GHS-R1a ratios compared with cells only expressing GHS-R1a (Figure R31A) were analysed by ANOVA followed by Bonferroni's corrections (\*,  $p < 0.05$ ; \*\*,  $p < 0.01$ ; \*\*\*,  $p < 0.001$ ).



According to the predominant coupling to  $G_{i/o}$  protein, ghrelin dose-dependently decreased forskolin-induced cAMP accumulation in cells only expressing GHS-R1a (Figure R26A). This effect was inhibited by YIL781 or by the PTX (Figure R26A). Again, this effect was not observed in cells only transfected with GHS-R1b (Figure R26B), and was dependent on the GHS-R1b/GHS-R1a expression ratio, with ghrelin being more efficient, similarly efficient and inefficient at expression ratios of 0.5, 1.4 and 5, respectively, compared with cells only transfected with GHS-R1a (Figure R26C).

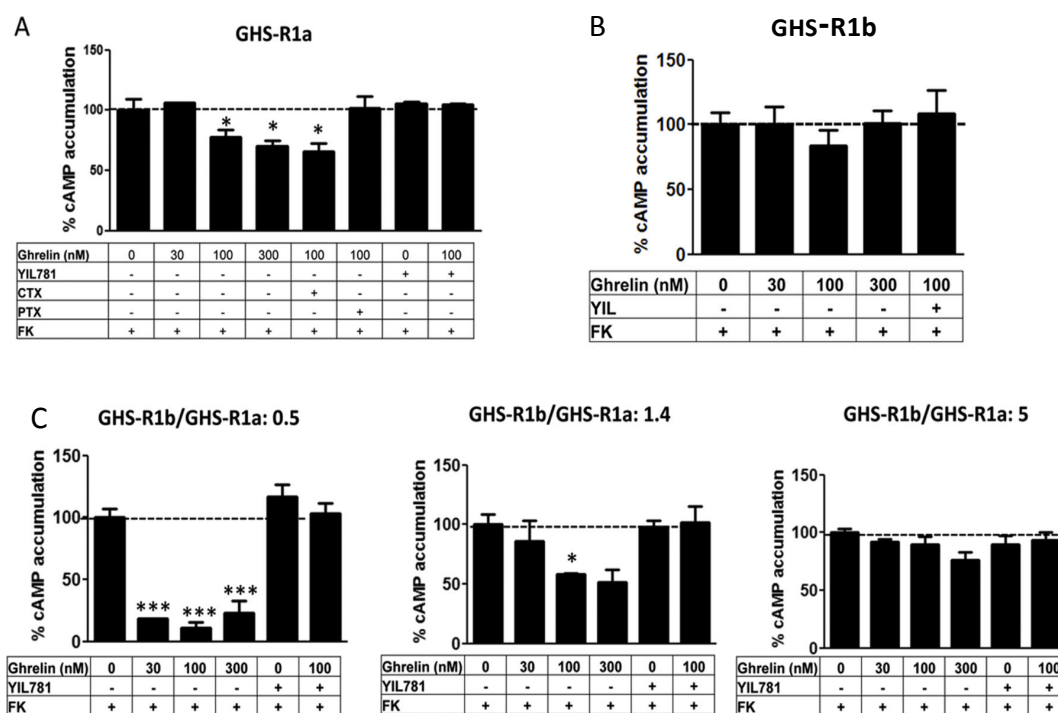


**Figure R26. Evaluation of cAMP GHS-R1a signalling upon GHS-R1a and GHS-R1a co-transfection.** HEK-293T cells transfected with GHS-R1a-YFP cDNA (1  $\mu$ g) (A), GHS-R1b-Rluc (0.5  $\mu$ g) (B) or GHS-R1a-YFP with increasing amounts of GHS-R1b-Rluc (0.05 to 0.6  $\mu$ g) according to the 0.5, 1.4 and 5 GHS-R1b/GHS-R1a ratio (C), were treated with ghrelin receptor antagonist YIL-781 (2  $\mu$ M) or vehicle (15 min) before activating the cells with ghrelin in the presence or absence of 0.5  $\mu$ M of forskolin. Values are means  $\pm$  S.E.M. of five to six experiments per treatment and expressed as decreases of forskolin-induced cAMP (100% dotted line). In A, cells were incubated overnight with vehicle, PTX or CTX prior to perform the experiment. Statistical differences of the effect of differently treated cells under different transfection conditions were analysed by ANOVA followed by Bonferroni's corrections (\*,  $p < 0.05$ ; \*\*\*,  $p < 0.001$  compared with the effect of forskolin alone).

Ghrelin also induced a dose-dependent increase in cytosolic  $Ca^{2+}$  (Figure R27),  $\beta$ -arrestin recruitment (Figure R28A and B) and ERK1/2 phosphorylation (Figure C and D) in HEK-293T cells only transfected with GHS-R1a. All measured ghrelin-activated signalling pathways were also inhibited by YIL781 (Figure R27A and Figure R28A and C), and they were not observed in cells only transfected with GHS-R1b (Figure R27A and Figure R28B and D). Importantly, these three signalling mechanisms were dependent on the GHS-

R1b/GHS-R1a expression ratio (Figure R27A and Figure R28A and C). As observed with DMR and cAMP accumulation experiments, at GHS-R1b/GHS-R1a expression ratios of 0.5, 1.4 and 5, ghrelin was more efficient, similarly efficient and significantly less efficient or inefficient, respectively, compared with cells only transfected with GHS-R1a (Figures R27A and R28A and C).

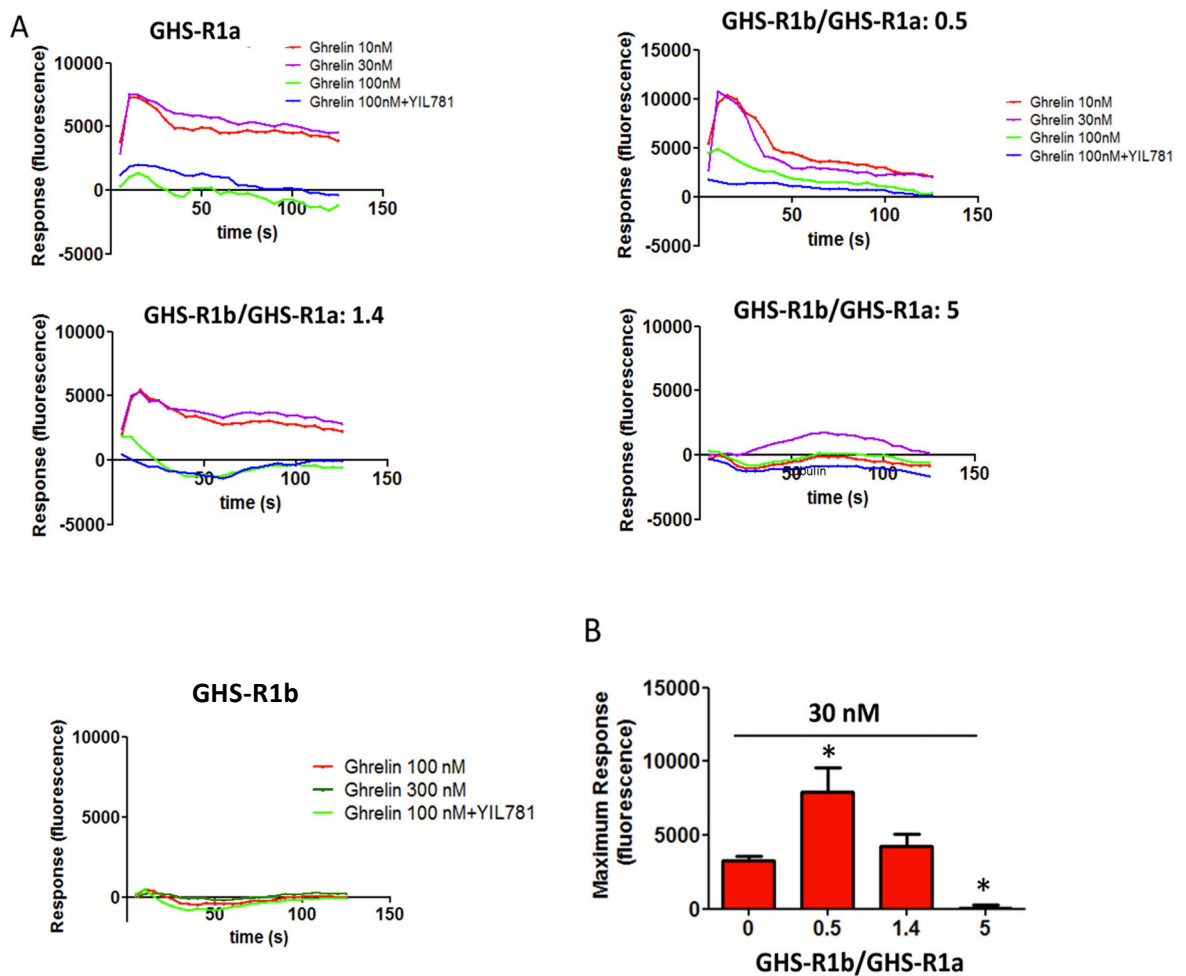


**Figure R27.** Evaluation of GHS-R1a-induced intracellular calcium mobilisation upon co-transfection with GHS-R1b. HEK-293T cells transfected with GHS-R1a-YFP cDNA (1  $\mu$ g), GHS-R1b-Rluc (0.5  $\mu$ g) or GHS-R1a-YFP with increasing amounts of GHS-R1b-Rluc (0.05 to 0.6  $\mu$ g) according to the 0.5, 1.4 and 5 GHS-R1b/GHS-R1a ratio, were treated with ghrelin receptor antagonist YIL-781 (2  $\mu$ M) or vehicle before activating the cells with ghrelin at 10, 30 100 or 300 nM concentrations. In (A) representative intracellular calcium release curves over time, and in (B), values of maximal calcium release (means  $\pm$  S.E.M. of four to six experiments) induced by 30 nM ghrelin were derived from the curves obtained at the different GHS-R1b/GHS-R1a ratios. Statistical differences of the effect of differently treated cells under different transfection conditions were analysed by ANOVA followed by Bonferroni's corrections (\*,  $p < 0.05$  compared with cells expressing GHS-R1a alone).

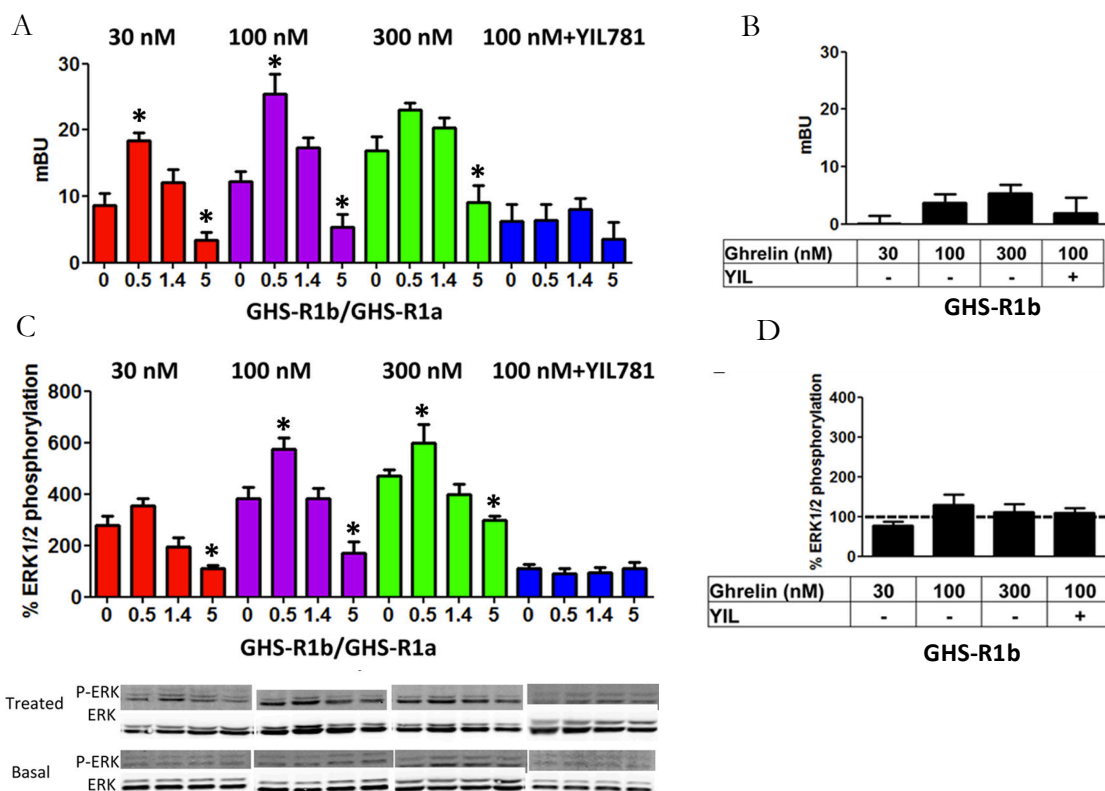


**Figure R28. Evaluation of  $\beta$ -arrestin and ERK1/2 phosphorylation GHS-R1a-mediated signalling upon co-transfection of HEK-293T cells with GHS-R1b.**  $\beta$ -arrestin-2 recruitment (means  $\pm$  S.E.M, n=5-7 experiments) was measured by BRET assay in cells transfected with 1  $\mu$ g  $\beta$ -arrestin-2 –Rluc, and GHS-R1a-YFP (1  $\mu$ g),  $\beta$ -arrestin-2 –Rluc, GHS-R1a-YFP and increasing amounts of increasing amounts of GHS-R1b-Rluc (0.05 to 0.6  $\mu$ g) according to the 0.5, 1.4 and 5 GHS-R1b/GHS-R1a ratio (A) or  $\beta$ -arrestin-2 –Rluc and GHS-R1a-YFP (1  $\mu$ g)(B). In all cases, cells were pre-treated (15 min) with vehicle or the GHS-R1a antagonist YIL-781 (2  $\mu$ M) followed by activation with ghrelin (30, 100 or 300 nM). ERK1/2 phosphorylation from the same transfected cell groups and treatments as in A and B, expressed as a percentage over values found in non-transfected cells (means  $\pm$  S.E.M, n=5-7 experiments). Representative Western blotting analyses are shown in the bottom of (C). Statistical differences of the effect of differently treated cells under different transfection conditions were analysed by ANOVA followed by Bonferroni's corrections (\*,  $p < 0.05$  compared with cells expressing GHS-R1a alone).

### IV.3.3 Homodimers and heterotetramers of GHS-R1a and GHS-R1b in HEK-293T-transfected cells

Biotinylation and signalling experiments therefore did not support a preferential intracellular localisation of GHS-R1b and GHS-R1a retention upon intracellular heteromerization with GHS-R1b as the basis for a dominant negative effect of GHS-R1b on GHS-R1a function (Chow *et al.*, 2012; Leung *et al.*, 2007). Our results instead fit with a negative effect of GHS-R1b on GHS-R1a signalling upon heteromerization in the plasma membrane (Mary *et al.*, 2013). Because GPCR homodimers seem to be a predominant species and oligomeric entities are viewed as multiples of dimers (Ferré *et al.*, 2014), we also investigated the possibility of homodimerization of GHS-R1b and heteromerization of GHS-R1a and

GHS-R1b homodimers. Saturable BRET curves were obtained in HEK-293T cells expressing a constant amount of GHS-R1a-Rluc and increasing amounts of GHS-R1a-GFP<sup>2</sup> (Figure R29A, BRET<sub>max</sub> of  $82 \pm 6$  mBU and BRET<sub>50</sub> of  $55 \pm 13$  mBU) or a constant amount of GHS-R1b-Rluc and increasing amounts of GHS-R1b-YFP (Figure R29B, BRET<sub>max</sub> of  $124 \pm 12$  mBU and BRET<sub>50</sub> of  $52 \pm 16$  mBU), strongly suggestive of homodimerization. As negative controls, linear plots with low BRET values were obtained using either CB<sub>1</sub>R-Rluc (Figure R36A) or CRF1-Rluc (Figure R29B).

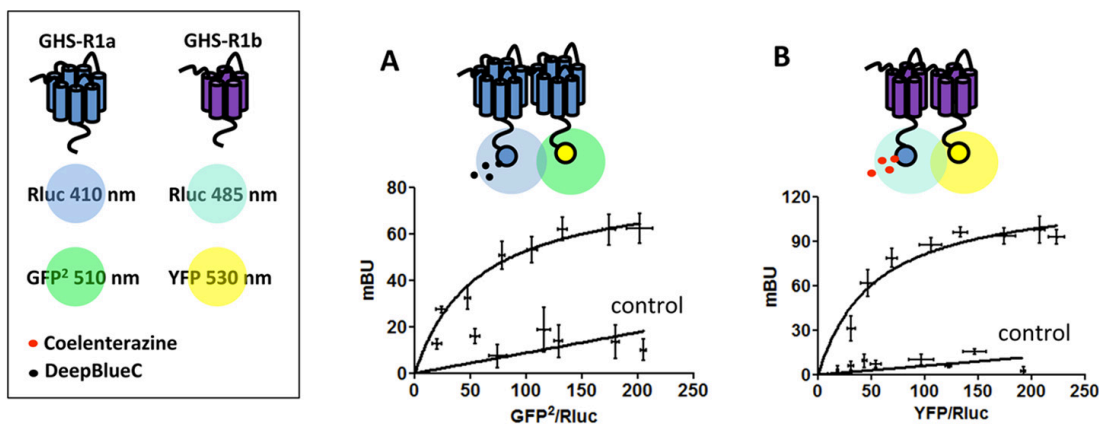


**Figure R29. Homomerization of GHS-R1a and GHS-R1b receptors.** GHS-R1a and GHS-R1b homodimers were detected by BRET saturation curves in HEK-293T cells co-transfected with GHS-R1a-Rluc cDNA (1.5  $\mu$ g) and increasing amounts of GHS-R1a-GFP<sup>2</sup> cDNA (0.5 to 3  $\mu$ g) (A), or co-transfecting GHS-R1b-Rluc (0.3  $\mu$ g) and increasing amounts of GHS-R1b-YFP (0.05 to 0.6  $\mu$ g) (B). As negative controls, linear and low BRET values were obtained by transfecting the cDNA to either cannabinoid receptor CB<sub>1</sub>R-Rluc (0.5  $\mu$ g) (A), or the corticotropin-releasing factor receptor CRFR<sub>1</sub>-Rluc (0.3  $\mu$ g) (B).

SRET assay was then used to evaluate the possibility of direct interactions between three receptor molecules, either two GHS-R1a and one GHS-R1b or two GHS-R1b and one GHS-R1a, as shown in Figures R30A and B. In this assay, Rluc was fused to one of the receptor units to act as BRET donor, GFP<sup>2</sup> was fused to a second receptor unit to act as BRET acceptor and FRET donor, and YFP was fused to act as FRET acceptor. The cDNA constructs were transfected in HEK-293T cells, and YFP emission was determined after adding DeepBlueC as luciferase donor. Positive SRET saturation curves were obtained with transfection of a constant amount of GHS-R1b-Rluc and GHS-R1a-GFP<sup>2</sup> and increasing amounts of GHS-R1a-YFP or GHS-R1b-YFP (Figure R30A and B), with SRET<sub>max</sub> values of  $222 \pm 18$  mSU and  $72 \pm 20$  mSU and SRET<sub>50</sub> values of  $48 \pm 14$  mSU and  $40 \pm 5$  mSU, respectively. As negative controls, linear plots with low SRET values were obtained when CB<sub>1</sub>R-Rluc was transfected as the BRET donor of GHS-R1a or GHS-R1b FRET pairs (Figure R30A and B). These results show the ability of GHS-R1a and GHS-R1b to assemble as heterotrimers and possibly heterotetramers. Support for heterotetramerformation was

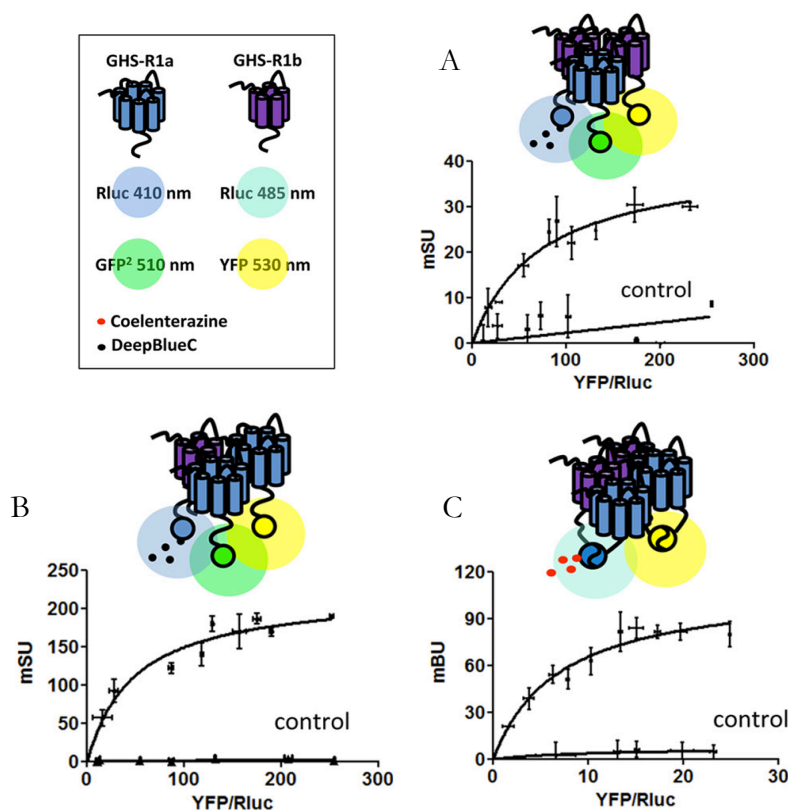


**Figure R30. Heterotetrameric structure of GHS-R1a and GHS-R1b heteromers.** SRET saturation curves were obtained in HEK-293T cells co-transfected with a constant amount of GHS-R1b-Rluc (0.4  $\mu$ g) and GHS-R1a-GFP<sup>2</sup> (1.5  $\mu$ g) and increasing amounts of GHS-R1b-YFP (0.5 to 3  $\mu$ g) (A) or increasing amounts of GHS-R1a-YFP (0.05 to 0.5  $\mu$ g) (B). As SRET negative controls, linear SRET values were obtained when CB<sub>1</sub>R-Rluc (0.4  $\mu$ g) was transfected as BRET donor of GHS-R1a or GHS-R1b FRET pairs. The BiLFC saturation curve was obtained in HEK-293T cells co-transfected with equal amounts of cDNA corresponding to GHS-R1a-cRluc and GHS-R1b-nRluc (1.5  $\mu$ g) and increasing amounts of GHS-R1a-cYFP and GHS-R1b-nYFP (0.5 to 2.5  $\mu$ g each). As negative control, linear BiLFC were obtained in cells transfected with adenosine A<sub>1</sub>R-cRluc (0.2  $\mu$ g) instead of GHS-R1a-cRluc. BRET and SRET amounts are given as a function of 100x the ratio between the fluorescence of the acceptor and the luminescence of the donor. BRET and SRET are expressed as miliBRET or miliSRET units and given as the means  $\pm$  S.D. of 4-5 experiments grouped as a function of the amount of BRET or SRET acceptor.

obtained by using BRET with double bimolecular luminescence complementation (BiLC) and bimolecular fluorescence complementation (BiFC) assays. In this assay, the two BRET sensors, the donor Rluc (a more efficient variant of Rluc) and the acceptor YFP Venus (a more efficient variant of YFP), are split into two hemiproteins, which each split sensor being fused to one of the four putative interacting receptors. BRET indicates reconstitution of both sensors and close proximity of the four receptors. A saturable BRET curve (BRET<sub>max</sub> of 111  $\pm$  10 mBU and BRET<sub>50</sub> of 7  $\pm$  2 mBU) was detected in HEK-293T cells co-transfected with equal amounts of GHS-R1a-cRluc and GHS-R1b-nRluc and increasing amounts of GHS-R1a-cYFP and GHS-R1b-nYFP cDNAs (Figure R30C). Negative controls were transfected with adenosine A<sub>1</sub>R-cRluc cDNA instead of GHS-R1a-cRluc cDNA (Figure R30C). Collectively,

these results indicate that GHS-R1a and GHS-R1b receptors can form oligomeric complexes that include heterodimers and homodimers.

#### IV.3.4 Differential GHS-R1b-mediated modulation of GHS-R1a signalling in rat striatal and hippocampal neurons

The significance of GHS-R1a-mediated signalling and its modulation by heteromerization with GHS-R1b was then addressed in primary neuronal cultures from striatum and hippocampus, brain areas that express functional GHS-R1a receptors (*Schellekens et al., 2010*). The relative expression of both GHS-R1a and GHS-R1b, determined by RT-PCR, was higher in striatal compared with hippocampal primary cultures (Figure R31).

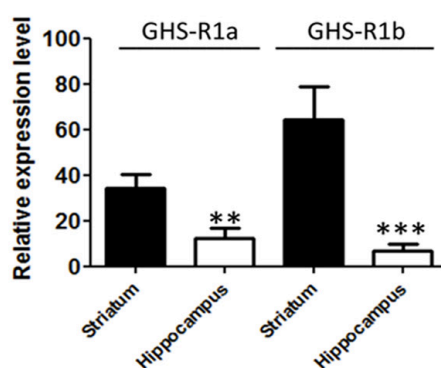


**Figure R31. Differential expression of GHS-R1a and GHS-R1b in primary neuron cultures.** Relative expression of GHS-R1a and GHS-R1b was determined by RT-PCR using primary cultures of rat hippocampus (white columns) and striatum (black columns) neurons. Values are the means  $\pm$  S.E.M. of five to seven experiments performed with independent primary cultures. Statistical differences of the expression of GHS-R1a and GHS-R1b in the different tissues were analysed by ANOVA followed by Bonferroni's corrections (\*\*,  $p < 0.01$ ; \*\*\*,  $p < 0.001$ ).

DMR was first analysed to evaluate the ghrelin-mediated signalling, and a dose-dependent response was obtained in primary cultures (Figure R32). Ghrelin, had a potent and efficient response in striatal than hippocampal neurons, and its effects were counteracted by YIL781 in both preparations (Figure R32). As shown in figure R31, the relative expression of GHS-R1b was higher than GHS-R1a expression in striatal neurons, while the opposite, a higher GHS-R1a than GHS-R1b expression, was observed in hippocampal neurons. Therefore, from the results obtained in HEK-293T cells, we anticipated that an increase in GHS-R1b expression could lead to opposite effects in hippocampal and striatal neurons. Indeed, in hippocampal primary cultures, transfection with increasing amounts of GHS-R1b cDNA (0.1 and 0.5  $\mu$ g) led to a progressive significant increase in the efficacy of ghrelin-induced DMR (Figure R33B), whereas in striatal primary cultures, GHS-R1b transfection led to the opposite effect (Figure R33A).



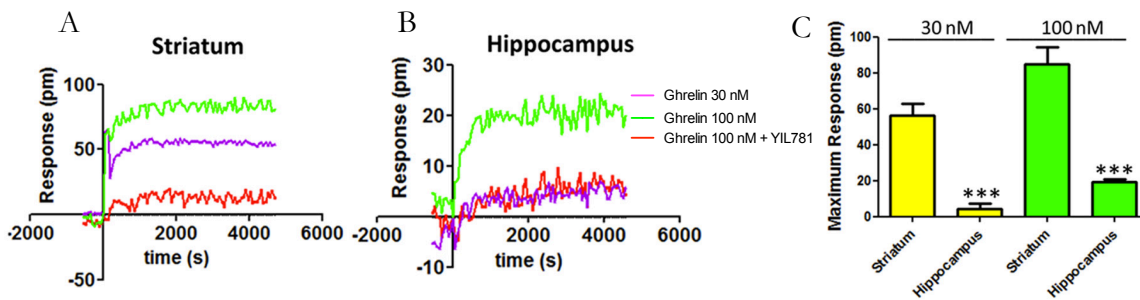


**Figure R32. Differential DMR ghrelin response in striatal and hippocampal neurons.** DMR was determined in striatal (A) or hippocampal (B) neuronal primary cultures pretreated (30 min) with vehicle or the GHS-R1a antagonist YIL-781 (2  $\mu$ M) followed by activation with ghrelin (30 or 100 nM). Representative picometer (pm) shifts of reflected light wavelength versus time curves are shown. Each curve represents the mean of an optical trace experiment carried out in triplicates. In (C) maximum responses of DMR at 2000 s induced by ghrelin at 30 or 100 nM are compared for striatal and hippocampal neuronal cultures. Values are the mean  $\pm$  S.E.M. of 5-7 experiments performed in independent primary cultures. Statistical differences of the ghrelin effect between tissue cultures were analysed by ANOVA followed by Bonferroni's corrections (\*\*\*,  $p < 0.001$ ).

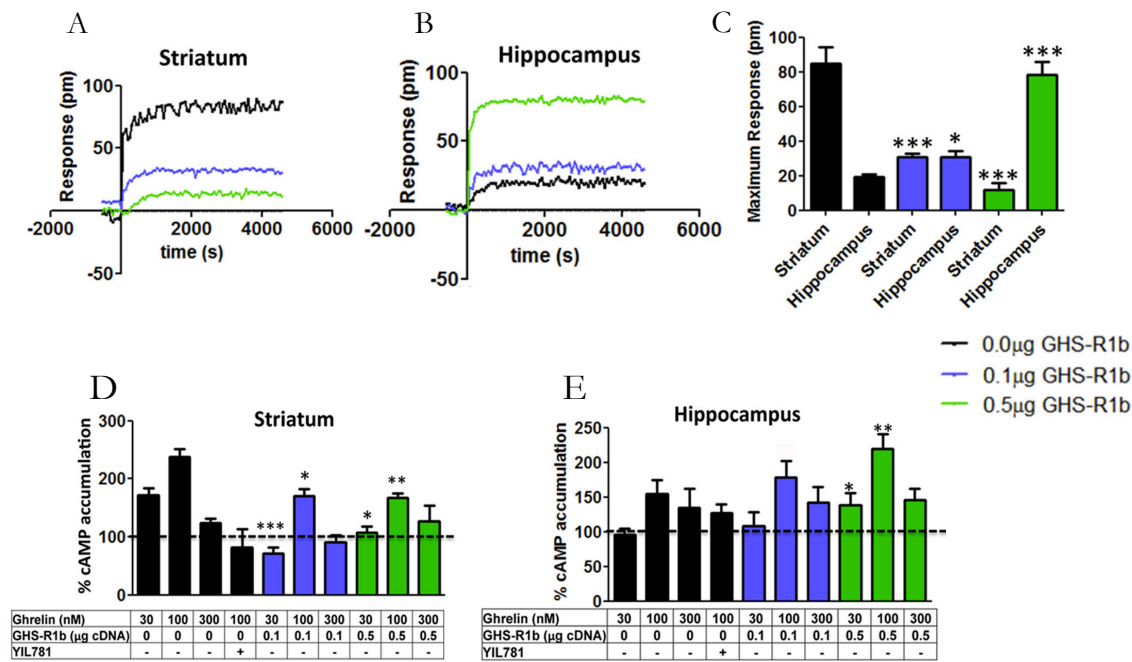


**Figure R33. GHS-R1b-mediated modulation of GHS-R1a signalling in striatal and hippocampal neurons.** DMR was determined in rat hippocampal (A and C) and striatal (B and C) primary cultures not transfected (black) or transfected with 0.1\_μg (blue) or 0.5\_μg (green) of GHS-R1b cDNA and activated with 100 nM ghrelin. Representative picometer (pm) shifts of reflected light wavelength versus time curves are shown in A and B. Each curve represents the mean of an optical trace experiment carried out in triplicate. C, ghrelin-induced maximum responses at 2000 s are compared for striatal and hippocampal neuronal cultures not transfected or transfected with 0.1 or 0.5\_μg of GHS-R1b cDNA. Statistical differences between differently transfected cells for each type of culture were analysed by ANOVA followed by Bonferroni's corrections. \*,  $p < 0.05$ ; \*\*\*,  $p < 0.001$  compared with non-transfected cells. D and E, cAMP accumulation was determined in rat hippocampal (D) and striatal (E) primary cultures not transfected (black) or transfected with 0.1\_μg (blue) or 0.5\_μg (green) of GHS-R1b cDNA. Cells were pretreated (15 min) with vehicle or the GHS-R1a antagonist YIL781 (2\_μM), followed by activation (15 min) with increasing ghrelin concentrations. Values are means  $\pm$  S.E. of four to six experiments and expressed as percentage of values from non-stimulated cells (100%, dotted line). Statistical differences between differently transfected cells were analyzed by ANOVA followed by Bonferroni's corrections. \*,  $p < 0.05$ ; \*\*\*,  $p < 0.001$  compared with non-transfected cells.

By analysing another signalling readout, the cAMP accumulation, unexpected results were obtained compared with HEK-293T cells in both hippocampal and striatal primary cultures. Ghrelin produced an increase in cAMP production with an inverted U-shaped dose-response (maximal effect at about 100 nM), indicating an agonist-induced desensitisation effect (Figure R33D and E). This effect was blocked by YIL781 in both preparations. The same as for DMR, in hippocampal and striatal primary cultures, transfection with increasing amounts of GHS-R1b cDNA (0.1 and 0.5  $\mu$ g) led to a progressive significant increase and decrease, respectively, in the effect of ghrelin-induced cAMP accumulation (Figures R33 D and E). The results also showed that, in neurons, GHS-R1b can positively or negatively modulate GHS-R1a function depending on the endogenous relative GHS-R1b/GHS-R1a expression ratio.

#### IV.3.5 Dopamine D<sub>1</sub>R interacts with GHS-R1a-GHS-R1b heteromers promoting a G<sub>s/olf</sub>-protein coupling

Previous studies have suggested that GHS-R1a-mediated signalling depends mostly on G<sub>q</sub> coupling, although, in this chapter, evidence of G<sub>i/o</sub> coupling in HEK-293T cells has also been obtained. Similarly, ghrelin-induced cAMP-PKA signalling has also been reported but suggested to be independent of G<sub>s/olf</sub> proteins. The G protein subtype involved in ghrelin-induced cAMP accumulation in striatal and hippocampal neurons in culture was first investigated by using the G<sub>s/olf</sub> toxin CTX, the G<sub>i/o</sub> toxin PTX, and the G<sub>q</sub> protein inhibitor YM254890. CTX, but not PTX or YM254890, prevented ghrelin-induced cAMP in both

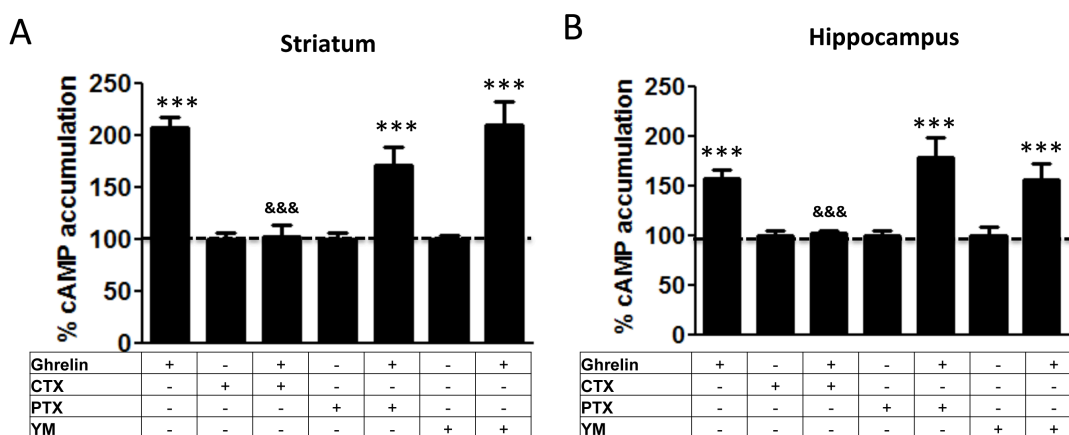


**Figure R34. G<sub>s/olf</sub>-coupling of ghrelin receptors in striatal and hippocampal neurons.** cAMP accumulation was determined in rat striatal (A) and hippocampal (B) primary cultures incubated overnight with vehicle, PTX (10 ng/ml), the G<sub>q</sub> inhibitor YM254890 (YM, 1  $\mu$ M) or for 2 h with CTX (100 ng/ml). Cells were then treated with vehicle or ghrelin (100 nM). Values are the mean  $\pm$  S.E.M. of three to four experiments and are expressed as percentage of the values of vehicle-treated cells (dotted line). Statistical differences between differently treated cells were analysed by ANOVA followed by Bonferroni's corrections (\*\*\*,  $p < 0.001$  compared with vehicle treated cells; &&&,  $p < 0.001$  compared with ghrelin-treated cells).





preparations (Figure R34), identifying  $G_{s/olf}$  as predominant G proteins coupled to GHS-R1a in neurons. Although CTX increased the basal levels of cAMP by 2- to 3-fold, this cannot explain an apparent inhibition of the ghrelin due to the saturation of the adenylyl cyclase activation because, under the same experimental conditions, forskolin increased cAMP levels by 10-fold (data not shown). A possible explanation for the unexpected preferential coupling of GHS-R1a to  $G_{s/olf}$  in neurons *versus* the  $G_{i/o}$  observed in HEK-293T cells could be the presence of additional receptors, that could interact with GHS-R1a or GHS-R1b, in the neuronal primary cultures. Indeed, dopamine  $D_1R$  is a canonical mediator of adenylyl cyclase activation that has been reported to heteromerise with GHS-R1a (Jiang *et al.*, 2006; Kern *et al.*, 2015). We then investigated its possible involvement in ghrelin-mediated cAMP accumulation in neurons in culture. In fact, the  $D_1R$  antagonist SCH23390 (1  $\mu$ M), but not the dopamine  $D_2R$  antagonist raclopride (1  $\mu$ M), was able to block the ghrelin-induced cAMP accumulation in striatal but not hippocampal neurons in culture (Figure R35). That  $D_1R$  co-expression can promote a switch in G protein coupling of GHS-R1a from  $G_{i/o}$  to  $G_{s/olf}$  was then demonstrated in HEK-293T cells transfected with GHS-R1b-Rluc (0.4  $\mu$ g), GHS-R1a-YFP (1  $\mu$ g, GHS-R1b/GHS-R1a ratio of 1.4) and with  $D_1R$  (0.4  $\mu$ g) (Figure R36A, C and D), or with  $D_2R$  (0.4  $\mu$ g) (Figure R36B and C). In the presence of  $D_1R$ , both ghrelin (100 nM) and the  $D_1R$  agonist SKF81297 (100 nM) increased cAMP production, an effect that was blocked by CTX but not by PTX or the  $G_q$ -inhibitor YM254890 (Figure R36A). In the presence of the  $D_2R$ , both ghrelin and the  $D_2R$  agonist quinpirole (1  $\mu$ M), decreased cAMP production, effect that was blocked by PTX but not the CTX or YM254890 (Figure R36B). Figure

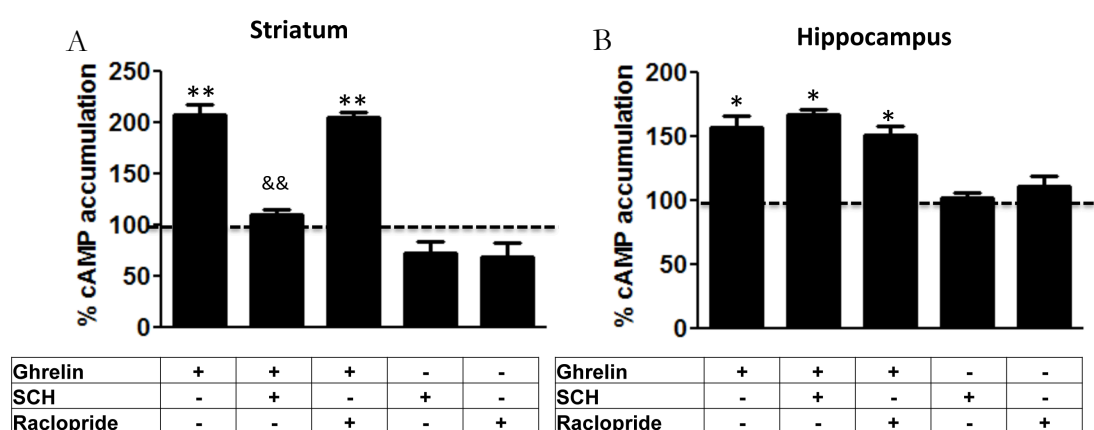


**Figure R35. Dopamine receptor antagonists block GHS-R1a cAMP signalling.** Striatal (A) and hippocampal (B) rat primary neurons were pretreated with vehicle, the  $D_1R$  antagonists SCH23390 (SCH, 1  $\mu$ M) or the  $D_2R$  antagonist Raclopride (2  $\mu$ M) followed by a treatment with vehicle or ghrelin (100 nM) and the cAMP levels evaluated. Values are the mean  $\pm$  S.E.M. of 5-6 experiments and are expressed as percentage of the values of vehicle-treated cells (100 % dotted line). Statistical comparison between differently treated cells were analysed by ANOVA followed by Bonferroni's corrections (\*,  $p < 0.05$ ; \*\*,  $p < 0.01$  compared with vehicle-treated cells; &&,  $p < 0.01$  compared with ghrelin-treated cells).

R36C demonstrates agonist selectivity at the concentrations used in cAMP experiments using cells only transfected with single receptors. In cells transfected with and SKF81294 (100 nM) did not produce an additive or synergic effect (Figure R36A), but blockade of either receptor with the D<sub>1</sub> receptor antagonist SCH23390 (1 μM) or the ghrelin antagonist YIL781 (1 μM) completely counteracted cAMP accumulation induced by both ghrelin and SKF81297 (Figure R36D). Because the interactions between GHS-R1a and D<sub>1</sub>R ligands, particularly the cross-antagonism, strongly suggested oligomerization, we investigated this possibility with BRET experiments. In HEK-293T cells transfected with a constant amount of D<sub>1</sub>R-Rluc (0.4 μg) and increasing amounts GHS-R1a-YFP (0.2 -1.5 μg) or GHS-R1b-YFP (0.1- 0.6 μg) showed low and linear plots, consistent with nonspecific interactions (Figure R37A and B). Similarly, low BRET values were obtained (at YFP/Rluc ratio of 100) when cells were exposed to

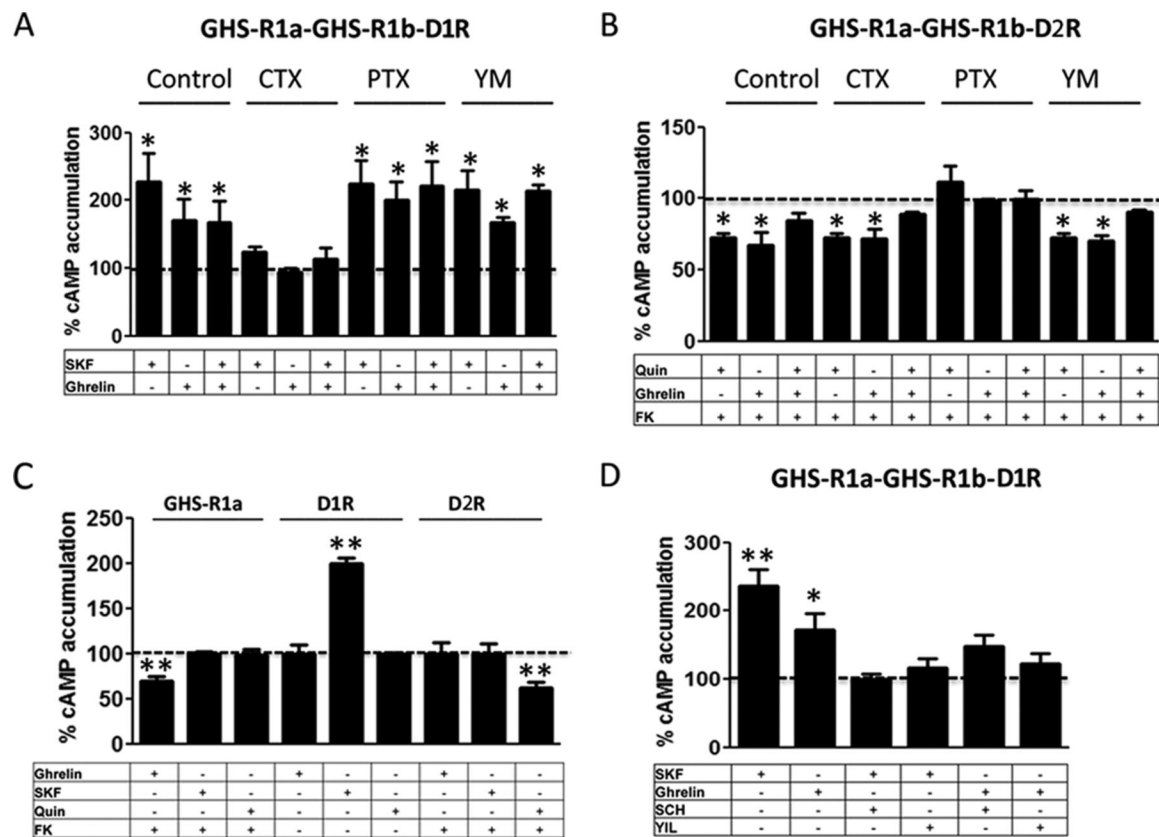


**Figure 36. D<sub>1</sub>R promotes GHS-R1a-GHS-R1b heteromers coupling to Gs/olf protein.** cAMP accumulation was determined in HEK-293T cells transfected with GHS-R1b-Rluc cDNA (0.2 μg), GHS-R1a-YFP cDNA (1 μg), and D<sub>1</sub>R cDNA (0.4 μg, A and D) or D<sub>2</sub>R cDNA (0.4 μg, B) or single-transfected with the same amount of the indicated receptors (C). Cells were incubated overnight with vehicle, PTX (10 ng/ml), or the Gq inhibitor YM254890 (YM, 1 μM) or for 2 h with CTX (100 ng/ml) and pretreated (15 min) with vehicle, the GHS-R1a antagonist YIL781 (YIL, 2 μM), or the D<sub>1</sub>R antagonist SCH23390 (SCH, 1 μM), followed by activation (15 min) with ghrelin (100 nM), the D<sub>1</sub>R agonist SKF81297 (SKF, 100 nM), or the D<sub>2</sub>R agonist quinpirole (Quin, 1 μM) alone or in combination in the absence (A and D) or presence (B and C) of forskolin (FK, 0.5 μM). Values are means ± S.E.M. of six to eight experiments and expressed as percentage of values of cells not treated with ghrelin (100%, dotted line). Statistical differences between differently treated cells were analyzed by ANOVA followed by Bonferroni's corrections (\*,  $p < 0.05$ ; \*\*,  $p < 0.01$  compared with vehicle-treated cells).

ghrelin, SKF81297 or both (100 nM in each case, Figure R37C and D). Nevertheless, a saturable BRET curve was obtained when cells were transfected with D<sub>1</sub>R-Rluc (0.4 μg), increasing amounts of GHS-R1b-YFP (0.1 to 0.6 μg) and GHS-R1a (0.8 μg), with BRET<sub>max</sub> and BRET<sub>50</sub> values of 36 ± 6 mBU and 93 ± 10 mBU, respectively (Figure R37E), indicating that D<sub>1</sub>R specifically interacts with GHS-R1a-GHS-R1b heteromers. In agreement, significant

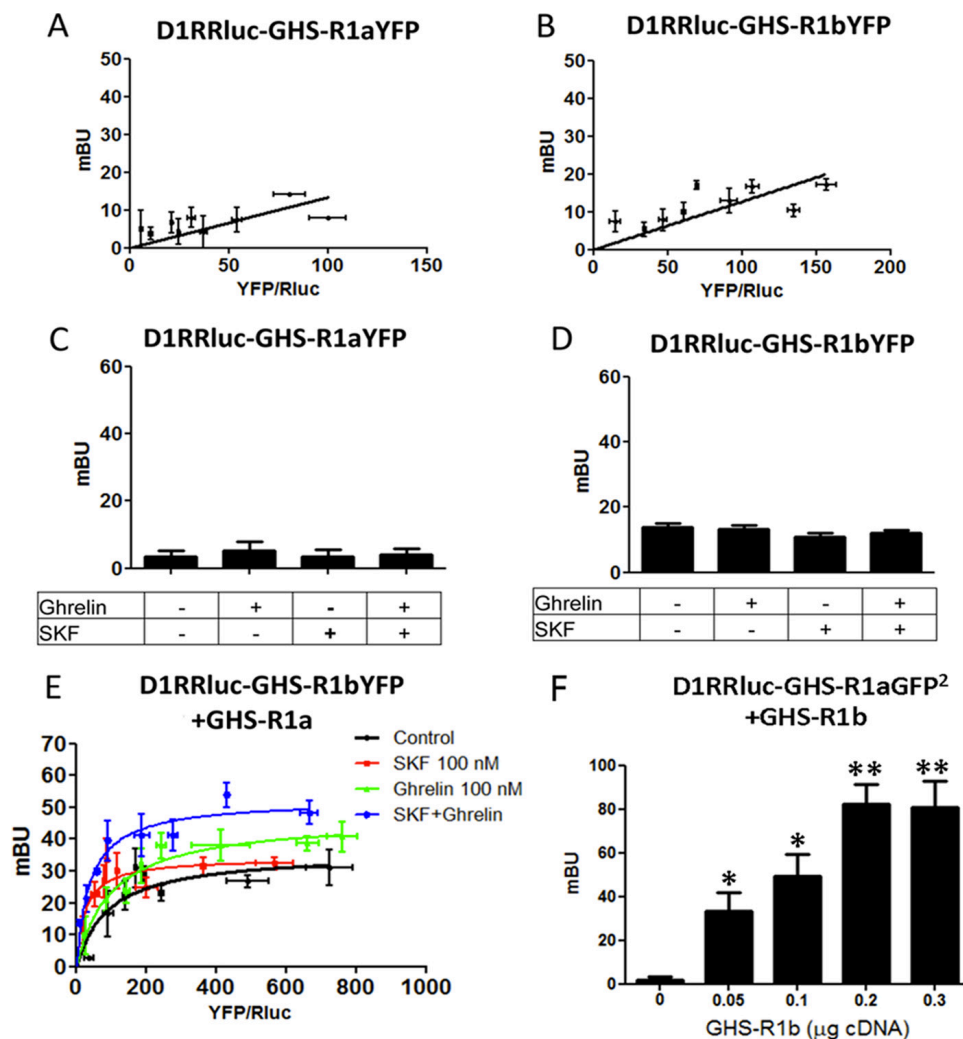


**Figure R37. Selective heteromerization of D<sub>1</sub>R with GHS-R1a-GH-R1b complexes.** BRET experiments in HEK-293T cells transfected with a constant amount of D<sub>1</sub>R-Rluc cDNA (0.4 μg) and increasing amounts of GHS-R1a-YFP cDNA (0.2-1.5 μg, A) or GHS-R1b-YFP cDNA (0.1-0.6 μg, B). BRET at a YFP/Rluc ratio of 100 was also determined in cells not activated or activated with ghrelin (100 nM), the D<sub>1</sub>R agonist SKF81297 (SKF, 100 nM), or both (C and D). E, BRET experiments were performed in HEK-293T cells transfected with D<sub>1</sub>R-Rluc cDNA (0.4 μg), GHS-R1a cDNA (0.8 μg), and increasing amounts of GHS-R1b-YFP cDNA (0.1– 0.6 μg), not stimulated (black curve), or stimulated with SKF81297 (SKF, 100 nM, red curve), ghrelin (100 nM, green curve), or both (blue curve). F, BRET experiments were performed in HEK-293T cells transfected with D<sub>1</sub>R-Rluc cDNA (0.4 μg), GHS-R1a-GFP<sup>2</sup> cDNA (1.0 μg), and increasing amounts of GHS-R1b cDNA (0.05– 0.3 μg). BRET values are given as a function of 100x the ratio between the fluorescence of the acceptor and the luciferase activity of the donor. BRET is expressed as milliBRET units and given as the means ±S.E.M. of 4-6 experiments grouped as a function of the amount of BRET acceptor. Statistical differences between differently transfected cells were analysed by ANOVA followed by Bonferroni's corrections (\*, p<0.05; \*\*, p <0.01 compared with cells not transfected with GHS-R1b).

BRET values could be only obtained in cells transfected with D<sub>1</sub>R-Rluc (0.4 µg), GHS-R1a-YFP (1 µg) when co-transfected with increasing amounts of GHS-R1b (0.05 to 0.3 µg) (Figure R37F). BRET saturation curves were also obtained in cells transfected with D<sub>1</sub>R-Rluc (0.4 µg), increasing amounts of GHS-R1b-YFP (0.1-0.6 µg) and GHS-R1a (0.8 µg), and treated with 100 nM SKF81297 (Figure R44 red line, BRET<sub>max</sub> and BRET<sub>50</sub> values of 34 ± 3 mBU and 25 ± 11 mBU, respectively), 100 nM ghrelin (Figure R44E green line, BRET<sub>max</sub> and BRET<sub>50</sub> values of 46 ± 3 mBU and 99 ± 12 mBU, respectively). The significant increase in BRET<sub>max</sub> upon treatment with ghrelin indicates a facilitation of energy transfer or an increase in the heteromer formation, whereas the significant decrease in BRET<sub>50</sub> upon treatment with SKF81297 suggest an increase in the affinity of the interaction between receptors. Both effects, a significant increase in BRET<sub>max</sub> and a significant decrease in BRET<sub>50</sub>, were observed upon co-treatment with ghrelin and SKF81297 (Figure R37E blue line, significant statistical differences in BRET<sub>max</sub> and BRET<sub>50</sub> compared with control non-treated cells were determined by ANOVA followed by Bonferroni's corrections, \*p < 0.05 in all cases). If D<sub>1</sub>R can only interact with GHS-R1a in the presence of GHS-R1b, the absence of GHS-R1b should disclose the properties that are dependent on GHS-R1a-GHS-R1b-D<sub>1</sub>R heteromerization. In fact, in cells transfected with D<sub>1</sub>R but only co-transfected with GHS-R1a, ghrelin (100 nM) did not produce cAMP accumulation, and YIL781 (1 µM) did not counteract cAMP accumulation induced by SKF81297 (100 nM) (Figure R38). Together, the results from

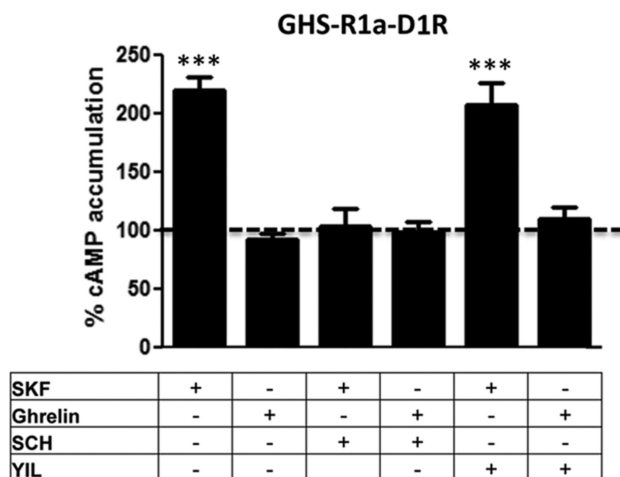


**Figure R38. Dependence on GHS-R1b for D<sub>1</sub>R-mediated modulation of GHS-R1a signalling.** cAMP accumulation was determined in cells transfected with GHS-R1a-YFP cDNA (1.5 µg) and D<sub>1</sub>R cDNA (0.5 µg). Cells were treated with vehicle, ghrelin (100 nM), or SKF 81297 (SKF, 100 nM) with and without YIL781 (YIL, 2 µM) or SCH23390 (SCH, 1 µM). Values are means ± S.E.M. of four to six experiments and are expressed as percentage values from cells only treated with vehicle (100%, dotted line). Statistical differences between differently treated cells were analysed by ANOVA followed by Bonferroni's corrections. \*\*, p < 0.01; \*\*\*, p < 0.001 compared with cells treated only with vehicle



transfected HEK-293T cells provide a very plausible mechanism for the results obtained in striatal cells in culture, demonstrating that GHS-R1b determines the ability of GHS-R1a to form oligomeric complexes with D<sub>1</sub>R, which allows ghrelin to activate G<sub>s/olf</sub> protein-

#### IV.3.6 Discussion

The spliced variant of the ghrelin receptor, GHS-R1b, negatively regulates the full and functional ghrelin receptor GHS-R1a. The proposed mechanisms through which this modulation could occur were, by GHS-R1b ability to retain the GHS-R1a in intracellular compartments (*Chow et al., 2012; Leung et al., 2007*) or by stabilising GHS-R1a in a non-signalling conformation (*Mary et al., 2013*). The results obtained in this chapter reveal a novel and more complex modulatory action of GHS-R1b on the trafficking and signalling of GHS-R1a. First, GHS-R1b is facilitating the traffic of GHS-R1a to the plasma membrane with an efficiency that depends on a specific GHS-R1b/GHS-R1a expression ratio. With further increases in the GHS-R1b/GHS-R1a ratio, this facilitation declines and disappears. Thus, higher and probably non-physiological amounts of GHS-R1b seem to be necessary to promote intracellular retention of GHS-R1a (*Chow et al., 2012; Leung et al., 2007*). On the other hand, GHS-R1b impairs GHS-R1a signalling upon oligomerization at the plasma membrane. The correlation between the results obtained with biotinylation and signalling assays performed in HEK-293T cells demonstrate that the main factor determining the ghrelin-induced signalling potency is the stoichiometry relationship of both proteins in the plasma membrane. Therefore, GHS-R1b may act as a dual modulator of GHS-R1a function: low relative GHS-R1b expression potentiates GHS-R1a function by facilitating the trafficking of the full-length ghrelin receptor and high relative expression of GHS-R1b inhibits GHS-R1a function exerting a negative allosteric effect on GHS-R1a signalling. One of the causes of the dual action might be the degree of GHS-R1a-GHS-R1b oligomerization. Because GHS-R1a seems to be the minimal functional unit (*Damian et al., 2015*), one possible scenario is that one GHS-R1b molecule per one GHS-R1a homodimer facilitates trafficking but not a negative allosteric modulation of ghrelin, whereas two (or more) GHS-R1b molecules would negatively affect GHS-R1a function and allosterically decrease ghrelin-mediated signalling.

To our knowledge, this study is the first addressing the modulatory role of GHS-R1b on GHS-R1a signalling in primary neurons in culture. First of all, the results in this chapter indicate that endogenous relative expression of GHS-R1a and GHS-R1b are in the same range in primary neuronal cultures that in our experiments in HEK-293T transfected cells. Significantly, from the experiments in HEK-293T cells, predictable changes in ghrelin-induced

signalling were demonstrated in striatal and hippocampal neurons in culture upon varying the GHS-R1b relative expression levels. Increasing the expression of GHS-R1b in a progressive manner, hippocampal and striatal cell cultures resulted in a, respectively, increase and decrease of the ghrelin-induced signalling, that depended on the initially low or high relative GHS-R1b/GHS-R1a expression ratio.

GHS-R1a couples to  $G_q$  proteins, therefore, ghrelin binding leads to activation of phospholipase C,  $IP_3$  and  $Ca^{2+}$  mobilisation (Damian *et al.*, 2015; Holst *et al.*, 2005; Mary *et al.*, 2013). It has also been reported that GHS-R1a-mediated signalling is pertussis toxin-sensitive (Bennett *et al.*, 2009; Dezaiki *et al.*, 2007). Thus, ghrelin may engage different signalling pathways depending on the cell context. In pituitary GH cells, GHS-R1a seems to couple preferentially to  $G_q$ , hence, stimulating GH release, whereas, in islet pancreatic  $\beta$  cells, it couples to  $G_{i/o}$  proteins and its activation leads to inhibition of insulin release (Dezaiki, 2013). Ghrelin can even lead to cAMP-PKA signalling (Cuellar and Isokawa, 2011; Malagón *et al.*, 2003; Sun *et al.*, 2014). The use of selective G protein toxins and inhibitors demonstrated a preferential  $G_{i/o}$  coupling of the GHS-R1a-GHS-R1b complex in HEK-293T cells and, unexpectedly, a preferential  $G_{s/olf}$  coupling in both striatal and hippocampal neurons in culture.

Interestingly, the results of this chapter demonstrate that oligomerization with GHS-R1b confers GHS-R1a-GHS-R1a complex the ability to heteromerise with a  $G_{s/olf}$ -coupled receptor. In fact, in HEK-293T cells transfected with GHS-R1a and GHS-R1b, co-transfection with  $D_1R$  promoted a switch of the ghrelin-mediated signalling from  $G_{i/o}$  to  $G_{s/olf}$  signalling. A previous study on transfected HEK-293T cells suggested that GHS-R1a can heteromerise and functionally interact with  $D_1R$ , but apparently without concomitant interaction with GHS-R1b. The same study, also suggested that, within the GHS-R1a- $D_1R$  heteromer, ghrelin amplifies  $D_1R$  signalling (Jiang *et al.*, 2006). A more recent study by the same research group suggests that GHS-R1a- $D_1R$  heteromerization allows  $D_1R$  to couple and signal through  $G_q$  proteins, once again, without involvement of the GHS-R1b receptor (Kern *et al.*, 2015). The BRET experiments shown in this chapter suggest that GHS-R1a- $D_1R$  heteromerization depends on the presence of GHS-R1b in the complex. In cells co-transfected with  $D_1R$ , GHS-R1a and GHS-R1b, ghrelin in the maximal effective concentration (100 nM) does not potentiate and, if anything, decreases cAMP accumulation induced by SKF81297. Furthermore, a significant cross-antagonism, a common biochemical property of receptor heteromers, was also observed. Thus, in cells transfected with the three receptors: GHS-R1a, GHS-R1b and  $D_1R$ , both GHS-R1a and  $D_1R$  antagonists were able to block SKF81297- and ghrelin-induced cAMP increases. The cross-antagonism phenomenon of



SCH23390 on ghrelin-induced cAMP accumulation was also observed in striatal but not hippocampal cells in culture. This lack of cross-antagonism phenomenon in hippocampal primary cultures could be due to the relative expression of GHS-R1b in striatal and hippocampal neurons. Moreover, molecular and functional interactions between GHS-R1a and D<sub>1</sub>R reported in hippocampus (*Kern et al., 2015*) may co-exist with complexes involving receptors other than D<sub>1</sub>R, suggesting that different complexes containing GHS-R1a-GHS-R1b heteromers can be differentially expressed in the brain.

In summary, GHS-R1b plays a much more active and complex role in ghrelin-induced signalling than previously assumed. The results of this chapter indicate that the relative expression of GHS-R1b not only determines the efficacy of ghrelin-induced and GHS-R1a-mediated signalling, but also determines the ability of GHS-R1a to form oligomeric complexes with other receptors, promoting profound qualitative changes in the ghrelin-induced signalling.

## Chapter 4.

### IV.4 Investigation of the relationship between cocaine and the loss of appetite

It has been established that addiction and eating disorders like binge eating, anorexia or bulimia, share a central control that involves reward circuitry of the brain. This leads to bidirectional influences: on one hand, previous history of binge eating predisposes to the addictive behaviour, whereas the cessation of exposure to drugs of abuse leads to persistent proclivity towards reward-providing activities, including the intake of palatable food. Since ancient times, it has been known that the use of cocaine is associated with a decreased food intake, with the inversion after the drug use is stopped. This creates a vicious circle in which the weight gain that follows the discontinuance of cocaine use secondarily causes a significant distress, which can make a patient more prone to the relapse. Many uncertainties remain about the biological substrate of these changes, particularly at the level of signalling systems involved. Thus, establishing the molecular mechanisms of such complex interactions is of immense biological and medical importance, even with social impact, particularly in the younger population.

Towards explaining the intricacies of drug and food intake interactions, our objective, in this chapter 4, was to establish and unravel the molecular mechanisms of the interactions between cocaine consumption and appetite consumption behaviours. The results in chapter 4 satisfy the **aim IV** of the thesis.

In this chapter, the author of this Thesis, Edgar Angelats, participated in the immunocytochemical and PLA assays using a variety of cell cultures treated or not with cocaine. These and other results developed by members of the laboratory and in collaboration





with other research groups, led to the paper entitled **‘Cocaine blocks effects of the hunger hormone, ghrelin, via neuronal interaction with sigma-1 receptors’**, whose authors are D. Aguinaga, M. Medrano, A. Cordoní, M. Jimenez, E. Angelats, M. Casanovas, I. Vega-Quiroga, M. Petrovic, K. Gysling, L. Pardo, R. Franco, G. Navarro. The paper has been accepted for publication in *Molecular Neurobiology* (May 2018), and the first author of the manuscript, D. Aguinaga, has included this work in his thesis.



#### IV.4.1 GHS-R1a forms heteromeric complexes with $\sigma_1$ -R

Immunocytochemical assays were performed to detect whether co-localisation between GHS-R1a and  $\sigma_1$ -R occurred in transfected HEK-293T cells. Cells were transfected with cDNA for  $\sigma_1$ -R fused to YFP (0.75  $\mu$ g cDNA) and for GHS-R1a fused to Rluc (1.66  $\mu$ g cDNA). In cells expressing only  $\sigma_1$ -R-YFP, the receptor was detected by the own YFP fluorescence, identifying  $\sigma_1$ -R-YFP mainly in intracellular structures. In HEK-293T cells expressing GHS-R1a-Rluc, the GHS-R1a was detected by a specific primary anti-Rluc and secondary Cy3 antibodies, being detected in intracellular structures and at the plasma membrane level. Interestingly, in HEK-293T cells co-expressing  $\sigma_1$ -R-YFP (0.75  $\mu$ g) and GHS-R1a-RLuc (1.66  $\mu$ g) co-localisation of both receptors was observed (Figure R39).

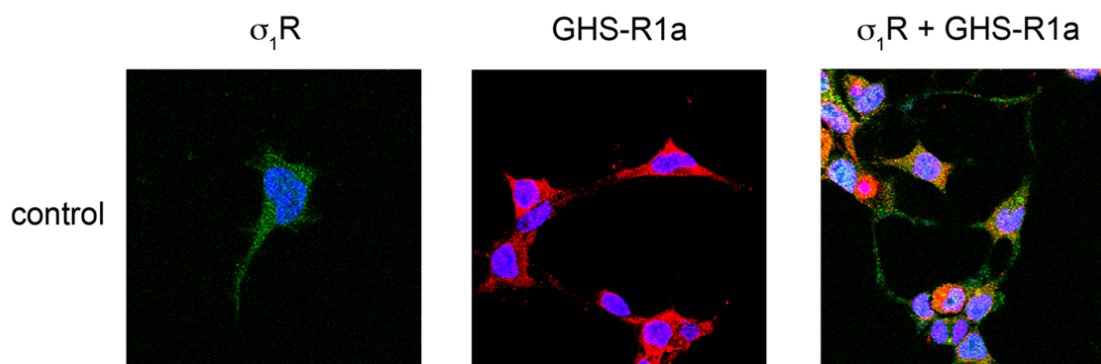


**Figure R39. Co-localisation of GHS-R1a with  $\sigma_1$ -R.** HEK-293T cells expressing  $\sigma_1$ -R, GHS-R1a-Rluc or both receptors, were monitored by YFP fluorescence (green) or using a monoclonal anti-Rluc primary antibody and a Cy-3 secondary antibody (red). Co-localisation is shown in yellow. Nuclei were stained in blue with Hoechst.

To identify and demonstrate a potential direct interaction between  $\sigma_1$ -R and GHS-R1a, we developed BRET experiments, transfecting constant amounts of  $\sigma_1$ -R-Rluc (0.075  $\mu$ g) and increasing amounts of the cDNA for GHS-R1a-GFP<sup>2</sup> (0.5 to 3  $\mu$ g). A saturation BRET curve was obtained, thus indicating a specific interaction between the  $\sigma_1$ -R and GHS-R1a (BRET<sub>max</sub> 371 ± 38 mBU and BRET<sub>50</sub> 68 ± 23) (Figure R40A, black line). Contrarily, when adenosine A<sub>2A</sub>-R-GFP<sup>2</sup> (0.5 to 2.5  $\mu$ g) was used as negative control, a linear plot with low BRET values was obtained (Figure R40A, red line).



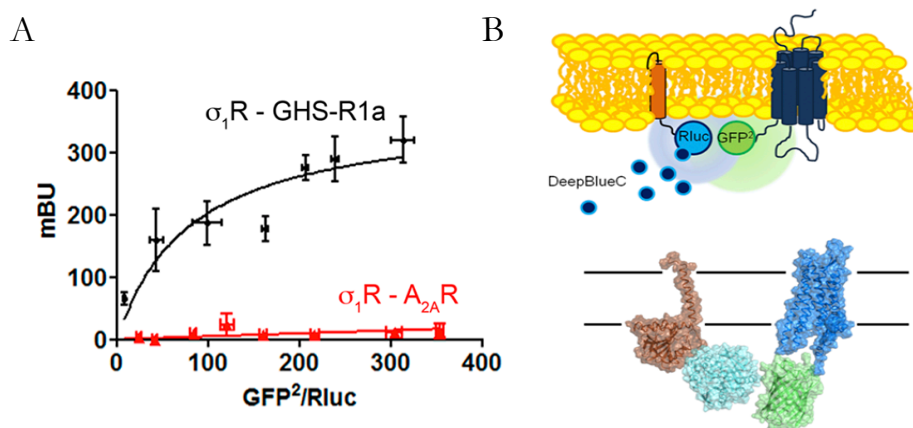


**Figure R40. BRET determination of GHS-R1a and  $\sigma_1$ -R interaction.** (A) BRET occurs in HEK-293T transfected cells with a constant amount of cDNA (0.075  $\mu$ g) for  $\sigma_1$ -R-Rluc and increasing amounts of GHS-R1a-GFP<sup>2</sup> (0.5 to 3  $\mu$ g) or A<sub>2A</sub>R-GFP<sup>2</sup> (0.5 to 2.5  $\mu$ g) as negative control. Values are the mean (in milliBRET units: mBU)  $\pm$  S.E.M. from 6 to 8 different experiments. (B) Scheme of the BRET<sup>2</sup> assay using  $\sigma_1$ -R-Rluc and GHS-R1a-GFP<sup>2</sup>.

#### IV.4.2 Quaternary structure of the heteromeric complex between $\sigma_1$ -R and GHS-R1a

We next addressed the quaternary structure of  $\sigma_1$ -R-GHS-R1a complexes, taking advantage of the recent publication of the crystal structure of  $\sigma_1$ -R in a trimeric receptor arrangement (*Schmidt et al., 2016*). The macromolecular complex cannot be understood without taking into account that the GHS-R1a receptor can form homomeric interactions with GHS-R1a and/or heteromeric interactions with GHS-R1b (*Chow et al., 2012; Mary et al., 2013*). Thus, to identify the TM interfaces involved in GHS-R1a-GHS-R1a homodimerization and GHS-R1a-GHS-R1b heterodimerization, as well as their TM interacting interfaces with  $\sigma_1$ -R, we used synthetic peptides with the amino acid sequence of individual TM domains 1 to 7 of GHS-R1a fused to the transactivator of transcription (TAT) peptide (Table R2). These cell-penetrating peptides interact with the TM domains of membrane proteins and can selectively disrupt interactions between proteins like GPCR protomers (*Hebert et al., 1996; Ng et al., 1996*). These peptides were first tested in HEK-293T cells expressing GHS-R1a-nYFP (0.75  $\mu$ g of cDNA) and GHS-R1a-cYFP (0.5  $\mu$ g) to explore whether BiFC occurs. Fluorescence complementation produced approximately read-outs of 4000 units, of indicative of the formation of GHS-R1a-homodimer complexes. Notably, in the presence of the interference peptides, we observed that the fluorescence decreased by two-fold only when TM5 or TM6 peptides were used (Figure R41A). These results pointed to the TM5/6 interface for GHS-R1a-GHS-R1a homodimerization. Similar results were obtained for GHS-R1a-GHS-R1b heterodimerization (TM 5/6 interface, Figure R41B), despite the fact that GHS-R1b lacks transmembrane domains 6 and 7 relative to GHS-R1a. Interestingly, when cells were

transfected with cDNA for GHS-R1a-nYFP, GHS-R1b-cYFP, and non-fused GHS-R1a, fluorescence was reduced in the presence of TM4, TM5 and TM6 peptides (Figure R41C). These results suggest an arrangement of protomers in which homodimerization of GHS-R1a occurs via the TM5/6 interfase, whereas heterodimerization of GHS-R1a and GHS-R1b occurs through the TM interface 4/5 (Figure R42A). The fluorescence decrease induced by the TM6 peptide of GHS-R1a (in addition to TM4 and TM5, Figure R42C) could indicate that this peptide also restricts the interactions with TM4 of GHS-R1b (Figure R42D).

TM1	APLLAGVTATSVALFVVGIAGNLLTMLVV-GRKKRRQRRR
TM2	RRRQRRKKRG-LYLSSMAFSDLLIFLSMPLDLV
TM3	FQFVSESSTYATVLTITALS-GRKKRRQRRR
TM4	RRRQRRKKRG-VKLVIFVIWAVAFSSAGPIFVL
TM5	LLTVMVWVSSIFFFCPVFSLTVLYSLI--GRKKRRQRRR
TM6	RRRQRRKKRG-MLAVVVFAFILCWLPFHVGRYLF
TM7	YCNVSFVLFYLSAAINPILYNIM-GRKKRRQRRR

**Table R2. Chemical structure of cell penetrating synthetic peptides.** Amino acid sequences of interference peptides corresponding with the amino acids of transmembrane domains of GHS-R1a fused to the transactivator of transcription (TAT) peptide (GRKKRRQRRR sequence) of the human immunodeficiency virus.

Next, we investigated the GHS-R1a TM domains involved in the interaction with  $\sigma_1$ -R. Remarkably, in the HEK-293T cells co-expressing GHS-R1a-nYFP (0.75  $\mu$ g) and  $\sigma_1$ -R-cYFP (0.5  $\mu$ g), fluorescence complementation (4000 units, which confirms the formation of GHS-R1a- $\sigma_1$ -R heteromers) was significantly reduced in the presence of TM1, TM2 or TM5 peptides; together with a marked tendency without statistical significance in the case of TM6 peptide (Figure R41D). This clearly indicated the existence of two different interacting interfaces between GHS-R1a and  $\sigma_1$ -R, involving either TM1/2 or TM5/6 interfaces of GHS-R1a and the single TM helix of  $\sigma_1$ -R. When similar experiments were performed with  $\sigma_1$ -R-cYFP (0.5  $\mu$ g) and GHS-R1b-nYFP (0.5  $\mu$ g), fluorescent signal (3500) units decreased in the presence of TM1 and TM2, but not with TM5 or TM6 (Figure R41E), due to the lack of TM 6 and TM 7 of GHS-R1b relative to GHS-R1a. All members of the GPCR family retain analogous tertiary structures at the seven-helical-bundle domain, thus, we hypothesised that TM1/2 or TM5/6 interfaces could be involved in the interaction between the GPCRs and  $\sigma_1$ -R. In addition, GPCR homo/heterodimerization must be taken into account to accommodate the  $\sigma_1$ -R in trimeric structure elucidated from structural studies. In order to achieve useful data in more physiological conditions, HEK-293T cells were transfected with cDNA for



GHS-R1a-nYFP and  $\sigma_1$ -R-cYFP in presence of non-fused GHS-R1b. In this case, the fluorescence complementation (5000 fluorescence units) was reduced only by TM1 and TM2 (Figure R41F), leading us to conclude that the formation of GHS-R1a-GHS-R1b heterotetramer via TM4/5 and TM5/6 (Figure R42A) only permits  $\sigma_1$ -R to interact with GHS-R1a via the free TM1/2 interface.

Using structural details of TM interfaces of GPCR oligomers (Cordomi *et al.*, 2015) and the crystal structure of the human  $\sigma_1$ -R (Schmidt *et al.*, 2016), together with the results from BiFC experiments in absence and presence of disrupting peptides, we constructed a computational molecular model of the GHS-R1a homodimer in complex with  $G_i$  protein and  $\sigma_1$ -R (Figure R42B). The model of the GHS-R1a homodimer contains two free TM4/5 interfaces that would allow binding of two GHS-R1b protomers (Figure R41F). However, the

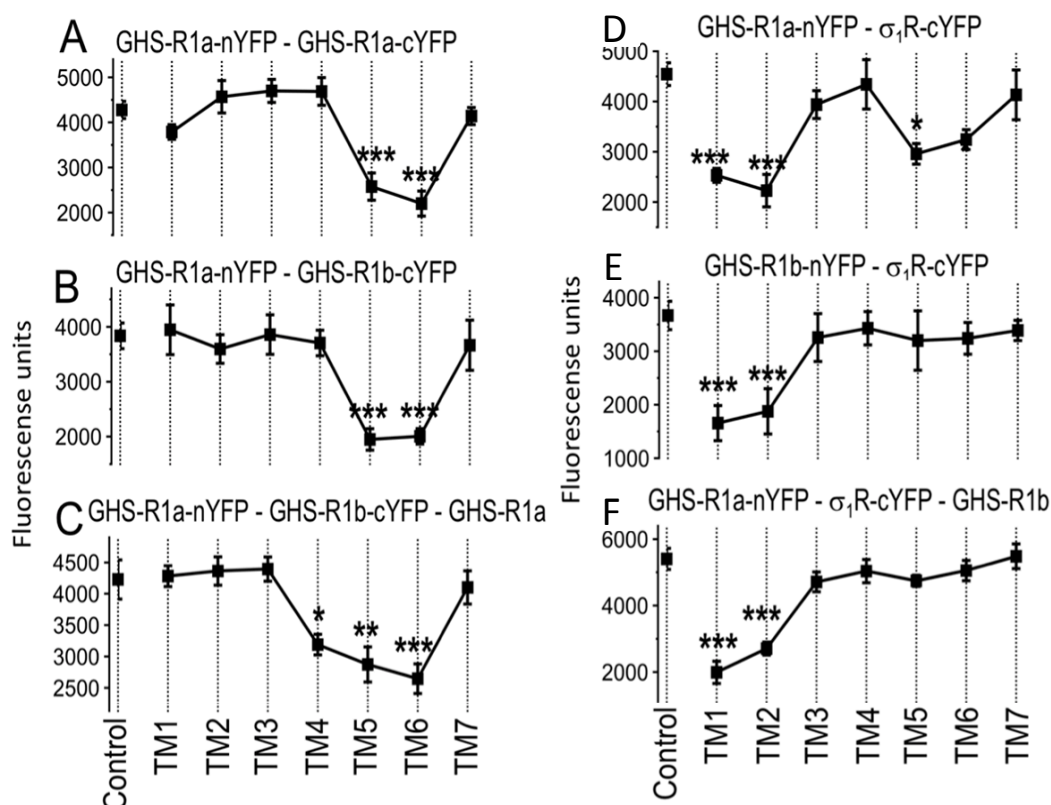


**Figure R41. BiFC complementation experiments in HEK-293T cells.** HEK-293T cells were transfected with GHS-R1a-nYFP (0.75  $\mu$ g) and GHS-R1a-cYFP (0.75  $\mu$ g) (A), GHS-R1a-nYFP (0.75  $\mu$ g) and GHS-R1b-cYFP (0.75  $\mu$ g) (B), GHS-R1a-nYFP (0.75  $\mu$ g) and GHS-R1b-cYFP (0.75  $\mu$ g) in presence of 1.5  $\mu$ g for GHS-R1a (C), GHS-R1a-nYFP (0.75  $\mu$ g) and  $\sigma_1$ -R-cYFP (0.75  $\mu$ g) (D), GHS-R1b-nYFP (0.5  $\mu$ g) and  $\sigma_1$ -R-cYFP (0.75  $\mu$ g) (E) and GHS-R1a-nYFP (0.75  $\mu$ g) and  $\sigma_1$ -R-cYFP (0.75  $\mu$ g) in the presence of GHS-R1b (1.5  $\mu$ g) (F). Prior to fluorescence determination, cells were treated with each of the interacting peptides (TM1 to TM7, 4  $\mu$ M) during 4 h. Values are the mean  $\pm$  S.E.M. from 6 to 8 different experiments. One-way ANOVA followed by Dunnett's post-hoc test showed a significant effect of treatments versus control conditions (\*,  $p < 0.05$ ; \*\*,  $p < 0.01$ ; \*\*\*,  $p < 0.001$ ).

$\sigma_1$ -R structural model is in favour of a homotrimer (*Schmidt et al., 2016*). Thus, accordingly to this fact, we constructed a computational model consisting of the GHS-R1a dimer, the  $\sigma_1$ -R trimer and a G protein that fits with the requirements of the biochemical data and takes into account all available structural constrains (Figure R41F). According to the experiments with GHS-R1a-derived peptides above described,  $\sigma_1$ -R can bind GHS-R1b through the TM1/2 interface and GHS-R1a through either TM1/2 or TM5/6 interfaces. Because GHS-R1a and GHS-R1b also employ TM5/6 interface for homo/heterodimerization, we assumed that at normal expression levels, TM1/2 is left as the only possible interface for the GHS-R1a- $\sigma_1$ -R

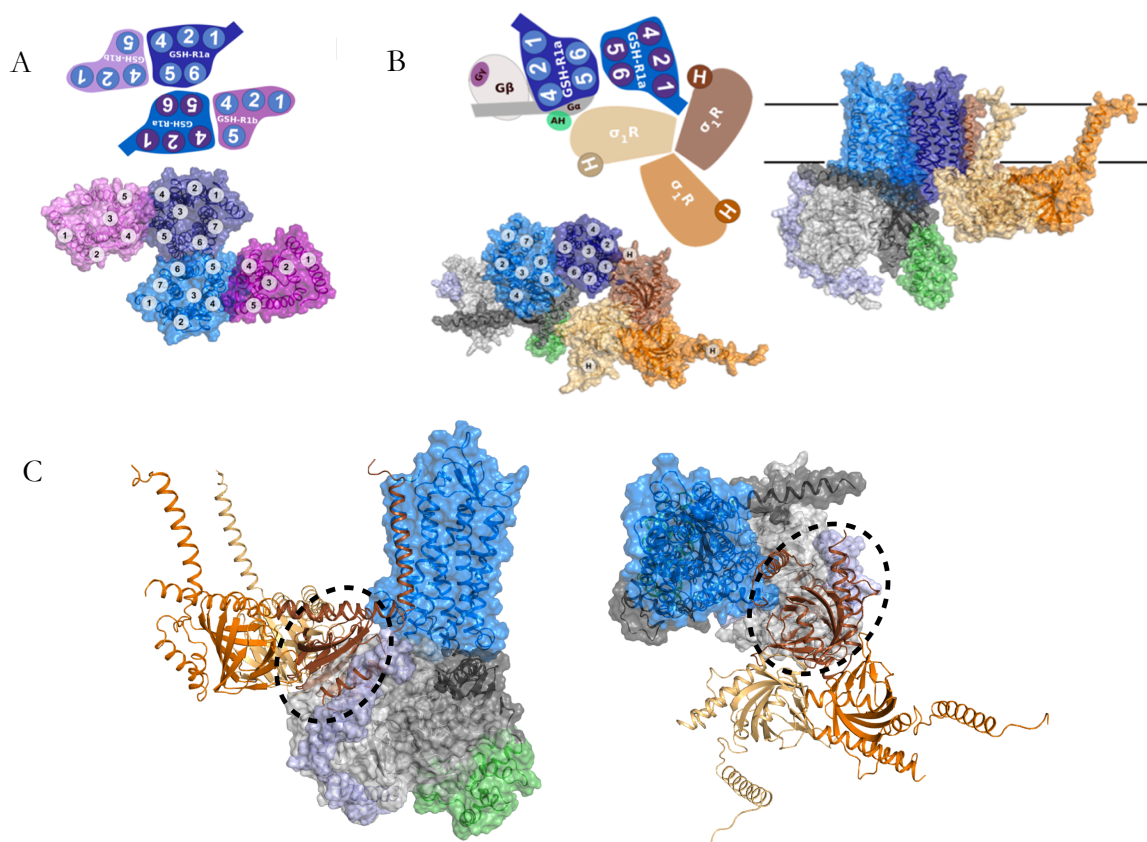


**Figure R42. Structural models of GHS-R1a-GHS-R1b and  $\sigma_1$ -R interactions.** (A) Structural model of the GHS-R1a-GHS-R1b heterotetramer (GHS-R1a protomers: blue, GHS-R1b protomers: purple) viewed from the extracellular side (scheme of the arrangement- top- and three-dimensional model (-bottom)). (B) At left, structural model consisting of a GHS-R1a homodimer (GHS-R1a G $\alpha$ -bound: light blue, GHS-R1a G $\alpha$ -unbound: dark blue) in complex with a  $\sigma_1$ -R homotrimer (in red, orange and yellow) coupled to Gi (G $\alpha$  Ras-like domain: light grey, G $\alpha$  alpha helical domain: green, G $\beta$ : dark grey and G $\gamma$ : purple) viewed from the extracellular side. At right, the same structural model viewed across the plane of the membrane. Proteins are displayed with a transparent surface and a cartoon. TM helices are indicated by circles (1-7 in GHS-R1a and H in  $\sigma_1$ -R). (C) Computational structural model viewed from the membrane illustrates that a GHS-R1a protomer bound to G $\alpha$  subunit of Gi cannot simultaneously bind  $\sigma_1$ -R via the TM 1/2 interface due to the steric clash between the intracellular voluminous C-terminal tail of  $\sigma_1$ -R. Proteins are displayed with a transparent surface and a cartoon, except  $\sigma_1$ -R which is displayed with a cartoon only. The colour code is: GHS-R1a (blue), Gi (G $\alpha$  Ras-like domain: light grey, G $\alpha$  alpha helical domain green, G $\beta$ : dark grey and G $\gamma$ : purple),  $\sigma_1$ -R heterotrimer (red, orange and yellow). The dashed ellipse outlines the regions that clash.



complex. This model indicates that a single GPCR protomer of GHS-R1a cannot simultaneously bind  $\sigma_1$ -R via the TM1/2 interface and a G protein due to a steric clash between the  $\beta\gamma$  subunits of  $G_i$  and the intracellular voluminous C-terminal tail of  $\sigma_1$ -R, containing a rigid cupin-like  $\beta$ -barrel fold that forms the buried ligand-binding site and the  $\beta\gamma$  subunits of  $G_i$  (Figure R42C). Thus, the minimal functional unit requires a GHS-R1a homodimer in which one protomer binds the G-protein and the second protomer is responsible for the binding of the  $\sigma_1$ -R TM helix (Figure R42B). Interestingly, this model predicts that the cytoplasmic domain of one protomer of the  $\sigma_1$ -R trimeric structure interacts with the  $\alpha$  subunit of  $G_i$ .

#### IV.4.3 Cocaine increased co-localisation of $\sigma_1$ -R and GHS-R1a at the cell surface

As cocaine binds  $\sigma_1$ -R (*Maurice and Romieu, 2004*), which establishes direct interactions with ghrelin receptors as shown above, we hypothesised if cocaine could affect ghrelin-mediated signals. Immunocytochemical assays were performed in cells expressing  $\sigma_1$ -R and GHS-R1a after the addition of cocaine (30  $\mu$ M for 30 minutes). Figure R43A shows that plasma membrane expression of  $\sigma_1$ -R increased when these cells were treated with a physiological relevant dose of cocaine. A similar increase was observed when cells were incubated with the  $\sigma_1$ -R agonist PRE-084 (100 nM for 30 min). The expression of GHS-R1a was not modified upon treatments with cocaine or PRE-084 but, interestingly, co-localisation of  $\sigma_1$ -R and GHS-R1a at the cell surface increased. Thus, cocaine and the  $\sigma_1$ -R specific ligand PRE-084 are able to concomitantly affect the co-expression of both receptors at the cell surface. Then, we evaluated the effect of cocaine and PRE-084 on the heteromerization of  $\sigma_1$ -R and GHS-R1a. The results in Figure R43B show the tendency to increase the energy transfer (without reaching statistical significance) between both receptors when 0.075  $\mu$ g of cDNA for  $\sigma_1$ -R-Rluc and 1.5  $\mu$ g GHS-R1a-GFP<sup>2</sup> transfected HEK-293T cells were in presence of cocaine (30  $\mu$ M) or PRE-084 (100 nM).

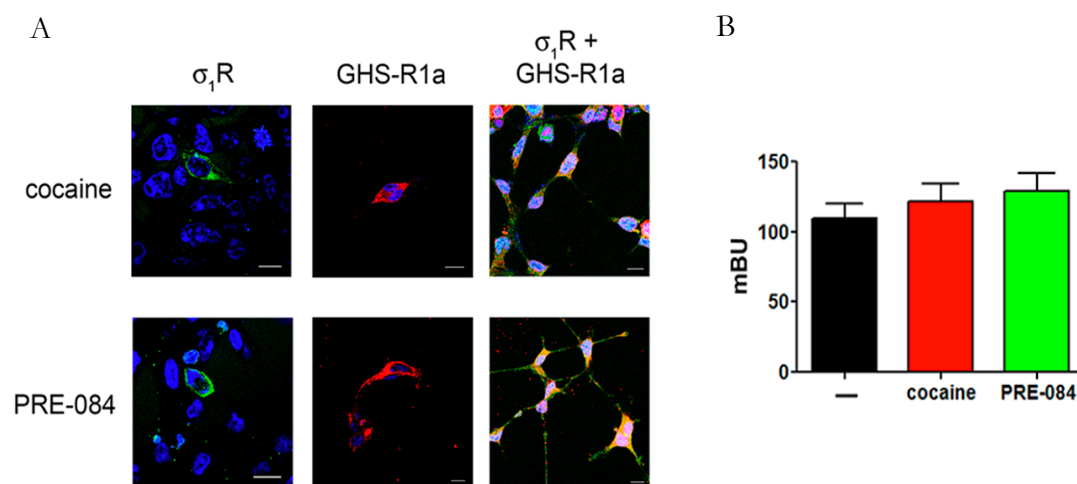


**Figure R43. Effects of cocaine and PRE-084 on GHS-R1a and  $\sigma_1$ -R interaction.** (A) HEK-293T cells transfected with 0.75  $\mu$ g cDNA for  $\sigma_1$ -R-YFP, 1.66  $\mu$ g cDNA for GHS-R1a or both were treated with 30  $\mu$ M cocaine or 100 nM PRE-084, then were monitored by the YFP fluorescence (green) or using a monoclonal anti-Rluc primary antibody and a Cy3 conjugated secondary antibody (red). Co-localisation is shown in yellow. Nuclei were stained with Hoechst (blue). Scale bar: 10  $\mu$ m. (B) BRET assay performed in HEK-293T cells transfected with 0.075  $\mu$ g of cDNA for  $\sigma_1$ -R-RLuc and 1.5  $\mu$ g of cDNA for GHS-R1a-GFP<sup>2</sup> treated with either 30  $\mu$ M cocaine, 100 nM PRE-084 or vehicle for 30 min. Afterwards, the energy transfer signals were measured. Values are the mean  $\pm$  S.E.M. of 7 different experiments. One-way ANOVA followed by Dunnett's *post-hoc* test did not show significant effects of treatment versus control.

#### IV.4.4 Cocaine inhibits GHS-R1a signalling

At first, we evaluated the effect of cocaine and PRE-084 on GHS-R1a-mediated signalling by measuring cAMP levels. HEK-293T cells endogenously express  $\sigma_1$ -R, but do not express ghrelin receptors. Moreover, it is known that low concentrations of GHS-R1b expression significantly increase GHS-R1a signalling. Thus to analyse GHS-R1a signalling pathways in HEK-293T cells, we co-expressed GHS-R1a (1.66  $\mu$ g of cDNA) with low amounts of GHS-R1b (0.25  $\mu$ g). Stimulation of these cells with ghrelin (100 nM) in the presence of forskolin (500 nM) significantly decreased cAMP levels (Figure R44A). This agrees with the previously reported coupling of GHS-R1a to  $G_i$ -proteins ([www.guidetopharmacology.org](http://www.guidetopharmacology.org)). The effect of ghrelin on forskolin-induced cAMP levels was completely blocked by pre-treatment with the GHS-R1a selective antagonist YIL-781 (2  $\mu$ M) (Figure R44A). Interestingly, when cells were treated either with cocaine (30  $\mu$ M, 15 min) or the  $\sigma_1$ -R agonist PRE-084 (100 nM, 15 min) prior to the ghrelin stimulation, the decrease in cAMP levels was prevented similarly to the GHS-R1a signalling blockade triggered by ghrelin receptor selective antagonist YIL-781 (Figure R44A). This suggests that cocaine





behaves as agonist of  $\sigma_1$ -R and inhibits GHS-R1a signalling as efficiently as the GHS-R1a antagonists.

Stimulation with ghrelin of HEK-293T cells transfected with GHS-R1a and GHS-R1b shows an increase of 80% over basal conditions (Figure R44B). Similarly to the cAMP measurements, the GHS-R1a antagonist YIL-781 and the  $\sigma_1$ -R agonists cocaine or PRE-084 inhibited the ghrelin effect (Figure R44B). This indicates that cocaine and PRE-084 not only affect the  $\alpha_i$ -dependent pathway, but also the signalling depending on  $\beta\gamma$  subunits. Moreover, a characteristic trace of intracellular calcium transient levels was obtained in HEK-293T cells expressing GHS-R1a, GHS-R1b and  $\sigma_1$ -R after activation with ghrelin (Figure R44C). Once again, the signalling was abrogated by the selective ghrelin antagonist and reduced by cocaine and PRE-084. Finally, to further test the inhibitory effect of agonist binding to  $\sigma_1$ -R in GHS-R1a, we performed Dynamic Mass Redistribution (DMR) recordings. Once again, the magnitude of the signalling by ghrelin significantly decreased in the presence of YIL-781,

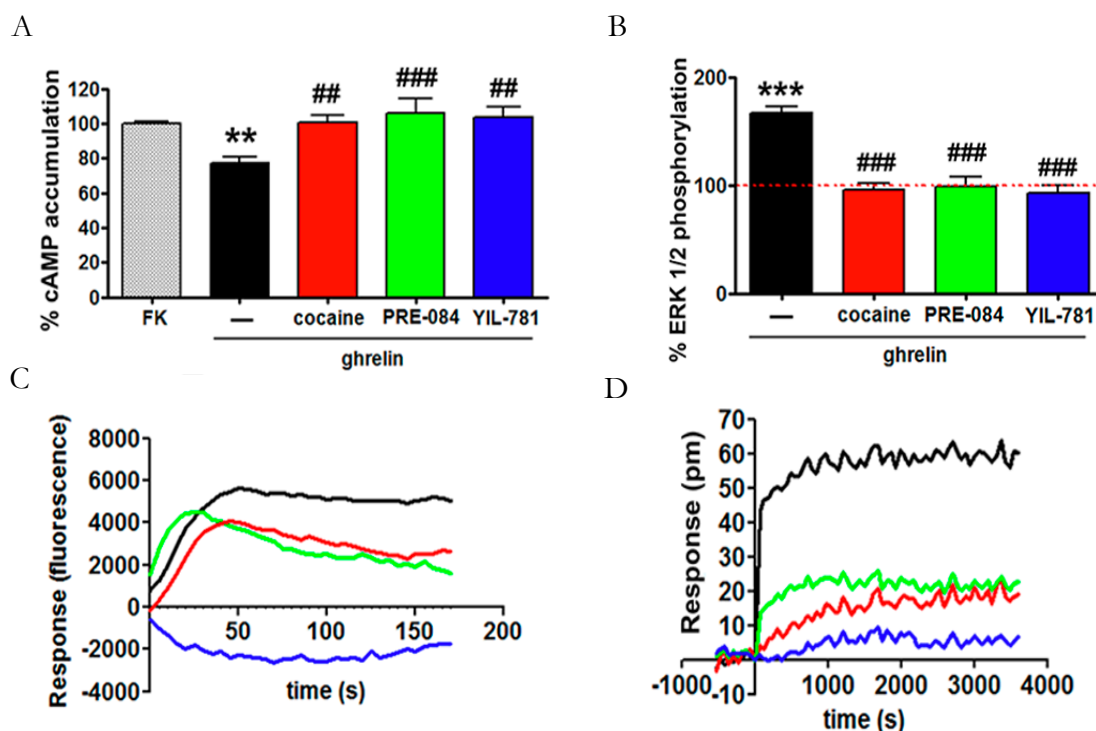


**Figure R44. Effects of cocaine on ghrelin-mediated signalling.** HEK-293T cells transfected with 1.66  $\mu\text{g}$  GHS-R1a cDNA and 0.25  $\mu\text{g}$  GHS-R1b cDNA were treated with 30  $\mu\text{M}$  cocaine (red), 2  $\mu\text{M}$  of the GHS-R1a antagonist YIL-781 (blue), 100 nM of  $\sigma_1$ -R agonist PRE-084 (green) or vehicle (black). Cells were then treated with 100 nM of ghrelin (in A, cells were also treated with 0.5  $\mu\text{M}$  forskolin (FK)) and cAMP levels (A), ERK1/2 phosphorylation (with the use of AlphaScreen® SureFit® kit (Perkin Elmer)), intracellular calcium mobilisation (employing the fluorescence of GCaMP6 sensor) or DMR label-free tracings analysed. Values are the mean  $\pm$  S.E.M. of 8 to 11 different experiments. One-way ANOVA followed by Dunnett's post-hoc test showed a significant effect of treatments versus forskolin (A) or control (B) (\*\*,  $p < 0.01$ ; \*\*\*,  $p < 0.001$ ) and a significant effect of treatments versus ghrelin (##,  $p < 0.01$ ; ###,  $p < 0.001$ )



cocaine and PRE-084 (Figure R44D). We can, thus, conclude that the GHS-R1a selective antagonist YIL-781, cocaine and PRE084 inhibited ghrelin effects, as measured by cAMP levels, ERK1/2 phosphorylation and DMR signal.

#### **IV.4.5 Cocaine inhibition of GHS-R1a signalling is mediated by $\sigma_1$ -R**

To check whether cocaine inhibition of ghrelin-induced signalling was due to its interaction with  $\sigma_1$ -R, HEK-293T cells expressing GHS-R1a (1.66  $\mu$ g of cDNA) and GHS-R1b (0.25  $\mu$ g) were transfected with a siRNA designed to knock-down the expression of  $\sigma_1$ -R (3  $\mu$ g of siRNA). Cells incorporating siRNA responded to 100 nM of ghrelin in both forskolin-induced cAMP determination and ERK1/2 phosphorylation (Figure R52A and B). However, while pre-treatment with YIL-781 blocked ghrelin-induced activation, neither cocaine nor PRE-084 had effect on ghrelin-induced signals, (Figure R45A and B). Also, the characteristic calcium mobilization (Figure R45C) and label-free recordings (Figure R45D) were not affected by cocaine or PRE-084 pre-treatment, while they were completely blocked by the ghrelin antagonist YIL-781 (Figure R45C and D). These results show that cocaine effects on GHS-R1a receptor are mediated by  $\sigma_1$ -R.

#### **IV.4.6 Disruption of the heteromeric complex between $\sigma_1$ -R and GHS-R1a by the TM1 interference peptide blocks the cocaine effect on GHS-R1a function**

The experiments using TAT-fused synthetic peptide above described show that the single TM helix of  $\sigma_1$ -R likely interacts with TM 1 and 2 of GHS-R1a. Accordingly, one may expect that addition of the TM1 interference peptide would abolish the effect of cocaine on GHS-R1a function. Thus, HEK-293T cells expressing GHS-R1a (1.66  $\mu$ g cDNA) were treated during 4 h with 4  $\mu$ M of TAT-TM1 (or TAT-TM7 as negative control). In agreement with our hypothesis, in the presence of TM1 peptide, only GHS-R1a selective antagonist YIL-781 (1  $\mu$ M) blocked the ghrelin (100 nM) stimulation, whereas cocaine (30  $\mu$ M) or PRE-084 (100 nM) did not display any effect on either cAMP levels (Figure R46) or DMR signals (Figure R47). Contrarily, cells treated with TM7 peptide displayed the  $\sigma_1$ -R-modulation of GHS-R1a upon binding of cocaine or PRE-084. These results demonstrate the involvement of TM1 in the GHS-R1a- $\sigma_1$ -R interaction, and the use of the TM1 peptides alter the cocaine effect on ghrelin receptors, thus reinforcing the idea that cocaine modulates GHS-R1a receptor via  $\sigma_1$ -R.



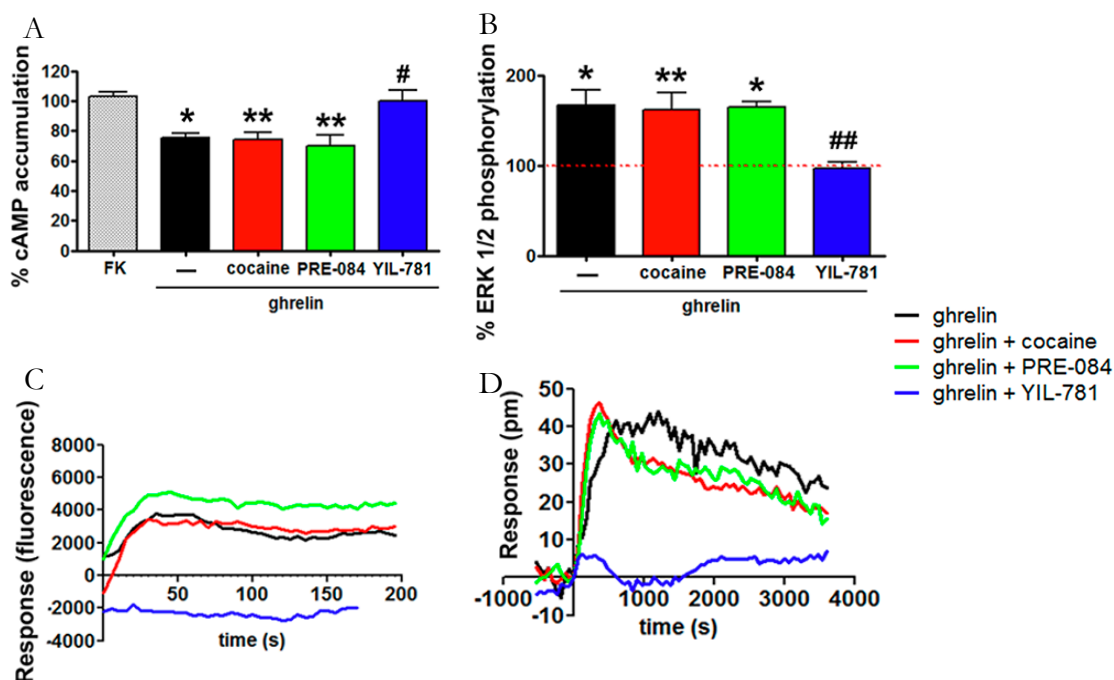


**Figure R45. Effects of cocaine on GHS-R1a signalling are dependent on  $\sigma_1$ R.** HEK-293T cells transfected with 1.66  $\mu$ g GHS-R1a cDNA, 0.25  $\mu$ g GHS-R1b cDNA and 3  $\mu$ g of siRNA for  $\sigma_1$ R were treated with 30  $\mu$ M cocaine (red), 2  $\mu$ M of the GHS-R1a antagonist YIL-781 (blue), 100 nM of  $\sigma_1$ -R agonist PRE-084 (green) or vehicle (black). Cells were then treated with 100 nM of ghrelin (in A, cells were also treated with 0.5  $\mu$ M forskolin (FK)) and cAMP levels (A), ERK1/2 phosphorylation, intracellular calcium mobilisation or DMR signals recorded. Values are the mean  $\pm$  S.E.M. of 8 to 11 different experiments. One-way ANOVA followed by Dunnett's post-hoc test showed a significant effect of treatments versus forskolin (A) or control (\*,  $p < 0.05$ ; \*\*,  $p < 0.01$ ) and a significant effect of treatments versus ghrelin (#,  $p < 0.05$ ; ##,  $p < 0.01$ ).

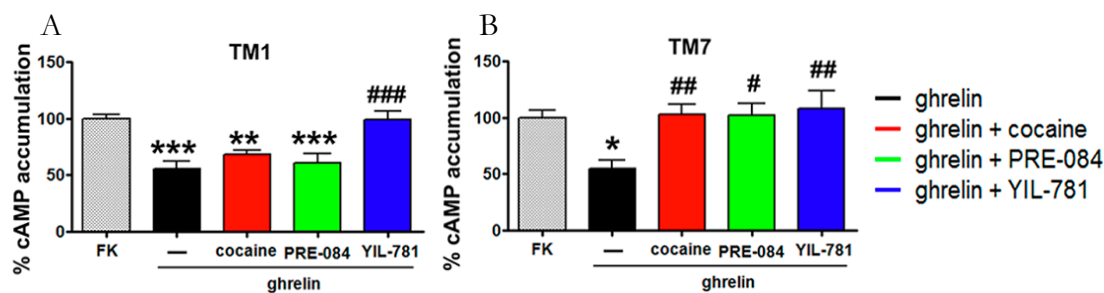


**Figure R46. Effects of TM peptides on cAMP GHS-R1a signalling.** HEK-293T cells expressing GHS-R1a (0.5  $\mu$ g) were treated for 4 h with TM1 (A) or TM7 (B) TAT-peptides. Cells were subsequently treated with 30  $\mu$ M cocaine (red), 100 nM PRE-084 (green), 1  $\mu$ M YIL-781 (blue) or vehicle (black). Then, cells were treated with 100 nM ghrelin and 0.5  $\mu$ M forskolin and cAMP levels measured. Values are the mean  $\pm$  S.E.M. of 6 different experiments. One-way ANOVA followed by Dunnett's *post-hoc* test showed significant effects of treatments versus forskolin (\*,  $p < 0.05$ ; \*\*,  $p < 0.01$ ; \*\*\*,  $p < 0.001$ ) and significant effects of treatments versus ghrelin (#,  $p < 0.05$ ; ##,  $p < 0.01$ ; ###,  $p < 0.001$ ).

Next, we attempted to provide deeper insight into the mechanism by which cocaine binds to  $\sigma_1$ -R and blocks GHS-R1a function. Our structural model predicts that a single protomer of GHS-R1a cannot simultaneously bind  $\sigma_1$ -R (via the TM1/2 interface) and  $G_i$  (Figure R42C). Accordingly,  $\sigma_1$ -R may impede  $G_i$  binding and in consequence GHS-R1a function. However, this does not seem reasonable due to the possible formation of GHS-R1a homodimer in which one protomer would bind  $G_i$  and the second protomer would bind the  $\sigma_1$ -R (Figure R42B). Notably, this model places the cytoplasmic domain of one protomer of the  $\sigma_1$ -R trimeric structure near to the  $\alpha$ -helical domain ( $\alpha$ AH) of the G-protein  $\alpha$ -subunit (Figure R49B). Due to the fact that the receptor-catalysed nucleotide exchange in G proteins involves a large-scale opening of  $\alpha$ AH to allow dissociation of the GDP (Dror *et al.*, 2015); the opening of  $\alpha$ AH is not feasible in the presence of the  $\sigma_1$ -R trimeric structure bound to TM1 and TM2 of GHS-R1a. Modification of the GHS-R1a- $\sigma_1$ -R interaction, by inserting the TAT-fused TM1 peptide, would increase the distance between cytoplasmic domain of  $\sigma_1$ -R and  $\alpha$ AH, facilitating  $G_i$  function as shown in our assays.

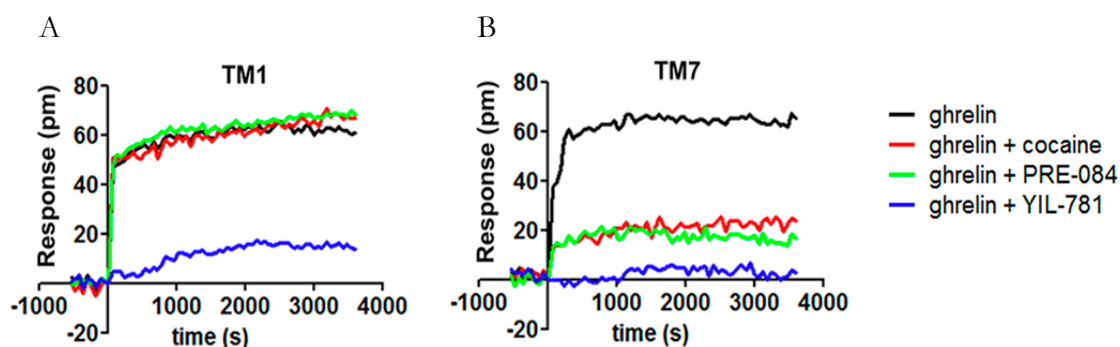


**Figure R47. Effects of TM TAT-peptides on DMR GHS-R1a signalling.** HEK-293T cells expressing GHS-R1a (0.5  $\mu$ g) were treated for 4 h with TM1 (A) or TM7 (B) TAT-peptides. Cells were subsequently treated with 30  $\mu$ M cocaine (red), 100 nM PRE-084 (green), 1  $\mu$ M YIL-781 (blue) or vehicle (black). Then, cells were treated with 100 nM ghrelin and DMR signals recorded. Traces representing DMR signal variation over time are represented.

#### IV.4.7 Effect of cocaine treatment on primary cultures of striatal neurons

Most of the cocaine effects in the central nervous system occur in the striatum (Borrotto-Escuela *et al.*, 2017; Joffe and Grueter, 2016). Consequently, we moved to primary cultures of striatal neurons to analyse in a more physiological environment the cocaine effects over GHS-R1a receptors. The *in situ* Proximity Ligation Assay (PLA) was used to identify GHS-R1a- $\sigma_1$ -R complexes (Figure R48A). In striatal primary cultures, the 43% of the cells presented red spots with 2 dots/cell-containing dots. However, when these cells were treated with 30  $\mu$ M cocaine



for 30 minutes, the number of cells containing red dots, and the number of dots per cell-containing dots increased significantly (54% of the cells with 3.2 dots/cell-containing dots). These results indicate that cocaine pre-treatment increases GHS-R1a-  $\sigma_1$ -R complexes in striatal primary cultures (Figure R48). Cocaine effects on GHS-R1a signalling were further analysed in primary cultures of striatal neurons in ERK1/2 phosphorylation assays. Cocaine and PRE-084 counteracted the ghrelin-induction of GHS-R1a signalling in a similar way as the

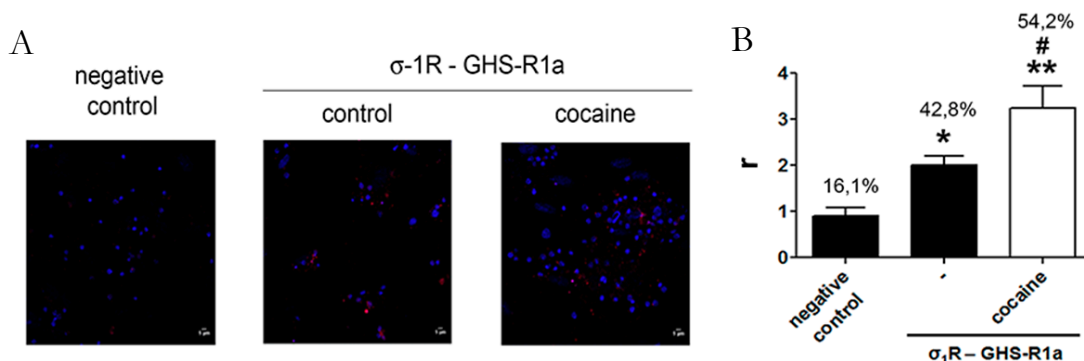


**Figure R48. Identification of GHS-R1a-  $\sigma_1$ -R heteromers in cocaine-treated primary neurons.** GHS-R1a- $\sigma_1$ R heteroreceptor complexes were identified in striatal primary cultures treated with 30  $\mu$ M cocaine, 100 nM PRE-084 or vehicle and detected by the use of a polyclonal anti- $\sigma_1$ R primary antibody and a polyclonal anti-GHS-R1a primary antibody in the presence of Hoechst. Then, cultures were treated with the PLA probes. (A) Representative PLA confocal images showing GHS-R1a-  $\sigma_1$ R complexes as red dots surrounding Hoechst-stained nuclei. Scale bar: 5  $\mu$ m. (B) Percentage of positive cells (containing one or more red dots, from cells in 5-6 different fields), and number (r) or red dots/cell-containing dots in primary cultures of striatal neurons. One-way ANOVA followed by Dunnett's post-hoc test showed a significant effect of treatments versus negative control (\*,  $p < 0.05$ ; \*\*,  $p < 0.01$ ) and a significant effect of treatments versus the untreated cells (#,  $p < 0.05$ ; ##,  $p < 0.01$ ).

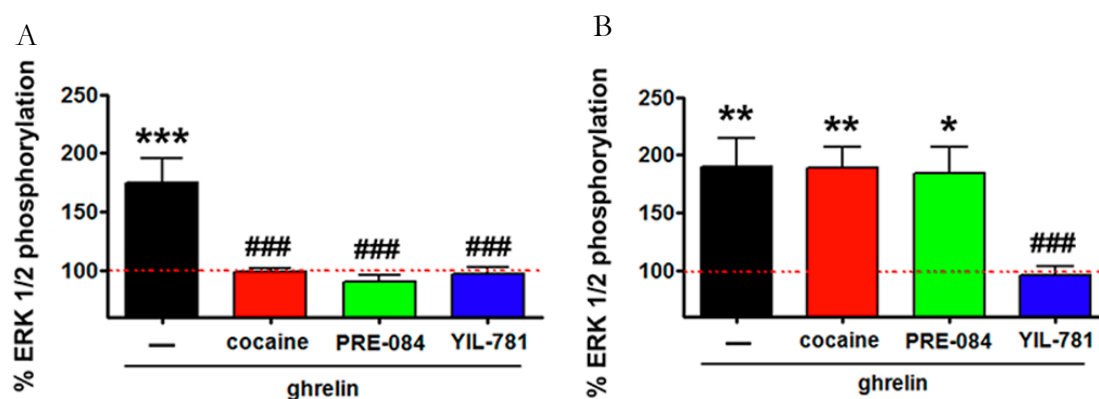


**Figure R49. Cocaine treatment inhibits GHS-R1a ERK1/2 signalling in primary cultures of striatal neurons.** Striatal primary neuron transfected (B) or not (A) with 3  $\mu$ g siRNA for  $\sigma_1$ R were treated with 30  $\mu$ M cocaine (red), 100 nM PRE-084 (green), 2  $\mu$ M of the GHS-R1a antagonist YIL-781 (blue) or vehicle (black) previous to a 100 nM ghrelin addition. ERK 1/2 phosphorylation was analysed using the AlphaScreen@SureFit@ kit. Values are mean  $\pm$  S.E.M. from 6 to 8 different experiments. One-way ANOVA followed by Dunnett's post-hoc test showed a significant effect of treatments versus control (\*,  $p < 0.05$ ; \*\*,  $p < 0.01$ , \*\*\*,  $p < 0.001$ ) and a significant effect of treatments versus ghrelin (#,  $p < 0.05$ ; ###,  $p < 0.001$ ).

GHS-R1a antagonist YIL-781 (Figure R49A). Such effect of cocaine was related to  $\sigma_1$ -R modulation of GHS-R1a, as in striatal primary cultures treated with siRNA for  $\sigma_1$ -R, neither cocaine nor PRE-084 exerted any significant effect (Figure R49B).

#### IV.4.8 Effects of cocaine administration on GHS-R1a- $\sigma_1$ -R heteromer expression in striatal sections from naïve and cocaine-treated animals

Rats following an i.p. administration of 15 mg/kg cocaine treatment for 1 (acute) or 14 (chronic) days, were sacrificed and 30  $\mu$ m-thick striatal sections were obtained from each group of animals and from vehicle-treated animals. *In situ* PLA was used to identify GHS-R1a- $\sigma_1$ -R heteroreceptor complexes (Figure 50A).

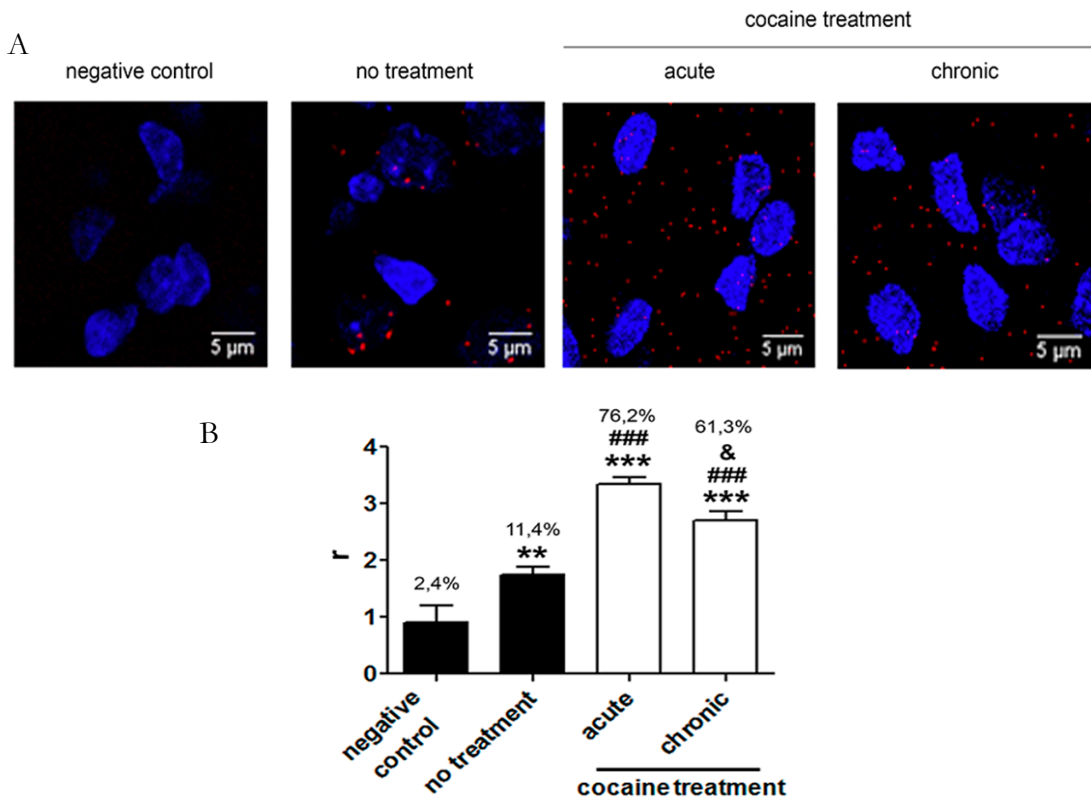


**Figure R50. Acute and chronic cocaine treatment increase the GHS-R1a- $\sigma_1$ -R heteromers expression in the rat striatum.** Male Sprague Dawley rats were i.p. administered with vehicle (control) or 15mg/kg cocaine for 1 (acute) or 14 (chronic) days. To identify  $\sigma_1$ -R-GHS-R1a complexes from each condition, rats were sacrificed and 30  $\mu$ m-thick striatal sections were obtained and treated with a polyclonal anti- $\sigma_1$ -R primary antibody and a polyclonal anti-ghrelin antibody in the presence of Hoechst and treated with the PLA probes. Representative PLA confocal images showing GHS-R1a- $\sigma_1$ -R complexes as red dots surrounding Hoechst-stained nuclei are shown for each condition (A). Scale bar: 5  $\mu$ m. Percentage of positive cells (containing one or more red dots; from cells in 4-6 different fields), and number ( $r$ ) or red dots/cell-containing dots in rat striatal sections. One-way ANOVA followed by Dunnett's post-hoc test showed a significant effect of treatments versus negative control (\*,  $p < 0.05$ ; \*\*,  $p < 0.01$ ), a significant effect of treatments versus the untreated cells (#,  $p < 0.05$ ) and a significant effect of chronic treatment versus acute treated sections (&,  $p < 0.05$ ).

When striatal sections of vehicle-treated animals were analysed, an 11% of cells displaying red dots with 1.6 dots/cell-containing dots were observed, indicating that around 10% of striatal cells expressed GHS-R1- $\sigma_1$ -R complexes. Interestingly, in the case of the chronic treatment, the number of the cells containing dots increased to 61%, and the number of dots/cell-containing dots also increased to 2.7. Both results are significantly higher when compared to control cells. Remarkably, the cocaine acute treatment led to values that were even higher than in the chronic condition (76% of the cells containing dots and 3.2 dots/cell-containing dots). These results indicate that cocaine treatment modulated GHS-R1a- $\sigma_1$ -R complex formation in striatal sections with a maximum increase in the heteromer formation found in acute conditions (Figure R50).

#### IV.4.9 Discussion

Due to its capability to interact with drugs of abuse, further knowledge about the structure and function of  $\sigma_1$ R is needed. To date,  $\sigma_1$ R has not been associated with a specific signalling machinery, although regulatory and modulatory actions of the receptor upon protein-protein interactions have been described (*Su et al., 2016; Wu and Bowen, 2008*). For instance,  $\sigma_1$ R has been related to the negative control that N-methyl-D-aspartate acid glutamate receptors (NMDARs) exert on opioid antinociception (*Rodríguez-Muñoz et al., 2015*). Thus,  $\sigma_1$ R antagonists would enhance antinociception and reduce the neuropathic pain induced by  $\mu$ -opioid receptors. Additionally, since the demonstration that cocaine binds to  $\sigma_1$ R even at doses attained at recreational use,  $\sigma_1$ R has been proposed to mediate locomotor activation (*Barr et al., 2015; Menkel et al., 1991*), seizures (*Matsumoto et al., 2001*), drug sensitisation (*Ujike et al., 1996*) or reward actions (*Romieu et al., 2000, 2002*) of the drug. Interestingly, reduction of  $\sigma_1$ R levels by antisense nucleotide injections, results in attenuated convulsive effects of the drug (*Matsumoto et al., 2002*), whereas, cocaine binding on  $\sigma_1$ R is capable of disrupting the orexin-1 receptor-corticotropin releasing factor receptor 1 heteromer promoting seeking behaviour and relapse (*Navarro et al., 2015*). Remarkably, the results presented in this chapter 4 disclose the underlying mechanisms through which  $\sigma_1$ R could mediate the hunger-suppressive actions of cocaine.

The nucleus accumbens, one of the striatal structures, is a key region within the CNS reward system. Activation of this system in response to food intake produces a pleasant sensation that helps in mammalian survival (*Kim and Hikosaka, 2015*). It should be noted that in these mesolimbic areas, GHS-R1a is co-expressed in neurons with the cocaine-sensitive

$\sigma_1$ R. From both mechanistic and molecular points of views, the results of this chapter highlight an interaction between  $\sigma_1$ R and GHS-R1a that is translated into a strong inhibition of the ghrelin-induced signalling pathways. It is shown that, in both transfected HEK-293T cells and in striatal primary cultures of neurons, a pre-treatment with  $\sigma_1$ R agonists cocaine or PRE-084 inhibits the ghrelin-mediated signalling in a similar manner than the inhibition produced by the GHS-R1a antagonist YIL-781. The implication of  $\sigma_1$ R in this inhibition is confirmed by the results obtained in  $\sigma_1$ R-siRNA treated cells, where cocaine or PRE-084 had no effect on ghrelin-induced signals, while the ghrelin receptor antagonist YIL-781 maintained its effect.

Kotagale and collaborators (*Kotagale et al., 2014*) have described the potent orexigenic effects of neuropeptide Y (NPY), which was described as the possible endogenous ligand for a subpopulation of sigma receptors, thus linking the stimulation of sigma receptors with hunger (*Roman et al., 1989*). However, no high binding affinity of NPY to brain  $\sigma_1$ R could be detected (*Tam and Mitchell, 1991*). Our results show that cocaine binding to  $\sigma_1$ R could counteract the feeling of hunger by a mechanism that excludes a direct competition between cocaine and NPY to interact with  $\sigma_1$ R. Moreover, it has been described that upon binding with cocaine,  $\sigma_1$ R is able to up-regulate  $D_1$ R signalling (*Navarro et al., 2010b*) while counteracting the effects of  $D_2$ R activation (*Navarro et al., 2013*). Altogether, it seems that  $\sigma_1$ R mediates the cocaine effects via several GPCR of the reward pathway, to overall, generate the seeking behaviour that favours and consumption of the drug, while reducing hunger upon interaction with GHS-R1a. Additionally, the results shown in this chapter 4 indicate that GHS-R1a- $\sigma_1$ R heteromer expression is increased in both acute and chronic cocaine administration. However, the effect was more marked in acute conditions. In fact, striatal sections of Sprague-Dawley rats injected for one day with 15 mg/kg cocaine displayed three-fold higher expression of  $\sigma_1$ R-GHS-R1a heteromers than control animals. Taking into account recent findings in the laboratory, it appears that  $D_1$ R could interact with either  $\sigma_1$ R or  $\sigma_2$ R, with a  $D_1$ R- $\sigma_1$ R heteromer predominance in acute cocaine consumption and increased  $D_1$ R- $\sigma_2$ R interactions in the chronic administrations of the drug (*Aguinaga et al., 2018*). It may be speculated that GHS-R1a would be undergoing a similar differential interaction between  $\sigma_1$ R- and  $\sigma_2$ R-interactions depending on the regime of the cocaine consumption.

Finally, in silico approaches using the structure of the receptor suggested that  $\sigma_1$ R consisted of two TM helical domains. However, the recently released crystal structure of  $\sigma_1$ R

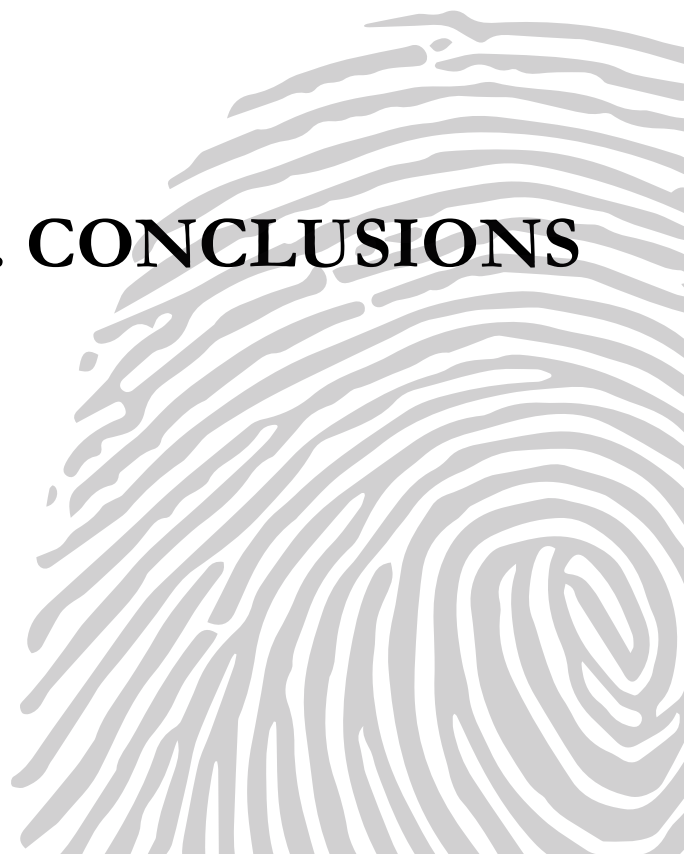




has shown a single TM domain and a C-terminal tail having a buried ligand-binding site and that the receptor arranges into homotrimers (*Schmidt et al., 2016*). Using TAT-fused synthetic peptides together with BiFC assays, we have been able to show that the single TM helix of  $\sigma_1$ R can be recognised by two different interacting interfaces of the 7TM bundle of GPCRs, either by TMs 1/2 or TMs 5/6 interfaces. Oligomerization of GPCRs via particular interface likely guides the interacting interface in the  $\sigma_1$ R. In the particular case of  $\sigma_1$ R-GHS-R1a, due to the formation of the GHS-R1a-GHS-R1b heterotetramer via TM 4/5 interface of GHS-R1b and TM 5/6 of GHS-R1a,  $\sigma_1$ R can interact with GHS-R1a via the free TM 1/2 interface. Additionally, it can be speculated that two additional TM helices in the  $\sigma_1$ R homotrimer can establish further interactions with GHS-R1a-GHS-R1b heteromers. Such macromolecular clusters may form specialised machineries for  $\sigma_1$ R mediated regulation.



## **V. CONCLUSIONS**



## CONCLUSIONS

## V. CONCLUSIONS

The conclusions derived from the results of the Chapter 1 of this thesis, corresponding with the aim 1; **to investigate the role of CB<sub>1</sub> and CB<sub>2</sub> receptors and the CB<sub>1</sub>-CB<sub>2</sub> receptor heteromer in different activation microglial phenotypes**, are:

- The CB<sub>2</sub>R expression levels are enhanced in primary microglia or in microglial cell lines activated using LPS and INF- $\gamma$ .
- The expression of the CB<sub>1</sub>-CB<sub>2</sub> receptor heteromer is increased in the microglial-derived N9 cells when activated with LPS and INF- $\gamma$ . The negative cross-talk between CB<sub>1</sub> and CB<sub>2</sub> observed in ‘resting’ conditions transforms into a potentiation of the receptors’ signalling in activated microglia.
- The CB<sub>1</sub>-CB<sub>2</sub> receptor heteromer is expressed in activated microglia in Parkinson’s disease and Alzheimer’s disease animal models. Remarkably, primary cultures of microglia obtained from the APP<sub>Sw,Ind</sub> mice model of Alzheimer’s disease displayed the activated phenotype in what concerns both the effect of cannabinoids and in the expression of the CB<sub>1</sub>-CB<sub>2</sub> receptor heteromers.

The conclusions derived from the results of the Chapter 2 of this thesis, which correspond with the aim 2 of this thesis, **to identify interactions between CB<sub>1</sub>R and the EF-hand domain-containing calcium proteins and their functional consequences**, are:

- The CB<sub>1</sub>R interacts with calneuron1 and NCS1 but not with caldendrin. The 3<sup>rd</sup> intracellular loop of the CB<sub>1</sub>R is involved in the interaction with calneuron1 and NCS1, while mutations at the C-terminal domain of the CB<sub>1</sub>R abolished the interaction with NCS1. The membrane-anchoring domain of calneuron1 and the N-terminal myristoylated domain of NCS1 are implicated in the interaction with the CB<sub>1</sub>R.



## CONCLUSIONS

- The increase in intracellular calcium levels leads to a predominant CB<sub>1</sub>R-calneuron1 interaction whereas at basal calcium levels the main interaction of the receptor is with NCS1.
- Remarkably, the increase in intracellular calcium in cultures of striatal neurons abolishes the canonical CB<sub>1</sub>R- mediated reduction of intracellular cAMP levels.

The conclusions inferred from aim 3 of the thesis: **to give insight into the functional role of the alternatively-spliced truncated form of the ghrelin receptor gene product** are:

- GHS-R1b modulates GHS-R1a trafficking and signalling depending on the specific GHS-R1b/GHS-R1a expression ratio. Low GHS-R1b/GHS-R1a expression ratios favour the trafficking of GHS-R1a towards the membrane, while in high GHS-R1b/ GHS-R1a expression levels, the truncated ghrelin receptor isoform exerts a negative allosteric regulation of GHS-R1a.
- The dimerization of GHS-R1b and GHS-R1a, with a consequential increase of the GHS-R1a at the plasma membrane determines the capacity of GHS-R1a to interact with other receptors like the dopamine receptor D<sub>1</sub>.
- The heteromerization of GHS-R1a, GHS-R1b and D<sub>1</sub>R produce a switch in the GHS-R1a signalling to Gs protein, radically altering the ghrelin receptor-mediated signalling.

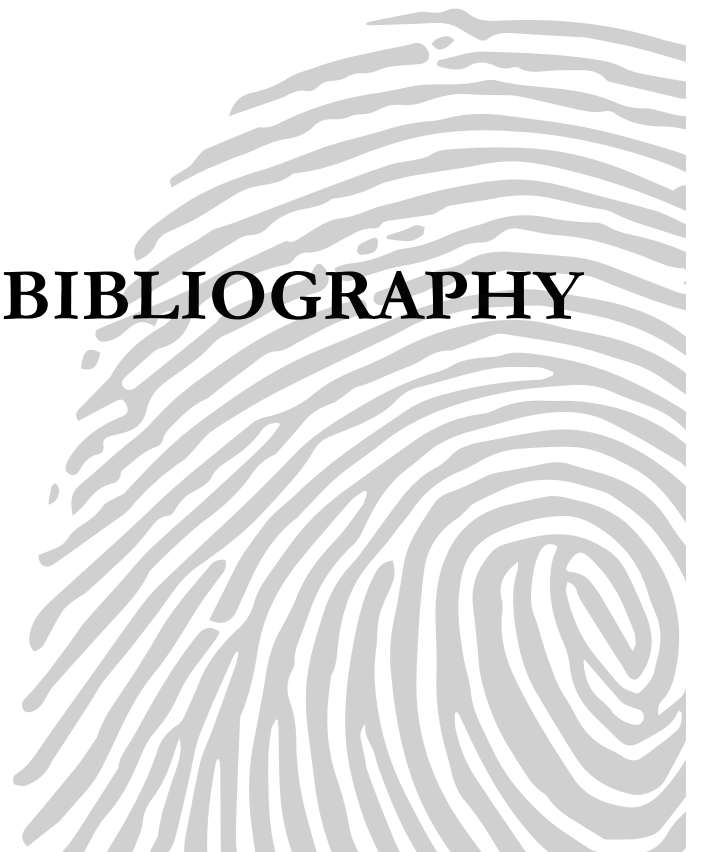
The conclusions derived from the results of the Chapter 4, which corresponds with the aim 4 of the thesis: **to investigate direct and indirect interactions between sigma-1 receptor and ghrelin receptor and to determinate the modulatory role of cocaine on the function of sigma-1-ghrelin receptor complexes**, are:

- Resonance energy transfer assays and confocal microscopy approaches show that GHS-R1a and sigma-1-receptors form macromolecular complexes in both transfected cell lines and in neuronal primary cultures.
- In the GHS-R1a-GHS-R1b-sigma-1 receptor macromolecular complex, GHS-R1a homodimers interact between each other through transmembrane domains 5 and 6, while GHS-R1a and GHS-R1b interfaces of interaction are transmembrane domains 4 and 5. Finally, GHS-R1a interacts through transmembrane domains 1 and 2 with the sigma-1 receptor trimeric complex.
- Upon interaction with cocaine, sigma-1 receptor blocks, in both transfected cells and striatal neurons, ghrelin-activated GHS-R1a cAMP signalling, the ERK1/2 phosphorylation and the intracellular calcium mobilisation.



## CONCLUSIONS

## **VI. BIBLIOGRAPHY**





BIBLIOGRAPHY

**VI. BIBLIOGRAFY**

Abadji, V., Lucas-Lenard, J.M., Chin, C., and Kendall, D.A. (1999). Involvement of the carboxyl terminus of the third intracellular loop of the cannabinoid CB1 receptor in constitutive activation of Gs. *J. Neurochem.* *72*, 2032–2038.

Abizaid, A., and Horvath, T.L. (2008). Brain circuits regulating energy homeostasis. *Regul. Pept.* *149*, 3–10.

Abizaid, A., Liu, Z.-W., Andrews, Z.B., Shanabrough, M., Borok, E., Elsworth, J.D., Roth, R.H., Sleeman, M.W., Picciotto, M.R., Tschöp, M.H., et al. (2006). Ghrelin modulates the activity and synaptic input organization of midbrain dopamine neurons while promoting appetite. *J. Clin. Invest.* *116*, 3229–3239.

Adamantidis, A.R., Tsai, H.-C., Boutrel, B., Zhang, F., Stuber, G.D., Budygin, E.A., Touriño, C., Bonci, A., Deisseroth, K., and de Lecea, L. (2011). Optogenetic interrogation of dopaminergic modulation of the multiple phases of reward-seeking behavior. *J. Neurosci. Off. J. Soc. Neurosci.* *31*, 10829–10835.

Aguinaga, D., Medrano, M., Vega-Quiroga, I., Gysling, K., Canela, E.I., Navarro, G., and Franco, R. (2018). Cocaine Effects on Dopaminergic Transmission Depend on a Balance between Sigma-1 and Sigma-2 Receptor Expression. *Front. Mol. Neurosci.* *11*, 17.

Ahmed, I.S., Rohe, H.J., Twist, K.E., and Craven, R.J. (2010). Pgrmc1 (progesterone receptor membrane component 1) associates with epidermal growth factor receptor and regulates erlotinib sensitivity. *J. Biol. Chem.* *285*, 24775–24782.

Ainscough, J.S., Gerberick, G.F., Kimber, I., and Dearman, R.J. (2015). Interleukin-1 $\beta$  Processing Is Dependent on a Calcium-mediated Interaction with Calmodulin. *J. Biol. Chem.* *290*, 31151–31161.

## BIBLIOGRAPHY

Alonso, G., Phan, V., Guillemain, I., Saunier, M., Legrand, A., Anoaï, M., and Maurice, T. (2000). Immunocytochemical localization of the sigma(1) receptor in the adult rat central nervous system. *Neuroscience* 97, 155–170.

Al-Saif, A., Al-Mohanna, F., and Bohlega, S. (2011). A mutation in sigma-1 receptor causes juvenile amyotrophic lateral sclerosis. *Ann. Neurol.* 70, 913–919.

Angulo, E., Casadó, V., Mallol, J., Canela, E.I., Viñals, F., Ferrer, I., Lluís, C., and Franco, R. (2003). A1 adenosine receptors accumulate in neurodegenerative structures in Alzheimer disease and mediate both amyloid precursor protein processing and tau phosphorylation and translocation. *Brain Pathol. Zurich Switz.* 13, 440–451.

Aron Badin, R., Spinnewyn, B., Gaillard, M.-C., Jan, C., Malgorn, C., Van Camp, N., Dollé, F., Guillermier, M., Boulet, S., Bertrand, A., et al. (2013). IRC-082451, a novel multitargeting molecule, reduces L-DOPA-induced dyskinesias in MPTP Parkinsonian primates. *PloS One* 8, e52680.

Ashton, J.C., and Glass, M. (2007). The cannabinoid CB2 receptor as a target for inflammation-dependent neurodegeneration. *Curr. Neuropharmacol.* 5, 73–80.

Aso, E., and Ferrer, I. (2014). Cannabinoids for treatment of Alzheimer's disease: moving toward the clinic. *Front. Pharmacol.* 5, 37.

Atwood, B.K., and Mackie, K. (2010). CB2: a cannabinoid receptor with an identity crisis. *Br. J. Pharmacol.* 160, 467–479.

Baldwin, J.M. (1994). Structure and function of receptors coupled to G proteins. *Curr. Opin. Cell Biol.* 6, 180–190.

Balenga, N.A., Martínez-Pinilla, E., Kargl, J., Schröder, R., Peinhaupt, M., Platzer, W., Bálint, Z., Zamarbide, M., Dopeso-Reyes, I.G., Ricobaraza, A., et al. (2014). Heteromerization of GPR55 and cannabinoid CB2 receptors modulates signalling. *Br. J. Pharmacol.* 171, 5387–5406.



- Baltoumas, F.A., Theodoropoulou, M.C., and Hamodrakas, S.J. (2016). Molecular dynamics simulations and structure-based network analysis reveal structural and functional aspects of G-protein coupled receptor dimer interactions. *J. Comput. Aided Mol. Des.* *30*, 489–512.
- Banères, J.-L., and Parello, J. (2003). Structure-based analysis of GPCR function: evidence for a novel pentameric assembly between the dimeric leukotriene B4 receptor BLT1 and the G-protein. *J. Mol. Biol.* *329*, 815–829.
- Bariselli, S., Glangetas, C., Tzanoulinou, S., and Bellone, C. (2016). Ventral tegmental area subcircuits process rewarding and aversive experiences. *J. Neurochem.* *139*, 1071–1080.
- Barnum, C.J., Eskow, K.L., Dupre, K., Blandino, P., Deak, T., and Bishop, C. (2008). Exogenous corticosterone reduces L-DOPA-induced dyskinesia in the hemi-parkinsonian rat: role for interleukin-1beta. *Neuroscience* *156*, 30–41.
- Barr, J.L., Deliu, E., Brailoiu, G.C., Zhao, P., Yan, G., Abood, M.E., Unterwald, E.M., and Brailoiu, E. (2015). Mechanisms of activation of nucleus accumbens neurons by cocaine via sigma-1 receptor-inositol 1,4,5-trisphosphate-transient receptor potential canonical channel pathways. *Cell Calcium* *58*, 196–207.
- Bayburt, T.H., Leitz, A.J., Xie, G., Oprian, D.D., and Sligar, S.G. (2007). Transducin activation by nanoscale lipid bilayers containing one and two rhodopsins. *J. Biol. Chem.* *282*, 14875–14881.
- Belin, D., and Everitt, B.J. (2008). Cocaine seeking habits depend upon dopamine-dependent serial connectivity linking the ventral with the dorsal striatum. *Neuron* *57*, 432–441.
- Benito, C., Núñez, E., Tolón, R.M., Carrier, E.J., Rábano, A., Hillard, C.J., and Romero, J. (2003). Cannabinoid CB2 receptors and fatty acid amide hydrolase are selectively overexpressed in neuritic plaque-associated glia in Alzheimer's disease brains. *J. Neurosci. Off. J. Soc. Neurosci.* *23*, 11136–11141.
- Benkirane, M., Jin, D.Y., Chun, R.F., Koup, R.A., and Jeang, K.T. (1997). Mechanism of transdominant inhibition of CCR5-mediated HIV-1 infection by ccr5delta32. *J. Biol. Chem.*



## BIBLIOGRAPHY

272, 30603–30606.

Bennett, K.A., Langmead, C.J., Wise, A., and Milligan, G. (2009). Growth hormone secretagogues and growth hormone releasing peptides act as orthosteric super-agonists but not allosteric regulators for activation of the G protein Galpha(o1) by the Ghrelin receptor. *Mol. Pharmacol.* 76, 802–811.

Berardi, F., Abate, C., Ferorelli, S., Uricchio, V., Colabufo, N.A., Niso, M., and Perrone, R. (2009). Exploring the importance of piperazine N-atoms for sigma(2) receptor affinity and activity in a series of analogs of 1-cyclohexyl-4-[3-(5-methoxy-1,2,3,4-tetrahydronaphthalen-1-yl)propyl]piperazine (PB28). *J. Med. Chem.* 52, 7817–7828.

Berchtold, M.W., and Villalobo, A. (2014). The many faces of calmodulin in cell proliferation, programmed cell death, autophagy, and cancer. *Biochim. Biophys. Acta* 1843, 398–435.

Berger, C., Schmid, P.C., Schabitz, W.-R., Wolf, M., Schwab, S., and Schmid, H.H.O. (2004). Massive accumulation of N-acylethanolamines after stroke. Cell signalling in acute cerebral ischemia? *J. Neurochem.* 88, 1159–1167.

Berridge, M.J. (1998). Neuronal calcium signaling. *Neuron* 21, 13–26.

Berthouze, M., Rivail, L., Lucas, A., Ayoub, M.A., Russo, O., Sicsic, S., Fischmeister, R., Berque-Bestel, I., Jockers, R., and Lezoualc'h, F. (2007). Two transmembrane Cys residues are involved in 5-HT4 receptor dimerization. *Biochem. Biophys. Res. Commun.* 356, 642–647.

Beuming, T., Kniazeff, J., Bergmann, M.L., Shi, L., Gracia, L., Raniszewska, K., Newman, A.H., Javitch, J.A., Weinstein, H., Gether, U., et al. (2008). The binding sites for cocaine and dopamine in the dopamine transporter overlap. *Nat. Neurosci.* 11, 780–789.

Bilkei-Gorzo, A. (2012). The endocannabinoid system in normal and pathological brain ageing. *Philos. Trans. R. Soc. Lond. B. Biol. Sci.* 367, 3326–3341.

Blasiolo, B., Kabbani, N., Boehmler, W., Thisse, B., Thisse, C., Canfield, V., and Levenson, R. (2005). Neuronal calcium sensor-1 gene ncs-1a is essential for semicircular canal formation in zebrafish inner ear. *J. Neurobiol.* 64, 285–297.



Bofill-Cardona, E., Kudlacek, O., Yang, Q., Ahorn, H., Freissmuth, M., and Nanoff, C. (2000). Binding of calmodulin to the D2-dopamine receptor reduces receptor signaling by arresting the G protein activation switch. *J. Biol. Chem.* *275*, 32672–32680.

Bonaventura, J., Rico, A.J., Moreno, E., Sierra, S., Sánchez, M., Luquin, N., Farré, D., Müller, C.E., Martínez-Pinilla, E., Cortés, A., et al. (2014). L-DOPA-treatment in primates disrupts the expression of A(2A) adenosine-CB(1) cannabinoid-D(2) dopamine receptor heteromers in the caudate nucleus. *Neuropharmacology* *79*, 90–100.

Bonaventura, J., Navarro, G., Casadó-Anguera, V., Azdad, K., Rea, W., Moreno, E., Brugarolas, M., Mallol, J., Canela, E.I., Lluís, C., et al. (2015). Allosteric interactions between agonists and antagonists within the adenosine A2A receptor-dopamine D2 receptor heterotetramer. *Proc. Natl. Acad. Sci. U. S. A.* *112*, E3609-3618.

Bonhaus, D.W., Chang, L.K., Kwan, J., and Martin, G.R. (1998). Dual activation and inhibition of adenylyl cyclase by cannabinoid receptor agonists: evidence for agonist-specific trafficking of intracellular responses. *J. Pharmacol. Exp. Ther.* *287*, 884–888.

Borroto-Escuela, D.O., Brito, I., Romero-Fernandez, W., Di Palma, M., Oflijan, J., Skieterska, K., Duchou, J., Van Craenenbroeck, K., Suárez-Boomgaard, D., Rivera, A., et al. (2014). The G protein-coupled receptor heterodimer network (GPCR-HetNet) and its hub components. *Int. J. Mol. Sci.* *15*, 8570–8590.

Borroto-Escuela, D.O., Narváez, M., Wydra, K., Pintsuk, J., Pinton, L., Jimenez-Beristain, A., Di Palma, M., Jastrzębska, J., Filip, M., and Fuxe, K. (2017). Cocaine self-administration specifically increases A2AR-D2R and D2R-sigma1R heteroreceptor complexes in the rat nucleus accumbens shell. Relevance for cocaine use disorder. *Pharmacol. Biochem. Behav.* *155*, 24–31.

Bourne, H.R., Sanders, D.A., and McCormick, F. (1991). The GTPase superfamily: conserved structure and molecular mechanism. *Nature* *349*, 117–127.

Bourne, Y., Dannenberg, J., Pollmann, V., Marchot, P., and Pongs, O. (2001).

## BIBLIOGRAPHY

Immunocytochemical localization and crystal structure of human frequenin (neuronal calcium sensor 1). *J. Biol. Chem.* *276*, 11949–11955.

Bouvier, M. (2001). Oligomerization of G-protein-coupled transmitter receptors. *Nat. Rev. Neurosci.* *2*, 274–286.

Braunewell, K.-H. (2005). The darker side of Ca<sup>2+</sup> signaling by neuronal Ca<sup>2+</sup>-sensor proteins: from Alzheimer's disease to cancer. *Trends Pharmacol. Sci.* *26*, 345–351.

Bridges, T.M., and Lindsley, C.W. (2008). G-protein-coupled receptors: from classical modes of modulation to allosteric mechanisms. *ACS Chem. Biol.* *3*, 530–541.

Brown, S.M., Wager-Miller, J., and Mackie, K. (2002). Cloning and molecular characterization of the rat CB2 cannabinoid receptor. *Biochim. Biophys. Acta* *1576*, 255–264.

Brusco, A., Tagliaferro, P.A., Saez, T., and Onaivi, E.S. (2008). Ultrastructural localization of neuronal brain CB2 cannabinoid receptors. *Ann. N. Y. Acad. Sci.* *1139*, 450–457.

Buchanan, J.D., Corbett, R.J., and Roche, R.S. (1986). The thermodynamics of calcium binding to thermolysin. *Biophys. Chem.* *23*, 183–199.

Bu, W., Ren, H., Deng, Y., Del Mar, N., Guley, N.M., Moore, B.M., Honig, M.G., and Reiner, A. (2016). Mild Traumatic Brain Injury Produces Neuron Loss That Can Be Rescued by Modulating Microglial Activation Using a CB2 Receptor Inverse Agonist. *Front. Neurosci.* *10*, 449.

Bulenger, S., Marullo, S., and Bouvier, M. (2005). Emerging role of homo- and heterodimerization in G-protein-coupled receptor biosynthesis and maturation. *Trends Pharmacol. Sci.* *26*, 131–137.

Burgoyne, R.D. (2007). Neuronal calcium sensor proteins: generating diversity in neuronal Ca<sup>2+</sup> signalling. *Nat. Rev. Neurosci.* *8*, 182–193.

Bush, G., Vogt, B.A., Holmes, J., Dale, A.M., Greve, D., Jenike, M.A., and Rosen, B.R. (2002). Dorsal anterior cingulate cortex: a role in reward-based decision making. *Proc. Natl. Acad. Sci.*

U. S. A. *99*, 523–528.

Bushlin, I., Gupta, A., Stockton, S.D., Miller, L.K., and Devi, L.A. (2012). Dimerization with cannabinoid receptors allosterically modulates delta opioid receptor activity during neuropathic pain. *PloS One* *7*, e49789.

Cabral, G.A., and Marciano-Cabral, F. (2005). Cannabinoid receptors in microglia of the central nervous system: immune functional relevance. *J. Leukoc. Biol.* *78*, 1192–1197.

Cabral, G.A., and Griffin-Thomas, L. (2009). Emerging role of the cannabinoid receptor CB2 in immune regulation: therapeutic prospects for neuroinflammation. *Expert Rev. Mol. Med.* *11*, e3.

Cabral, A., López Soto, E.J., Epelbaum, J., and Perelló, M. (2017). Is Ghrelin Synthesized in the Central Nervous System? *Int. J. Mol. Sci.* *18*.

Caenazzo, L., Hoehe, M.R., Hsieh, W.T., Berrettini, W.H., Bonner, T.I., and Gershon, E.S. (1991). HindIII identifies a two allele DNA polymorphism of the human cannabinoid receptor gene (CNR). *Nucleic Acids Res.* *19*, 4798.

Cahill, M.A. (2007). Progesterone receptor membrane component 1: an integrative review. *J. Steroid Biochem. Mol. Biol.* *105*, 16–36.

Callén, L., Moreno, E., Barroso-Chinea, P., Moreno-Delgado, D., Cortés, A., Mallol, J., Casadó, V., Lanciego, J.L., Franco, R., Lluís, C., et al. (2012). Cannabinoid receptors CB1 and CB2 form functional heteromers in brain. *J. Biol. Chem.* *287*, 20851–20865.

Campbell, V.A., and Gowran, A. (2007). Alzheimer's disease; taking the edge off with cannabinoids? *Br. J. Pharmacol.* *152*, 655–662.

Canals, M., Burgueño, J., Marcellino, D., Cabello, N., Canela, E.I., Mallol, J., Agnati, L., Ferré, S., Bouvier, M., Fuxe, K., et al. (2004). Homodimerization of adenosine A2A receptors: qualitative and quantitative assessment by fluorescence and bioluminescence energy transfer. *J. Neurochem.* *88*, 726–734.



## BIBLIOGRAPHY

Carafoli, E. (2002). Calcium signaling: a tale for all seasons. *Proc. Natl. Acad. Sci. U. S. A.* *99*, 1115–1122.

Carriba, P., Ortiz, O., Patkar, K., Justinova, Z., Stroik, J., Themann, A., Müller, C., Woods, A.S., Hope, B.T., Ciruela, F., et al. (2007). Striatal adenosine A2A and cannabinoid CB1 receptors form functional heteromeric complexes that mediate the motor effects of cannabinoids. *Neuropsychopharmacol. Off. Publ. Am. Coll. Neuropsychopharmacol.* *32*, 2249–2259.

Carriba, P., Navarro, G., Ciruela, F., Ferré, S., Casadó, V., Agnati, L., Cortés, A., Mallol, J., Fuxe, K., Canela, E.I., et al. (2008). Detection of heteromerization of more than two proteins by sequential BRET-FRET. *Nat. Methods* *5*, 727–733.

Castillo, P.E., Younts, T.J., Chávez, A.E., and Hashimotodani, Y. (2012). Endocannabinoid signaling and synaptic function. *Neuron* *76*, 70–81.

Catterall, W.A., and Few, A.P. (2008). Calcium channel regulation and presynaptic plasticity. *Neuron* *59*, 882–901.

Chaplin, R., Thach, L., Hollenberg, M.D., Cao, Y., Little, P.J., and Kamato, D. (2017). Insights into cellular signalling by G protein coupled receptor transactivation of cell surface protein kinase receptors. *J. Cell Commun. Signal.* *11*, 117–125.

Chen, X.P., Yang, W., Fan, Y., Luo, J.S., Hong, K., Wang, Z., Yan, J.F., Chen, X., Lu, J.X., Benovic, J.L., et al. (2010). Structural determinants in the second intracellular loop of the human cannabinoid CB1 receptor mediate selective coupling to G(s) and G(i). *Br. J. Pharmacol.* *161*, 1817–1834.

Cherezov, V., Rosenbaum, D.M., Hanson, M.A., Rasmussen, S.G.F., Thian, F.S., Kobilka, T.S., Choi, H.-J., Kuhn, P., Weis, W.I., Kobilka, B.K., et al. (2007). High-resolution crystal structure of an engineered human beta2-adrenergic G protein-coupled receptor. *Science* *318*, 1258–1265.



- Chow, K.B.S., Sun, J., Chu, K.M., Tai Cheung, W., Cheng, C.H.K., and Wise, H. (2012). The truncated ghrelin receptor polypeptide (GHS-R1b) is localized in the endoplasmic reticulum where it forms heterodimers with ghrelin receptors (GHS-R1a) to attenuate their cell surface expression. *Mol. Cell. Endocrinol.* *348*, 247–254.
- Christian, D.T., Wang, X., Chen, E.L., Sehgal, L.K., Ghassemloo, M.N., Miao, J.J., Estepanian, D., Araghi, C.H., Stutzmann, G.E., and Wolf, M.E. (2017). Dynamic Alterations of Rat Nucleus Accumbens Dendritic Spines over 2 Months of Abstinence from Extended-Access Cocaine Self-Administration. *Neuropsychopharmacol. Off. Publ. Am. Coll. Neuropsychopharmacol.* *42*, 748–756.
- Chung, Y.C., Bok, E., Huh, S.H., Park, J.-Y., Yoon, S.-H., Kim, S.R., Kim, Y.-S., Maeng, S., Park, S.H., and Jin, B.K. (2011). Cannabinoid receptor type 1 protects nigrostriatal dopaminergic neurons against MPTP neurotoxicity by inhibiting microglial activation. *J. Immunol. Baltim. Md 1950* *187*, 6508–6517.
- Ciruela, F., Casadó, V., Rodrigues, R.J., Luján, R., Burgueño, J., Canals, M., Borycz, J., Rebola, N., Goldberg, S.R., Mallol, J., et al. (2006). Presynaptic control of striatal glutamatergic neurotransmission by adenosine A1-A2A receptor heteromers. *J. Neurosci. Off. J. Soc. Neurosci.* *26*, 2080–2087.
- Coke, C.J., Scarlett, K.A., Chetram, M.A., Jones, K.J., Sandifer, B.J., Davis, A.S., Marcus, A.I., and Hinton, C.V. (2016). Simultaneous Activation of Induced Heterodimerization between CXCR4 Chemokine Receptor and Cannabinoid Receptor 2 (CB2) Reveals a Mechanism for Regulation of Tumor Progression. *J. Biol. Chem.* *291*, 9991–10005.
- Colabufo, N.A., Berardi, F., Contino, M., Niso, M., Abate, C., Perrone, R., and Tortorella, V. (2004). Antiproliferative and cytotoxic effects of some sigma2 agonists and sigma1 antagonists in tumour cell lines. *Naunyn. Schmiedebergs Arch. Pharmacol.* *370*, 106–113.
- Colpaert, F.C., Niemegeers, C.J., and Janssen, P.A. (1978). Discriminative stimulus properties of cocaine and d-amphetamine, and antagonism by haloperidol: a comparative study. *Neuropharmacology* *17*, 937–942.

## BIBLIOGRAPHY

Concannon, R.M., Okine, B.N., Finn, D.P., and Dowd, E. (2016). Upregulation of the cannabinoid CB2 receptor in environmental and viral inflammation-driven rat models of Parkinson's disease. *Exp. Neurol.* *283*, 204–212.

Cordomí, A., Navarro, G., Aymerich, M.S., and Franco, R. (2015). Structures for G-Protein-Coupled Receptor Tetramers in Complex with G Proteins. *Trends Biochem. Sci.* *40*, 548–551.

Costa, T., and Herz, A. (1989). Antagonists with negative intrinsic activity at delta opioid receptors coupled to GTP-binding proteins. *Proc. Natl. Acad. Sci. U. S. A.* *86*, 7321–7325.

Costa-Neto, C.M., Parreiras-E-Silva, L.T., and Bouvier, M. (2016). A Pluridimensional View of Biased Agonism. *Mol. Pharmacol.* *90*, 587–595.

Crawford, K.W., and Bowen, W.D. (2002). Sigma-2 receptor agonists activate a novel apoptotic pathway and potentiate antineoplastic drugs in breast tumor cell lines. *Cancer Res.* *62*, 313–322.

Creed, M., Kaufling, J., Fois, G.R., Jalabert, M., Yuan, T., Lüscher, C., Georges, F., and Bellone, C. (2016). Cocaine Exposure Enhances the Activity of Ventral Tegmental Area Dopamine Neurons via Calcium-Impermeable NMDARs. *J. Neurosci. Off. J. Soc. Neurosci.* *36*, 10759–10768.

Cuellar, J.N., and Isokawa, M. (2011). Ghrelin-induced activation of cAMP signal transduction and its negative regulation by endocannabinoids in the hippocampus. *Neuropharmacology* *60*, 842–851.

Cvejic, S., and Devi, L.A. (1997). Dimerization of the delta opioid receptor: implication for a role in receptor internalization. *J. Biol. Chem.* *272*, 26959–26964.

Daaka, Y., Luttrell, L.M., Ahn, S., Della Rocca, G.J., Ferguson, S.S., Caron, M.G., and Lefkowitz, R.J. (1998). Essential role for G protein-coupled receptor endocytosis in the activation of mitogen-activated protein kinase. *J. Biol. Chem.* *273*, 685–688.

Damian, M., Mary, S., Maingot, M., M'Kadmi, C., Gagne, D., Leyris, J.-P., Denoyelle, S.,

- Gaibelet, G., Gavara, L., Garcia de Souza Costa, M., et al. (2015). Ghrelin receptor conformational dynamics regulate the transition from a preassembled to an active receptor:Gq complex. *Proc. Natl. Acad. Sci. U. S. A.* *112*, 1601–1606.
- Davis, R.J. (1995). Transcriptional regulation by MAP kinases. *Mol. Reprod. Dev.* *42*, 459–467.
- De Castro, E., Nef, S., Fiumelli, H., Lenz, S.E., Kawamura, S., and Nef, P. (1995). Regulation of rhodopsin phosphorylation by a family of neuronal calcium sensors. *Biochem. Biophys. Res. Commun.* *216*, 133–140.
- De Filippis, D., Steardo, A., D’Amico, A., Scuderi, C., Cipriano, M., Esposito, G., and Iuvone, T. (2009). Differential cannabinoid receptor expression during reactive gliosis: a possible implication for a nonpsychotropic neuroprotection. *ScientificWorldJournal* *9*, 229–235.
- De Jesús, M.L., Sallés, J., Meana, J.J., and Callado, L.F. (2006). Characterization of CB1 cannabinoid receptor immunoreactivity in postmortem human brain homogenates. *Neuroscience* *140*, 635–643.
- De Wit, H., and Wise, R.A. (1977). Blockade of cocaine reinforcement in rats with the dopamine receptor blocker pimozide, but not with the noradrenergic blockers phentolamine or phenoxybenzamine. *Can. J. Psychol.* *31*, 195–203.
- DeFea, K.A., Zalevsky, J., Thoma, M.S., Déry, O., Mullins, R.D., and Bunnett, N.W. (2000). beta-arrestin-dependent endocytosis of proteinase-activated receptor 2 is required for intracellular targeting of activated ERK1/2. *J. Cell Biol.* *148*, 1267–1281.
- Della Rocca, G.J., van Biesen, T., Daaka, Y., Luttrell, D.K., Luttrell, L.M., and Lefkowitz, R.J. (1997). Ras-dependent mitogen-activated protein kinase activation by G protein-coupled receptors. Convergence of Gi- and Gq-mediated pathways on calcium/calmodulin, Pyk2, and Src kinase. *J. Biol. Chem.* *272*, 19125–19132.
- Delgado-Peraza, F., Nogueras-Ortiz, C., Acevedo Canabal, A.M., Roman-Vendrell, C., and Yudowski, G.A. (2016). Imaging GPCRs trafficking and signaling with total internal reflection

## BIBLIOGRAPHY

fluorescence microscopy in cultured neurons. *Methods Cell Biol.* 132, 25–33.

Devane, W.A., Breuer, A., Sheskin, T., Järbe, T.U., Eisen, M.S., and Mechoulam, R. (1992). A novel probe for the cannabinoid receptor. *J. Med. Chem.* 35, 2065–2069.

DeWire, S.M., Kim, J., Whalen, E.J., Ahn, S., Chen, M., and Lefkowitz, R.J. (2008). Beta-arrestin-mediated signaling regulates protein synthesis. *J. Biol. Chem.* 283, 10611–10620.

Dezaki, K. (2013). Ghrelin function in insulin release and glucose metabolism. *Endocr. Dev.* 25, 135–143.

Dezaki, K., Kakei, M., and Yada, T. (2007). Ghrelin uses Galphai2 and activates voltage-dependent K<sup>+</sup> channels to attenuate glucose-induced Ca<sup>2+</sup> signaling and insulin release in islet beta-cells: novel signal transduction of ghrelin. *Diabetes* 56, 2319–2327.

Di Chiara, G., and Imperato, A. (1988). Drugs abused by humans preferentially increase synaptic dopamine concentrations in the mesolimbic system of freely moving rats. *Proc. Natl. Acad. Sci. U. S. A.* 85, 5274–5278.

Di Ciano, P., Cardinal, R.N., Cowell, R.A., Little, S.J., and Everitt, B.J. (2001). Differential involvement of NMDA, AMPA/kainate, and dopamine receptors in the nucleus accumbens core in the acquisition and performance of pavlovian approach behavior. *J. Neurosci. Off. J. Soc. Neurosci.* 21, 9471–9477.

Di Donato, V., Auer, T.O., Duroure, K., and Del Bene, F. (2013). Characterization of the calcium binding protein family in zebrafish. *PloS One* 8, e53299.

Di Marzo, V., Bisogno, T., De Petrocellis, L., Brandi, I., Jefferson, R.G., Winckler, R.L., Davis, J.B., Dasse, O., Mahadevan, A., Razdan, R.K., et al. (2001). Highly selective CB(1) cannabinoid receptor ligands and novel CB(1)/VR(1) vanilloid receptor “hybrid” ligands. *Biochem. Biophys. Res. Commun.* 281, 444–451.

Díaz-Alonso, J., de Salas-Quiroga, A., Paraíso-Luna, J., García-Rincón, D., Garcez, P.P., Parsons, M., Andradas, C., Sánchez, C., Guillemot, F., Guzmán, M., et al. (2017). Loss of

Cannabinoid CB1 Receptors Induces Cortical Migration Malformations and Increases Seizure Susceptibility. *Cereb. Cortex N. Y. N* 1991 *27*, 5303–5317.

Dieterich, D.C., Karpova, A., Mikhaylova, M., Zdobnova, I., König, I., Landwehr, M., Kreutz, M., Smalla, K.-H., Richter, K., Landgraf, P., et al. (2008). Caldendrin-Jacob: a protein liaison that couples NMDA receptor signalling to the nucleus. *PLoS Biol.* *6*, e34.

DiLeone, R.J., Taylor, J.R., and Picciotto, M.R. (2012). The drive to eat: comparisons and distinctions between mechanisms of food reward and drug addiction. *Nat. Neurosci.* *15*, 1330–1335.

Dorn, G.W., Oswald, K.J., McCluskey, T.S., Kuhel, D.G., and Liggett, S.B. (1997). Alpha 2A-adrenergic receptor stimulated calcium release is transduced by Gi-associated G(beta gamma)-mediated activation of phospholipase C. *Biochemistry (Mosc.)* *36*, 6415–6423.

Downes, G.B., and Gautam, N. (1999). The G protein subunit gene families. *Genomics* *62*, 544–552.

Dror, R.O., Mildorf, T.J., Hilger, D., Manglik, A., Borhani, D.W., Arlow, D.H., Philippsen, A., Villanueva, N., Yang, Z., Lerch, M.T., et al. (2015). SIGNAL TRANSDUCTION. Structural basis for nucleotide exchange in heterotrimeric G proteins. *Science* *348*, 1361–1365.

Egecioglu, E., Jerlhag, E., Salomé, N., Skibicka, K.P., Haage, D., Bohlooly-Y, M., Andersson, D., Bjursell, M., Perrissoud, D., Engel, J.A., et al. (2010). Ghrelin increases intake of rewarding food in rodents. *Addict. Biol.* *15*, 304–311.

El Far, O., Bofill-Cardona, E., Airas, J.M., O'Connor, V., Boehm, S., Freissmuth, M., Nanoff, C., and Betz, H. (2001). Mapping of calmodulin and Gbetagamma binding domains within the C-terminal region of the metabotropic glutamate receptor 7A. *J. Biol. Chem.* *276*, 30662–30669.

El Moustaine, D., Granier, S., Doumazane, E., Scholler, P., Rahmeh, R., Bron, P., Mouillac, B., Banères, J.-L., Rondard, P., and Pin, J.-P. (2012). Distinct roles of metabotropic glutamate receptor dimerization in agonist activation and G-protein coupling. *Proc. Natl. Acad. Sci. U. S. A.* *109*, 16342–16347.

## BIBLIOGRAPHY

Ellis, J., Pediani, J.D., Canals, M., Milasta, S., and Milligan, G. (2006). Orexin-1 receptor-cannabinoid CB1 receptor heterodimerization results in both ligand-dependent and -independent coordinated alterations of receptor localization and function. *J. Biol. Chem.* *281*, 38812–38824.

Fagan, S.G., and Campbell, V.A. (2014). The influence of cannabinoids on generic traits of neurodegeneration. *Br. J. Pharmacol.* *171*, 1347–1360.

Fakhoury, M. (2015). Role of Immunity and Inflammation in the Pathophysiology of Neurodegenerative Diseases. *Neurodegener. Dis.* *15*, 63–69.

Faure, M., Voyno-Yasenetskaya, T.A., and Bourne, H.R. (1994). cAMP and beta gamma subunits of heterotrimeric G proteins stimulate the mitogen-activated protein kinase pathway in COS-7 cells. *J. Biol. Chem.* *269*, 7851–7854.

Feng, Z., Alqarni, M.H., Yang, P., Tong, Q., Chowdhury, A., Wang, L., and Xie, X.-Q. (2014). Modeling, molecular dynamics simulation, and mutation validation for structure of cannabinoid receptor 2 based on known crystal structures of GPCRs. *J. Chem. Inf. Model.* *54*, 2483–2499.

Ferguson, S.S. (2001). Evolving concepts in G protein-coupled receptor endocytosis: the role in receptor desensitization and signaling. *Pharmacol. Rev.* *53*, 1–24.

Fernández-Ruiz, J., Romero, J., Velasco, G., Tolón, R.M., Ramos, J.A., and Guzmán, M. (2007). Cannabinoid CB2 receptor: a new target for controlling neural cell survival? *Trends Pharmacol. Sci.* *28*, 39–45.

Fernández-Ruiz, J., Romero, J., and Ramos, J.A. (2015). Endocannabinoids and Neurodegenerative Disorders: Parkinson's Disease, Huntington's Chorea, Alzheimer's Disease, and Others. *Handb. Exp. Pharmacol.* *231*, 233–259.

Ferré, S. (2010). Role of the central ascending neurotransmitter systems in the psychostimulant effects of caffeine. *J. Alzheimers Dis. JAD 20 Suppl 1*, S35-49.

Ferré, S., Karcz-Kubicha, M., Hope, B.T., Popoli, P., Burgueño, J., Gutiérrez, M.A., Casadó, V., Fuxe, K., Goldberg, S.R., Lluís, C., et al. (2002). Synergistic interaction between adenosine A2A and glutamate mGlu5 receptors: implications for striatal neuronal function. *Proc. Natl. Acad. Sci. U. S. A.* *99*, 11940–11945.

Ferré, S., Ciruela, F., Woods, A.S., Lluís, C., and Franco, R. (2007). Functional relevance of neurotransmitter receptor heteromers in the central nervous system. *Trends Neurosci.* *30*, 440–446.

Ferré, S., Baler, R., Bouvier, M., Caron, M.G., Devi, L.A., Durroux, T., Fuxe, K., George, S.R., Javitch, J.A., Lohse, M.J., et al. (2009). Building a new conceptual framework for receptor heteromers. *Nat. Chem. Biol.* *5*, 131–134.

Ferré, S., Casadó, V., Devi, L.A., Filizola, M., Jockers, R., Lohse, M.J., Milligan, G., Pin, J.-P., and Guitart, X. (2014). G protein-coupled receptor oligomerization revisited: functional and pharmacological perspectives. *Pharmacol. Rev.* *66*, 413–434.

Ferreira, S.G., Gonçalves, F.Q., Marques, J.M., Tomé, Â.R., Rodrigues, R.J., Nunes-Correia, I., Ledent, C., Harkany, T., Venance, L., Cunha, R.A., et al. (2015). Presynaptic adenosine A2A receptors dampen cannabinoid CB1 receptor-mediated inhibition of corticostriatal glutamatergic transmission. *Br. J. Pharmacol.* *172*, 1074–1086.

Filippula, S., Yaddanapudi, S., Mercier, R., Xu, W., Pavlopoulos, S., and Makriyannis, A. (2004). Purification and mass spectroscopic analysis of human CB2 cannabinoid receptor expressed in the baculovirus system. *J. Pept. Res. Off. J. Am. Pept. Soc.* *64*, 225–236.

Fishbein-Kaminietsky, M., Gafni, M., and Sarne, Y. (2014). Ultralow doses of cannabinoid drugs protect the mouse brain from inflammation-induced cognitive damage. *J. Neurosci. Res.* *92*, 1669–1677.

Flower, D.R. (1999). Modelling G-protein-coupled receptors for drug design. *Biochim. Biophys. Acta* *1422*, 207–234.





## BIBLIOGRAPHY

Fowler, C.J., Rojo, M.L., and Rodriguez-Gaztelumendi, A. (2010). Modulation of the endocannabinoid system: neuroprotection or neurotoxicity? *Exp. Neurol.* *224*, 37–47.

Franco, R., and Fernández-Suárez, D. (2015). Alternatively activated microglia and macrophages in the central nervous system. *Prog. Neurobiol.* *131*, 65–86.

Franco, R., Casadó, V., Ciruela, F., Mallol, J., Lluís, C., and Canela, E.I. (1996). The cluster-arranged cooperative model: a model that accounts for the kinetics of binding to A1 adenosine receptors. *Biochemistry (Mosc.)* *35*, 3007–3015.

Franco, R., Canals, M., Marcellino, D., Ferré, S., Agnati, L., Mallol, J., Casadó, V., Ciruela, F., Fuxe, K., Lluís, C., et al. (2003). Regulation of heptaspanning-membrane-receptor function by dimerization and clustering. *Trends Biochem. Sci.* *28*, 238–243.

Franco, R., Ciruela, F., Casadó, V., Cortes, A., Canela, E.I., Mallol, J., Agnati, L.F., Ferré, S., Fuxe, K., and Lluís, C. (2005). Partners for adenosine A1 receptors. *J. Mol. Neurosci.* *MN 26*, 221–232.

Franco, R., Lluís, C., Canela, E.I., Mallol, J., Agnati, L., Casadó, V., Ciruela, F., Ferré, S., and Fuxe, K. (2007). Receptor-receptor interactions involving adenosine A1 or dopamine D1 receptors and accessory proteins. *J. Neural Transm. Vienna Austria 1996* *114*, 93–104.

Franco, R., Casadó, V., Cortés, A., Mallol, J., Ciruela, F., Ferré, S., Lluís, C., and Canela, E.I. (2008). G-protein-coupled receptor heteromers: function and ligand pharmacology. *Br. J. Pharmacol.* *153 Suppl 1*, S90-98.

Franco, R., Martínez-Pinilla, E., Ricobaraza, A., and McCormick, P.J. (2013). Challenges in the development of heteromer-GPCR-based drugs. *Prog. Mol. Biol. Transl. Sci.* *117*, 143–162.

Franco, R., Martínez-Pinilla, E., Lanciego, J.L., and Navarro, G. (2016). Basic Pharmacological and Structural Evidence for Class A G-Protein-Coupled Receptor Heteromerization. *Front. Pharmacol.* *7*, 76.

- Franklin, A., and Stella, N. (2003). Arachidonycyclopropylamide increases microglial cell migration through cannabinoid CB2 and abnormal-cannabidiol-sensitive receptors. *Eur. J. Pharmacol.* *474*, 195–198.
- Franklin, A., Parmentier-Batteur, S., Walter, L., Greenberg, D.A., and Stella, N. (2003). Palmitoylethanolamide increases after focal cerebral ischemia and potentiates microglial cell motility. *J. Neurosci. Off. J. Soc. Neurosci.* *23*, 7767–7775.
- Fredriksson, R., Lagerström, M.C., Lundin, L.-G., and Schiöth, H.B. (2003). The G-protein-coupled receptors in the human genome form five main families. Phylogenetic analysis, paralogon groups, and fingerprints. *Mol. Pharmacol.* *63*, 1256–1272.
- Fredriksson, S., Gullberg, M., Jarvius, J., Olsson, C., Pietras, K., Gústafsdóttir, S.M., Ostman, A., and Landegren, U. (2002). Protein detection using proximity-dependent DNA ligation assays. *Nat. Biotechnol.* *20*, 473–477.
- Friedberg, F., and Rhoads, A.R. (2001). Evolutionary aspects of calmodulin. *IUBMB Life* *51*, 215–221.
- Fuenzalida, J., Galaz, P., Araya, K.A., Slater, P.G., Blanco, E.H., Campusano, J.M., Ciruela, F., and Gysling, K. (2014). Dopamine D1 and corticotrophin-releasing hormone type-2 $\alpha$  receptors assemble into functionally interacting complexes in living cells. *Br. J. Pharmacol.* *171*, 5650–5664.
- Fujita, W., Gomes, I., and Devi, L.A. (2014). Revolution in GPCR signalling: opioid receptor heteromers as novel therapeutic targets: IUPHAR review 10. *Br. J. Pharmacol.* *171*, 4155–4176.
- Fung, J.J., Deupi, X., Pardo, L., Yao, X.J., Velez-Ruiz, G.A., Devree, B.T., Sunahara, R.K., and Kobilka, B.K. (2009). Ligand-regulated oligomerization of beta(2)-adrenoceptors in a model lipid bilayer. *EMBO J.* *28*, 3315–3328.
- Fuxe, K., Ferré, S., Genedani, S., Franco, R., and Agnati, L.F. (2007). Adenosine receptor-dopamine receptor interactions in the basal ganglia and their relevance for brain function.

## BIBLIOGRAPHY

*Physiol. Behav.* *92*, 210–217.

Gahbauer, S., and Böckmann, R.A. (2016). Membrane-Mediated Oligomerization of G Protein Coupled Receptors and Its Implications for GPCR Function. *Front. Physiol.* *7*, 494.

Galiègue, S., Mary, S., Marchand, J., Dussossoy, D., Carrière, D., Carayon, P., Bouaboula, M., Shire, D., Le Fur, G., and Casellas, P. (1995). Expression of central and peripheral cannabinoid receptors in human immune tissues and leukocyte subpopulations. *Eur. J. Biochem.* *232*, 54–61.

Galve-Roperh, I., Aguado, T., Palazuelos, J., and Guzmán, M. (2008). Mechanisms of control of neuron survival by the endocannabinoid system. *Curr. Pharm. Des.* *14*, 2279–2288.

Galve-Roperh, I., Chiurchiù, V., Díaz-Alonso, J., Bari, M., Guzmán, M., and Maccarrone, M. (2013). Cannabinoid receptor signaling in progenitor/stem cell proliferation and differentiation. *Prog. Lipid Res.* *52*, 633–650.

Gandía, J., Lluís, C., Ferré, S., Franco, R., and Ciruela, F. (2008). Light resonance energy transfer-based methods in the study of G protein-coupled receptor oligomerization. *BioEssays News Rev. Mol. Cell. Dev. Biol.* *30*, 82–89.

Gantz, I., Muraoka, A., Yang, Y.K., Samuelson, L.C., Zimmerman, E.M., Cook, H., and Yamada, T. (1997). Cloning and chromosomal localization of a gene (GPR18) encoding a novel seven transmembrane receptor highly expressed in spleen and testis. *Genomics* *42*, 462–466.

Garcés-Ramírez, L., Green, J.L., Hiranita, T., Kopajtic, T.A., Mereu, M., Thomas, A.M., Mesangeau, C., Narayanan, S., McCurdy, C.R., Katz, J.L., et al. (2011). Sigma receptor agonists: receptor binding and effects on mesolimbic dopamine neurotransmission assessed by microdialysis. *Biol. Psychiatry* *69*, 208–217.

George, S.R., O'Dowd, B.F., and Lee, S.P. (2002). G-protein-coupled receptor oligomerization and its potential for drug discovery. *Nat. Rev. Drug Discov.* *1*, 808–820.

- Gerdes, D., Wehling, M., Leube, B., and Falkenstein, E. (1998). Cloning and tissue expression of two putative steroid membrane receptors. *Biol. Chem.* 379, 907–911.
- German, D.C., and Manaye, K.F. (1993). Midbrain dopaminergic neurons (nuclei A8, A9, and A10): three-dimensional reconstruction in the rat. *J. Comp. Neurol.* 331, 297–309.
- Gether, U. (2000). Uncovering molecular mechanisms involved in activation of G protein-coupled receptors. *Endocr. Rev.* 21, 90–113.
- Ghosh, A., and Greenberg, M.E. (1995). Calcium signaling in neurons: molecular mechanisms and cellular consequences. *Science* 268, 239–247.
- Ghosh, D., Syed, A.U., Prada, M.P., Nystoriak, M.A., Santana, L.F., Nieves-Cintrón, M., and Navedo, M.F. (2017). Calcium Channels in Vascular Smooth Muscle. *Adv. Pharmacol. San Diego Calif* 78, 49–87.
- Gidon, A., Feinstein, T.N., Xiao, K., and Vilardaga, J.-P. (2016). Studying the regulation of endosomal cAMP production in GPCR signaling. *Methods Cell Biol.* 132, 109–126.
- Ginés, S., Hillion, J., Torvinen, M., Le Crom, S., Casadó, V., Canela, E.I., Rondin, S., Lew, J.Y., Watson, S., Zoli, M., et al. (2000). Dopamine D1 and adenosine A1 receptors form functionally interacting heteromeric complexes. *Proc. Natl. Acad. Sci. U. S. A.* 97, 8606–8611.
- Giros, B., Jaber, M., Jones, S.R., Wightman, R.M., and Caron, M.G. (1996). Hyperlocomotion and indifference to cocaine and amphetamine in mice lacking the dopamine transporter. *Nature* 379, 606–612.
- Glass, M., and Felder, C.C. (1997). Concurrent stimulation of cannabinoid CB1 and dopamine D2 receptors augments cAMP accumulation in striatal neurons: evidence for a Gs linkage to the CB1 receptor. *J. Neurosci. Off. J. Soc. Neurosci.* 17, 5327–5333.
- Glass, M., Dragunow, M., and Faull, R.L. (1997). Cannabinoid receptors in the human brain: a detailed anatomical and quantitative autoradiographic study in the fetal, neonatal and adult human brain. *Neuroscience* 77, 299–318.

## BIBLIOGRAPHY

Golan, M., Schreiber, G., and Avissar, S. (2009). Antidepressants, beta-arrestins and GRKs: from regulation of signal desensitization to intracellular multifunctional adaptor functions. *Curr. Pharm. Des.* *15*, 1699–1708.

Gomes, I., Jordan, B.A., Gupta, A., Trapaidze, N., Nagy, V., and Devi, L.A. (2000). Heterodimerization of mu and delta opioid receptors: A role in opiate synergy. *J. Neurosci. Off. J. Soc. Neurosci.* *20*, RC110.

Gomez, M., De Castro, E., Guarin, E., Sasakura, H., Kuhara, A., Mori, I., Bartfai, T., Bargmann, C.I., and Nef, P. (2001). Ca<sup>2+</sup> signaling via the neuronal calcium sensor-1 regulates associative learning and memory in *C. elegans*. *Neuron* *30*, 241–248.

Gonzalez, A., Cordero, A., Matsoukas, M., Zachmann, J., and Pardo, L. (2014). Modeling of G protein-coupled receptors using crystal structures: from monomers to signaling complexes. *Adv. Exp. Med. Biol.* *796*, 15–33.

González-Maeso, J., Ang, R.L., Yuen, T., Chan, P., Weisstaub, N.V., López-Giménez, J.F., Zhou, M., Okawa, Y., Callado, L.F., Milligan, G., et al. (2008). Identification of a serotonin/glutamate receptor complex implicated in psychosis. *Nature* *452*, 93–97.

Goudet, C., Kniazeff, J., Hlavackova, V., Malhaire, F., Maurel, D., Acher, F., Blahos, J., Prézeau, L., and Pin, J.-P. (2005). Asymmetric functioning of dimeric metabotropic glutamate receptors disclosed by positive allosteric modulators. *J. Biol. Chem.* *280*, 24380–24385.

Gorny, X., Mikhaylova, M., Seeger, C., Reddy, P.P., Reissner, C., Schott, B.H., Helena Danielson, U., Kreutz, M.R., and Seidenbecher, C. (2012). AKAP79/150 interacts with the neuronal calcium-binding protein caldendrin. *J. Neurochem.* *122*, 714–726.

de Graaf, C., Song, G., Cao, C., Zhao, Q., Wang, M.-W., Wu, B., and Stevens, R.C. (2017). Extending the Structural View of Class B GPCRs. *Trends Biochem. Sci.* *42*, 946–960.

Greer, P.L., and Greenberg, M.E. (2008). From synapse to nucleus: calcium-dependent gene transcription in the control of synapse development and function. *Neuron* *59*, 846–860.

- Guitart, X., Codony, X., and Monroy, X. (2004). Sigma receptors: biology and therapeutic potential. *Psychopharmacology (Berl.)* 174, 301–319.
- Guitart, X., Navarro, G., Moreno, E., Yano, H., Cai, N.-S., Sánchez-Soto, M., Kumar-Barodia, S., Naidu, Y.T., Mallol, J., Cortés, A., et al. (2014). Functional selectivity of allosteric interactions within G protein-coupled receptor oligomers: the dopamine D1-D3 receptor heterotetramer. *Mol. Pharmacol.* 86, 417–429.
- Guo, W., Urizar, E., Kralikova, M., Mobarec, J.C., Shi, L., Filizola, M., and Javitch, J.A. (2008). Dopamine D2 receptors form higher order oligomers at physiological expression levels. *EMBO J.* 27, 2293–2304.
- Haeseleer, F., Imanishi, Y., Sokal, I., Filipek, S., and Palczewski, K. (2002). Calcium-binding proteins: intracellular sensors from the calmodulin superfamily. *Biochem. Biophys. Res. Commun.* 290, 615–623.
- Hanner, M., Moebius, F.F., Flandorfer, A., Knaus, H.G., Striessnig, J., Kempner, E., and Glossmann, H. (1996). Purification, molecular cloning, and expression of the mammalian sigma1-binding site. *Proc. Natl. Acad. Sci. U. S. A.* 93, 8072–8077.
- Hanus, L., Abu-Lafi, S., Fride, E., Breuer, A., Vogel, Z., Shalev, D.E., Kustanovich, I., and Mechoulam, R. (2001). 2-arachidonyl glyceryl ether, an endogenous agonist of the cannabinoid CB1 receptor. *Proc. Natl. Acad. Sci. U. S. A.* 98, 3662–3665.
- Hasbi, A., Perreault, M.L., Shen, M.Y.F., Zhang, L., To, R., Fan, T., Nguyen, T., Ji, X., O'Dowd, B.F., and George, S.R. (2014). A peptide targeting an interaction interface disrupts the dopamine D1-D2 receptor heteromer to block signaling and function in vitro and in vivo: effective selective antagonism. *FASEB J. Off. Publ. Fed. Am. Soc. Exp. Biol.* 28, 4806–4820.
- Hashimoto, K., and Kudla, J. (2011). Calcium decoding mechanisms in plants. *Biochimie* 93, 2054–2059.
- Hausdorff, W.P., Bouvier, M., O'Dowd, B.F., Irons, G.P., Caron, M.G., and Lefkowitz, R.J.

## BIBLIOGRAPHY

(1989). Phosphorylation sites on two domains of the beta 2-adrenergic receptor are involved in distinct pathways of receptor desensitization. *J. Biol. Chem.* *264*, 12657–12665.

Hayashi, T., and Su, T. (2005). The sigma receptor: evolution of the concept in neuropsychopharmacology. *Curr. Neuropharmacol.* *3*, 267–280.

Hayashi, T., and Su, T.-P. (2007). Sigma-1 receptor chaperones at the ER-mitochondrion interface regulate Ca(2+) signaling and cell survival. *Cell* *131*, 596–610.

Haynes, L.P., Thomas, G.M.H., and Burgoyne, R.D. (2005). Interaction of neuronal calcium sensor-1 and ADP-ribosylation factor 1 allows bidirectional control of phosphatidylinositol 4-kinase beta and trans-Golgi network-plasma membrane traffic. *J. Biol. Chem.* *280*, 6047–6054.

He, Y., Appel, S., and Le, W. (2001). Minocycline inhibits microglial activation and protects nigral cells after 6-hydroxydopamine injection into mouse striatum. *Brain Res.* *909*, 187–193.

Hebert, T.E., Moffett, S., Morello, J.P., Loisel, T.P., Bichet, D.G., Barret, C., and Bouvier, M. (1996). A peptide derived from a beta2-adrenergic receptor transmembrane domain inhibits both receptor dimerization and activation. *J. Biol. Chem.* *271*, 16384–16392.

Heikkila, R.E., Cabbat, F.S., and Duvoisin, R.C. (1979). Motor activity and rotational behavior after analogs of cocaine: correlation with dopamine uptake blockade. *Commun. Psychopharmacol.* *3*, 285–290.

Hellewell, S.B., Bruce, A., Feinstein, G., Orringer, J., Williams, W., and Bowen, W.D. (1994). Rat liver and kidney contain high densities of sigma 1 and sigma 2 receptors: characterization by ligand binding and photoaffinity labeling. *Eur. J. Pharmacol.* *268*, 9–18.

Herkenham, M., Lynn, A.B., Little, M.D., Johnson, M.R., Melvin, L.S., de Costa, B.R., and Rice, K.C. (1990). Cannabinoid receptor localization in brain. *Proc. Natl. Acad. Sci. U. S. A.* *87*, 1932–1936.

Herrick-Davis, K., Grinde, E., and Mazurkiewicz, J.E. (2004). Biochemical and biophysical characterization of serotonin 5-HT<sub>2C</sub> receptor homodimers on the plasma membrane of

living cells. *Biochemistry (Mosc.)* *43*, 13963–13971.

Herrick-Davis, K., Weaver, B.A., Grinde, E., and Mazurkiewicz, J.E. (2006). Serotonin 5-HT<sub>2C</sub> receptor homodimer biogenesis in the endoplasmic reticulum: real-time visualization with confocal fluorescence resonance energy transfer. *J. Biol. Chem.* *281*, 27109–27116.

Herrick-Davis, K., Grinde, E., Lindsley, T., Teitler, M., Mancía, F., Cowan, A., and Mazurkiewicz, J.E. (2015). Native serotonin 5-HT<sub>2C</sub> receptors are expressed as homodimers on the apical surface of choroid plexus epithelial cells. *Mol. Pharmacol.* *87*, 660–673.

Hilger, D., Masureel, M., and Kobilka, B.K. (2018). Structure and dynamics of GPCR signaling complexes. *Nat. Struct. Mol. Biol.* *25*, 4–12.

Hirschberg, B.T., and Schimerlik, M.I. (1994). A kinetic model for oxotremorine M binding to recombinant porcine m<sub>2</sub> muscarinic receptors expressed in Chinese hamster ovary cells. *J. Biol. Chem.* *269*, 26127–26135.

Hlavackova, V., Goudet, C., Kniazeff, J., Zikova, A., Maurel, D., Vol, C., Trojanova, J., Prézeau, L., Pin, J.-P., and Blahos, J. (2005). Evidence for a single heptahelical domain being turned on upon activation of a dimeric GPCR. *EMBO J.* *24*, 499–509.

Hnasko, T.S., Sotak, B.N., and Palmiter, R.D. (2007). Cocaine-conditioned place preference by dopamine-deficient mice is mediated by serotonin. *J. Neurosci. Off. J. Soc. Neurosci.* *27*, 12484–12488.

Hoehe, M.R., Caenazzo, L., Martinez, M.M., Hsieh, W.T., Modi, W.S., Gershon, E.S., and Bonner, T.I. (1991). Genetic and physical mapping of the human cannabinoid receptor gene to chromosome 6q14-q15. *New Biol.* *3*, 880–885.

Hojo, M., Sudo, Y., Ando, Y., Minami, K., Takada, M., Matsubara, T., Kanaide, M., Taniyama, K., Sumikawa, K., and Uezono, Y. (2008).  $\mu$ -Opioid receptor forms a functional heterodimer with cannabinoid CB<sub>1</sub> receptor: electrophysiological and FRET assay analysis. *J. Pharmacol. Sci.* *108*, 308–319.



## BIBLIOGRAPHY

Holst, B., Brandt, E., Bach, A., Heding, A., and Schwartz, T.W. (2005). Nonpeptide and peptide growth hormone secretagogues act both as ghrelin receptor agonist and as positive or negative allosteric modulators of ghrelin signaling. *Mol. Endocrinol. Baltim. Md* 19, 2400–2411.

Howard, A.D., Feighner, S.D., Cully, D.F., Arena, J.P., Liberato, P.A., Rosenblum, C.I., Hamelin, M., Hreniuk, D.L., Palyha, O.C., Anderson, J., et al. (1996). A receptor in pituitary and hypothalamus that functions in growth hormone release. *Science* 273, 974–977.

Howard, A.D., McAllister, G., Feighner, S.D., Liu, Q., Nargund, R.P., Van der Ploeg, L.H., and Patchett, A.A. (2001). Orphan G-protein-coupled receptors and natural ligand discovery. *Trends Pharmacol. Sci.* 22, 132–140.

Howick, K., Griffin, B.T., Cryan, J.F., and Schellekens, H. (2017). From Belly to Brain: Targeting the Ghrelin Receptor in Appetite and Food Intake Regulation. *Int. J. Mol. Sci.* 18.

Howlett, A.C., Qualy, J.M., and Khachatrian, L.L. (1986). Involvement of Gi in the inhibition of adenylate cyclase by cannabimimetic drugs. *Mol. Pharmacol.* 29, 307–313.

Howlett, A.C., Barth, F., Bonner, T.I., Cabral, G., Casellas, P., Devane, W.A., Felder, C.C., Herkenham, M., Mackie, K., Martin, B.R., et al. (2002). International Union of Pharmacology. XXVII. Classification of cannabinoid receptors. *Pharmacol. Rev.* 54, 161–202.

Hradsky, J., Bernstein, H.-G., Marunde, M., Mikhaylova, M., and Kreutz, M.R. (2015). Alternative splicing, expression and cellular localization of Calneuron-1 in the rat and human brain. *J. Histochem. Cytochem. Off. J. Histochem. Soc.* 63, 793–804.

Hu, C.-D., Chinenov, Y., and Kerppola, T.K. (2002). Visualization of interactions among bZIP and Rel family proteins in living cells using bimolecular fluorescence complementation. *Mol. Cell* 9, 789–798.

Hu, J., Thor, D., Zhou, Y., Liu, T., Wang, Y., McMillin, S.M., Mistry, R., Challiss, R.A.J., Costanzi, S., and Wess, J. (2012). Structural aspects of M<sub>3</sub> muscarinic acetylcholine receptor dimer formation and activation. *FASEB J. Off. Publ. Fed. Am. Soc. Exp. Biol.* 26, 604–616.

- Hua, T., Vemuri, K., Pu, M., Qu, L., Han, G.W., Wu, Y., Zhao, S., Shui, W., Li, S., Korde, A., et al. (2016). Crystal Structure of the Human Cannabinoid Receptor CB1. *Cell* *167*, 750–762.e14.
- Huang, J., Chen, S., Zhang, J.J., and Huang, X.-Y. (2013). Crystal structure of oligomeric  $\beta$ 1-adrenergic G protein-coupled receptors in ligand-free basal state. *Nat. Struct. Mol. Biol.* *20*, 419–425.
- Huang, S.M., Bisogno, T., Trevisani, M., Al-Hayani, A., De Petrocellis, L., Fezza, F., Tognetto, M., Petros, T.J., Krey, J.F., Chu, C.J., et al. (2002). An endogenous capsaicin-like substance with high potency at recombinant and native vanilloid VR1 receptors. *Proc. Natl. Acad. Sci. U. S. A.* *99*, 8400–8405.
- Ikura, M., and Ames, J.B. (2006). Genetic polymorphism and protein conformational plasticity in the calmodulin superfamily: two ways to promote multifunctionality. *Proc. Natl. Acad. Sci. U. S. A.* *103*, 1159–1164.
- J Gingell, J., Simms, J., Barwell, J., Poyner, D.R., Watkins, H.A., Pioszak, A.A., Sexton, P.M., and Hay, D.L. (2016). An allosteric role for receptor activity-modifying proteins in defining GPCR pharmacology. *Cell Discov.* *2*, 16012.
- Jaakola, V.-P., Griffith, M.T., Hanson, M.A., Cherezov, V., Chien, E.Y.T., Lane, J.R., Ijzerman, A.P., and Stevens, R.C. (2008). The 2.6 angstrom crystal structure of a human A2A adenosine receptor bound to an antagonist. *Science* *322*, 1211–1217.
- Jacoby, E., Bouhelal, R., Gerspacher, M., and Seuwen, K. (2006). The 7 TM G-protein-coupled receptor target family. *ChemMedChem* *1*, 761–782.
- Janssen, B., Vugts, D.J., Funke, U., Molenaar, G.T., Kruijer, P.S., van Berckel, B.N.M., Lammertsma, A.A., and Windhorst, A.D. (2016). Imaging of neuroinflammation in Alzheimer's disease, multiple sclerosis and stroke: Recent developments in positron emission tomography. *Biochim. Biophys. Acta* *1862*, 425–441.



## BIBLIOGRAPHY

- Jääntti, M.H., Mandrika, I., and Kukkonen, J.P. (2014). Human orexin/hypocretin receptors form constitutive homo- and heteromeric complexes with each other and with human CB1 cannabinoid receptors. *Biochem. Biophys. Res. Commun.* *445*, 486–490.
- Jarrahan, A., Watts, V.J., and Barker, E.L. (2004). D2 dopamine receptors modulate G $\alpha$ -subunit coupling of the CB1 cannabinoid receptor. *J. Pharmacol. Exp. Ther.* *308*, 880–886.
- Jastrzebska, B., Orban, T., Golczak, M., Engel, A., and Palczewski, K. (2013). Asymmetry of the rhodopsin dimer in complex with transducin. *FASEB J. Off. Publ. Fed. Am. Soc. Exp. Biol.* *27*, 1572–1584.
- Jastrzebska, B., Chen, Y., Orban, T., Jin, H., Hofmann, L., and Palczewski, K. (2015). Disruption of Rhodopsin Dimerization with Synthetic Peptides Targeting an Interaction Interface. *J. Biol. Chem.* *290*, 25728–25744.
- Jay, T.M. (2003). Dopamine: a potential substrate for synaptic plasticity and memory mechanisms. *Prog. Neurobiol.* *69*, 375–390.
- Jerlhag, E., Egecioglu, E., Dickson, S.L., Andersson, M., Svensson, L., and Engel, J.A. (2006). Ghrelin stimulates locomotor activity and accumbal dopamine-overflow via central cholinergic systems in mice: implications for its involvement in brain reward. *Addict. Biol.* *11*, 45–54.
- Jerlhag, E., Egecioglu, E., Landgren, S., Salomé, N., Heilig, M., Moechars, D., Datta, R., Perrissoud, D., Dickson, S.L., and Engel, J.A. (2009). Requirement of central ghrelin signaling for alcohol reward. *Proc. Natl. Acad. Sci. U. S. A.* *106*, 11318–11323.
- Jia, J., Peng, J., Li, Z., Wu, Y., Wu, Q., Tu, W., and Wu, M. (2016). Cannabinoid CB2 Receptor Mediates Nicotine-Induced Anti-Inflammation in N9 Microglial Cells Exposed to  $\beta$  Amyloid via Protein Kinase C. *Mediators Inflamm.* *2016*, 4854378.
- Kaplan, B.L.F. (2013). The role of CB1 in immune modulation by cannabinoids. *Pharmacol. Ther.* *137*, 365–374.
- Jiang, H., Betancourt, L., and Smith, R.G. (2006). Ghrelin amplifies dopamine signaling by cross talk involving formation of growth hormone secretagogue receptor/dopamine receptor



subtype 1 heterodimers. *Mol. Endocrinol. Baltim. Md* 20, 1772–1785.

Jockers, R., Angers, S., Da Silva, A., Benaroch, P., Strosberg, A.D., Bouvier, M., and Marullo, S. (1999). Beta(2)-adrenergic receptor down-regulation. Evidence for a pathway that does not require endocytosis. *J. Biol. Chem.* 274, 28900–28908.

Joffe, M.E., Grueter, C.A., and Grueter, B.A. (2014). Biological substrates of addiction. *Wiley Interdiscip. Rev. Cogn. Sci.* 5, 151–171.

Joffe, M.E., and Grueter, B.A. (2016). Cocaine Experience Enhances Thalamo-Accumbens N-Methyl-D-Aspartate Receptor Function. *Biol. Psychiatry* 80, 671–681.

Johnston, J.M., Aburi, M., Provasi, D., Bortolato, A., Urizar, E., Lambert, N.A., Javitch, J.A., and Filizola, M. (2011). Making structural sense of dimerization interfaces of delta opioid receptor homodimers. *Biochemistry (Mosc.)* 50, 1682–1690.

Jones, K.A., Borowsky, B., Tamm, J.A., Craig, D.A., Durkin, M.M., Dai, M., Yao, W.J., Johnson, M., Gunwaldsen, C., Huang, L.Y., et al. (1998). GABA(B) receptors function as a heteromeric assembly of the subunits GABA(B)R1 and GABA(B)R2. *Nature* 396, 674–679.

Jonhede, S., Petersen, A., Zetterberg, M., and Karlsson, J.-O. (2010). Acute effects of the sigma-2 receptor agonist siramesine on lysosomal and extra-lysosomal proteolytic systems in lens epithelial cells. *Mol. Vis.* 16, 819–827.

Jordan, B.A., and Devi, L.A. (1999). G-protein-coupled receptor heterodimerization modulates receptor function. *Nature* 399, 697–700.

Kabbani, N., Negyessy, L., Lin, R., Goldman-Rakic, P., and Levenson, R. (2002). Interaction with neuronal calcium sensor NCS-1 mediates desensitization of the D2 dopamine receptor. *J. Neurosci. Off. J. Soc. Neurosci.* 22, 8476–8486.

Kabbani, N., Woll, M.P., Nordman, J.C., and Levenson, R. (2012). Dopamine receptor interacting proteins: targeting neuronal calcium sensor-1/D2 dopamine receptor interaction for antipsychotic drug development. *Curr. Drug Targets* 13, 72–79.

## BIBLIOGRAPHY

- Kang, D.S., Tian, X., and Benovic, J.L. (2014). Role of  $\beta$ -arrestins and arrestin domain-containing proteins in G protein-coupled receptor trafficking. *Curr. Opin. Cell Biol.* 27, 63–71.
- Kang, Y., Zhou, X.E., Gao, X., He, Y., Liu, W., Ishchenko, A., Barty, A., White, T.A., Yefanov, O., Han, G.W., et al. (2015). Crystal structure of rhodopsin bound to arrestin by femtosecond X-ray laser. *Nature* 523, 561–567.
- Kapp-Barnea, Y., Melnikov, S., Shefler, I., Jeromin, A., and Sagi-Eisenberg, R. (2003). Neuronal calcium sensor-1 and phosphatidylinositol 4-kinase beta regulate IgE receptor-triggered exocytosis in cultured mast cells. *J. Immunol. Baltim. Md 1950* 171, 5320–5327.
- Kargl, J., Balenga, N., Parzmair, G.P., Brown, A.J., Heinemann, A., and Waldhoer, M. (2012). The cannabinoid receptor CB1 modulates the signaling properties of the lysophosphatidylinositol receptor GPR55. *J. Biol. Chem.* 287, 44234–44248.
- Kasai, R.S., and Kusumi, A. (2014). Single-molecule imaging revealed dynamic GPCR dimerization. *Curr. Opin. Cell Biol.* 27, 78–86.
- Katona, I., and Freund, T.F. (2008). Endocannabinoid signaling as a synaptic circuit breaker in neurological disease. *Nat. Med.* 14, 923–930.
- Kaupmann, K., Malitschek, B., Schuler, V., Heid, J., Froestl, W., Beck, P., Mosbacher, J., Bischoff, S., Kulik, A., Shigemoto, R., et al. (1998). GABA(B)-receptor subtypes assemble into functional heteromeric complexes. *Nature* 396, 683–687.
- Kawasaki, H., Nakayama, S., and Kretsinger, R.H. (1998). Classification and evolution of EF-hand proteins. *Biometals Int. J. Role Met. Ions Biol. Biochem. Med.* 11, 277–295.
- Kearn, C.S., Blake-Palmer, K., Daniel, E., Mackie, K., and Glass, M. (2005). Concurrent stimulation of cannabinoid CB1 and dopamine D2 receptors enhances heterodimer formation: a mechanism for receptor cross-talk? *Mol. Pharmacol.* 67, 1697–1704.

- Kelly, E., Bailey, C.P., and Henderson, G. (2008). Agonist-selective mechanisms of GPCR desensitization. *Br. J. Pharmacol.* *153 Suppl 1*, S379-388.
- Kenakin, T. (2014). What is pharmacological “affinity”? Relevance to biased agonism and antagonism. *Trends Pharmacol. Sci.* *35*, 434–441.
- Kenakin, T., and Christopoulos, A. (2013). Signalling bias in new drug discovery: detection, quantification and therapeutic impact. *Nat. Rev. Drug Discov.* *12*, 205–216.
- Kenakin, T., and Miller, L.J. (2010). Seven transmembrane receptors as shapeshifting proteins: the impact of allosteric modulation and functional selectivity on new drug discovery. *Pharmacol. Rev.* *62*, 265–304.
- Kermer, P., Klöcker, N., Labes, M., Thomsen, S., Srinivasan, A., and Bähr, M. (1999). Activation of caspase-3 in axotomized rat retinal ganglion cells in vivo. *FEBS Lett.* *453*, 361–364.
- Kern, A., Mavrikaki, M., Ullrich, C., Albarran-Zeckler, R., Brantley, A.F., and Smith, R.G. (2015). Hippocampal Dopamine/DRD1 Signaling Dependent on the Ghrelin Receptor. *Cell* *163*, 1176–1190.
- Khan, S.S., and Lee, F.J.S. (2014). Delineation of domains within the cannabinoid CB1 and dopamine D2 receptors that mediate the formation of the heterodimer complex. *J. Mol. Neurosci.* *MN 53*, 10–21.
- Kim, F.J. (2017). Introduction to Sigma Proteins: Evolution of the Concept of Sigma Receptors. *Handb. Exp. Pharmacol.* *244*, 1–11.
- Kim, H., Lee, B.-K., Naider, F., and Becker, J.M. (2009). Identification of specific transmembrane residues and ligand-induced interface changes involved in homo-dimer formation of a yeast G protein-coupled receptor. *Biochemistry (Mosc.)* *48*, 10976–10987.
- Kim, H.F., and Hikosaka, O. (2015). Parallel basal ganglia circuits for voluntary and automatic behaviour to reach rewards. *Brain J. Neurol.* *138*, 1776–1800.

## BIBLIOGRAPHY

Klein Herenbrink, C., Sykes, D.A., Donthamsetti, P., Canals, M., Coudrat, T., Shonberg, J., Scammells, P.J., Capuano, B., Sexton, P.M., Charlton, S.J., et al. (2016). The role of kinetic context in apparent biased agonism at GPCRs. *Nat. Commun.* 7, 10842.

Koch, W.J., Hawes, B.E., Allen, L.F., and Lefkowitz, R.J. (1994). Direct evidence that Gi-coupled receptor stimulation of mitogen-activated protein kinase is mediated by G beta gamma activation of p21ras. *Proc. Natl. Acad. Sci. U. S. A.* 91, 12706–12710.

Koh, P.O., Undie, A.S., Kabbani, N., Levenson, R., Goldman-Rakic, P.S., and Lidow, M.S. (2003). Up-regulation of neuronal calcium sensor-1 (NCS-1) in the prefrontal cortex of schizophrenic and bipolar patients. *Proc. Natl. Acad. Sci. U. S. A.* 100, 313–317.

Kohno, M., Hasegawa, H., Inoue, A., Muraoka, M., Miyazaki, T., Oka, K., and Yasukawa, M. (2006). Identification of N-arachidonylglycine as the endogenous ligand for orphan G-protein-coupled receptor GPR18. *Biochem. Biophys. Res. Commun.* 347, 827–832.

Kojima, M., Hosoda, H., Date, Y., Nakazato, M., Matsuo, H., and Kangawa, K. (1999). Ghrelin is a growth-hormone-releasing acylated peptide from stomach. *Nature* 402, 656–660.

Kolakowski, L.F. (1994). GCRDb: a G-protein-coupled receptor database. *Receptors Channels* 2, 1–7.

Kong, M.M.C., Hasbi, A., Mattocks, M., Fan, T., O'Dowd, B.F., and George, S.R. (2007). Regulation of D1 dopamine receptor trafficking and signaling by caveolin-1. *Mol. Pharmacol.* 72, 1157–1170.

Koob, G.F., and Volkow, N.D. (2016). Neurobiology of addiction: a neurocircuitry analysis. *Lancet Psychiatry* 3, 760–773.

Kotagale, N.R., Upadhyay, M., Hadole, P.N., Kokare, D.M., and Taksande, B.G. (2014). Involvement of hypothalamic neuropeptide Y in pentazocine induced suppression of food intake in rats. *Neuropeptides* 48, 133–141.

- Kovacs, J.J., Hara, M.R., Davenport, C.L., Kim, J., and Lefkowitz, R.J. (2009). Arrestin development: emerging roles for beta-arrestins in developmental signaling pathways. *Dev. Cell* 17, 443–458.
- Krebs, C.J., Jarvis, E.D., Chan, J., Lydon, J.P., Ogawa, S., and Pfaff, D.W. (2000). A membrane-associated progesterone-binding protein, 25-Dx, is regulated by progesterone in brain regions involved in female reproductive behaviors. *Proc. Natl. Acad. Sci. U. S. A.* 97, 12816–12821.
- Krupnick, J.G., and Benovic, J.L. (1998). The role of receptor kinases and arrestins in G protein-coupled receptor regulation. *Annu. Rev. Pharmacol. Toxicol.* 38, 289–319.
- Kuszak, A.J., Pitchiaya, S., Anand, J.P., Mosberg, H.I., Walter, N.G., and Sunahara, R.K. (2009). Purification and functional reconstitution of monomeric mu-opioid receptors: allosteric modulation of agonist binding by Gi2. *J. Biol. Chem.* 284, 26732–26741.
- de Lago, E., and Fernández-Ruiz, J. (2007). Cannabinoids and neuroprotection in motor-related disorders. *CNS Neurol. Disord. Drug Targets* 6, 377–387.
- Lanciego, J.L., Barroso-Chinea, P., Rico, A.J., Conte-Perales, L., Callén, L., Roda, E., Gómez-Bautista, V., López, I.P., Lluís, C., Labandeira-García, J.L., et al. (2011). Expression of the mRNA coding the cannabinoid receptor 2 in the pallidal complex of *Macaca fascicularis*. *J. Psychopharmacol. Oxf. Engl.* 25, 97–104.
- Laprairie, R.B., Bagher, A.M., Kelly, M.E.M., and Denovan-Wright, E.M. (2015). Cannabidiol is a negative allosteric modulator of the cannabinoid CB1 receptor. *Br. J. Pharmacol.* 172, 4790–4805.
- Laprairie, R.B., Kelly, M.E.M., and Denovan-Wright, E.M. (2012). The dynamic nature of type 1 cannabinoid receptor (CB1) gene transcription. *Br. J. Pharmacol.* 167, 1583–1595.
- Leach, K., and Gregory, K.J. (2017). Molecular insights into allosteric modulation of Class C G protein-coupled receptors. *Pharmacol. Res.* 116, 105–118.



## BIBLIOGRAPHY

Lee, S.P., So, C.H., Rashid, A.J., Varghese, G., Cheng, R., Lança, A.J., O'Dowd, B.F., and George, S.R. (2004). Dopamine D1 and D2 receptor Co-activation generates a novel phospholipase C-mediated calcium signal. *J. Biol. Chem.* *279*, 35671–35678.

Lefkowitz, R.J. (1998). G protein-coupled receptors. III. New roles for receptor kinases and beta-arrestins in receptor signaling and desensitization. *J. Biol. Chem.* *273*, 18677–18680.

Lefkowitz, R.J., Cotecchia, S., Kjelsberg, M.A., Pitcher, J., Koch, W.J., Inglese, J., and Caron, M.G. (1993). Adrenergic receptors: recent insights into their mechanism of activation and desensitization. *Adv. Second Messenger Phosphoprotein Res.* *28*, 1–9.

Leonelli, M., Torráo, A.S., and Britto, L.R.G. (2009). Unconventional neurotransmitters, neurodegeneration and neuroprotection. *Braz. J. Med. Biol. Res. Rev. Bras. Pesqui. Medicas E Biol.* *42*, 68–75.

Leung, P.-K., Chow, K.B.S., Lau, P.-N., Chu, K.-M., Chan, C.-B., Cheng, C.H.K., and Wise, H. (2007). The truncated ghrelin receptor polypeptide (GHS-R1b) acts as a dominant-negative mutant of the ghrelin receptor. *Cell. Signal.* *19*, 1011–1022.

Lever, J.R., Miller, D.K., Green, C.L., Ferguson-Cantrell, E.A., Watkinson, L.D., Carmack, T.L., Fan, K.-H., and Lever, S.Z. (2014). A selective sigma-2 receptor ligand antagonizes cocaine-induced hyperlocomotion in mice. *Synap. N. Y. N* *68*, 73–84.

Li, Y., and Kim, J. (2015). Neuronal expression of CB2 cannabinoid receptor mRNAs in the mouse hippocampus. *Neuroscience* *311*, 253–267.

Lian, L.-Y., Pandalaneni, S.R., Patel, P., McCue, H.V., Haynes, L.P., and Burgoyne, R.D. (2011). Characterisation of the interaction of the C-terminus of the dopamine D2 receptor with neuronal calcium sensor-1. *PloS One* *6*, e27779.

Limbäck-Stokin, K., Korzus, E., Nagaoka-Yasuda, R., and Mayford, M. (2004). Nuclear calcium/calmodulin regulates memory consolidation. *J. Neurosci. Off. J. Soc. Neurosci.* *24*,

10858–10867.

Limbird, L.E., Meyts, P.D., and Lefkowitz, R.J. (1975). Beta-adrenergic receptors: evidence for negative cooperativity. *Biochem. Biophys. Res. Commun.* *64*, 1160–1168.

Liu, Y., Buck, D.C., Macey, T.A., Lan, H., and Neve, K.A. (2007). Evidence that calmodulin binding to the dopamine D2 receptor enhances receptor signaling. *J. Recept. Signal Transduct. Res.* *27*, 47–65.

López-Moreno, J.A., López-Jiménez, A., Gorriti, M.A., and de Fonseca, F.R. (2010). Functional interactions between endogenous cannabinoid and opioid systems: focus on alcohol, genetics and drug-addicted behaviors. *Curr. Drug Targets* *11*, 406–428.

Lu, H.-C., and Mackie, K. (2016). An Introduction to the Endogenous Cannabinoid System. *Biol. Psychiatry* *79*, 516–525.

Lu, M., and Wu, B. (2016). Structural studies of G protein-coupled receptors. *IUBMB Life* *68*, 894–903.

Lüscher, C. (2016). The Emergence of a Circuit Model for Addiction. *Annu. Rev. Neurosci.* *39*, 257–276.

Luttrell, L.M. (2005). Composition and function of g protein-coupled receptor signalsomes controlling mitogen-activated protein kinase activity. *J. Mol. Neurosci.* *MN 26*, 253–264.

Luttrell, L.M., and Lefkowitz, R.J. (2002). The role of beta-arrestins in the termination and transduction of G-protein-coupled receptor signals. *J. Cell Sci.* *115*, 455–465.

Mach, R.H., Zeng, C., and Hawkins, W.G. (2013). The  $\sigma_2$  receptor: a novel protein for the imaging and treatment of cancer. *J. Med. Chem.* *56*, 7137–7160.

Mackie, K. (2005). Cannabinoid receptor homo- and heterodimerization. *Life Sci.* *77*, 1667–1673.

## BIBLIOGRAPHY

Magalhaes, A.C., Dunn, H., and Ferguson, S.S. (2012). Regulation of GPCR activity, trafficking and localization by GPCR-interacting proteins. *Br. J. Pharmacol.* *165*, 1717–1736.

Maggio, R., Vogel, Z., and Wess, J. (1993). Coexpression studies with mutant muscarinic/adrenergic receptors provide evidence for intermolecular “cross-talk” between G-protein-linked receptors. *Proc. Natl. Acad. Sci. U. S. A.* *90*, 3103–3107.

Makriyannis, A. (2014). 2012 Division of medicinal chemistry award address. Trekking the cannabinoid road: a personal perspective. *J. Med. Chem.* *57*, 3891–3911.

Malagón, M.M., Luque, R.M., Ruiz-Guerrero, E., Rodríguez-Pacheco, F., García-Navarro, S., Casanueva, F.F., Gracia-Navarro, F., and Castaño, J.P. (2003). Intracellular signaling mechanisms mediating ghrelin-stimulated growth hormone release in somatotropes. *Endocrinology* *144*, 5372–5380.

Malek, N., Popiolek-Barczyk, K., Mika, J., Przewlocka, B., and Starowicz, K. (2015). Anandamide, Acting via CB2 Receptors, Alleviates LPS-Induced Neuroinflammation in Rat Primary Microglial Cultures. *Neural Plast.* *2015*, 130639.

Manglik, A., Kruse, A.C., Kobilka, T.S., Thian, F.S., Mathiesen, J.M., Sunahara, R.K., Pardo, L., Weis, W.I., Kobilka, B.K., and Granier, S. (2012). Crystal structure of the  $\mu$ -opioid receptor bound to a morphinan antagonist. *Nature* *485*, 321–326.

Marcellino, D., Ferré, S., Casadó, V., Cortés, A., Le Foll, B., Mazzola, C., Drago, F., Saur, O., Stark, H., Soriano, A., et al. (2008a). Identification of dopamine D1-D3 receptor heteromers. Indications for a role of synergistic D1-D3 receptor interactions in the striatum. *J. Biol. Chem.* *283*, 26016–26025.

Marcellino, D., Carriba, P., Filip, M., Borgkvist, A., Frankowska, M., Bellido, I., Tanganelli, S., Müller, C.E., Fisone, G., Llus, C., et al. (2008b). Antagonistic cannabinoid CB1/dopamine D2 receptor interactions in striatal CB1/D2 heteromers. A combined neurochemical and behavioral analysis. *Neuropharmacology* *54*, 815–823.

Marcelo, K.L., Means, A.R., and York, B. (2016). The Ca(2+)/Calmodulin/CaMKK2 Axis:

Nature's Metabolic CaMshaft. *Trends Endocrinol. Metab.* *TEM* 27, 706–718.

Maresz, K., Carrier, E.J., Ponomarev, E.D., Hillard, C.J., and Dittel, B.N. (2005). Modulation of the cannabinoid CB2 receptor in microglial cells in response to inflammatory stimuli. *J. Neurochem.* *95*, 437–445.

Margeta-Mitrovic, M., Jan, Y.N., and Jan, L.Y. (2000). A trafficking checkpoint controls GABA(B) receptor heterodimerization. *Neuron* 27, 97–106.

Marinissen, M.J., and Gutkind, J.S. (2001). G-protein-coupled receptors and signaling networks: emerging paradigms. *Trends Pharmacol. Sci.* *22*, 368–376.

Martin, W.R., Eades, C.G., Thompson, J.A., Huppler, R.E., and Gilbert, P.E. (1976). The effects of morphine- and nalorphine- like drugs in the nondependent and morphine-dependent chronic spinal dog. *J. Pharmacol. Exp. Ther.* *197*, 517–532.

Martínez-Pinilla, E., Rabal, O., Reyes-Resina, I., Zamarbide, M., Navarro, G., Sánchez-Arias, J.A., de Miguel, I., Lanciego, J.L., Oyarzabal, J., and Franco, R. (2016). Two Affinity Sites of the Cannabinoid Subtype 2 Receptor Identified by a Novel Homogeneous Binding Assay. *J. Pharmacol. Exp. Ther.* *358*, 580–587.

Martire, A., Tebano, M.T., Chiodi, V., Ferreira, S.G., Cunha, R.A., Köfalvi, A., and Popoli, P. (2011). Pre-synaptic adenosine A2A receptors control cannabinoid CB1 receptor-mediated inhibition of striatal glutamatergic neurotransmission. *J. Neurochem.* *116*, 273–280.

Mary, S., Fehrentz, J.-A., Damian, M., Gaibelet, G., Orcel, H., Verdié, P., Mouillac, B., Martinez, J., Marie, J., and Banères, J.-L. (2013). Heterodimerization with Its splice variant blocks the ghrelin receptor 1a in a non-signaling conformation: a study with a purified heterodimer assembled into lipid discs. *J. Biol. Chem.* *288*, 24656–24665.

Mason, B.L., Wang, Q., and Zigman, J.M. (2014). The central nervous system sites mediating the orexigenic actions of ghrelin. *Annu. Rev. Physiol.* *76*, 519–533.

Matsuda, L.A., Lolait, S.J., Brownstein, M.J., Young, A.C., and Bonner, T.I. (1990). Structure

## BIBLIOGRAPHY

of a cannabinoid receptor and functional expression of the cloned cDNA. *Nature* *346*, 561–564.

Matsumoto, R.R., Hewett, K.L., Pouw, B., Bowen, W.D., Husbands, S.M., Cao, J.J., and Newman, A.H. (2001). Rimcazole analogs attenuate the convulsive effects of cocaine: correlation with binding to sigma receptors rather than dopamine transporters. *Neuropharmacology* *41*, 878–886.

Matsumoto, R.R., McCracken, K.A., Pouw, B., Zhang, Y., and Bowen, W.D. (2002). Involvement of sigma receptors in the behavioral effects of cocaine: evidence from novel ligands and antisense oligodeoxynucleotides. *Neuropharmacology* *42*, 1043–1055.

Matsumoto, R.R., Liu, Y., Lerner, M., Howard, E.W., and Brackett, D.J. (2003). Sigma receptors: potential medications development target for anti-cocaine agents. *Eur. J. Pharmacol.* *469*, 1–12.

Matsumoto, R.R., Gilmore, D.L., Pouw, B., Bowen, W.D., Williams, W., Kausar, A., and Coop, A. (2004). Novel analogs of the sigma receptor ligand BD1008 attenuate cocaine-induced toxicity in mice. *Eur. J. Pharmacol.* *492*, 21–26.

Matsumoto, R.R., Pouw, B., Mack, A.L., Daniels, A., and Coop, A. (2007). Effects of UMB24 and (+/-)-SM 21, putative sigma2-preferring antagonists, on behavioral toxic and stimulant effects of cocaine in mice. *Pharmacol. Biochem. Behav.* *86*, 86–91.

Mattera, R., Pitts, B.J., Entman, M.L., and Birnbaumer, L. (1985). Guanine nucleotide regulation of a mammalian myocardial muscarinic receptor system. Evidence for homo- and heterotropic cooperativity in ligand binding analyzed by computer-assisted curve fitting. *J. Biol. Chem.* *260*, 7410–7421.

Maurice, T., and Romieu, P. (2004). Involvement of the sigma1 receptor in the appetitive effects of cocaine. *Pharmacopsychiatry* *37 Suppl 3*, S198-207.

Mavlyutov, T.A., Epstein, M.L., Verbny, Y.I., Huerta, M.S., Zaitoun, I., Ziskind-Conhaim, L., and Ruoho, A.E. (2013). Lack of sigma-1 receptor exacerbates ALS progression in mice.

Neuroscience 240, 129–134.

May, L.T., Leach, K., Sexton, P.M., and Christopoulos, A. (2007). Allosteric modulation of G protein-coupled receptors. *Annu. Rev. Pharmacol. Toxicol.* 47, 1–51.

McAllister, S.D., and Glass, M. (2002). CB(1) and CB(2) receptor-mediated signalling: a focus on endocannabinoids. *Prostaglandins Leukot. Essent. Fatty Acids* 66, 161–171.

McClure, S.M., Daw, N.D., and Montague, P.R. (2003). A computational substrate for incentive salience. *Trends Neurosci.* 26, 423–428.

McCue, H.V., Haynes, L.P., and Burgoyne, R.D. (2010a). The diversity of calcium sensor proteins in the regulation of neuronal function. *Cold Spring Harb. Perspect. Biol.* 2, a004085.

McCue, H.V., Haynes, L.P., and Burgoyne, R.D. (2010b). Bioinformatic analysis of CaBP/calneuron proteins reveals a family of highly conserved vertebrate Ca<sup>2+</sup>-binding proteins. *BMC Res. Notes* 3, 118.

McFerran, B.W., Graham, M.E., and Burgoyne, R.D. (1998). Neuronal Ca<sup>2+</sup> sensor 1, the mammalian homologue of frequenin, is expressed in chromaffin and PC12 cells and regulates neurosecretion from dense-core granules. *J. Biol. Chem.* 273, 22768–22772.

McHugh, D., Tanner, C., Mechoulam, R., Pertwee, R.G., and Ross, R.A. (2008). Inhibition of human neutrophil chemotaxis by endogenous cannabinoids and phytocannabinoids: evidence for a site distinct from CB1 and CB2. *Mol. Pharmacol.* 73, 441–450.

McKay, M.M., and Morrison, D.K. (2007). Integrating signals from RTKs to ERK/MAPK. *Oncogene* 26, 3113–3121.

Mecha, M., Feliú, A., Carrillo-Salinas, F.J., Rueda-Zubiaurre, A., Ortega-Gutiérrez, S., de Sola, R.G., and Guaza, C. (2015). Endocannabinoids drive the acquisition of an alternative phenotype in microglia. *Brain. Behav. Immun.* 49, 233–245.

Mecha, M., Carrillo-Salinas, F.J., Feliú, A., Mestre, L., and Guaza, C. (2016). Microglia

## BIBLIOGRAPHY

activation states and cannabinoid system: Therapeutic implications. *Pharmacol. Ther.* *166*, 40–55.

Mechoulam, R., Spatz, M., and Shohami, E. (2002). Endocannabinoids and neuroprotection. *Sci. STKE Signal Transduct. Knowl. Environ.* *2002*, re5.

Medina, M., and Avila, J. (2014). The need for better AD animal models. *Front. Pharmacol.* *5*, 227.

Menkel, M., Terry, P., Pontecorvo, M., Katz, J.L., and Witkin, J.M. (1991). Selective sigma ligands block stimulant effects of cocaine. *Eur. J. Pharmacol.* *201*, 251–252.

Mésangeau, C., Narayanan, S., Green, A.M., Shaikh, J., Kaushal, N., Viard, E., Xu, Y.-T., Fishback, J.A., Poupaert, J.H., Matsumoto, R.R., et al. (2008). Conversion of a highly selective sigma-1 receptor-ligand to sigma-2 receptor preferring ligands with anticocaine activity. *J. Med. Chem.* *51*, 1482–1486.

Métayé, T., Gibelin, H., Perdrisot, R., and Kraimps, J.-L. (2005). Pathophysiological roles of G-protein-coupled receptor kinases. *Cell. Signal.* *17*, 917–928.

Miczek, K.A., Thompson, M.L., and Shuster, L. (1982). Opioid-like analgesia in defeated mice. *Science* *215*, 1520–1522.

Mifsud, W., and Bateman, A. (2002). Membrane-bound progesterone receptors contain a cytochrome b5-like ligand-binding domain. *Genome Biol.* *3*, RESEARCH0068.

Mikhaylova, M., Sharma, Y., Reissner, C., Nagel, F., Aravind, P., Rajini, B., Smalla, K.-H., Gundelfinger, E.D., and Kreutz, M.R. (2006). Neuronal Ca<sup>2+</sup> signaling via caldendrin and calneurons. *Biochim. Biophys. Acta* *1763*, 1229–1237.

Mikhaylova, M., Reddy, P.P., Munsch, T., Landgraf, P., Suman, S.K., Smalla, K.-H., Gundelfinger, E.D., Sharma, Y., and Kreutz, M.R. (2009). Calneurons provide a calcium threshold for trans-Golgi network to plasma membrane trafficking. *Proc. Natl. Acad. Sci. U. S. A.* *106*, 9093–9098.

- Mikhaylova, M., Hradsky, J., and Kreutz, M.R. (2011). Between promiscuity and specificity: novel roles of EF-hand calcium sensors in neuronal Ca<sup>2+</sup> signalling. *J. Neurochem.* *118*, 695–713.
- Miller, E.K., Freedman, D.J., and Wallis, J.D. (2002). The prefrontal cortex: categories, concepts and cognition. *Philos. Trans. R. Soc. Lond. B. Biol. Sci.* *357*, 1123–1136.
- Milligan, G., and Kostenis, E. (2006). Heterotrimeric G-proteins: a short history. *Br. J. Pharmacol.* *147 Suppl 1*, S46-55.
- Min, L., Strushkevich, N.V., Harnastai, I.N., Iwamoto, H., Gilep, A.A., Takemori, H., Usanov, S.A., Nonaka, Y., Hori, H., Vinson, G.P., et al. (2005). Molecular identification of adrenal inner zone antigen as a heme-binding protein. *FEBS J.* *272*, 5832–5843.
- Miura, S.-I., Karnik, S.S., and Saku, K. (2005). Constitutively active homo-oligomeric angiotensin II type 2 receptor induces cell signaling independent of receptor conformation and ligand stimulation. *J. Biol. Chem.* *280*, 18237–18244.
- Mochida, S., Few, A.P., Scheuer, T., and Catterall, W.A. (2008). Regulation of presynaptic Ca(V)2.1 channels by Ca<sup>2+</sup> sensor proteins mediates short-term synaptic plasticity. *Neuron* *57*, 210–216.
- Montero, C., Campillo, N.E., Goya, P., and Páez, J.A. (2005). Homology models of the cannabinoid CB1 and CB2 receptors. A docking analysis study. *Eur. J. Med. Chem.* *40*, 75–83.
- Moore, K.E., and Gudelsky, G.A. (1977). Drug actions on dopamine turnover in the median eminence. *Adv. Biochem. Psychopharmacol.* *16*, 227–235.
- Moore, C.A.C., Milano, S.K., and Benovic, J.L. (2007). Regulation of receptor trafficking by GRKs and arrestins. *Annu. Rev. Physiol.* *69*, 451–482.
- Morales, M., and Margolis, E.B. (2017). Ventral tegmental area: cellular heterogeneity, connectivity and behaviour. *Nat. Rev. Neurosci.* *18*, 73–85.



## BIBLIOGRAPHY

Morales, P., Hernandez-Folgado, L., Goya, P., and Jagerovic, N. (2016). Cannabinoid receptor 2 (CB2) agonists and antagonists: a patent update. *Expert Opin. Ther. Pat.* *26*, 843–856.

Moreno, E., Hoffmann, H., Gonzalez-Sepúlveda, M., Navarro, G., Casadó, V., Cortés, A., Mallol, J., Vignes, M., McCormick, P.J., Canela, E.I., et al. (2011). Dopamine D1-histamine H3 receptor heteromers provide a selective link to MAPK signaling in GABAergic neurons of the direct striatal pathway. *J. Biol. Chem.* *286*, 5846–5854.

Moreno, E., Andradas, C., Medrano, M., Caffarel, M.M., Pérez-Gómez, E., Blasco-Benito, S., Gómez-Cañas, M., Pazos, M.R., Irving, A.J., Lluís, C., et al. (2014). Targeting CB2-GPR55 receptor heteromers modulates cancer cell signaling. *J. Biol. Chem.* *289*, 21960–21972.

Moreno, E., Quiroz, C., Rea, W., Cai, N.-S., Mallol, J., Cortés, A., Lluís, C., Canela, E.I., Casadó, V., and Ferré, S. (2017). Functional  $\mu$ -Opioid-Galanin Receptor Heteromers in the Ventral Tegmental Area. *J. Neurosci. Off. J. Soc. Neurosci.* *37*, 1176–1186.

Mucke, L., Masliah, E., Yu, G.Q., Mallory, M., Rockenstein, E.M., Tatsuno, G., Hu, K., Kholodenko, D., Johnson-Wood, K., and McConlogue, L. (2000). High-level neuronal expression of abeta 1-42 in wild-type human amyloid protein precursor transgenic mice: synaptotoxicity without plaque formation. *J. Neurosci. Off. J. Soc. Neurosci.* *20*, 4050–4058.

Mukhopadhyay, S., McIntosh, H.H., Houston, D.B., and Howlett, A.C. (2000). The CB(1) cannabinoid receptor juxtamembrane C-terminal peptide confers activation to specific G proteins in brain. *Mol. Pharmacol.* *57*, 162–170.

Munro, S., Thomas, K.L., and Abu-Shaar, M. (1993). Molecular characterization of a peripheral receptor for cannabinoids. *Nature* *365*, 61–65.

Muñoz, A., Garrido-Gil, P., Dominguez-Mejide, A., and Labandeira-Garcia, J.L. (2014). Angiotensin type 1 receptor blockage reduces l-dopa-induced dyskinesia in the 6-OHDA model of Parkinson's disease. Involvement of vascular endothelial growth factor and interleukin-1 $\beta$ . *Exp. Neurol.* *261*, 720–732.

Muthian, S., Rademacher, D.J., Roelke, C.T., Gross, G.J., and Hillard, C.J. (2004).

Anandamide content is increased and CB1 cannabinoid receptor blockade is protective during transient, focal cerebral ischemia. *Neuroscience* 129, 743–750.

Nakamura, T.Y., Jeromin, A., Smith, G., Kurushima, H., Koga, H., Nakabeppu, Y., Wakabayashi, S., and Nabekura, J. (2006). Novel role of neuronal Ca<sup>2+</sup> sensor-1 as a survival factor up-regulated in injured neurons. *J. Cell Biol.* 172, 1081–1091.

Navarro, G., Carriba, P., Gandía, J., Ciruela, F., Casadó, V., Cortés, A., Mallol, J., Canela, E.I., Lluís, C., and Franco, R. (2008). Detection of heteromers formed by cannabinoid CB1, dopamine D2, and adenosine A2A G-protein-coupled receptors by combining bimolecular fluorescence complementation and bioluminescence energy transfer. *ScientificWorldJournal* 8, 1088–1097.

Navarro, G., Aymerich, M.S., Marcellino, D., Cortés, A., Casadó, V., Mallol, J., Canela, E.I., Agnati, L., Woods, A.S., Fuxe, K., et al. (2009). Interactions between calmodulin, adenosine A2A, and dopamine D2 receptors. *J. Biol. Chem.* 284, 28058–28068.

Navarro, G., Ferré, S., Cordomi, A., Moreno, E., Mallol, J., Casadó, V., Cortés, A., Hoffmann, H., Ortiz, J., Canela, E.I., et al. (2010a). Interactions between Intracellular Domains as Key Determinants of the Quaternary Structure and Function of Receptor Heteromers. *J. Biol. Chem.* 285, 27346–27359.

Navarro, G., Moreno, E., Aymerich, M., Marcellino, D., McCormick, P.J., Mallol, J., Cortés, A., Casadó, V., Canela, E.I., Ortiz, J., et al. (2010b). Direct involvement of sigma-1 receptors in the dopamine D1 receptor-mediated effects of cocaine. *Proc. Natl. Acad. Sci. U. S. A.* 107, 18676–18681.

Navarro, G., Hradsky, J., Lluís, C., Casadó, V., McCormick, P.J., Kreutz, M.R., and Mikhaylova, M. (2012). NCS-1 associates with adenosine A(2A) receptors and modulates receptor function. *Front. Mol. Neurosci.* 5, 53.

Navarro, G., Moreno, E., Bonaventura, J., Brugarolas, M., Farré, D., Aguinaga, D., Mallol, J., Cortés, A., Casadó, V., Lluís, C., et al. (2013). Cocaine inhibits dopamine D2 receptor signaling via sigma-1-D2 receptor heteromers. *PloS One* 8, e61245.

## BIBLIOGRAPHY

Navarro, G., Borroto-Escuela, D.O., Fuxe, K., and Franco, R. (2014a). Potential of caveolae in the therapy of cardiovascular and neurological diseases. *Front. Physiol.* *5*, 370.

Navarro, G., Aguinaga, D., Moreno, E., Hradsky, J., Reddy, P.P., Cortés, A., Mallol, J., Casadó, V., Mikhaylova, M., Kreutz, M.R., et al. (2014b). Intracellular Calcium Levels Determine Differential Modulation of Allosteric Interactions within G Protein-Coupled Receptor Heteromers. *Chem. Biol.* *21*, 1546–1556.

Navarro, G., Quiroz, C., Moreno-Delgado, D., Sierakowiak, A., McDowell, K., Moreno, E., Rea, W., Cai, N.-S., Aguinaga, D., Howell, L.A., et al. (2015). Orexin-corticotropin-releasing factor receptor heteromers in the ventral tegmental area as targets for cocaine. *J. Neurosci. Off. J. Soc. Neurosci.* *35*, 6639–6653.

Navarro, G., Cordoní, A., Zelman-Femiak, M., Brugarolas, M., Moreno, E., Aguinaga, D., Perez-Benito, L., Cortés, A., Casadó, V., Mallol, J., et al. (2016a). Quaternary structure of a G-protein-coupled receptor heterotetramer in complex with Gi and Gs. *BMC Biol.* *14*, 26.

Navarro, G., Morales, P., Rodríguez-Cueto, C., Fernández-Ruiz, J., Jagerovic, N., and Franco, R. (2016b). Targeting Cannabinoid CB2 Receptors in the Central Nervous System. *Medicinal Chemistry Approaches with Focus on Neurodegenerative Disorders. Front. Neurosci.* *10*, 406.

Navarro, G., Cordoní, A., Brugarolas, M., Moreno, E., Aguinaga, D., Pérez-Benito, L., Ferre, S., Cortés, A., Casadó, V., Mallol, J., et al. (2018). Cross-communication between Gi and Gs in a G-protein-coupled receptor heterotetramer guided by a receptor C-terminal domain. *BMC Biol.* *16*, 24.

Nef, S., Fiumelli, H., de Castro, E., Raes, M.B., and Nef, P. (1995). Identification of neuronal calcium sensor (NCS-1) possibly involved in the regulation of receptor phosphorylation. *J. Recept. Signal Transduct. Res.* *15*, 365–378.

Negyessy, L., and Goldman-Rakic, P.S. (2005). Subcellular localization of the dopamine D2 receptor and coexistence with the calcium-binding protein neuronal calcium sensor-1 in the primate prefrontal cortex. *J. Comp. Neurol.* *488*, 464–475.



- Neubig, R.R., Spedding, M., Kenakin, T., Christopoulos, A., and International Union of Pharmacology Committee on Receptor Nomenclature and Drug Classification (2003). International Union of Pharmacology Committee on Receptor Nomenclature and Drug Classification. XXXVIII. Update on terms and symbols in quantitative pharmacology. *Pharmacol. Rev.* *55*, 597–606.
- Ng, G.Y., O'Dowd, B.F., Lee, S.P., Chung, H.T., Brann, M.R., Seeman, P., and George, S.R. (1996). Dopamine D2 receptor dimers and receptor-blocking peptides. *Biochem. Biophys. Res. Commun.* *227*, 200–204.
- Oades, R.D., and Halliday, G.M. (1987). Ventral tegmental (A10) system: neurobiology. 1. Anatomy and connectivity. *Brain Res.* *434*, 117–165.
- Oka, S., Nakajima, K., Yamashita, A., Kishimoto, S., and Sugiura, T. (2007). Identification of GPR55 as a lysophosphatidylinositol receptor. *Biochem. Biophys. Res. Commun.* *362*, 928–934.
- Orrenius, S., Zhivotovsky, B., and Nicotera, P. (2003). Regulation of cell death: the calcium-apoptosis link. *Nat. Rev. Mol. Cell Biol.* *4*, 552–565.
- Ostrom, R.S., and Insel, P.A. (2004). The evolving role of lipid rafts and caveolae in G protein-coupled receptor signaling: implications for molecular pharmacology. *Br. J. Pharmacol.* *143*, 235–245.
- Ozcan, L., and Tabas, I. (2010). Pivotal role of calcium/calmodulin-dependent protein kinase II in ER stress-induced apoptosis. *Cell Cycle Georget. Tex* *9*, 223–224.
- Pacher, P., and Mechoulam, R. (2011). Is lipid signaling through cannabinoid 2 receptors part of a protective system? *Prog. Lipid Res.* *50*, 193–211.
- Pak, Y., O'Dowd, B.F., Wang, J.B., and George, S.R. (1999). Agonist-induced, G protein-dependent and -independent down-regulation of the mu opioid receptor. The receptor is a direct substrate for protein-tyrosine kinase. *J. Biol. Chem.* *274*, 27610–27616.

## BIBLIOGRAPHY

Palazuelos, J., Ortega, Z., Díaz-Alonso, J., Guzmán, M., and Galve-Roperh, I. (2012). CB2 cannabinoid receptors promote neural progenitor cell proliferation via mTORC1 signaling. *J. Biol. Chem.* *287*, 1198–1209.

Palczewski, K., Kumasaka, T., Hori, T., Behnke, C.A., Motoshima, H., Fox, B.A., Le Trong, I., Teller, D.C., Okada, T., Stenkamp, R.E., et al. (2000). Crystal structure of rhodopsin: A G protein-coupled receptor. *Science* *289*, 739–745.

Pandalaneni, S., Karuppiyah, V., Saleem, M., Haynes, L.P., Burgoyne, R.D., Mayans, O., Derrick, J.P., and Lian, L.-Y. (2015). Neuronal Calcium Sensor-1 Binds the D2 Dopamine Receptor and G-protein-coupled Receptor Kinase 1 (GRK1) Peptides Using Different Modes of Interactions. *J. Biol. Chem.* *290*, 18744–18756.

Paradis, J.S., Ly, S., Blondel-Tepaz, É., Galan, J.A., Beaudrait, A., Scott, M.G.H., Enslin, H., Marullo, S., Roux, P.P., and Bouvier, M. (2015). Receptor sequestration in response to  $\beta$ -arrestin-2 phosphorylation by ERK1/2 governs steady-state levels of GPCR cell-surface expression. *Proc. Natl. Acad. Sci. U. S. A.* *112*, E5160-5168.

Park, P.S.-H., Lodowski, D.T., and Palczewski, K. (2008). Activation of G protein-coupled receptors: beyond two-state models and tertiary conformational changes. *Annu. Rev. Pharmacol. Toxicol.* *48*, 107–141.

Parmar, V.K., Grinde, E., Mazurkiewicz, J.E., and Herrick-Davis, K. (2017). Beta2-adrenergic receptor homodimers: Role of transmembrane domain 1 and helix 8 in dimerization and cell surface expression. *Biochim. Biophys. Acta* *1859*, 1445–1455.

Parton, R.G., and del Pozo, M.A. (2013). Caveolae as plasma membrane sensors, protectors and organizers. *Nat. Rev. Mol. Cell Biol.* *14*, 98–112.

Pascoli, V., Terrier, J., Hiver, A., and Lüscher, C. (2015). Sufficiency of Mesolimbic Dopamine Neuron Stimulation for the Progression to Addiction. *Neuron* *88*, 1054–1066.

Paulmurugan, R., and Gambhir, S.S. (2003). Monitoring protein-protein interactions using

split synthetic renilla luciferase protein-fragment-assisted complementation. *Anal. Chem.* *75*, 1584–1589.

Pazos, M.R., Mohammed, N., Lafuente, H., Santos, M., Martínez-Pinilla, E., Moreno, E., Valdizan, E., Romero, J., Pazos, A., Franco, R., et al. (2013). Mechanisms of cannabidiol neuroprotection in hypoxic-ischemic newborn pigs: role of 5HT(1A) and CB2 receptors. *Neuropharmacology* *71*, 282–291.

Pei, L., Li, S., Wang, M., Diwan, M., Anisman, H., Fletcher, P.J., Nobrega, J.N., and Liu, F. (2010). Uncoupling the dopamine D1-D2 receptor complex exerts antidepressant-like effects. *Nat. Med.* *16*, 1393–1395.

Perello, M., Sakata, I., Birnbaum, S., Chuang, J.-C., Osborne-Lawrence, S., Rovinsky, S.A., Woloszyn, J., Yanagisawa, M., Lutter, M., and Zigman, J.M. (2010). Ghrelin increases the rewarding value of high-fat diet in an orexin-dependent manner. *Biol. Psychiatry* *67*, 880–886.

Perreault, M.L., Hasbi, A., Shen, M.Y.F., Fan, T., Navarro, G., Fletcher, P.J., Franco, R., Lanciego, J.L., and George, S.R. (2016). Disruption of a dopamine receptor complex amplifies the actions of cocaine. *Eur. Neuropsychopharmacol. J. Eur. Coll. Neuropsychopharmacol.* *26*, 1366–1377.

Pertwee, R.G. (2010). Receptors and channels targeted by synthetic cannabinoid receptor agonists and antagonists. *Curr. Med. Chem.* *17*, 1360–1381.

Pettit, H.O., and Justice, J.B. (1991). Effect of dose on cocaine self-administration behavior and dopamine levels in the nucleus accumbens. *Brain Res.* *539*, 94–102.

Pfleger, K.D.G., and Eidne, K.A. (2005). Monitoring the formation of dynamic G-protein-coupled receptor-protein complexes in living cells. *Biochem. J.* *385*, 625–637.

Phillipson, O.T. (1979). The cytoarchitecture of the interfascicular nucleus and ventral tegmental area of Tsai in the rat. *J. Comp. Neurol.* *187*, 85–98.

Pin, J.-P., Galvez, T., and Prézeau, L. (2003). Evolution, structure, and activation mechanism

## BIBLIOGRAPHY

of family 3/C G-protein-coupled receptors. *Pharmacol. Ther.* *98*, 325–354.

Pinna, A., Bonaventura, J., Farré, D., Sánchez, M., Simola, N., Mallol, J., Lluís, C., Costa, G., Baqi, Y., Müller, C.E., et al. (2014). L-DOPA disrupts adenosine A(2A)-cannabinoid CB(1)-dopamine D(2) receptor heteromer cross-talk in the striatum of hemiparkinsonian rats: biochemical and behavioral studies. *Exp. Neurol.* *253*, 180–191.

Pongs, O., Lindemeier, J., Zhu, X.R., Theil, T., Engelkamp, D., Krah-Jentgens, I., Lambrecht, H.G., Koch, K.W., Schwemer, J., and Rivosecchi, R. (1993). Frequentin--a novel calcium-binding protein that modulates synaptic efficacy in the *Drosophila* nervous system. *Neuron* *11*, 15–28.

Poulter, N.S., Pitkeathly, W.T.E., Smith, P.J., and Rappoport, J.Z. (2015). The physical basis of total internal reflection fluorescence (TIRF) microscopy and its cellular applications. *Methods Mol. Biol. Clifton NJ* *1251*, 1–23.

Price, D.A., Martinez, A.A., Seillier, A., Koek, W., Acosta, Y., Fernandez, E., Strong, R., Lutz, B., Marsicano, G., Roberts, J.L., et al. (2009). WIN55,212-2, a cannabinoid receptor agonist, protects against nigrostriatal cell loss in the 1-methyl-4-phenyl-1,2,3,6-tetrahydropyridine mouse model of Parkinson's disease. *Eur. J. Neurosci.* *29*, 2177–2186.

Probst, W.C., Snyder, L.A., Schuster, D.I., Brosius, J., and Sealfon, S.C. (1992). Sequence alignment of the G-protein coupled receptor superfamily. *DNA Cell Biol.* *11*, 1–20.

Racioppi, L., and Means, A.R. (2008). Calcium/calmodulin-dependent kinase IV in immune and inflammatory responses: novel routes for an ancient traveller. *Trends Immunol.* *29*, 600–607.

Ragusa, G., Gómez-Cañas, M., Morales, P., Hurst, D.P., Deligia, F., Pazos, R., Pinna, G.A., Fernández-Ruiz, J., Goya, P., Reggio, P.H., et al. (2015). Synthesis, pharmacological evaluation and docking studies of pyrrole structure-based CB2 receptor antagonists. *Eur. J. Med. Chem.* *101*, 651–667.

Rana, B.K., Shiina, T., and Insel, P.A. (2001). Genetic variations and polymorphisms of G

- protein-coupled receptors: functional and therapeutic implications. *Annu. Rev. Pharmacol. Toxicol.* *41*, 593–624.
- Ranjan, R., Gupta, P., and Shukla, A.K. (2016). GPCR Signaling:  $\beta$ -arrestins Kiss and Remember. *Curr. Biol. CB* *26*, R285-288.
- Ribeiro, R., Wen, J., Li, S., and Zhang, Y. (2013). Involvement of ERK1/2, cPLA2 and NF- $\kappa$ B in microglia suppression by cannabinoid receptor agonists and antagonists. *Prostaglandins Other Lipid Mediat.* *100–101*, 1–14.
- Richardson, N.R., and Gratton, A. (1998). Changes in medial prefrontal cortical dopamine levels associated with response-contingent food reward: an electrochemical study in rat. *J. Neurosci. Off. J. Soc. Neurosci.* *18*, 9130–9138.
- Ritz, M.C., Lamb, R.J., Goldberg, S.R., and Kuhar, M.J. (1987). Cocaine receptors on dopamine transporters are related to self-administration of cocaine. *Science* *237*, 1219–1223.
- Roberts, D.C., Corcoran, M.E., and Fibiger, H.C. (1977). On the role of ascending catecholaminergic systems in intravenous self-administration of cocaine. *Pharmacol. Biochem. Behav.* *6*, 615–620.
- Robinson, T.E., and Kolb, B. (1999). Alterations in the morphology of dendrites and dendritic spines in the nucleus accumbens and prefrontal cortex following repeated treatment with amphetamine or cocaine. *Eur. J. Neurosci.* *11*, 1598–1604.
- Robinson, T.E., Gorny, G., Mitton, E., and Kolb, B. (2001). Cocaine self-administration alters the morphology of dendrites and dendritic spines in the nucleus accumbens and neocortex. *Synap. N. Y. N* *39*, 257–266.
- Rocha, B.A. (2003). Stimulant and reinforcing effects of cocaine in monoamine transporter knockout mice. *Eur. J. Pharmacol.* *479*, 107–115.
- Rocheville, M., Lange, D.C., Kumar, U., Sasi, R., Patel, R.C., and Patel, Y.C. (2000). Subtypes of the somatostatin receptor assemble as functional homo- and heterodimers. *J. Biol. Chem.*



## BIBLIOGRAPHY

275, 7862–7869.

Rodríguez-Cueto, C., Benito, C., Fernández-Ruiz, J., Romero, J., Hernández-Gálvez, M., and Gómez-Ruiz, M. (2014). Changes in CB(1) and CB(2) receptors in the post-mortem cerebellum of humans affected by spinocerebellar ataxias. *Br. J. Pharmacol.* *171*, 1472–1489.

Rodríguez-Muñoz, M., Cortés-Montero, E., Pozo-Rodrigálvarez, A., Sánchez-Blázquez, P., and Garzón-Niño, J. (2015). The ON:OFF switch,  $\sigma$ 1R-HINT1 protein, controls GPCR-NMDA receptor cross-regulation: implications in neurological disorders. *Oncotarget* *6*, 35458–35477.

Rohe, H.J., Ahmed, I.S., Twist, K.E., and Craven, R.J. (2009). PGRMC1 (progesterone receptor membrane component 1): a targetable protein with multiple functions in steroid signaling, P450 activation and drug binding. *Pharmacol. Ther.* *121*, 14–19.

Rom, S., and Persidsky, Y. (2013). Cannabinoid receptor 2: potential role in immunomodulation and neuroinflammation. *J. Neuroimmune Pharmacol. Off. J. Soc. NeuroImmune Pharmacol.* *8*, 608–620.

Roman, F.J., Pascaud, X., Duffy, O., Vauche, D., Martin, B., and Junien, J.L. (1989). Neuropeptide Y and peptide YY interact with rat brain sigma and PCP binding sites. *Eur. J. Pharmacol.* *174*, 301–302.

Romano, C., Yang, W.L., and O'Malley, K.L. (1996). Metabotropic glutamate receptor 5 is a disulfide-linked dimer. *J. Biol. Chem.* *271*, 28612–28616.

Romano, C., Miller, J.K., Hyrc, K., Dikranian, S., Mennerick, S., Takeuchi, Y., Goldberg, M.P., and O'Malley, K.L. (2001). Covalent and noncovalent interactions mediate metabotropic glutamate receptor mGlu5 dimerization. *Mol. Pharmacol.* *59*, 46–53.

Romieu, P., Martin-Fardon, R., and Maurice, T. (2000). Involvement of the sigma1 receptor in the cocaine-induced conditioned place preference. *Neuroreport* *11*, 2885–2888.

Romieu, P., Phan, V.L., Martin-Fardon, R., and Maurice, T. (2002). Involvement of the

sigma(1) receptor in cocaine-induced conditioned place preference: possible dependence on dopamine uptake blockade. *Neuropsychopharmacol. Off. Publ. Am. Coll. Neuropsychopharmacol.* *26*, 444–455.

Rosenbaum, D.M., Rasmussen, S.G.F., and Kobilka, B.K. (2009). The structure and function of G-protein-coupled receptors. *Nature* *459*, 356–363.

Ross, S.B., and Renyi, A.L. (1967). Inhibition of the uptake of tritiated catecholamines by antidepressant and related agents. *Eur. J. Pharmacol.* *2*, 181–186.

Rozenfeld, R., Gupta, A., Gagnidze, K., Lim, M.P., Gomes, I., Lee-Ramos, D., Nieto, N., and Devi, L.A. (2011). AT1R-CB<sub>1</sub>R heteromerization reveals a new mechanism for the pathogenic properties of angiotensin II. *EMBO J.* *30*, 2350–2363.

Rozenfeld, R., Bushlin, I., Gomes, I., Tzavaras, N., Gupta, A., Neves, S., Battini, L., Gusella, G.L., Lachmann, A., Ma'ayan, A., et al. (2012). Receptor heteromerization expands the repertoire of cannabinoid signaling in rodent neurons. *PloS One* *7*, e29239.

Ryberg, E., Larsson, N., Sjögren, S., Hjorth, S., Hermansson, N.-O., Leonova, J., Elebring, T., Nilsson, K., Drmota, T., and Greasley, P.J. (2007). The orphan receptor GPR55 is a novel cannabinoid receptor. *Br. J. Pharmacol.* *152*, 1092–1101.

Salahpour, A., Angers, S., Mercier, J.-F., Lagacé, M., Marullo, S., and Bouvier, M. (2004). Homodimerization of the beta2-adrenergic receptor as a prerequisite for cell surface targeting. *J. Biol. Chem.* *279*, 33390–33397.

Saura, C.A., Chen, G., Malkani, S., Choi, S.-Y., Takahashi, R.H., Zhang, D., Gouras, G.K., Kirkwood, A., Morris, R.G.M., and Shen, J. (2005). Conditional inactivation of presenilin 1 prevents amyloid accumulation and temporarily rescues contextual and spatial working memory impairments in amyloid precursor protein transgenic mice. *J. Neurosci. Off. J. Soc. Neurosci.* *25*, 6755–6764.

Savonenko, A.V., Melnikova, T., Wang, Y., Ravert, H., Gao, Y., Koppel, J., Lee, D., Pletnikova, O., Cho, E., Sayyida, N., et al. (2015). Cannabinoid CB2 Receptors in a Mouse

## BIBLIOGRAPHY

Model of A $\beta$  Amyloidosis: Immunohistochemical Analysis and Suitability as a PET Biomarker of Neuroinflammation. *PloS One* 10, e0129618.

Scheerer, P., Park, J.H., Hildebrand, P.W., Kim, Y.J., Krauss, N., Choe, H.-W., Hofmann, K.P., and Ernst, O.P. (2008). Crystal structure of opsin in its G-protein-interacting conformation. *Nature* 455, 497–502.

Schellekens, H., Dinan, T.G., and Cryan, J.F. (2010). Lean mean fat reducing “ghrelin” machine: hypothalamic ghrelin and ghrelin receptors as therapeutic targets in obesity. *Neuropharmacology* 58, 2–16.

Schlyer, S., and Horuk, R. (2006). I want a new drug: G-protein-coupled receptors in drug development. *Drug Discov. Today* 11, 481–493.

Schmidt, H.R., Zheng, S., Gurpinar, E., Koehl, A., Manglik, A., and Kruse, A.C. (2016). Crystal structure of the human  $\sigma$ 1 receptor. *Nature* 532, 527–530.

Schröder, B., Schlumbohm, C., Kaune, R., and Breves, G. (1996). Role of calbindin-D9k in buffering cytosolic free Ca<sup>2+</sup> ions in pig duodenal enterocytes. *J. Physiol.* 492 ( Pt 3), 715–722.

Schultz, W., Dayan, P., and Montague, P.R. (1997). A neural substrate of prediction and reward. *Science* 275, 1593–1599.

Schwaller, B. (2009). The continuing disappearance of “pure” Ca<sup>2+</sup> buffers. *Cell. Mol. Life Sci. CMLS* 66, 275–300.

Scotter, E.L., Abood, M.E., and Glass, M. (2010). The endocannabinoid system as a target for the treatment of neurodegenerative disease. *Br. J. Pharmacol.* 160, 480–498.

Seidenbecher, C.I., Langnaese, K., Sanmartí-Vila, L., Boeckers, T.M., Smalla, K.H., Sabel, B.A., Garner, C.C., Gundelfinger, E.D., and Kreutz, M.R. (1998). Caldendrin, a novel neuronal calcium-binding protein confined to the somato-dendritic compartment. *J. Biol. Chem.* 273, 21324–21331.

Seidenbecher, C.I., Landwehr, M., Smalla, K.-H., Kreutz, M., Dieterich, D.C., Zuschratter, W., Reissner, C., Hammarback, J.A., Böckers, T.M., Gundelfinger, E.D., et al. (2004). Caldendrin but not calmodulin binds to light chain 3 of MAP1A/B: an association with the microtubule cytoskeleton highlighting exclusive binding partners for neuronal Ca(2+)-sensor proteins. *J. Mol. Biol.* *336*, 957–970.

Seifert, R., and Wenzel-Seifert, K. (2002). Constitutive activity of G-protein-coupled receptors: cause of disease and common property of wild-type receptors. *Naunyn. Schmiedebergs Arch. Pharmacol.* *366*, 381–416.

Sexton, P.M., Poyner, D.R., Simms, J., Christopoulos, A., and Hay, D.L. (2009). Modulating receptor function through RAMPs: can they represent drug targets in themselves? *Drug Discov. Today* *14*, 413–419.

Shao, Z., Yin, J., Chapman, K., Grzemska, M., Clark, L., Wang, J., and Rosenbaum, D.M. (2016). High-resolution crystal structure of the human CB1 cannabinoid receptor. *Nature*.

Sheng, M., and Hoogenraad, C.C. (2007). The postsynaptic architecture of excitatory synapses: a more quantitative view. *Annu. Rev. Biochem.* *76*, 823–847.

Shintani, M., Ogawa, Y., Ebihara, K., Aizawa-Abe, M., Miyanaga, F., Takaya, K., Hayashi, T., Inoue, G., Hosoda, K., Kojima, M., et al. (2001). Ghrelin, an endogenous growth hormone secretagogue, is a novel orexigenic peptide that antagonizes leptin action through the activation of hypothalamic neuro peptide Y/Y1 receptor pathway. *Diabetes* *50*, 227–232.

Shonberg, J., Kling, R.C., Gmeiner, P., and Löber, S. (2015). GPCR crystal structures: Medicinal chemistry in the pocket. *Bioorg. Med. Chem.* *23*, 3880–3906.

Sierra, S., Luquin, N., Rico, A.J., Gómez-Bautista, V., Roda, E., Dopeso-Reyes, I.G., Vázquez, A., Martínez-Pinilla, E., Labandeira-García, J.L., Franco, R., et al. (2015). Detection of cannabinoid receptors CB1 and CB2 within basal ganglia output neurons in macaques: changes following experimental parkinsonism. *Brain Struct. Funct.* *220*, 2721–2738.

Silver, R., and Balsam, P. (2010). Oscillators entrained by food and the emergence of

## BIBLIOGRAPHY

anticipatory timing behaviors. *Sleep Biol. Rhythms* 8, 120–136.

Simon, K., Hennen, S., Merten, N., Blättermann, S., Gillard, M., Kostenis, E., and Gomeza, J. (2016). The Orphan G Protein-coupled Receptor GPR17 Negatively Regulates Oligodendrocyte Differentiation via  $G\alpha i/o$  and Its Downstream Effector Molecules. *J. Biol. Chem.* 291, 705–718.

Sippy, T., Cruz-Martín, A., Jeromin, A., and Schweizer, F.E. (2003). Acute changes in short-term plasticity at synapses with elevated levels of neuronal calcium sensor-1. *Nat. Neurosci.* 6, 1031–1038.

Skibicka, K.P., Hansson, C., Alvarez-Crespo, M., Friberg, P.A., and Dickson, S.L. (2011). Ghrelin directly targets the ventral tegmental area to increase food motivation. *Neuroscience* 180, 129–137.

Soares-Cunha, C., Coimbra, B., Sousa, N., and Rodrigues, A.J. (2016). Reappraising striatal D1- and D2-neurons in reward and aversion. *Neurosci. Biobehav. Rev.* 68, 370–386.

Solas, M., Francis, P.T., Franco, R., and Ramirez, M.J. (2013). CB2 receptor and amyloid pathology in frontal cortex of Alzheimer's disease patients. *Neurobiol. Aging* 34, 805–808.

Sorensen, A.B., Søndergaard, M.T., and Overgaard, M.T. (2013). Calmodulin in a heartbeat. *FEBS J.* 280, 5511–5532.

Stadel, R., Ahn, K.H., and Kendall, D.A. (2011). The cannabinoid type-1 receptor carboxyl-terminus, more than just a tail. *J. Neurochem.* 117, 1–18.

Steketee, J.D., and Kalivas, P.W. (2011). Drug wanting: behavioral sensitization and relapse to drug-seeking behavior. *Pharmacol. Rev.* 63, 348–365.

Stella, N. (2010). Cannabinoid and cannabinoid-like receptors in microglia, astrocytes, and astrocytomas. *Glia* 58, 1017–1030.

van der Stelt, M., and Di Marzo, V. (2005). Cannabinoid receptors and their role in

- neuroprotection. *Neuromolecular Med.* 7, 37–50.
- van der Stelt, M., Veldhuis, W.B., Maccarrone, M., Bär, P.R., Nicolay, K., Veldink, G.A., Di Marzo, V., and Vliegthart, J.F.G. (2002). Acute neuronal injury, excitotoxicity, and the endocannabinoid system. *Mol. Neurobiol.* 26, 317–346.
- Stone, J.M., Arstad, E., Erlandsson, K., Waterhouse, R.N., Ell, P.J., and Pilowsky, L.S. (2006). [123I]TPCNE--a novel SPET tracer for the sigma-1 receptor: first human studies and in vivo haloperidol challenge. *Synap. N. Y. N* 60, 109–117.
- Stryer, L. (1978). Fluorescence energy transfer as a spectroscopic ruler. *Annu. Rev. Biochem.* 47, 819–846.
- Su, T.-P., Hayashi, T., Maurice, T., Buch, S., and Ruoho, A.E. (2010). The sigma-1 receptor chaperone as an inter-organelle signaling modulator. *Trends Pharmacol. Sci.* 31, 557–566.
- Su, T.-P., Su, T.-C., Nakamura, Y., and Tsai, S.-Y. (2016). The Sigma-1 Receptor as a Pluripotent Modulator in Living Systems. *Trends Pharmacol. Sci.* 37, 262–278.
- Sugiura, T., Kondo, S., Sukagawa, A., Nakane, S., Shinoda, A., Itoh, K., Yamashita, A., and Waku, K. (1995). 2-Arachidonoylglycerol: a possible endogenous cannabinoid receptor ligand in brain. *Biochem. Biophys. Res. Commun.* 215, 89–97.
- Sun, Y., Shi, N., Li, H., Liu, K., Zhang, Y., Chen, W., and Sun, X. (2014). Ghrelin suppresses Purkinje neuron P-type Ca(2+) channels via growth hormone secretagogue type 1a receptor, the  $\beta\gamma$  subunits of Go-protein, and protein kinase a pathway. *Cell. Signal.* 26, 2530–2538.
- Syrovatkina, V., Alegre, K.O., Dey, R., and Huang, X.-Y. (2016). Regulation, Signaling, and Physiological Functions of G-Proteins. *J. Mol. Biol.* 428, 3850–3868.
- Tam, S.W., and Mitchell, K.N. (1991). Neuropeptide Y and peptide YY do not bind to brain sigma and phencyclidine binding sites. *Eur. J. Pharmacol.* 193, 121–122.
- Tadross, M.R., Dick, I.E., and Yue, D.T. (2008). Mechanism of local and global Ca<sup>2+</sup> sensing

## BIBLIOGRAPHY

by calmodulin in complex with a Ca<sup>2+</sup> channel. *Cell* *133*, 1228–1240.

Tebano, M.T., Martire, A., Chiodi, V., Pepponi, R., Ferrante, A., Domenici, M.R., Frank, C., Chen, J.-F., Ledent, C., and Popoli, P. (2009). Adenosine A<sub>2A</sub> receptors enable the synaptic effects of cannabinoid CB<sub>1</sub> receptors in the rodent striatum. *J. Neurochem.* *110*, 1921–1930.

Tecuapetla, F., Patel, J.C., Xenias, H., English, D., Tadros, I., Shah, F., Berlin, J., Deisseroth, K., Rice, M.E., Tepper, J.M., et al. (2010). Glutamatergic signaling by mesolimbic dopamine neurons in the nucleus accumbens. *J. Neurosci. Off. J. Soc. Neurosci.* *30*, 7105–7110.

Thomsen, A.R.B., Plouffe, B., Cahill, T.J., Shukla, A.K., Tarrasch, J.T., Dosey, A.M., Kahsai, A.W., Strachan, R.T., Pani, B., Mahoney, J.P., et al. (2016). GPCR-G Protein-β-Arrestin Super-Complex Mediates Sustained G Protein Signaling. *Cell* *166*, 907–919.

Tsien, R.W., and Tsien, R.Y. (1990). Calcium channels, stores, and oscillations. *Annu. Rev. Cell Biol.* *6*, 715–760.

Turner, J.H., Gelasco, A.K., and Raymond, J.R. (2004). Calmodulin interacts with the third intracellular loop of the serotonin 5-hydroxytryptamine<sub>1A</sub> receptor at two distinct sites: putative role in receptor phosphorylation by protein kinase C. *J. Biol. Chem.* *279*, 17027–17037.

Ujike, H., Kuroda, S., and Otsuki, S. (1996). sigma Receptor antagonists block the development of sensitization to cocaine. *Eur. J. Pharmacol.* *296*, 123–128.

Ulrich, C.D., Holtmann, M., and Miller, L.J. (1998). Secretin and vasoactive intestinal peptide receptors: members of a unique family of G protein-coupled receptors. *Gastroenterology* *114*, 382–397.

Valdeolivas, S., Sagredo, O., Delgado, M., Pozo, M.A., and Fernández-Ruiz, J. (2017). Effects of a Sativex-Like Combination of Phytocannabinoids on Disease Progression in R6/2 Mice, an Experimental Model of Huntington's Disease. *Int. J. Mol. Sci.* *18*.

Van Craenenbroeck, K., Borroto-Escuela, D.O., Skieterska, K., Duchou, J., Romero-

- Fernandez, W., and Fuxe, K. (2014). Role of dimerization in dopamine D(4) receptor biogenesis. *Curr. Protein Pept. Sci.* *15*, 659–665.
- Vaupel, D.B. (1983). Naltrexone fails to antagonize the sigma effects of PCP and SKF 10,047 in the dog. *Eur. J. Pharmacol.* *92*, 269–274.
- Vázquez, C., Tolón, R.M., Grande, M.T., Caraza, M., Moreno, M., Koester, E.C., Villaescusa, B., Ruiz-Valdepeñas, L., Fernández-Sánchez, F.J., Cravatt, B.F., et al. (2015). Endocannabinoid regulation of amyloid-induced neuroinflammation. *Neurobiol. Aging* *36*, 3008–3019.
- Villardaga, J.-P., Nikolaev, V.O., Lorenz, K., Ferrandon, S., Zhuang, Z., and Lohse, M.J. (2008). Conformational cross-talk between alpha2A-adrenergic and mu-opioid receptors controls cell signaling. *Nat. Chem. Biol.* *4*, 126–131.
- Villar, V.A.M., Cuevas, S., Zheng, X., and Jose, P.A. (2016). Localization and signaling of GPCRs in lipid rafts. *Methods Cell Biol.* *132*, 3–23.
- Viñals, X., Moreno, E., Lanfumey, L., Cordoní, A., Pastor, A., de La Torre, R., Gasperini, P., Navarro, G., Howell, L.A., Pardo, L., et al. (2015). Cognitive Impairment Induced by Delta9-tetrahydrocannabinol Occurs through Heteromers between Cannabinoid CB1 and Serotonin 5-HT2A Receptors. *PLoS Biol.* *13*, e1002194.
- van Waarde, A., Rybczynska, A.A., Ramakrishnan, N., Ishiwata, K., Elsinga, P.H., and Dierckx, R.A.J.O. (2010). Sigma receptors in oncology: therapeutic and diagnostic applications of sigma ligands. *Curr. Pharm. Des.* *16*, 3519–3537.
- van Waarde, A., Rybczynska, A.A., Ramakrishnan, N.K., Ishiwata, K., Elsinga, P.H., and Dierckx, R.A.J.O. (2015). Potential applications for sigma receptor ligands in cancer diagnosis and therapy. *Biochim. Biophys. Acta* *1848*, 2703–2714.
- Wager-Miller, J., Westenbroek, R., and Mackie, K. (2002). Dimerization of G protein-coupled receptors: CB1 cannabinoid receptors as an example. *Chem. Phys. Lipids* *121*, 83–89.





## BIBLIOGRAPHY

Walker, D.G., and Lue, L.-F. (2015). Immune phenotypes of microglia in human neurodegenerative disease: challenges to detecting microglial polarization in human brains. *Alzheimers Res. Ther.* 7, 56.

Walther, C., and Ferguson, S.S.G. (2015). Minireview: Role of intracellular scaffolding proteins in the regulation of endocrine G protein-coupled receptor signaling. *Mol. Endocrinol. Baltim. Md* 29, 814–830.

Wang, D., Sadée, W., and Quillan, J.M. (1999). Calmodulin binding to G protein-coupling domain of opioid receptors. *J. Biol. Chem.* 274, 22081–22088.

Wang, J., Xu, Y., Zhu, L., Zou, Y., Kong, W., Dong, B., Huang, J., Chen, Y., Xue, W., Huang, Y., et al. (2018). Cannabinoid receptor 2 as a novel target for promotion of renal cell carcinoma prognosis and progression. *J. Cancer Res. Clin. Oncol.* 144, 39–52.

Wang, W., Jia, Y., Pham, D.T., Palmer, L.C., Jung, K.-M., Cox, C.D., Rumbaugh, G., Piomelli, D., Gall, C.M., and Lynch, G. (2017). Atypical Endocannabinoid Signaling Initiates a New Form of Memory-Related Plasticity at a Cortical Input to Hippocampus. *Cereb. Cortex N. Y. N* 1991 1–14.

Wehbi, V.L., Stevenson, H.P., Feinstein, T.N., Calero, G., Romero, G., and Vilardaga, J.-P. (2013). Noncanonical GPCR signaling arising from a PTH receptor-arrestin-G $\beta\gamma$  complex. *Proc. Natl. Acad. Sci. U. S. A.* 110, 1530–1535.

Weis, W.I., and Kobilka, B.K. (2008). Structural insights into G-protein-coupled receptor activation. *Curr. Opin. Struct. Biol.* 18, 734–740.

Weiss, J.L., Archer, D.A., and Burgoyne, R.D. (2000). Neuronal Ca<sup>2+</sup> sensor-1/frequenin functions in an autocrine pathway regulating Ca<sup>2+</sup> channels in bovine adrenal chromaffin cells. *J. Biol. Chem.* 275, 40082–40087.

van der Westhuizen, E.T., Breton, B., Christopoulos, A., and Bouvier, M. (2014). Quantification of ligand bias for clinically relevant  $\beta$ 2-adrenergic receptor ligands: implications for drug taxonomy. *Mol. Pharmacol.* 85, 492–509.

- Weston, C., Lu, J., Li, N., Barkan, K., Richards, G.O., Roberts, D.J., Skerry, T.M., Poyner, D., Pardamwar, M., Reynolds, C.A., et al. (2015). Modulation of Glucagon Receptor Pharmacology by Receptor Activity-modifying Protein-2 (RAMP2). *J. Biol. Chem.* *290*, 23009–23022.
- Whalen, E.J., Rajagopal, S., and Lefkowitz, R.J. (2011). Therapeutic potential of  $\beta$ -arrestin- and G protein-biased agonists. *Trends Mol. Med.* *17*, 126–139.
- White, J.H., Wise, A., Main, M.J., Green, A., Fraser, N.J., Disney, G.H., Barnes, A.A., Emson, P., Foord, S.M., and Marshall, F.H. (1998). Heterodimerization is required for the formation of a functional GABA(B) receptor. *Nature* *396*, 679–682.
- Whorton, M.R., Bokoch, M.P., Rasmussen, S.G.F., Huang, B., Zare, R.N., Kobilka, B., and Sunahara, R.K. (2007). A monomeric G protein-coupled receptor isolated in a high-density lipoprotein particle efficiently activates its G protein. *Proc. Natl. Acad. Sci. U. S. A.* *104*, 7682–7687.
- Will, R.G., Martz, J.R., and Dominguez, J.M. (2016). The medial preoptic area modulates cocaine-induced locomotion in male rats. *Behav. Brain Res.* *305*, 218–222.
- Wilson, R.I., and Nicoll, R.A. (2002). Endocannabinoid signaling in the brain. *Science* *296*, 678–682.
- Wingard, J.N., Chan, J., Bosanac, I., Haeseleer, F., Palczewski, K., Ikura, M., and Ames, J.B. (2005). Structural analysis of Mg<sup>2+</sup> and Ca<sup>2+</sup> binding to CaBP1, a neuron-specific regulator of calcium channels. *J. Biol. Chem.* *280*, 37461–37470.
- Wise, R.A. (2002). Brain reward circuitry: insights from unsensed incentives. *Neuron* *36*, 229–240.
- Wolf, M.E. (2016). Synaptic mechanisms underlying persistent cocaine craving. *Nat. Rev. Neurosci.* *17*, 351–365.

## BIBLIOGRAPHY

Woll, M.P., De Cotiis, D.A., Bewley, M.C., Tacelosky, D.M., Levenson, R., and Flanagan, J.M. (2011). Interaction between the D2 dopamine receptor and neuronal calcium sensor-1 analyzed by fluorescence anisotropy. *Biochemistry (Mosc.)* 50, 8780–8791.

Woods, A.S., Marcellino, D., Jackson, S.N., Franco, R., Ferré, S., Agnati, L.F., and Fuxe, K. (2008). How calmodulin interacts with the adenosine A(2A) and the dopamine D(2) receptors. *J. Proteome Res.* 7, 3428–3434.

Wooten, D., Christopoulos, A., and Sexton, P.M. (2013). Emerging paradigms in GPCR allostery: implications for drug discovery. *Nat. Rev. Drug Discov.* 12, 630–644.

Wreggett, K.A., and Wells, J.W. (1995). Cooperativity manifest in the binding properties of purified cardiac muscarinic receptors. *J. Biol. Chem.* 270, 22488–22499.

Wu, Z., and Bowen, W.D. (2008). Role of sigma-1 receptor C-terminal segment in inositol 1,4,5-trisphosphate receptor activation: constitutive enhancement of calcium signaling in MCF-7 tumor cells. *J. Biol. Chem.* 283, 28198–28215.

Wu, D.-F., Yang, L.-Q., Goschke, A., Stumm, R., Brandenburg, L.-O., Liang, Y.-J., Höllt, V., and Koch, T. (2008). Role of receptor internalization in the agonist-induced desensitization of cannabinoid type 1 receptors. *J. Neurochem.* 104, 1132–1143.

Wu, H., Wacker, D., Mileni, M., Katritch, V., Han, G.W., Vardy, E., Liu, W., Thompson, A.A., Huang, X.-P., Carroll, F.I., et al. (2012). Structure of the human  $\kappa$ -opioid receptor in complex with JDTic. *Nature* 485, 327–332.

Xu, J., Zeng, C., Chu, W., Pan, F., Rothfuss, J.M., Zhang, F., Tu, Z., Zhou, D., Zeng, D., Vangveravong, S., et al. (2011). Identification of the PGRMC1 protein complex as the putative sigma-2 receptor binding site. *Nat. Commun.* 2, 380.

Xu, W., Filppula, S.A., Mercier, R., Yaddanapudi, S., Pavlopoulos, S., Cai, J., Pierce, W.M., and Makriyannis, A. (2005). Purification and mass spectroscopic analysis of human CB1 cannabinoid receptor functionally expressed using the baculovirus system. *J. Pept. Res. Off. J. Am. Pept. Soc.* 66, 138–150.



- Yang, Y., and Raine, A. (2009). Prefrontal structural and functional brain imaging findings in antisocial, violent, and psychopathic individuals: a meta-analysis. *Psychiatry Res.* *174*, 81–88.
- Yang, J., Brown, M.S., Liang, G., Grishin, N.V., and Goldstein, J.L. (2008). Identification of the acyltransferase that octanoylates ghrelin, an appetite-stimulating peptide hormone. *Cell* *132*, 387–396.
- Yin, Y., Zhou, X.E., Hou, L., Zhao, L.-H., Liu, B., Wang, G., Jiang, Y., Melcher, K., and Xu, H.E. (2016). An intrinsic agonist mechanism for activation of glucagon-like peptide-1 receptor by its extracellular domain. *Cell Discov.* *2*, 16042.
- Zampese, E., and Pizzo, P. (2012). Intracellular organelles in the saga of Ca<sup>2+</sup> homeostasis: different molecules for different purposes? *Cell. Mol. Life Sci. CMLS* *69*, 1077–1104.
- Zeng, C., Vangveravong, S., Xu, J., Chang, K.C., Hotchkiss, R.S., Wheeler, K.T., Shen, D., Zhuang, Z.-P., Kung, H.F., and Mach, R.H. (2007). Subcellular localization of sigma-2 receptors in breast cancer cells using two-photon and confocal microscopy. *Cancer Res.* *67*, 6708–6716.
- Zeng, C., Rothfuss, J.M., Zhang, J., Vangveravong, S., Chu, W., Li, S., Tu, Z., Xu, J., and Mach, R.H. (2014). Functional assays to define agonists and antagonists of the sigma-2 receptor. *Anal. Biochem.* *448*, 68–74.
- Zhang, X.C., Liu, J., and Jiang, D. (2014). Why is dimerization essential for class-C GPCR function? New insights from mGluR1 crystal structure analysis. *Protein Cell* *5*, 492–495.
- Zhou, H., Kim, S.-A., Kirk, E.A., Tippens, A.L., Sun, H., Haeseleer, F., and Lee, A. (2004). Ca<sup>2+</sup>-binding protein-1 facilitates and forms a postsynaptic complex with Cav1.2 (L-type) Ca<sup>2+</sup> channels. *J. Neurosci. Off. J. Soc. Neurosci.* *24*, 4698–4708.
- Zhu, X., and Wess, J. (1998). Truncated V2 vasopressin receptors as negative regulators of wild-type V2 receptor function. *Biochemistry (Mosc.)* *37*, 15773–15784.

## BIBLIOGRAPHY

Zhu, W., Mao, Z., Zhu, C., Li, M., Cao, C., Guan, Y., Yuan, J., Xie, G., and Guan, X. (2016). Adolescent exposure to cocaine increases anxiety-like behavior and induces morphologic and neurochemical changes in the hippocampus of adult rats. *Neuroscience* 313, 174–183.

Zigman, J.M., Jones, J.E., Lee, C.E., Saper, C.B., and Elmquist, J.K. (2006). Expression of ghrelin receptor mRNA in the rat and the mouse brain. *J. Comp. Neurol.* 494, 528–548.

Zoppi, S., Pérez Nievas, B.G., Madrigal, J.L.M., Manzanares, J., Leza, J.C., and García-Bueno, B. (2011). Regulatory role of cannabinoid receptor 1 in stress-induced excitotoxicity and neuroinflammation. *Neuropsychopharmacol. Off. Publ. Am. Coll. Neuropsychopharmacol.* 36, 805–818.